LOCATION-BASED FORWARDING IN VEHICULAR NETWORKS

by WOUTER KLEIN WOLTERINK

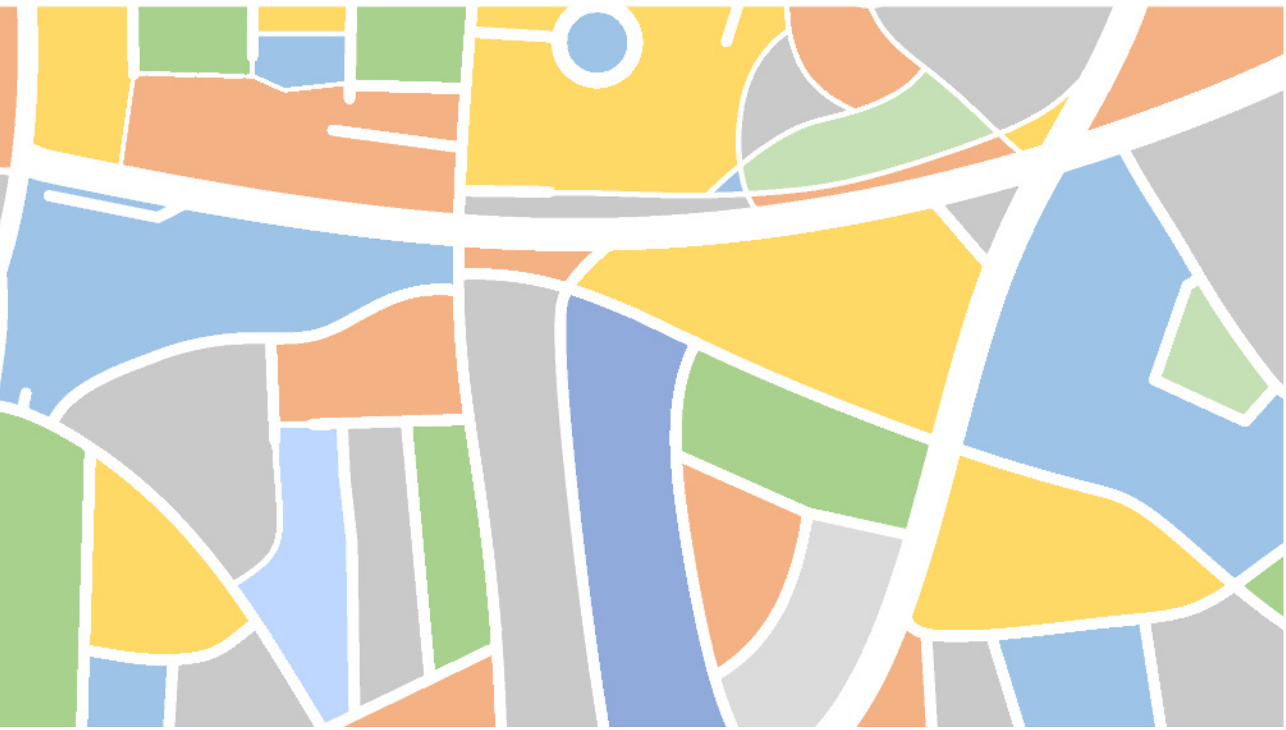

Location-based Forwarding in Vehicular Networks

Wouter Klein Wolterink

Graduation committee:

Chairman:	prof. dr. ir. P.H. Veltink, University of Twente
Promoter:	prof. dr. J.L. van den Berg, University of Twente, TNO
Assistant promoter:	dr. ir. G.J. Heijenk, University of Twente

Members:	
Dr. ir. G. Karagiannis	University of Twente
Prof. dr. ing. P.J.M. Havinga	University of Twente
Prof. dr. rer. nat. F.E. Kargl	University of Twente, Ulm University
Prof. dr. rer. nat. H. Hartenstein	Karlsruhe Institute of Technology
Prof. dr. R.D. van der Mei	Centrum Wiskunde & Informatica, VU University

CTIT

CTIT Ph.D.-thesis Series No. 13-275
Centre for Telematics and Information Technology
University of Twente
P.O. Box 217, NL – 7500 AE Enschede

ISSN 1381-3617
ISBN 978-90-365-3560-1
DOI 10.3990/1.9789036535601
http://dx.doi.org/10.3990/1.9789036535601

Cover design by Wouter Klein Wolterink. All images have been created by Wouter Klein Wolterink unless noted otherwise. This thesis was printed by Wöhrmann Print Service.

LOCATION-BASED FORWARDING IN VEHICULAR NETWORKS

PROEFSCHRIFT

ter verkrijging van
de graad van doctor aan de Universiteit Twente,
op gezag van de rector magnificus,
prof. dr. H. Brinksma,
volgens besluit van het College voor Promoties,
in het openbaar te verdedigen
op vrijdag 1 november 2013 om 12.45 uur

door

Wouter Klein Wolterink

geboren op 22 december 1982
te Emmen, Nederland

This dissertation has been approved by:
Prof. dr. J.L. van den Berg (promoter)
Dr. ir. G.J. Heijenk (assistant promoter)

"In the end, you must clarify your goals. Once they have been clarified you must exercise your mental and physical energy in the most effective way in order to achieve them."

– Jigoro Kano,
in MIND OVER MUSCLE: WRITINGS FROM THE FOUNDER OF JUDO

Acknowledgements

This thesis would not have been possible without the help of my supervisors Geert Heijenk, Hans van den Berg, and Georgios Karagiannis. For the last years they have guided me, helped me, stimulated me, and formed me, and I am thankful for having had the opportunity of working with them. Likewise, I count myself lucky with all of my colleagues at DACS for the past four and a half years. I found it to be a group of people whom I consider to be both competent and kind, a combination one should never take for granted. In particular I will remember my roommates Martijn van Eenennaam, with whom I shared all of the confusions that come with obtaining a PhD, and Sarwar Morshed.

Outside of work my main priority was to refresh body & mind. Judo proved to be most effective at this, both by its uncompromising nature and the group's unaffected camaraderie. It was here that I found my two paranymphs, Bram Dil and Sietse Jongsma, both of whom embody these particular qualities to a great extent.

Finally I would like to thank family and friends for any support and distractions given. Above all my gratitude goes out towards my parents, who have always supported my siblings and me in every way possible.

Wouter Klein Wolterink
Enschede, October 2013

Abstract

In this thesis we focus on location-based message forwarding in vehicular networks to support intelligent transport systems (ITSs). ITSs are transport systems that utilise information and communication technologies to increase their level of automation, in this way levering the performance of such a system beyond the capabilities of the human driver. Such systems provide an increased level of traffic safety, traffic efficiency, and driving comfort, and reduce the environmental impact of traffic. An example ITS application is platoon driving, a form of automated driving in which vehicles cooperatively control their speed using wireless communication. The field of wireless networking that enables such systems is called vehicular networking. In a vehicular network vehicles, or nodes, act both as end-user and as router. Direct vehicle-to-vehicle (V2V) communication is possible using short-range communication technologies such as the IEEE 802.11p standard. Communication with more distant vehicles is supported by multi-hop forwarding protocols, typically using georouting. Georouting is a form of location-based forwarding in which data is addressed to a specific geographic location, and delivered to all nodes that are inside the geographic location at the time of delivery. It has been made possible by means of positioning techniques such as the global positioning system (GPS) and is used to disseminate location-relevant data.

In this thesis we consider two distinct challenges related to location-based forwarding in vehicular networks. The first challenges concerns georouting. Although it is currently the method of choice to disseminate data over multiple hops, georouting has a number of challenges left open. Specifically, its method of addressing does not always fit the requirements of the higher-level ITS application, causing data to be routed in an inefficient manner. This inefficiency stems from the fact that with standard georouting nodes are distinguished based on their current position only, a method which poorly meets the requirements of a typical ITS scenario where a node's trajectory from its current position onward is important. We address this shortcoming by proposing constrained geocast, a novel form of georouting in which destination nodes are addressed based on their conjectured future position rather than their current position. This allows data to be routed in a more selective manner, such that it only reaches those parts of the network where it is needed, i.e., where there are nodes that are headed in the direction of the event location and for that reason have interest in the data. We define a set of generic forwarding rules for constrained geocast and test it by means of simulation of a small-scale scenario, demonstrating the effectiveness of our solution.

The second challenge concerns the analytical modelling of multi-hop location-based forwarding inside vehicular networks. Despite the fact that several multi-hop forwarding protocols have already been standardised for use in vehicular networks, a thorough understanding of the performance of these protocols is still lacking. In particular, there is hardly

any analytical work available on the subject. To analytically model a multi-hop forwarding protocol in a realistic manner is a challenging task because of the size of the system and the inter-dependencies of successive hops, such that the complexity of such an analysis increases with each following hop. Existing analytical studies are therefore typically based on overly-simplified assumptions and give only limited insights. In this thesis we analytically model three multi-hop forwarding protocols in detail. One of these protocols is also referred to as beacon dissemination, or piggybacking. Another has recently been standardised as the contention-based forwarding (CBF) protocol. We express the behaviour of all three protocols in a number of fast-to-evaluate analytical expressions, with a high level of detail. Our models cover the multi-hop transmission of a single message from source to sink over a straight road with results including the full probability distribution of *(i)* the length of each hop, *(ii)* the delay of each hop, *(iii)* the success probability of each hop, *(iv)* the position of successive forwarders, *(v)* the required number of hops to have the message delivered, and *(vi)* the end-to-end delay to have the message delivered. Extensive verification of our analyses by detailed simulation showed the analytical results to be very accurate.

Our analytical models allow for easy and fast evaluation of the performance of the considered multi-hop forwarding protocols. In addition, they provide useful insights regarding the behaviour of the respective protocols, such as the way they are influenced by the various network and protocol parameters. Because of their high evaluation speed compared to existing simulation models, our analytical models can also speed up and, hence, considerably improve the usability of ITS application level simulations by emulating the communication layer.

The results of this thesis improve the efficiency and understanding of location-based forwarding in vehicular networks. The insights provided by our work can be used to increase the effectiveness of vehicular communication protocols and in this way advance the overall performance of ITS applications.

Samenvatting

Dit proefschrift richt zich op het locatiegebaseerd verzenden van berichten in een netwerk van voertuigen ter ondersteuning van zogeheten intelligente transportsystemen (ITS'en). Een ITS is een geautomatiseerd transportsysteem dat veiliger, efficiënter, comfortabeler en duurzamer is dan bestaande systemen. Een voorbeeld hiervan is het automatisch rijden in colonne, waarbij voertuigen onderling hun afstand tot elkaar bepalen door middel van draadloze communicatie. Een dergelijk communicatienetwerk wordt een vehiculair (communicatie)netwerk genoemd. In zulke netwerken acteren de voertuigen (ook wel nodes genoemd) als zowel eindgebruiker als router. Directe communicatie tussen nabijgelegen voertuigen is mogelijk door draadloze communicatietechnieken zoals de recent vastgestelde IEEE 802.11p-standaard, een variant van WiFi. Communicatie met voertuigen verder weg is mogelijk door berichten één of meerdere malen door te sturen. Dit wordt ook wel multi-hop-communicatie genoemd, waarbij elke 'hop' voor het verder doorsturen van een bericht staat. Multi-hop-communicatie in een vehiculair netwerk wordt meestal gedaan met behulp van geo-routeren, een techniek waarbij berichten worden geaddresseerd aan een bepaalde locatie, en worden geleverd aan alle voertuigen die zich op die locatie bevinden. Deze techniek is mogelijk dankzij ruime beschikbaarheid van locatietechnologieën zoals GPS en wordt gebruikt om informatie te versturen die alleen relevant is op een bepaalde locatie.

Locatiegebaseerde berichtverzending brengt verschillende onderzoeksuitdagingen met zich mee; in dit proefschrift richten we ons op twee daarvan. De eerste betreft het geo-routeren van berichten. Hoewel het de huidige standaardmethode is om berichten meerdere hops te verzenden, komt de adresseringsmethode van geo-routeren de eisen van de bovenliggende applicatie soms slecht tegemoet. Berichten worden hierdoor inefficiënt gerouteerd, naar delen van het netwerk waar ze geen enkel nut hebben. Deze inefficiënte komt voort uit het feit dat met geo-routeren een node wordt onderscheiden op basis van zijn huidige positie, terwijl in een typisch ITS-scenario de toekomstige locatie veel bepalender is. In dit proefschrift stellen wij daarom constrained geocast voor, een nieuwe vorm van geo-routeren waarbij nodes worden geadresseerd op basis van hun verwachte toekomstige locatie. Met constrained geocast kunnen berichten op meer selectieve wijze dan voorheen worden gerouteerd, zodat een bericht alleen die delen van het netwerk bereikt waar het van belang is, dat wil zeggen waar zich nodes bevinden die zich in de toekomst op een bepaalde locatie zullen bevinden. We definiëren een set van algemene regels die bepalen hoe berichten moeten worden verzonden met constrained geocast, en tonen de effectiviteit van onze oplossing aan door het op kleine schaal te testen.

De tweede uitdaging betreft het analytisch modelleren van locatiegebaseerde multi-hop-communicatie in een vehiculair netwerk. Communicatie tussen nodes is erg onzeker in zo'n netwerk: nodes kunnen soms maar kort met elkaar communiceren en berichten kunnen

verloren gaan. Ondanks het feit dat verscheidene van dergelijke communicatieprotocollen al zijn gestandaardiseerd, ontbreekt vanwege deze onzekerheden nog steeds een volledig begrip van deze protocollen. Het is bijvoorbeeld nog altijd onduidelijk hoe de prestaties van deze protocollen worden beïnvloed door omgevings- en protocolparameters, zoals bijv. de verkeersdrukte op de weg of de frequentie waarmee berichten worden verstuurd. Dit soort verbanden worden meestal uitgedrukt met behulp van analytische modellen, die het gedrag van een protocol in formules proberen te vangen. Om multi-hop-communicatie in een vehiculair netwerk analytisch te modelleren is echter zeer complex, vanwege de grootte van een dergelijk netwerk, de onderlinge afhankelijkheden tussen opeenvolgende hops, en de genoemde onzekerheid van communicatie. Bestaande analytische modellen maken daarom veelal gebruik van vereenvoudigde aannames en bieden slechts in beperkte mate inzicht in de prestaties van een protocol. In dit proefschrift modelleren wij daarom op analytische wijze drie multi-hop-communicatieprotocollen, waarbij we gebruik maken van meer realistische aannames dan voorheen het geval was. We beschrijven het gedrag van de protocollen in een aantal formules die snel te evalueren zijn en een grote mate van detail geven. Onze modellen behandelen het scenario waarin een bericht van bron naar ontvanger wordt verstuurd over een rechte weg, en elk model geeft als uitkomst onder andere de volledige kansverdeling van (i) de lengte van elke hop, (ii) de wachttijd van elke hop, (iii) de kans van succes van elke hop, (iv) de positie van de opeenvolgende nodes die het bericht verder zenden, (v) het benodigd aantal hops om het bericht aan de ontvanger te leveren en (vi) de totale wachttijd om het bericht aan de ontvanger te leveren. Een uitgebreide evaluatie laat zien dat de resultaten van onze modellen zeer nauwkeurig zijn.

Onze modellen maken het mogelijk om de prestaties van een multi-hop-communicatieprotocol makkelijk en snel te evalueren, en maken de invloed van de verschillende omgevings- en protocolparameters zichtbaar. Bovendien kunnen onze modellen, vanwege hun snelheid vergeleken met bestaande simulatiemodellen, worden gebruikt om de simulatiemodellen van communicatieprotocollen te vervangen, om op die manier de effectiviteit van ITS-simulatie op applicatieniveau te vergroten.

De resultaten beschreven in dit proefschrift vebeteren de efficiëntie en het begrip van het locatiegebaseerd verzenden van berichten in vehiculaire netwerken. De inzichten die zij geven kunnen worden gebruikt om de effectiviteit van vehiculaire communicatieprotocollen te verhogen en op die manier ITS-applicaties in het algemeen naar een hoger plan te tillen.

Contents

Part I

Introduction

CHAPTER 1

Introduction

Intelligent transport systems (ITSs) are transport systems that use recent advances in the field of information and communication technologies to provide an increased level of traffic safety, traffic efficiency, and user comfort, and to reduce the environmental impact of traffic. One of the main strengths of ITS is that it allows for a stronger, automated level of cooperation between traffic participants using wireless communication. This form of wireless networking is referred to as vehicular networking and it can be considered to be the main enabler of ITS applications.

The main objective of vehicular networking is to disseminate traffic information. By its very nature traffic information is mostly only relevant to a specific geographical location, e.g., information regarding a traffic accident in the city of Enschede is relevant only to traffic participants in that general area. Traffic information is therefore typically routed using geographical routing, or georouting for short: a form of location-based forwarding with which information is addressed and disseminated to a specific geographical location.

The subject of this thesis is vehicular networking, in particular the multi-hop dissemination of messages using location-based forwarding techniques such as georouting. The goal of this first chapter is to introduce both the thesis itself and the subject of our research.

The outline of this chapter is as follows. In Section 1.1 a very brief introduction to ITS, vehicular networking, and georouting is given. We discuss the research challenges that are still left open in this field in Section 1.2, formulate our research questions in Section 1.3, and summarise our research contributions in Section 1.4. Finally, we outline the thesis in Section 1.5.

Image on previous page: a cul-de-sac in Enschede.

Figure 1.1: Test drive of an automated driving system. The vehicles have WiFi antennas and GPS receivers mounted on top. Picture by Bart Klaassen.

1.1 Intelligent transport systems and vehicular networking

ITSs utilise information and communication technologies to make transportation more automated, in this way levering the performance of these systems beyond the limitations of human traffic participants. An ITS has the possibility to increase traffic safety, traffic efficiency, driving comfort, and to reduce the environmental impact of traffic, among others. Because of its many advantages ITS development is currently actively being pushed and pursued by governments and organisations world wide. An example of an ITS application is automated platoon driving; Fig. 1.1 shows prototype testing of such a system during the Connect & Drive project [1]. Because of their superior reaction time compared to human drivers vehicles in such platoons can drive relatively close together, making more efficient use of the road, improving driver comfort, lessen traffic disturbances, and reducing fuel costs [2]. Other examples of applications are electronic tollbooths, traffic information systems, or traffic navigation systems. In all of these cases the most important enabling technology is wireless communication, allowing traffic participants to share information and cooperatively control their behaviour.

The field of wireless networking that enables these kind of applications is referred to as vehicular networking. A vehicular network is made up out of vehicles themselves and infrastructure nodes, and encompasses different types of communication techniques, both short range (up to a few hundred meters) and long range (several kilometres). In this thesis we focus on vehicular networking using short-range communication only. In such a network both vehicles and infrastructure nodes can communicate directly with other nodes that are

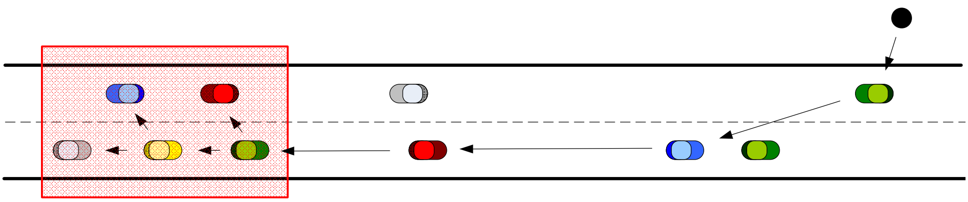

Figure 1.2: An example of georouting: an infrastructure node initiates a transmission. The message is routed to all nodes inside the destination area (in red).

within their communication range. To disseminate information beyond the communication range of a node multi-hop communication between nodes is used.

One of the main objectives of vehicular networking is to disseminate information regarding traffic events. Such traffic information is often only relevant to a specific geographical location: information regarding bad road conditions is for instance only interesting for vehicles that are driving on that particular road, and when a vehicle is about to crash then following vehicles should be warned, not vehicles driving well ahead of the crash. Georouting is therefore typically used to disseminate traffic information in vehicular networks: it is a form of location-based forwarding in which information (or data) is addressed to a specific geographical destination, such as a specific section of a road. The data is forwarded to the destination using some location-based forwarding protocol and delivered to all nodes located at the destination at the time the data reaches it, see Fig. 1.2. Location-based forwarding in general, and georouting in particular, is made possible by means of positioning techniques such as global positioning system (GPS). It is a type of routing that is strongly different from more traditional forms of routing in which information is targeted to specific nodes, regardless of the location of these nodes. With georouting however the source will often not even know which nodes receive the information.

1.2 Research challenges

Vehicular networking is a young field of research that still contains many relevant unsolved problems. In this section we discuss two specific challenges that are still left open. These two challenges will be the focal points of the rest of this thesis. For each challenge we motivate why the current state of research is not adequate and present how the work in this thesis aims to tackle this challenge. The first challenge relates to the inefficiency of georouting: due to the way in which information is addressed information is often routed to parts of the network where it is not needed, thus creating a considerable amount of network overhead. The second challenge relates to the limited understanding that still exists of multi-hop location-based message forwarding inside a vehicular network. Although plenty of work on the subject is available and some multi-hop forwarding protocols have already reached an advanced level of standardisation, there is still a considerable lack of understanding of the impact that network and protocol parameters have on the performance of such protocols.

Figure 1.3: A tightly interwoven city road network crossed by a highway (in blue). Taken from the Open Street Map project.

1.2.1 The inadequacies of spatial addressing

The *de facto* method of disseminating traffic information in a vehicular network is georouting. With georouting spatial constraints determine whether a node is a destination node and should receive the information or not. This method of addressing using spatial constraints is referred to as geocast. The goal of geocast is to route messages effectively (every destination node receives the information) and efficiently (only destination nodes receive the information). Below we show however that for a typical traffic application spatial constrains alone are not able to distinguish between nodes that should receive traffic information and nodes that should not receive traffic information, and that using geocast inherently means choosing between either efficiency or effectiveness. We then propose a different method of addressing traffic information in which information is routed based on spatiotemporal constraints. With this method a destination node is determined based on its expected location at a future time rather than its current location.

Typically, information about a traffic event is relevant only to those nodes that are currently at the location of the event or – if the event takes place for an extended time period, such as a traffic jam – that are expected to be at the location of the event in the near future. In the latter case nodes that are interested in information regarding the event can therefore be spread out over a large geographical area. Likewise, nodes that are relatively close to the location of an event may not be interested in the event at all, e.g., because they are driving on a road lane that is not affected by the event. Clearly in such a scenario spatial constraints alone – i.e., the current location of a node – are not enough to distinguish between nodes that are interested in the information and nodes that are not. With geocast information may thus be routed to parts of the network where it is not needed, creating inefficiency. Below we illustrate this by means of an example.

Consider a busy city road network crossed by a highway, as illustrated by Fig. 1.3. The city road network is a tightly interwoven mesh of streets with local-bound traffic, the speed of vehicles not exceeding 50 km/h. In contrast, the highway is a single road with few ramps, its traffic travelling at speeds of 120 km/h and higher to destinations typically tens or hundreds of kilometres away. Now consider that an accident has happened on the highway, causing one of its lanes to become blocked. To prevent mass queuing from occurring on the highway we wish to inform any drivers approaching the blockage of this fact while they are still able to choose an alternate route. However, because the wireless medium is a scarce resource, any communication solution should have as little impact on the network as possible and information about the blockage should therefore only be routed to parts of the road network where it is needed.

When using georouting to disseminate the information, how should it be addressed? A geocast destination area can have a circular, square, or ellipsoidal shape. How big should the area be when we want to inform vehicles of the highway blockage? To inform drivers on the highway in a timely manner information about the blockage should travel tens of kilometres upstream and the destination area should be set accordingly. As can be judged from the figure however, any such destination area inevitably encompasses large areas of the road network where traffic is local-bound and the information is largely irrelevant to drivers, making our solution inefficient. If we on the other hand avoid such waste by choosing a smaller destination area then highway drivers will not be warned in time of the blockage, making our solution ineffective.

The choice between efficiency and effectiveness illustrated in the example is inherent for geocast. In this thesis we therefore investigate a different approach. Consider a traffic event that takes place at a certain location for an extended period of time, similar to the example of the blocked road presented above. Instead of addressing information to all nodes that are within a certain distance of the event at the moment the information is disseminated, as is done with geocast, with our approach information is addressed to all nodes that are expected to be at the location of the event itself, during the period of time that the event takes place, and information is delivered before the nodes reaches the event location. This is achieved by keeping the information alive inside the network for the duration of the event, but only in those parts of the network where there are nodes headed for the event area. Information is thus not forwarded to parts of the network where it is not needed, improving the efficiency and overall scalability of the network.

1.2.2 A lack of understanding of multi-hop forwarding

To properly design vehicular applications the performance of the underlying communication system must be well-understood, and its performance should preferably be expressed in a quantitative manner. Although considerable advances have been made in this field for the single-hop dissemination of messages, regarding multi-hop location-based forwarding of messages such a level of understanding is still lacking, even though an increasing number of such protocols are being standardised [3]. This thesis addresses this shortcoming by presenting a number of analytical models that are able to express the behaviour of a multi-hop location-based forwarding protocol, giving full distributions of relevant performance metrics. Below we briefly discuss the current state of performance modelling of such multi-hop forwarding protocols, its limitations, and how we aim to enhance it.

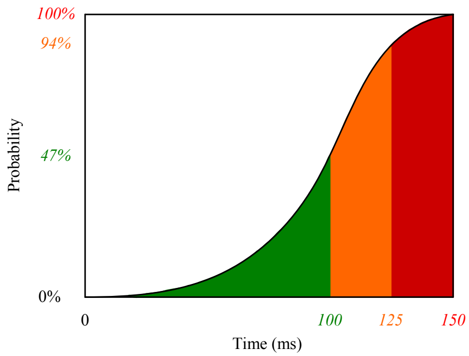

Figure 1.4: An example end-to-end delay distribution of a safety message application, divided into time intervals.

Existing research on multi-hop location-based forwarding protocols in vehicular networks is mainly based on simulation. Simulation is a powerful tool with which with relative ease networking protocols can be evaluated in great detail. Because of this level of detail of the simulation models however, interpreting the results of such a study can be quite difficult. The insights such studies provide can therefore be limited and any obtained results may only be valid for the specific set of parameters that was simulated. Additionally, in order to gain reliable results extremely long simulation runs are necessary; depending on the scenario this may take hours, days, or even weeks.

Analytical models have in many cases strong advantages over simulation models, in particular regarding the insight they provide and their relative speed compared to simulation: analytical models will typically provide results within seconds to minutes. Analytical models may also allow for speedier simulation of ITS applications, e.g., by replacing the (computationally highly demanding) communication parts of the simulation model by analytical models. The number of existing analytical models is limited however and as of yet do not give a satisfactory level of understanding of the protocols they model. Model assumptions are often overly simplistic and results often focus on specific performance metrics such as network connectivity, rather than on the behaviour of the protocol as a whole. Moreover, instead of expressing full performance distributions these models tend to give average values or upper/lower bounds.

In order to better understand the performance of multi-hop forwarding inside a vehicular network, it is important that we can analytically model the behaviour of such protocols in a manner that is more realistic and gives more complete insights on their performance than is currently the case. We attempt to answer this need in this thesis by presenting a new modelling approach which we apply to a number of multi-hop location-based forwarding protocols. Our approach uses very realistic assumptions and expresses the performance of the protocols in a high level of detail, often including full distributions of relevant performance metrics such as the end-to-end delay. Such a level of detail is important to evaluate the performance of higher-level performance applications, as messages are often required to be delivered within a certain delay margin in order to be relevant, see Fig. 1.4.

1.3 Research questions

In the previous section we addressed a number of open research challenges in the field of vehicular networking that we focus on in this thesis. In this section we formulate a number of specific research questions regarding these challenges. The rest of our thesis will focus on answering these research questions. We have separated our questions for the two topics that we address, routing with spatiotemporal constraints and analytically modelling multi-hop location-based forwarding.

1.3.1 Routing with spatiotemporal constraints

It was shown in the previous section that to effectively disseminate ITS application data using georouting a high level of inefficiency is often inevitable, i.e., to ensure that the data reaches all parts of the network where it is relevant, it is also spread to parts of the network where it is irrelevant. It is our goal to disseminate data in a more selective manner. To achieve this we first need to determine which nodes require the data. Typically ITS data regarding some traffic event is only relevant to those nodes that will be at the location of the event during the event's lifetime. Data should therefore be disseminated to nodes that will be at the event location, now or in some future time during the event's lifetime. In a vehicular network the only information that can be assumed available however is a node's current location, heading, speed, acceleration, etc., but with limited information regarding its future route. This leads us to the following research questions.

Research question 1. How can we distinguish destination nodes that require certain ITS application data from other nodes?

Research question 2. How can we route the ITS application data both effectively (to as many destination nodes as possible) and efficiently (to as few non-destination nodes as possible)?

1.3.2 Analytically modelling multi-hop forwarding protocols

It was shown in the previous section that the current state of performance modelling is not able to give a full understanding of the behaviour of multi-hop location-based forwarding protocols in a vehicular network.

Research question 3. How can we express the behaviour of a multi-hop location-based forwarding protocol in a vehicular network in an analytical manner, using realistic assumptions that fully capture the behaviour of the protocol and the network?

Existing studies on multi-hop forwarding protocols typically do not define the behaviour of a multi-hop forwarding protocol in detail but give average values or upper/lower bounds of performance metrics.

Research question 4. How can we express performance of a multi-hop location-based forwarding protocol in more detail?

1.4 Contribution

The contribution of this thesis is split into two parts: Part II and Part III.

The main contribution of the second part is the introduction, implementation, and evaluation of *routing with spatiotemporal constraints*, or *constrained geocast* for short: a novel method of georouting that aims to disseminate traffic event information only to nodes that require the information because they are expected to reach the location of the traffic event at some specific (future) time during the event's lifetime. In particular we specify the destination set based on the spatiotemporal constraints of nodes and specify how to route information only to those parts of the network where there are interested nodes. Our approach is based on the idea that only nodes that are part of a traffic flow leading to the event area are interested in the traffic event information; information is therefore always routed against the flow of traffic (i.e., upstream) from the event area outward. We formulate a number of generic rules to implement constrained geocast and give a full implementation and evaluation of constrained geocast in the context of automated merging application.

The main contribution of the third part is the analytical modelling of a number of multi-hop location-based forwarding protocols. For a given network density, single-hop transmission model, and set of forwarding rules we explicitly calculate the behaviour of each forwarding hop, taking into account all relevant dependencies between hops. By expressing protocol behaviour in terms of protocol and network parameters we fully quantify the impact of these parameters on protocol performance. We consider the source-to-sink forwarding of separate messages and give the full distribution of a number of performance metrics, including *(i)* the end-to-end delay, *(ii)* the required number of hops, *(iii)* the position of intermediate forwarders, *(iv)* the length of each hop, *(v)* the delay of each hop, and *(vi)* the end-to-end reception probability. We can thus for instance express the probability that a sink receives a message within a certain interval of time, a relevant performance metric for vehicular safety applications.

1.5 Outline

This thesis spans nine chapters that are divided over four parts. The first part gives an introduction to the thesis itself as well as to the subject of the thesis, the second part focuses on routing with spatiotemporal constraints, the third part focuses on analytically modelling multi-hop location-based forwarding in vehicular networks, and the fourth part concludes the thesis. Although the two parts with the main contributions of this thesis, i.e., Part II and Part III, are clearly related they can be read independently of each other. Below we give a brief per-chapter overview of the contents of this thesis.

This chapter, Chapter 1, is the first chapter of Part I. It has given a very brief introduction to the research areas of ITS and vehicular networking, explained our motivation, formulated the research questions this thesis addresses, and summarized our contributions. In Chapter 2 a more elaborate background is given on the subject of ITS, further establishing the context of our research. Specifically we describe in detail an example ITS application that has served as motivation for part of our work. Finally, Chapter 3 serves to give both background on vehicular networking and to give the state of the art of the research in this field.

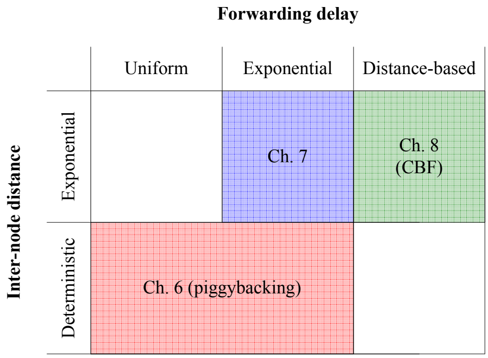

Figure 1.5: The model assumptions employed in each chapter in Part III.

In Part II first we introduce the concept of constrained geocast in Chapter 4. We have implemented the concept of constrained geocast on a small scale for an automated highway merging application in Chapter 5. We first present the automated highway merging application, then show how to implement constrained geocast, and finally evaluate how well the protocol performs.

In Part III we model three multi-hop location-based forwarding protocols in different scenarios. The protocols themselves differ in how forwarding delays are determined and the scenarios differ in how the nodes are distributed on the road. In the scenario in Chapter 6 nodes (vehicles) are equidistantly distributed over the road and the forwarding delays are either uniformly or exponentially distributed. When forwarding delays are uniformly distributed the protocol is functionally equivalent to a so-called piggybacking protocol, the forwarding protocol used in Chapter 5. In the scenarios in Chapter 7 and Chapter 8 inter-node distances are exponentially distributed. In Chapter 7 forwarding delays are exponentially distributed, while in Chapter 8 forwarding delays are distance-based, i.e., nodes that lie further in the direction of the destination have shorter forwarding delays. The latter model can be applied to model the performance of the recently standardised contention-based forwarding (CBF) protocol [3]. Fig. 1.5 shows the main characteristics regarding forwarding delay and inter-node distances of the systems investigated in Chapters 6, 7, and 8.

Part IV consists solely of Chapter 9 and concludes the thesis. We summarise our contributions, answer the research questions, give conclusions on the work presented and sketch directions for future work.

The work presented in Chapters 4 and 5 was published, in increasing levels of maturity, at the ERCIM Workshop on eMobility (ERCIM) 2010 [4], the IEEE Vehicular Networking Conference (VNC) 2010 [5], ERCIM 2011 [6], and the International Conference on ITS Telecommunications (ITST) 2011 [7]. The work in [8] served as a basis for all of the modelling work presented in Part III of the thesis and has been published in the proceedings of VNC 2011. The work presented in Chapter 6 was first published at the ACM International Workshop on VehiculAr Inter-NETworking, Systems, and Applications (VANET) 2012 [9], while the work presented in Chapter 7 was first published at VNC 2012 [10]. The work presented in Chapter 8 is currently being prepared for publication.

While writing we have tried to structure the thesis in such a way that chapters can be read on their own, without relying too much on other chapters. There is therefore some overlap among the chapters.


3A-0481

CHAPTER 2

Intelligent transport systems

ITSs are systems that employ information and communication technologies to provide an increased level of traffic safety, traffic efficiency, and user comfort, and to reduce the environmental impact of traffic. All of the research presented in this thesis has been performed in the context of ITS; the main goal of the present chapter is to provide the necessary background on this topic.

The outline of this chapter is as follows. In Section 2.1 we explain the concept of ITS, give some background on its potential benefits to increase the safety and efficiency of road traffic, and discuss the political drive that lies behind the ongoing development of ITS applications. In Section 2.2 cooperative adaptive cruise control (CACC) is discussed; it is a type of cruise control in which vehicles cooperatively control their speed using wireless communication, allowing for automatic driving. The work presented in Part II has been based on this CACC use case. CACC is also a good example of the (technological) challenges that ITS applications have to deal with, as it applies control engineering, telecommunication, traffic engineering, and human-machine interfacing.

Image on previous page: a bus stop near Siem Reap, Cambodia.

Figure 2.1: Car accident in Tokyo [11].

2.1 Driven by need

The term ITS is used to imply any type of transport system in which information and communication technology has been used to improve the system's performance. Examples of ITS applications are electronic toll booths, advanced types of cruise control, and in-car navigation systems. Improvements may include increases in safety, security, reliability, efficiency, and flexibility, and a decrease in environmental pollution. Technologies that can be applied are diverse – they can range from wireless communication systems to support electronic toll booths or in-car traffic navigation systems, to automatic number plate recognition using video cameras.

Interest in ITS is driven both by need and by opportunity. Due to the cascading effects of an expanding world population, an increasing urbanisation, and a growing motorisation, transportation infrastructures are being put under more and more pressure. Direct results of this are an increase in traffic congestion, road accidents, and environmental pollution. In 2006 the European Commission published a report [12] in which the total number of traffic accidents in Europe was estimated at a total of 1.4 million, with 40.000 fatalities. On a daily basis 10% of the European road network suffered from congestion and 25% of the total EU energy consumption came from road transport, leading to an annual CO_2 emission of 835 million tonnes. The combined economic cost of traffic congestion and traffic accidents was estimated at a yearly amount of 250 billion Euro.

As the report was aimed at raising awareness of the potential benefits of ITS, it also gave specific examples of where these benefits could be gained. Up to 50% of fuel consumption is caused by congested traffic situations and non optimal driving behaviour. The latter is caused by the inability of drivers to correctly anticipate the behaviour of preceding vehicles,

Figure 2.2: Prototype testing of a CACC system during the Connect & Drive project. Picture taken by Bart Klaassen.

causing both unnecessary braking and accelerating. Another quoted study shows that in case of an accident human error was involved in 93% of the cases, and in almost 75% of the cases it was the sole cause. And while it has been shown that at a driving speed of 50 km/h the energy of a crash can be halved when drivers would brake half a second earlier, an analysis of German accidents showed that 39% of passenger vehicles and 26% of trucks that were involved in a collision did not brake at all, and some 40% did not brake effectively. The main goals of ITS applications are therefore to improve road safety and road efficiency by improving driver reaction time and anticipatory capabilities. In the next section we highlight such an application that has served as a context for our work.

2.2 Cooperative adaptive cruise control

CACC is a form of cruise control in which the longitudinal velocity of a vehicle is automatically controlled based on the behaviour of its preceding vehicles [1]. Information about the behaviour of the preceding vehicles is obtained by means of a front-end radar and wireless communication between the vehicles. Because of the superior reaction time of a CACC-operated vehicle compared to a human driver, CACC vehicles can drive relatively close together (at less than 0.5s time headway). Such strings of vehicles are called *vehicle platoons*. By keeping the distances between vehicles constant and relatively small, a flow of traffic is created that is both stable and compact. Such a flow of traffic increases traffic throughput – thus reducing congestion – and requires less fuel consumption [2].

CACC evolved from adaptive cruise control (ACC), which in turn evolved from the

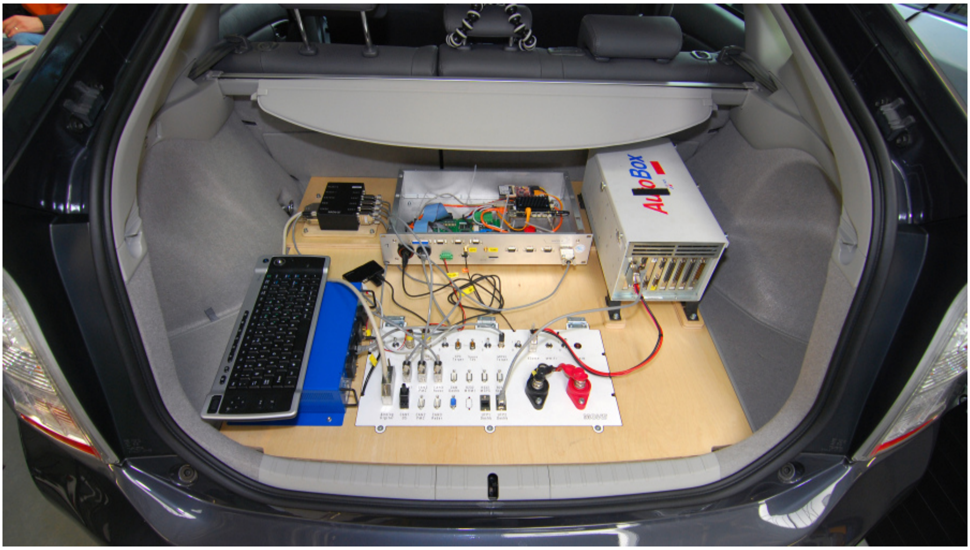

Figure 2.3: Interior of a CACC-equipped vehicle during prototype testing of the Connect & Drive project. Picture taken by Bart Klaassen.

'standard' form of cruise control (CC). With CC the driver can select a cruise speed, and the CC system will control the throttle of the car to maintain this speed. With ACC the vehicle also has a front-end radar that is able to measure the (time) headway to a preceding vehicle. Drivers can select a preferred cruise speed and following distance (in seconds). If there is no preceding vehicle within range of the radar the ACC system will maintain the cruise speed in the same way as the CC system. If there is a preceding vehicle, and it drives slower than the preferred cruise speed, then the ACC system will aim to maintain the preferred following distance by controlling the throttle of the car based on the measured time headway.

From a user's perspective CACC operates in the same way as ACC: again a preferred cruise speed and following distance can be selected, and the CACC system will either try to maintain the preferred cruise speed or following distance. The difference with the ACC system lies in the fact that the CACC system also uses the acceleration values of the preceding vehicle(s) as input to maintain the preferred following distance. It is therefore better able to anticipate to speed disturbances of these vehicles. It acquires the acceleration values by means of wireless communication; the specific technique used may differ per implementation. As an example, in the Connect & Drive project [1] (see Fig. 2.2 and Fig. 2.3) a CACC prototype application was developed using commercial off-the-shelf WiFi-equipment.

The main goal of CACC is to achieve string stability. A platoon of vehicles is said to be string stable if any traffic disturbances – such as braking – are not amplified in the upstream direction, e.g., if a vehicle brakes, following vehicles should not brake harder than the reference vehicle. When traffic is string unstable any traffic disturbances are amplified in the upstream direction, which may lead to unsafe traffic situations and phantom traffic

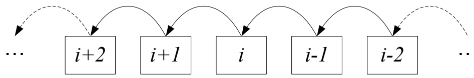

(a) Preceding vehicle only.

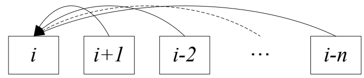

(b) With n preceding vehicles.

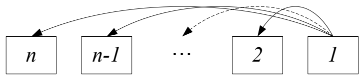

(c) With a leader vehicle.

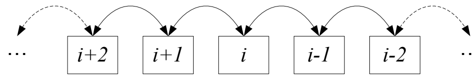

(d) Preceding and following vehicle.

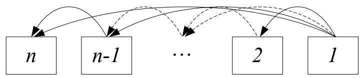

(e) Preceding and leading vehicle.

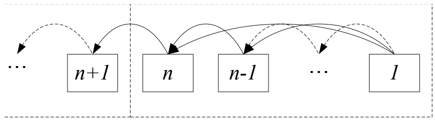

(f) Mini platoons.

Figure 2.4: CACC control modes.

jams. The latter has been effectively visualized in a well-known Japanese experiment, see [13] [14].

CACC takes the acceleration of preceding vehicles into account. Which vehicles are taken into account differs per design and is an important design choice. A number of possibilities exist, as can be seen in Fig. 2.4. The designs mainly differ in whether or not there is a platoon leader, and the number of vehicles that are taken into account. A vehicle that acts as platoon leader controls the manoeuvres taken by the platoon, such as creation, joining, merging, etc. When there is no platoon leader the platooning is said to be ad-hoc, i.e., vehicles decide each action on their own. As the acceleration of more preceding vehicles are taken into account the string stability of the platoon increases; this also makes the communication requirements more demanding however.

Platoon manoeuvres include joining and merging inside a platoon. In case of ad-hoc platooning a vehicle (or a platoon of vehicles) joins a platoon simply by driving either directly in front or behind the platoon. The vehicle will then automatically adapt its speed to that of the platoon's. If there is a platoon leader the joining vehicle must also explicitly request to join the platoon. When a vehicle joins a platoon somewhere in the middle it is referred to as merging. When platoon vehicles drive close together a merging vehicle must always explicitly request the platoon to make room inside the platoon before it can merge. In Chapter 5 we focus on a single vehicle merging inside an ad-hoc controlled platoon at a highway on-ramp.

Although prototypes have proven that string stable platoons of vehicles can be created using CACC [1], there is still a long way to go before CACC can be used in everyday traffic. On a technological level the main problem is that wireless communication becomes a bottleneck as the system scales up. With current communication techniques the reliability decreases as the number of vehicles increases, causing CACC to become less string stable [15] [16]. Research is also still ongoing on how drivers are influenced by CACC since it is still required that they remain alert, even though they no longer actively control the speed of the car. When applied on a large scale however research suggests that CACC can significantly improve traffic throughput, even for low penetration rates [2].


MADAME
TUSSAUDS
REGA
MODELL'S
EMPIRE
amc THEATRES
villa
BUS

CHAPTER 3

Vehicular networking

Vehicular networks are wireless networks in which the main nodes are vehicles, supported by infrastructure nodes. Vehicular networking is a relatively new field and has its own challenges. In this chapter we give the background on vehicular networking that is necessary for the rest of the thesis, present the current state of vehicular networking, and discuss its challenges.

The outline of this chapter is as follows. We first discuss the general properties of a vehicular network in Section 3.1. We then discuss the first three layers of the networking stack in a bottom-up fashion: Section 3.2 discusses at the physical layer those radio wave propagation effects that are most relevant for higher layers, Section 3.3 discusses IEEE 802.11p, the link layer technology that is used in this thesis, and at the network level we first focus on geocast in Section 3.4 and on georouting techniques in Section 3.5. A number of relevant aspects related to vehicular networking are discussed in Section 3.6. Finally, Section 3.7 gives an overview of standardisation efforts that have been made regarding vehicular networking technologies, while Section 3.8 goes into simulation of vehicular networks.

Image on previous page: the corner of 7th Avenue and 42nd Street in Manhattan, New York.

3.1 Properties of a vehicular network

A vehicular network is a wireless network in which the principal nodes are vehicles, supported by a host of infrastructure entities. Supported communication interfaces include, but are not limited to, IEEE 802.11p, WiFi, UMTS, LTE, WiMAX, and satellite communication. Examples of infrastructure nodes include road-side units (RSUs), cellular base stations, and satellites. RSUs are entities that are placed at the side of a road (hence the name) and employ short-range communication techniques such as IEEE 802.11p and WiFi. Both vehicles and RSUs can communicate directly to back office applications using cellular techniques such as UMTS, LTE, or WiMAX. Satellites are mainly used for positioning (GPS [17], GALILEO [18]), but may also be used for broadcast communication.

In this thesis we focus on vehicle-to-vehicle (V2V) and vehicle-to-infrastructure (V2I) communication using IEEE 802.11p; the only network nodes that are considered are vehicles and RSUs. A vehicular network that only includes vehicles and RSUs and only considers short-range, ad-hoc communication is also referred to as a vehicular ad-hoc network (VANET).

Nodes can communicate directly with any other node that falls within their transmission range without having to perform any initialisation (authentication, association, etc.) – hence the name vehicular *ad-hoc* network. Due to the limited (up to 1km) communication range of IEEE 802.11p and the high speed with which vehicles move, communication between nodes is best effort and of an erratic nature. Transmission channel properties change continuously due to movement of the nodes themselves and their surroundings, and environmental conditions such as high-rise buildings may have a decremental effect on the channel's quality. Vehicles driving in opposite directions on a highway may have connection times that last less than 10s. The set of nodes with which a node can directly communicate is therefore very dynamic, making multi-hop routing a challenge.

The topology of the network is constrained by the road topology. RSUs are statically placed next to roads, while vehicles move along the road according to the rules of traffic. Two distinct environments are usually considered: urban and highway. In an urban environment the road network is dense, vehicle speeds are low, and the space between roads is filled up with buildings, trees, road signs, and similar obstacles. Due to these obstacles communication is often constrained to the road network, since wireless signals have trouble reaching 'around the corner'. In a highway environment often only a single (straight) road is considered, sometimes combined with a ramp. Speed limits are high and there are little to no urban obstacles besides the road. A distinction is sometimes made between forest regions and regions with sparse vegetation as this effects the transmission channel.

All nodes in a VANET are assumed to know their own position with sub-meter accuracy, making it possible for vehicles to pinpoint their position up to the lane in which they are travelling [19]. Positioning is performed using a global navigation satellite system (GNSS), such as GPS or GALILEO, in combination with other positioning technologies, e.g., an in-vehicle gyroscope. Being stationary, RSUs will often have more exact knowledge about their position and may aid vehicles in their positioning. Moreover, all nodes may have the availability of road topology data. Time synchronisation is also based on a GNSS and has an accuracy of 10-15ns [20]. Using on-board sensors vehicles also know their own speed, acceleration, heading, and similar mobility-related properties.

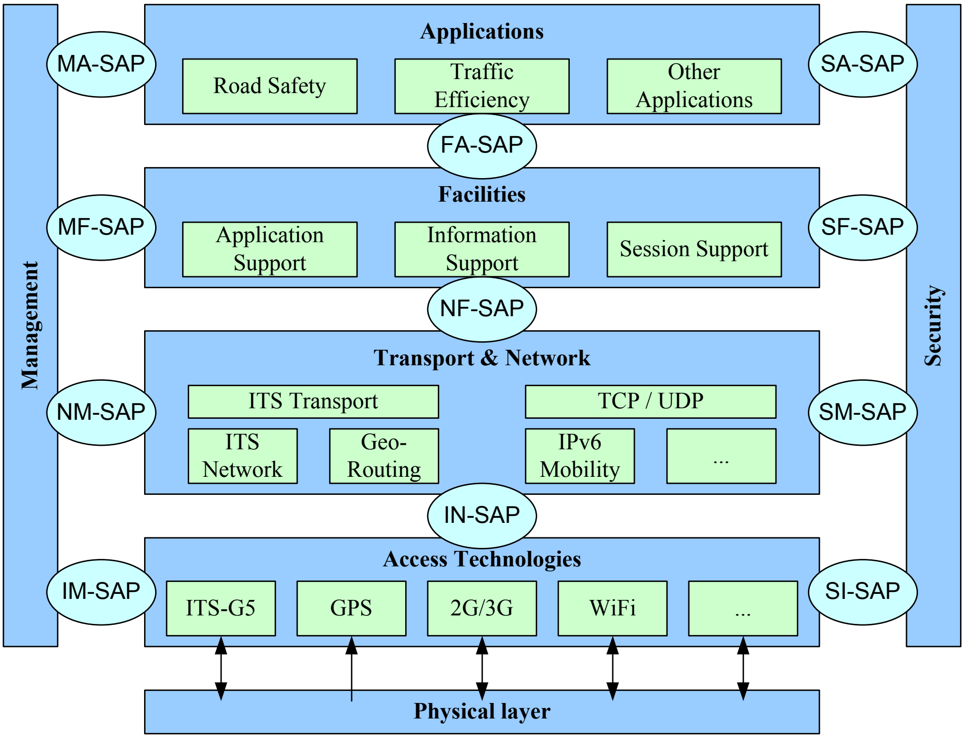

Figure 3.1: The ISO CALM architecture [21].

Vehicular networking encompasses a wide variety of concerns at different levels of the open systems interconnection (OSI) model. Although standardisation of lower-layer technologies has been finalised, this is still ongoing for higher layers. Three standardisation tracks currently exist and are being actively being pushed in different parts of the world. This thesis follows the standardisation track pursued in Europe, which has adopted the international organisation for standardisation's (ISO) CALM [21] architecture (which stand for communications access for land mobiles), see Fig. 3.1. As can be seen in the figure, functionality has been split between different layers, in a manner strongly resembling the OSI model. In this thesis we focus on georouting using IEEE 802.11p as the link layer technology, which in Fig. 3.1 has been included as ITS-G5.

3.2 Radio wave propagation

At the physical layer radio wave propagation is the behaviour of a signal once it has been transmitted by a node. It is a key factor in the performance of wireless communication systems. IEEE 802.11p transmits in the 5.9 GHz frequency band with wavelengths of roughly 5 cm in length. The propagation of these radio waves is influenced by many environmental

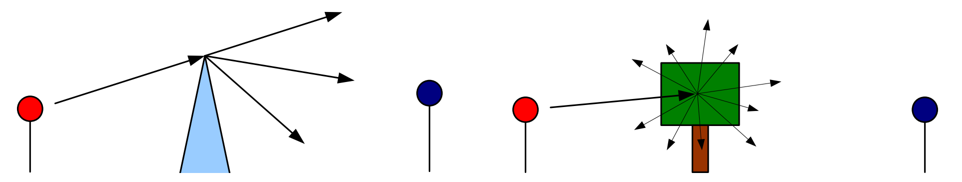

(a) Line of sight.

(b) Reflection.

(c) Diffraction.

(d) Scattering.

Figure 3.2: Propagation effects.

factors such as the (non-)existence of a line-of-sight, obstructions by buildings, foliage, or vehicles, and the speed of the respective nodes. In this section we discuss those propagation effects that have the largest impact on the propagation behaviour in a vehicular network. Our discussion is based mainly on [22].

Propagation effects are usually divided into two categories: large-scale effects and small-scale effects. The large-scale effects include reflection, diffraction, and scattering; they can be seen in Fig. 3.2. They all relate to the different paths a signal may take as it travels from transmitter to receiver. Due to these effects a receiver may receive multiple versions of the same signal, all with differing amplitudes, frequency phases, and time delays. Combined, these multipath waves may fluctuate rapidly over short periods of time and space. These small-scale effects are referred to as (multipath) fading. Another small-scale effect is Doppler shifting. Below we briefly describe the mentioned propagation effects.

Reflection occurs when a radio wave encounters a smooth surface much larger than its wavelength, such as the ground, buildings, or other vehicles. How much energy the reflected wave contains depends on the permittivity and the conductivity of the materials involved, the wave's angle of incidence, and the transmitting frequency.

When the path of a wave is obstructed by a sharp edge, a secondary front of waves will be generated at this point, called diffraction. This secondary front will propagate through space in the original direction, but will also reach behind the obstacle. Signals can thus bend around obstacles, and reach receivers that would otherwise be obstructed.

Scattering occurs when a radio wave encounters an object that is small compared to its wavelength, or has a rough surface. When this happens, the waves of a signal are reflected in random directions. Sources of scattering may be foliage, street signs, and lamp posts.

Doppler shift is the shifting of a signal's frequency due to movement of either the transmitter, the receiver, or one of the objects in the signal's path. In case of multipath, different versions of the same signal may have different Doppler shifts, causing the signal bandwidth

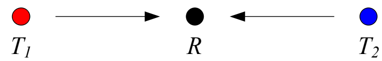

Figure 3.3: The hidden node problem. Two transmitters that are outside each other's transmission range simultaneously transmit a message to an in-between receiver, causing a link layer collision.

to increase. This is called Doppler spread.

Due to the effects described above a receiver will often receive multiple versions of the same signal, each with differing amplitudes, frequency shifts, phase shifts, and time delays. These different versions are combined at the receiver, and can cause the resulting signal to distort or fade. This is referred to as multipath fading. Multipath fading can cause rapid fluctuations as nodes move only a short distance. Even if the transmitter-receiver pair is static, movement of objects in the signal path can cause fading.

3.3 IEEE 802.11p / ITS-G5 link layer technology

IEEE 802.11p is an amendment to the IEEE 802.11 standard – also known as WiFi – specifically designed to be used in a vehicular environment. Both the standard and all of its amendments are specified in [23]. The ITS-G5 standard [24] has been based on IEEE 802.11p and mainly gives details on how to operate IEEE 802.11p in a vehicular network, such as which channels to use. In the remainder of this thesis we will refer to IEEE 802.11p only, but also give details on relevant specifics regarding ITS-G5.

The IEEE 802.11p amendment mainly focuses on being able to cope with the high speed of nodes. The physical layer has for instance been made more robust to be able to cope with the increased Doppler shift and Doppler spread that are a result of node movement. Furthermore, only ad-hoc mode is supported, i.e., nodes communicate directly with each other without use of an intermediate access point (AP). Because connection times between nodes are typically very short no authentication or association is needed, as this would take too much time. Nodes can therefore exchange messages directly with any node within transmission range.

Nodes access the wireless medium using the enhanced distributed channel access (EDCA) mechanism[1]. The request-to-send/clear-to-send (RTS/CTS) mechanism has been dropped since its effectiveness is limited when node movement is high. IEEE 802.11p is therefore vulnerable to hidden nodes, i.e., a node receiving a transmission from a sender may be hindered by a transmission from a second sender that is outside the range of the first sender. Because the two senders are outside each other's range they are unaware of the problem, but the resulting collision of both transmissions may prevent the receiver from receiving any data. The hidden node problem is illustrated in Fig 3.3. It is a major source of performance degradation in VANETs [25].

[1] In 'standard' IEEE 802.11 there exist also the distributed coordination function (DCF) and the point coordination function (PCF), but these are not used in IEEE 802.11p.

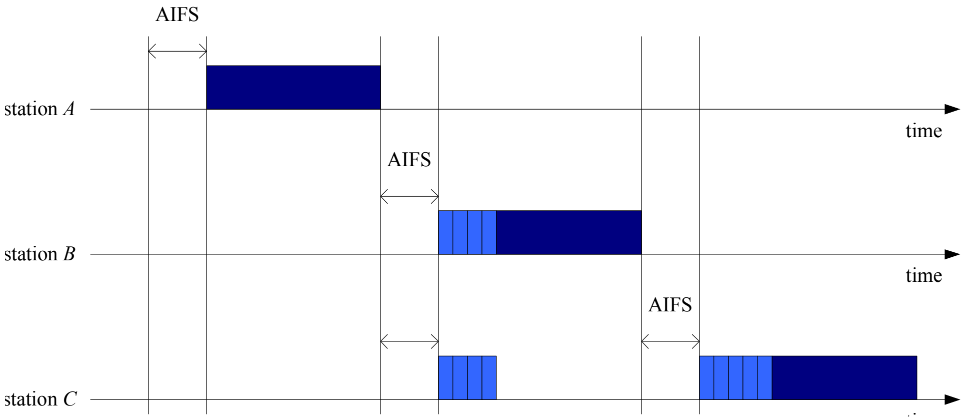

Figure 3.4: The EDCA access mechanism for three broadcast transmissions.

The EDCA medium access control (MAC) mechanism works as follows. Time is divided into slots of $13\mu s$. Time slots are unsynchronised although nodes tend to mutually synchronise their timeslots as a result of link-level traffic [26]. When a node has a message to send it will first sense the medium whether it is busy (i.e., a signal is detected meaning that another node is already transmitting) or free. If the medium is free and has been free for a specified amount of time – called the arbitrary inter-frame space (AIFS) – it will immediately start transmitting. If the medium is busy then the node will go into contention by choosing a contention number randomly from a specified range of numbers, and decrementing this number at the start of each time slot after the medium has been free for at least AIFS seconds. If the number is decremented to zero then the node starts its transmission at the start of the next time slot. If the transmission was a broadcast transmission then the node is finished. If the transmission was a unicast transmission then the node will wait for a specified time interval in which it should receive an acknowledgement (ACK). If it does not receive this acknowledgement it will go through the same process of contention, but with a higher range of numbers from which the contention number is chosen. Fig. 3.4 illustrates the EDCA MAC for both unicast and broadcast transmissions. Station A finds the medium free for AIFS seconds and immediately starts transmitting. Station B and C first query the medium during A's transmission; finding it busy they randomly draw a contention number and start decrementing it once the medium has been free for AIFS seconds. Station B has the shortest contention number and will therefore transmit before node C, who will pause decrementing its contention number until the medium has again been free for AIFS seconds.

EDCA supports prioritisation of messages in four different access categories (ACs). Each higher-priority AC has a shorter AIFS and a lower range of numbers from which the contention number is chosen. High-priority messages thus have a higher probability of winning the contention for the medium. EDCA furthermore defines a transmission opportunity (TXOP): a bounded time interval in which a station has exclusive access to the medium and can potentially send multiple packets.

Different channels have been allocated for use of IEEE 802.11p in Europe and the USA.

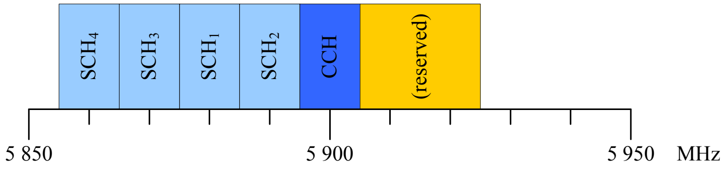

(a) The European ITS frequency allocation, based on [24].

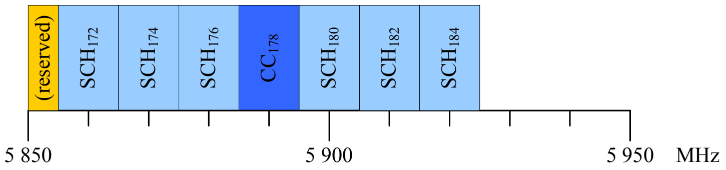

(b) The US ITS frequency allocation, based on [28].

Figure 3.5: Frequency band allocation for use of IEEE 802.11p for ITS applications in Europe and the USA.

Fig. 3.5 shows the frequency band allocation for both regions. In both cases a single control channel and multiple service channels have been defined. The control channel is used for high-priority traffic such as safety messages and must be regularly listened to by a node [27]. The service channels serve less demanding traffic and may be used by efficiency applications. Current standards assume the use of a single radio transceiver and therefore require a node to switch between the control channel and service channels. Work is ongoing however on designs that support multiple transceivers; in that case one transceiver is dedicated to the control channel and the other switches between service channels.

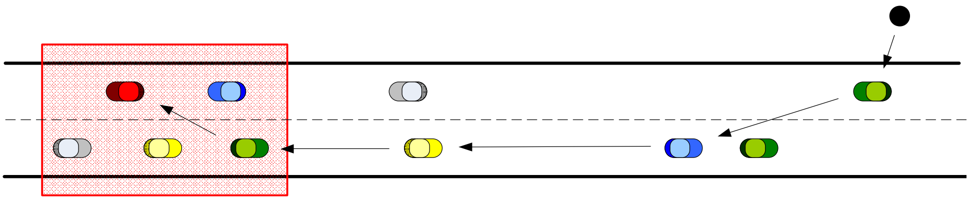

(a) Geo-unicast with a square destination area.

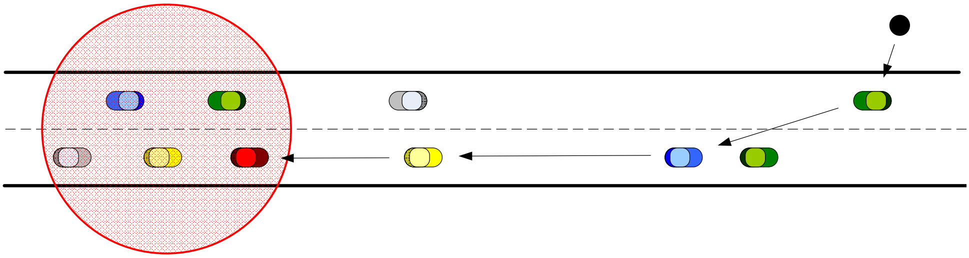

(b) Geo-anycast with a circular destination area. Note that the choice of destination vehicle is arbitrary, as long as it is inside the destination area.

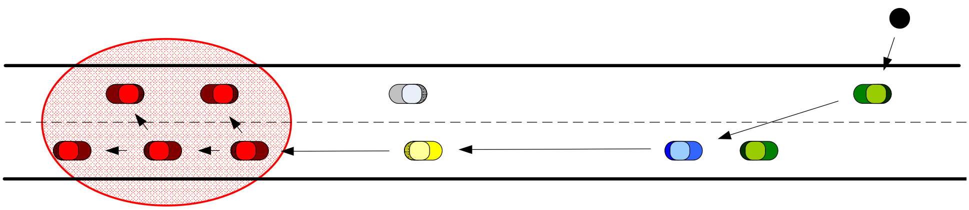

(c) Geo-broadcast with an ellipsoidal destination area.

Figure 3.6: Three forms of geocast, each with a differently shaped geographical destination area. The red vehicles are destination vehicles.

3.4 Geocast

The addressing of data to a geographical destination area is referred to as geocasting, analogue to broadcasting. It is part of the network layer. It is in strong contrast to more traditional forms of routing in which data is routed to a specific node. Geocast is a form of addressing well suited to vehicular networks because data (such as traffic information) is often targeted at a specific region instead of at specific users. The shape of the destination area can be a circle, an ellipsoid, or a square [29].

Within the context of vehicular networking four types of geocast are distinguished: geo-unicast, geo-anycast, geo-broadcast, and abiding geo-broadcast [30]. The first three types of geocast have been standardised by the European Telecommunications Standards Institute (ETSI) [3]. The latter type is also referred to as information hovering [31] in literature. For the first three types the address is defined as a combination of a geographic destination area and a node identifier; for abiding geo-broadcast time information is also used. With geo-unicast information is addressed to a *specific* node that is inside the destination area the moment the information arrives at the area. With geo-anycast information is addressed to *any* node, regardless which, that is inside the destination area the moment the information arrives at the area. With geo-broadcast information is addressed to *all* nodes that are inside the destination area the moment the information arrives at the area. With abiding geo-broadcast information is addressed to *all* nodes that are inside the destination area *during a certain time period*. Fig. 3.6 illustrates these different types of geocast and the three possible destination area shapes.

The source node may or may not be inside the destination area. If not, then the information must first be routed towards the destination area using some kind of multi-hop georouting technique. These are discussed in the next section.

3.5 Georouting

At the network layer geocast data is routed through the network based on geographic position information. Nodes base their forwarding decisions on their own position, the positions of their neighbours, and the geocast destination address. This is referred to as geographic routing, or georouting for short. In this section we discuss a number of georouting techniques, both single-hop and multi-hop, using IEEE 802.11p as the link layer technology. Single hops are made using either unicast or broadcast, as was described in Section 3.3, and multi-hop addressing is done using geocast, as was discussed in the previous section. The only network nodes that are considered are vehicles and RSUs.

With unicast georouting information is routed from the source to a single destination node via a number of intermediate forwarders; intermediate forwarding is done using unicast. With broadcast georouting information is routed to all nodes within the destination area and intermediate forwarding is done using broadcast – this is also referred to as flooding.

Beaconing refers to the periodical single-hop broadcasting of network-level status messages, also called beacons. The status messages contain information such as the location of a vehicle, its speed, its acceleration, its direction of travel, but also information such as whether a vehicle has its lights on. The main function of these messages is to provide a level of awareness both at the network level and at the application level. At the application level almost all co-operative road safety applications defined by ETSI are based on beaconing, and the same holds for the CACC application described in Section 2.2. At the network level received beacons are used to create location tables that are then used by georouting protocols [3]. Creating a scalable beaconing algorithm that can be used for cooperative awareness applications is far from trivial and is receiving an extensive amount of attention [15] [32] [33] [34] [35] [36] [37]. Approaches mainly focus on varying the frequency and the power with which messages are transmitted, while keeping the size of a message as small as possible. Because of their function, beacons have been defined by ETSI in [38] as cooperative awareness messages (CAMs).

All VANET unicast routing protocols to some extent use the location tables that are created by means of beaconing. Position-based routing protocols base their choice of a next forwarder on the positions of their neighbours with respect to the destination. In the simplest case the node closest to the destination is chosen as the next forwarder, this is referred to as greedy forwarding. It was first proposed in [39] and was recently standardised by the ETSI [3]. This simple algorithm is very effective as long as a message can be routed along a straight road that goes from the source to the destination, but if the environment becomes more complex, such as in a city, additional mechanisms must be employed to deal with problems such as indirect routes and routing loops [40]. Some unicast routing protocols assume that knowledge about the road topology is available and can be used for routing [41] [42] [43] [44]; whether this is a valid assumption remains to be seen as long as standardisation of the network stack is still an ongoing process. For more information on unicast georouting in VANETs the reader is referred to [45] [46].

Nodes may not always have a next forwarder to forward a message to, in which case they must store the message until they do find a next forwarder. This principle is referred to as store-carry-forward and applies both for flooding and unicast routing protocols [47].

The main goal of flooding protocols is to deliver a message to every node inside the destination area as efficiently as possible. In its simplest form every node in the destination area rebroadcasts every message once; we refer to this form of flooding as simple geo-broadcast forwarding as standardised by the ETSI in [3]. Simple geo-broadcast gives a high probability of success, but wastes a lot of bandwidth. A more advanced approach is distance-based delay forwarding: in this approach nodes will attempt to rebroadcast a message after a certain delay. The delay is lower as a node is closer to the end of the destination region, and at its maximum close to the previous forwarder. If a node has received the message from someone that is closer to the destination region than itself before its delay has ended, it will not rebroadcast the message. In this way the distance between two forwarders is maximised and a a message is transmitted towards the end of the destination in as few hops as possible. This approach was implemented using deterministic time slots in [48] as slotted 1-persistence broadcasting and has currently been standardised by the ETSI as the contention-based forwarding, also in [3]. In [49] a solution is given to optimise the end-to-end delay when using such a distance-based delay scheme.

Piggybacking is a forwarding technique in which messages are attached to and broadcasted along with beacons. Preferably this should be done without changing the timing of the beacons, since creating a scalable beaconing process is far from trivial. By transmitting messages together with beacons piggybacking aims to minimise the number of times that the medium needs to be accessed by a node, thus keeping contention for the wireless medium low. This comes at the cost of an increased forwarding delay, since nodes have to wait for the next scheduled beacon before being able to forward a message. Piggybacking is therefore mainly used to flood delay-insensitive information [7] [50].

Finally, with cluster-based routing a virtual backbone is created and used for multi-hop forwarding. Nodes are either part of the backbone or have a neighbour that is part of the backbone. Messages are first forwarded to a backbone node and are then forwarded in the direction of their destination. Because of the short connection times in a VANET clustering is quite a challenge, and attention on clustering has so far been limited [51] [52] [53].

3.6 Other aspects

There are a number of challenges in vehicular networking that are not in a direct way functional to the work presented in this thesis, but that are nevertheless relevant for gaining a broad understanding of vehicular networking. In this section we discuss a number of these challenges.

3.6.1 Security

Security in vehicular networks encompasses authentication, integrity, and privacy. It is of critical importance in vehicular networks for two reasons. Firstly, an unsecure system is vulnerable to attacks which may lead to performance degradation, to the point that the system may become unusable. Secondly, a system that is not able to guarantee a minimum level of privacy will most likely be rejected by potential users. For both reasons the topic of security is receiving a lot of attention by academia, industry, and governments.

The following security requirements have been identified in [54]: message authentication, message integrity, message non-repudiation, entity authentication, message confidentiality, accountability, and privacy protection. Message authentication allows a receiver to verify the sender of the message, while message integrity ensures that the message was not altered. Message non-repudiation ensures that a sender cannot deny having sent the message, which enables accountability. Entity authentication ensures that only authorised entities can generate messages. Message confidentiality ensures that the content of a message is kept secret from those network entities that are not authorised to access it. Finally, privacy protection ensures that vehicles cannot be tracked.

To meet some of these requirements, public keys are used to digitally sign messages. Before transmitting a message a sender s digitally signs the message using a secret key that has been assigned to it by a certification authority (CA). It then attaches a certificate, which has also been assigned to it by the CA, which contains the public key of s. Upon reception the receiver will first validate the certificate, after which it can validate the digital signature of the message using the public key of the sender contained in the certificate.

The use of public keys to digitally sign messages, in combination with certificates, ensures entity authentication, since only entities that have been assigned a key and a certificate set by a CA can digitally sign their messages. Message authentication and message non-repudiation are ensured since messages are signed using the secret key, while message integrity is ensured because alteration of a message are detected by means of the digital signature. Finally, to ensure the privacy of vehicles, each vehicle will have a large set of keys and continuously switches between the key it uses to sign its messages. In this way two messages that are signed using different keys cannot readily be matched to the same vehicle. Each key is referred to as a pseudonym.

The addition of digital signatures and certificates to messages severely increases the size of these messages, sometimes more than doubling the size of the original message.

Efforts are therefore being made to decrease this impact by adding digital signatures and certificates in a selective way, instead of adding them to every message [55].

For a more detailed discussion on security challenges in vehicular networks and how to meet them see [54] and [56].

3.6.2 Scalability

Because of the scarceness of the wireless medium *scalability* is a major issue in wireless networks and a primary design concern for any vehicular network protocol. IEEE 802.11p is a carrier sense multiple access with collision avoidance (CSMA/CA) technique that employs random access. In such networks it is a given that as the load increases beyond a certain saturation point, the throughput declines due to an increase in collisions and contention of the medium. To achieve a good utilisation of the medium it is therefore desirable to keep the offered load at or below this saturation point. When the medium does become congested message delivery drops and delays increase rapidly.

Designing scalable vehicular network protocols is a challenging task due to the variability of the network density. Vehicle densities may range from an empty high way to a city-wide traffic jam, each giving rise to different challenges. In a sparse network vehicles must buffer data when there are no (useful) nodes to forward it to, and forward it at a later time. In a dense network transmissions should be suppressed as much as possible to avoid the medium from becoming congested.

Scalability is especially an issue for beaconing, i.e., the regular one-hop broadcasting of awareness messages. Cooperative awareness applications require that vehicles regularly receive beacons from nearby vehicles at frequencies of 10 Hz or higher [57]. As traffic densities increase however supporting such high frequencies becomes problematic [15].

To ensure that safety and awareness transmissions do not suffer from other, less relevant types of transmissions, multiple transmission channels have been defined. The control channel (CCH) is reserved for beaconing (to support awareness) and safety related transmissions. Two service channels (SCHs) have been designed for less critical transmissions, such as to support efficiency applications. Moreover, to ensure that safety messages can still be transmitted even when the medium is congested, a priority mechanism is employed. Messages with a higher transmission priority – such as safety messages – have a higher probability of winning the contention for the wireless medium.

3.6.3 Short-range vs. long-range communication

There is an ongoing discussion in the field of vehicular networking which of the two alternatives is better suited for specific ITS applications: short-range communication (i.e., IEEE 802.11p) or long-range communication (i.e., LTE), see for instance [58]. Both techniques have their pros and cons. IEEE 802.11p has the advantage of being cheap: hardware costs are relatively low and no licenses are required. The quality of service (QoS) is at best variable however, without any guarantee of delivery and without any given delay bounds [59]. In contrast, LTE, being cell-based, gives clear QoS: delays are fixed and delivery of a message can often be guaranteed. However, use of LTE requires a license, making it relatively costly, as well as infrastructure to provide coverage. The latter is problematic for two reasons: in rural areas it may well be the case that there is no coverage, while in areas in which traffic is dense it cannot always be guaranteed that there are enough base stations to provide the required coverage at all times. For both IEEE 802.11p and LTE the issue of scalability is one of the most critical performance issues and is still being researched [60] [15]. Which of the two techniques is more scalable is as of yet undecided and will most likely depend on the specific application at hand. Neither IEEE 802.11p nor LTE has the definite advantage over the other and current architectures are being designed to support both these techniques, as well as other communication techniques, with nodes switching between communication interfaces based on how a certain technique meets an application's requirements. This thesis focuses on short range communication techniques and IEEE 802.11p specifically.

3.7 Standardisation

ITS advancement is mainly being pursued in three parts of the world: Europe, the USA, and Japan. Each has its own set of governmental organisations, joint initiatives, projects, and standardisation bodies. As a result three different ITS architectures are currently being standardised. We briefly discuss the relevant organisation and resulting standards for each region. Note that in this thesis we follow the European architecture and protocol suite.

In Europe the ISO CALM architecture is used [21]. It defines user entities and communication interfaces, see Fig. 3.1. It is being developed in close cooperation with the ETSI, as well as the International Telecommunications Union (ITU) and the CAR 2 CAR Communication Consortium (C2C-CC). The latter is a non-profit industrial driven organisation initiated by European vehicle manufacturers and supported by equipment suppliers, research organisations and other partners. Vehicular networking protocols are being standardised by the ETSI and are based on results of European research and development projects such as SAFESPOT [61], CVIS [62], NoW [63], COMeSafety [64] and SeVeCom [65].

In the USA the ITS architecture has been defined by the U.S. Department of Transportation (DoT) and is referred to as NITSA (which stand for national ITS architecture, see [66]). The NITSA architecture defines user entities, information flows, and functional requirements. The vehicular networking protocol standards used are the wireless access in vehicular environments (WAVE) protocol standards that are standardised by the IEEE in the IEEE 802.11p and IEEE 1609 protocol set [67] [68] [69] [27]. The development of these protocols has been based on results from national projects such as Intellidrive [70], PATH [71], and V2V [72]. The message format used by the IEEE 1609 protocols has been standardised by the Society of Automotive Engineers (SAE).

Similar to Europe Japan uses the ISO CALM architecture. Vehicular networking protocols are standardised by the Association of Radio Industries and Businesses (ARIB). Results from national projects such as ETC [73] and AHSRA [74] have been used both by ARIB and the ISO.

Both in Europa and in the USA V2V communication is implemented using IEEE 802.11p although there exist differences in how the technology is used. In Europe IEEE 802.11p has been included in the ISO CALM architecture as CALM M5 [75] while in the USA it is part of IEEE WAVE. Both in Europe and the USA one control channel (CCH) and multiple service channels (SCH) have been defined. The CCH is reserved for beaconing and safety applications; the SCHs are either reserved for safety applications, non-safety applications (e.g., traffic efficiency applications), or future applications that are as of yet unknown.

3.8 Simulation of vehicular networks

Vehicular network simulation brings together two forms of simulation that operate on wholly different time scales. On the one hand there is the simulation of vehicular traffic, which operates on the scale of seconds, minutes, or even hours. On the other hand there is the simulation of the network communication between the vehicles, which operates at a scale of milliseconds or even smaller. Because of this difference, and the fact that in both fields already quite some mature simulators exist, most VANET simulation frameworks have opted to combine existing simulators instead of creating a single simulator that encompasses all complexity. Communication between the different components is done using standardised interfaces. An additional advantage of this approach is that the framework becomes more modular, making it easier to interchange for example different mobility models, radio wave propagation models, communication protocols, etc.

Traffic can be observed at different scales. At the microscopic level the behaviour of each and every vehicle is taken into account. Such an amount of detail is necessary when communication actively influences the behaviour of a vehicle, such as with CACC. At the macroscopic level traffic is described in terms of flows, e.g., how many vehicles have passed a certain point for the last hour. In between there is the mesoscopic level, which tries to combine the advantages of the previous two levels by dividing the road network into small cells, which are in turn modelled at a macroscopic level.

Coupling between the traffic simulator and the mobility simulator can be one-way (from the traffic simulator to the network simulator) or two-way. Traffic mobility may be either be pre-generated (e.g., based on accurate traffic measurements) or based on a mobility model. To simulate the effectiveness of a communication protocol that does not affect traffic for a certain traffic situation, a one-way coupling with pre-generated mobility suffices. To measure the effect of communication on traffic two-way coupling is required.

When simulating radio wave propagation inevitably a choice has to be made between accuracy and speed. When the propagation model takes too little detail into account results will be inaccurate and misleading. However, simply choosing a propagation model that takes as much detail into account as possible will lead to overly long simulations, taking hours, days, or even weeks. Generally speaking one should choose a propagation model that is able to model relevant effects of the environment that is considered, and can deliver the amount of detail that is required, within a limited time frame.

Veins [76] is a simulation framework that combines the open source network simulator OMNET++ [77] with the open source traffic simulator SUMO [78]. Network communication is modelled using the simulation package MiXiM [79]. Veins supports two-way microsimulation. TraNS [80] is a simulation framework that combines the open source network simulator NS2 [81] with SUMO. TraNS also supports two-way microsimulation. In the SeVeCom [65] project the open source JiST/SWANS simulation framework [82] was extended to support VANET simulation.

Part II

Routing with spatiotemporal constraints


107.50
FM
777
COSMIC
コスミック
HONDA
1AN-7290
1C-3375
HONDA

CHAPTER 4

Constrained geocast

Geocast is a method of addressing in which a message is given a destination area and any node inside the destination area is considered a destination node. Although it is the de facto method of addressing in vehicular networks we show in this chapter that it does not properly meet the requirements of the overlaying ITS applications, and present a novel form of geocast that aims to better meet these requirements, called constrained geocast. We do so in the context of an application scenario in which information concerning a traffic event must be disseminated throughout the network, and show that for standard geocast to be effective in such a scenario it becomes inherently inefficient, delivering messages to parts of the network where they are not needed. In contrast, constrained geocast aims to disseminate information to only those nodes that are expected to be at the location of the event.

The outline of this chapter is as follows. We first discuss the limitations of standard geocast in Section 4.1 and then introduce the concept of constrained geocast in Section 4.2. Note that geocast itself was discussed in detail in Section 3.4.

Image on previous page: motorbike riders in Phnom Penh, Cambodia.

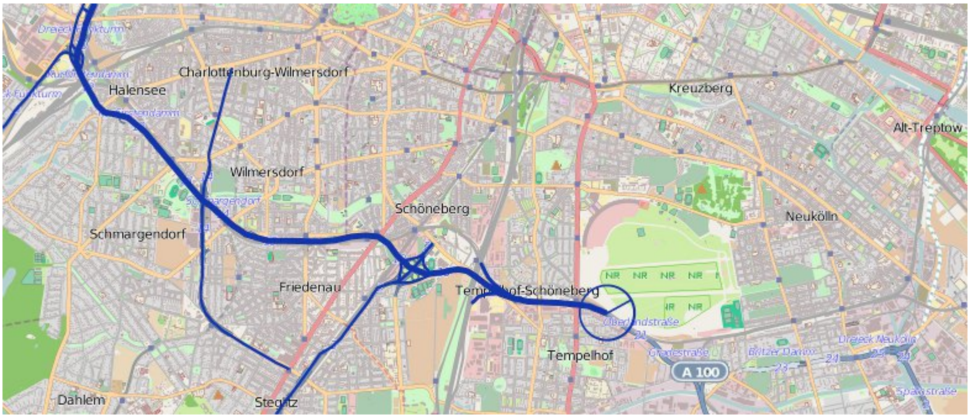

Figure 4.1: The location where a highway road lane is blocked (denoted by the circle) and the primary and secondary traffic flows leading to the blockage area (in blue).

4.1 Limitations of geocast

In this section we discuss the limitations of standard[1] geocast when disseminating traffic event information in a vehicular network. These limitations stem from the fact that with geocast information is addressed using spatial constraints only, which in a vehicular network is often not enough to distinguish between nodes to whom the traffic information is relevant and nodes to whom it is not relevant. Because of this there is often an inherent choice between efficiency and effectiveness when using geocast. Below we discuss this issue in more detail and illustrate it by means of an example.

Typically, information about a traffic event is relevant only to those nodes that are currently at the location of the event or – if the event takes place for an extended time period, such as a traffic jam – that are expected to be at the location of the event in the near future. In the latter case nodes that are interested in information regarding a certain event are therefore spread out over a large geographical area. Likewise, nodes that are relatively close to the location of the event may not be interested in the event at all, e.g., because they are driving on a road lane that is not affected by the event, or because they are driving away from the event. Clearly, using only spatial constraints to address and disseminate information regarding such a traffic event does not allow to distinguish between nodes that are interested in the information and nodes that are not. Information is thus almost by definition routed to parts of the network where it is not needed, creating inefficiency. Moreover, because of the speed with which vehicles move, in some scenarios the destination area must necessarily be large in order for the application to be effective, thus increasing inefficiency. As has already been discussed in Section 3.6.2 bandwidth scarcity is a major issue in vehicular networking and such inefficiency should be avoided whenever possible. We illustrate these problems of standard geocast by means of an example.

Consider a busy city road network crossed by a highway, as illustrated by Fig. 1.3.

[1] I.e., as standardised in [3].

Figure 4.2: A minimum-size destination area covering the primary and secondary traffic flows.

The city road network is a tightly interwoven mesh of streets with local-bound traffic, the speed of vehicles not exceeding 50 km/h. In contrast, the highway is a single road with few ramps, its traffic travelling at speeds of 120 km/h and higher to destinations typically tens or hundreds of kilometres away. Now consider that an accident has happened on the highway, causing a blockage of one its lanes.

To prevent mass queuing from occurring on the highway we wish to inform any drivers approaching the blockage of this fact while they are still able to choose an alternate route. Information about the traffic event should be disseminated several kilometres upstream[2] of the event, giving highway drivers the opportunity to exit the highway. Likewise the information should be disseminated to local drivers that are about to the enter the highway at a point leading to the event, to prevent them from doing so.

In order to visualise the location of drivers that are, or may be, approaching the blockage, we have highlighted the location of the blockage and the primary[3] and secondary road lanes leading to the blockage in Fig. 4.1. Any traffic headed for the event area must come via the primary road lane and must therefore be warned; any traffic driving on for instance a secondary or tertiary road lane is less likely to be headed for the event area as it may still turn away, and should not necessarily be warned. The further in advance a driver is warned however, the more options he has to choose an alternate route to avoid the event area. Note that we exclude road lanes on which traffic moves away from the event area, i.e., any downstream road lanes. Although our choice of highlighting is somewhat arbitrary (we could also have included the tertiary roads that lead to the secondary roads, etc.), the figure clearly shows that spatial constraints alone are not enough to distinguish nodes that are headed towards the event area from nodes that are not. This is further exemplified by Fig. 4.2 which shows a minimum-sized geocast destination area covering the primary and

[2]Upstream here means against the flow of traffic.

[3]In this context a primary road lane is a road lane that leads directly to the event area; a secondary road lane leads directly to the primary road lane.

secondary roads leading to the blockage area (although the highway continues on outside the figure so the destination area does not cover the primary road in full). It can be seen that the greater part of the destination area covers parts of the road network where information about the highway blockage is not relevant. Traffic event messages are therefore considered overhead in these parts. Overhead may be reduced by choosing a smaller destination area but this will diminish the effectiveness of the application, as drivers are warned less far in advance of reaching the blockage and may not be able to choose an alternate route.

Apart from the size of the destination area the frequency with which data is disseminated is also relevant. With current geocast solutions a message is disseminated just once to its destination area. Event messages concerning the blockage must therefore be repeatedly retransmitted for the entire duration of the blockage in order to ensure that all approaching nodes receive a warning. For those parts of the network where the message is not relevant the overhead is therefore also present for the entire duration of the blockage. *Abiding geocast* [30] solves part of this problem by specifying both a destination area and a time interval during which all nodes in the event area should receive the message. With abiding geocast information can typically be flooded throughout the destination area once, and then kept alive at the edges to inform nodes that enter the destination area. This reduces the overhead compared to basic geocast, but still does not prevent information from reaching parts of the network where it is not relevant. In the following section we therefore propose a new form of geocast in which messages do reach only those parts of the network where they are relevant.

4.2 Constrained geocast

We propose *constrained geocast* as a novel form of geographical addressing aimed to better meet the communication requirements of ITS applications. In this section we explain the concept of constrained geocast, address some of the peculiarities of its resulting destination set, explain how to implement it in a vehicular network, and discuss issues that must be solved in order to implement constrained geocast. Note that we do not fully implement constrained geocast in this chapter. In Chapter 5 constrained geocast is implemented for a one-dimensional scenario.

4.2.1 Concept

Consider again a scenario in which a traffic event has occurred, e.g., a road lane has been blocked. The event has a specific location and takes place for a specific amount of time. In case of the blockage the location is the point where the road is blocked and is referred to as the *event area*. The size of the event area is variable and may be as precise as to indicate a specific road lane. The time interval that an event takes place is referred to as the *event time*. We consider the routing of *event messages*: messages that inform a vehicle (and its driver) about the situation at the event area. Note that events can be both small and large in area and short and long in time. Road works can for instance affect long stretches of road for long periods of time, whereas a vehicle that merges at an intersection is a short-lived event that affects few vehicles.

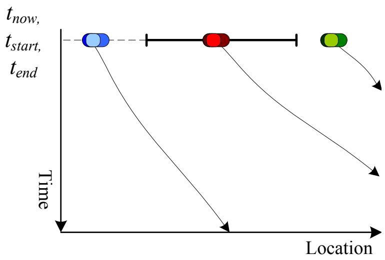

(a) Destination area of standard geocast.

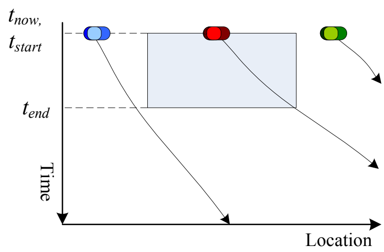

(b) Destination area of abiding geocast.

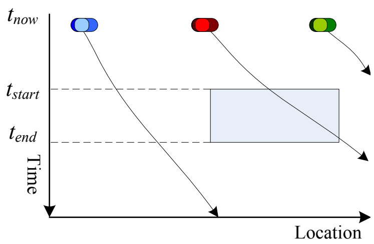

(c) Constrained geocast event area.

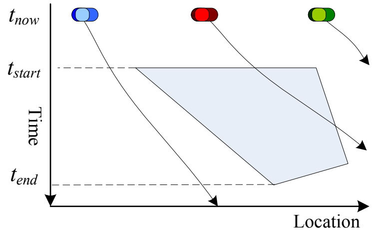

(d) Dynamic constrained geocast event area.

Figure 4.3: Spatiotemporal diagrams illustrating one-dimensional areas in time as well as the trajectories of three vehicles. Time runs from the current moment in time t_{now} onwards (downwards). For all figures holds that only the red node is a destination node.

A vehicle is considered interested in the traffic event information if it is expected to be inside the event area during the event time. From this point forward we refer to interested nodes as *destination nodes*. Every message transmitted or received by a node that is not a destination node is considered overhead. The goal of constrained geocast is to have event messages only routed to parts of the network where there are destination nodes.

Constrained geocast differs from standard geocast and abiding geocast in that destination nodes are defined by their future location instead of their current location. We discuss this difference in detail using Fig. 4.3, which depicts the destination areas of geocast and abiding geocast and two event areas of constrained geocast. For the sake of our discussion we define t_{start} to be the moment in time when an area is first defined and t_{end} the moment when it ends. Let t_{now} furthermore be the current time. We consider when a node is defined a destination node of an event message that it receives at t_{now} for all three forms of geocast.

With standard geocast the destination area is a flat line at t_{now}, i.e., $t_{start} = t_{end} = t_{now}$. A node is considered a destination node if it is inside the destination area at t_{now}, see Fig. 4.3a.

With abiding geocast the destination area is a flat line that starts at t_{now} ($t_{start} = t_{now}$) and moves through time for the duration of the event until t_{end} ($t_{end} > t_{now}$). A node is considered a destination node when it is inside the destination area during the event time

$[t_{start}, t_{end}]$, see Fig. 4.3b.

With constrained geocast the event area is a flat line that starts at some (future) time ($t_{start} \geq t_{now}$) and moves through time for the duration of the event until t_{end}, see Fig. 4.3c and Fig. 4.3d. A node is considered a destination *the moment it determines that it expects to be inside the event area during the event time* $[t_{start}, t_{end}]$. I.e., even though the node may not be inside the event area at time t_{now}, $t_{now} < t_{start}$, if at t_{now} it expects to be inside the event area during the event time $[t_{start}, t_{end}]$ it is considered a destination node at t_{now}. The event area may move through time as is illustrated in Fig. 4.3d. An example scenario of a moving event area is an emergency vehicle that broadcasts event messages concerning its route. In this case the event area is the emergency vehicle's location, which changes in time according to its route, and the messages must be routed to any node that is expected at some future time to be in the emergency vehicle's path.

Because with constrained geocast destination nodes are determined based on their future location the resulting destination set is considerably different from a standard geocast destination set. We therefore discuss the properties of such a destination set below, before defining how to implement a routing protocol that can support it.

4.2.2 Destination set

We consider the destination set of a given event message. Firstly, there is a difference between the set of nodes that will eventually be in the event area during the event time, and the set of nodes that, at a certain moment in time, is estimated to be in the event area during the event time. In some cases reception of an event message by a vehicle will result in the vehicle actively changing its route to avoid the event area, e.g., in case of a blockage. In the remainder of our discussion we use the latter definition of a destination set.

The destination set is dynamic and may change every few seconds as vehicles change route, as they enter or exit a road leading to the event area, or as changing traffic speeds cause vehicles to reach the event area at an earlier or later time. As the event area and the duration of the event become smaller, the destination set becomes more susceptible to traffic disturbances and therefore becomes more dynamic.

The destination set is geographically spread out and unconnected. Destination vehicles may approach the event area from all directions and can be widely dispersed, with no necessary communication connection to other destination vehicles. This may hold even for a single road lane if speed differences are high.

4.2.3 Routing issues

To implement a routing protocol that is able to deliver messages to a destination set with properties such as the above a number of implementation issues must be considered. We discuss some of these issues here but do not necessarily solve them. In the next chapter we solve these issues for the case of one-dimensional constrained geocast.

We first formally define the concept of a traffic flow as we will use it in our discussion. A traffic flow consists of one or more adjoining road lanes that have the same direction of travel. We order the flows of traffic with respect to the event area: a traffic flow that leads

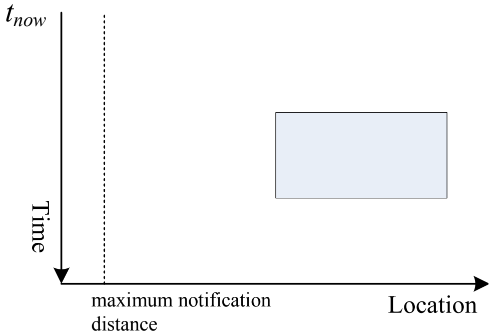

Figure 4.4: Spatiotemporal diagram of the event area and the maximum dissemination distance.

directly to an event area is defined as a primary traffic flow, a traffic flow that leads to a primary traffic flow is defined as a secondary traffic flow, etc.

The first issue is how to decide whether a vehicle will be in the event area. It is impossible to predict with full certainty the future position of a node so some level of uncertainty must be taken into account. We therefore assume that any node part of a primary traffic flow will reach the event area at some moment. Furthermore, any node part of a secondary traffic flow *may* join the primary flow of traffic at some future moment, any node part of a tertiary traffic flow may join the secondary traffic at some future point, etc. For every lower order traffic flow the probability that a vehicle will eventually reach the event area becomes less.

Assuming that the vehicle will eventually arrive at the event area, the next issue is how to decide when it will do so. The arrival time of a vehicle can be estimated based on the vehicle's distance (e.g., shortest route) to the event area, its current speed and acceleration, but also traffic factors such as the speed of preceding vehicles, the state of traffic lights, etc. The exact method of estimation can be abstracted from, as long as the method is reasonably accurate and relatively simple. The required level of accuracy may differ per scenario and is a subject of further research. The method should be simple to prevent routing decisions from becoming too complex and requiring too much computation time.

Once it has been determined that a node is a destination node, how far in advance of reaching the event area should a destination node receive the event message? This may differ per application as applications have different requirements: either to simply inform the driver of the situation on the road ahead (e.g., a slippery road) or to inform them to choose another road (e.g., in case of a blockage). In the former scenario a driver need only be warned a small distance in advance in order to slow down; in the latter the driver must be warned well in advance to be able to choose an alternate route. If the event takes place a limited time in the future destination nodes will by definition be relatively close by and messages can be routed to all destination nodes. If the event takes place for an extended period of time however (e.g., in case of road works) this is not an option, as destination nodes can potentially be hundreds of kilometres away. In such a scenario a limit must be

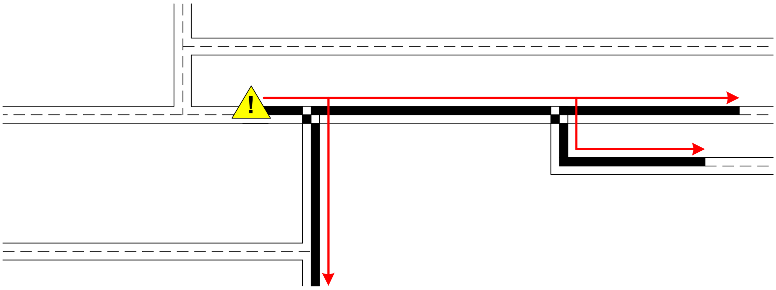

Figure 4.5: Routing against the flow of traffic from the event area outward.

set to the maximum distance in advance of the event area that a node should be notified, see Fig. 4.4.

Due to the dynamicity of traffic the expected route of a vehicle and its expected arrival time at the event area may change continuously. A node's membership of the destination set can thus change with every update of the vehicle's route, speed, or heading until the moment that the event has ended. A vehicle's membership of the destination area must therefore regularly be re-evaluated.

Information regarding a traffic event may need to be updated, e.g., because the event area has changed. In such a case a new event message should be sent out, obsoleting any previous event messages.

Implementation rules: routing against the flow of traffic

Having introduced the concept of constrained geocast and discussed some of its properties, we give a number of general rules for implementing constrained geocast.

Routing of event messages is initiated at the event area itself. Messages are routed against the flow of traffic, initially along the primary traffic flow and branching out along lower-order traffic flows. An event message is routed upstream until either *(i)* it has been routed along a predefined maximum number of traffic flows, *(ii)* it has reached a point where traffic can no longer reach the event area during the event time, or *(iii)* it has been routed a predefined distance ahead of the event area called the maximum notification distance. As an example Fig. 4.5 shows a road network in which each road has two opposite-moving flows of traffic and an event on one of the roads affects one of the road lanes. We assume right-hand traffic. The primary and secondary traffic flows are shown in black up to the maximum notification distance. The red arrows denote where information is routed. Information about the event is routed against the flow of traffic, along the primary and secondary traffic flow, up to the maximum notification distance.

To have vehicles route messages against the flow of traffic and a specific number of flows deep, vehicles must be able to identify the flow they are themselves part of as well as other flows, and be able to determine how flows are related to each other (e.g., distinguish primary flows from secondary flows). This is possible if vehicles have access to road topology information and are able to identify their own driving lane (and the direction of

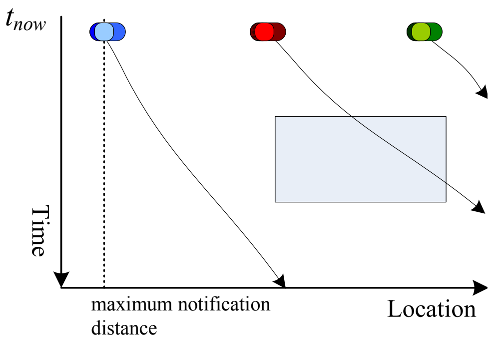

Figure 4.6: Spatiotemporal diagram of the event area and vehicle trajectories. The arrows represent a vehicle's location in time.

travel). Based on results reported by the European SAFESPOT project [19] the latter assumption seems fair. Whether road topology information can be assumed to be available at the network level is as of yet unclear.

A node must be able to determine whether it is headed for the event area or not, and if so when it will reach it. It must be able to do so both for itself and for nodes with whom it can communicate directly. Destination nodes are estimated to be at the event area sometime during the event time, see for instance the red vehicle in Fig. 4.6. Non-destination nodes are estimated to have either already have passed the event area during the entire event time, such as the green vehicle in Fig. 4.6, or to have not yet reached the event area during the entire event time, see the blue vehicle in Fig. 4.6. The former group of nodes is said to reach the event area too soon while the other group of nodes is said to reach the event area too late.

We now formulate a number of rules for forwarding constrained geocast event messages. These rules are meant as generic rules and together do not yet form a complete protocol. We abstract from the method of forwarding.

A message should be forward upstream if:

1. it is forwarded along a traffic flow that is less than or equal to the maximum number of traffic flows a message should be routed away from the event area;
2. the forwarder's distance to the event area is within the event area's notification distance;
3. the forwarder is a destination node;
4. the forwarder is estimated to reach the event area too soon;
5. there are nodes located upstream of the forwarder that are headed towards the event area and that are either destination nodes or are estimated to reach the event area too soon.

When a message is no longer forwarded upstream, either because it has been forward up a predefined number of traffic flows, because it has reached the notification distance, or because it has reached a point where traffic can no longer reach the event area during the event time, the message must be kept alive at the point where forwarding stopped, i.e., at the dissemination edge. Any node that passes this point in the direction of the event area should be forwarded the event message.

4.3 Conclusions

In this chapter we have shown that existing geocast can be very inefficient when used to disseminate traffic information. As a solution to this we have proposed constrained geocast as a means to address and route messages in a way that is both effective and efficient. We have explained the concept of constrained geocast and have given a number of general rules for implementing it. In the next chapter we show how to implement constrained geocasting in full detail for a scenario in which messages are routed along the primary traffic flow only, with no predefined maximum to the distance that messages should be routed upstream.

CHAPTER 5

Application: CACC merging at a junction

CACC is a form of cruise control in which vehicles cooperatively control their speed using wireless communication. Because of their superior reaction time to traffic disturbances CACC vehicles can drive relatively close together. In situations where other vehicles wish to join a flow of CACC traffic CACC vehicles must therefore be explicitly told to make room for them.

In this section we look more closely at merging inside a platoon of CACC vehicles at a junction. We present an application to support CACC merging at a junction and show that this is a scenario in which destination nodes are defined based on their location at a future moment in time rather than on their current location. The communication requirements of such a scenario are therefore typical for constrained geocast, a form of addressing that we explained in the previous chapter. In this chapter we show how to implement a constrained geocast protocol for such a scenario and evaluate its performance compared to standard geocast protocols.

The outline of this chapter is as follows. We first present the problem of CACC merging at a junction and present an extension to the CACC system to support such merging in Section 5.1. In Section 5.2 we show that such a scenario is a typical example of constrained geocast and show how to implement a constrained geocast aimed at this particular situation. We evaluate its performance in Section and finally give conclusions in Section 5.4.

Image on previous page: a lone bicyclist on a mountain road on Doi Suthep, near Chiang Mai, Thailand.

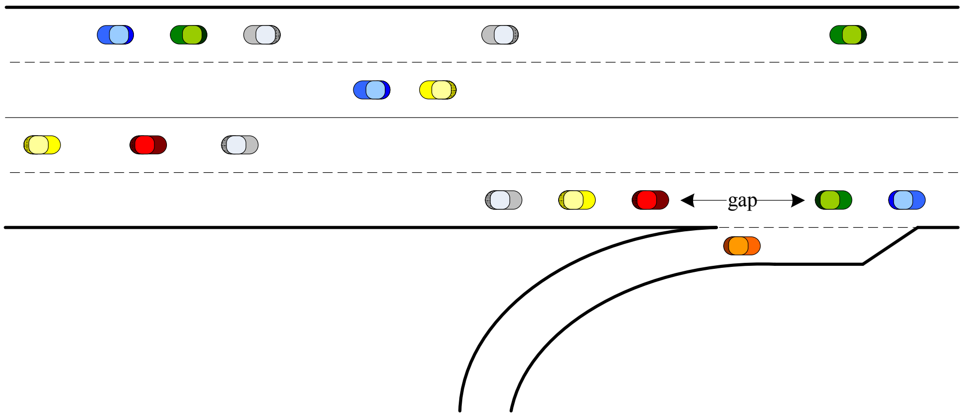

Figure 5.1: Merging at a junction. We consider right-hand traffic. The double-headed arrow denotes the merging gap required by the merging vehicle to merge inside the flow of traffic.

5.1 Introduction

In this section we introduce the scenario of merging at a ajunction, show that it is currently not supported by CACC, and present a CACC merging application to fill this gap in functionality.

5.1.1 CACC merging at a junction

The work presented in this chapter has been performed in the context of the Connect & Drive project [1]. This project focused on the creation of a CACC system that is able to operate with a mix of CACC and non-CACC vehicles, i.e., the system does not require all traffic participants to be CACC operated. The advantage of such a system is that it can be introduced on the public road without requiring a minimum system penetration rate. Research has shown that introducing CACC vehicles on the public road increases the overall throughput of traffic [83]. CACC is explained in detail in Section 2.2.

The Connect & Drive CACC system is based on beaconing. With beaconing each node in the network regularly broadcasts a short status message. The status messages are called beacons and contain information such as a node's location, speed, acceleration, etc. A node uses the information contained in the beacons as input to its CACC control algorithm.

Because of the superior reaction time of the CACC system compared to a human driver CACC vehicles can drive relatively close together, e.g., at distances of 0.5 s or less. [83] A string of CACC vehicles is called a platoon; in case of ad-hoc platooning, as is done in the Connect & Drive CACC system, there is no maximum length to a platoon. Vehicles that wish to join a platoon can either do so by joining the platoon at the front end or rear end simply by driving in front of or behind the platoon, or somewhere in the middle. In the latter case the platoon must explicitly make room for the merging vehicle to allow it to merge inside the platoon.

The most basic form of merging is when a vehicle that is driving on a road lane wishes to join a platoon that is driving on an adjoining road lane. The merging vehicle initiates the merging procedure by driving next to the vehicle it wishes to join in front of, and indicates that it wishes to join the platoon by sending a merge request. The platoon vehicle in question then creates a merging gap by increasing its headway by temporarily slowing down. Once the merging vehicle has merged, normal CACC operation is resumed. The distance and time it takes for a platoon vehicle to increase its headway to such an extent that a merging vehicle can merge inside the platoon depends on the speed of the platoon and the required headway. The latter in turn depends on the size of the vehicle and again the speed of the platoon. Increasing the headway should be done with some care to prevent traffic disturbances from occurring so as to keep the platoon string stable.

In some scenarios vehicles are forced to merge inside a platoon. A vehicle attempting to join the flow of highway traffic at a junction may for instance find that the lane it attempts to join is fully occupied by a platoon of CACC vehicles. The only way for the merging vehicle to join the flow of traffic is if the platoon creates a gap for the vehicle to merge in. Merging at a junction is a more demanding procedure than basic merging however: the merging procedure must be finished by the time the merging vehicle reaches the end of the merging lane, and there is only a limited length of road to execute the procedure. The basic merging procedure described above cannot be applied in such a situation therefore: either the merging gap will not be ready soon enough to allow the merging vehicle to merge, or the merging gap will not be created in a string-stable manner, causing traffic disturbances.

To avoid these problems the platoon should have a merging gap ready by the time it reaches the merging area, see Fig. 5.1. In this way the merging vehicle has plenty of time to perform the merging procedure before the end of the merging area. The platoon should therefore start creating the merging gap well in advance of the merging area. Doing so is somewhat problematic however. Firstly, as both vehicles are part of different, usually non-adjoining traffic flows, and the merging vehicle is typically accelerating, estimating in advance which vehicle in the platoon should increase its headway for the merging vehicle is non-trivial. Furthermore, at the moment the platoon should start creating the merging gap there may very likely be no direct communication possible between the merging vehicle and the platoon vehicle. The merging vehicle can therefore not request the platoon to create a gap in time. Finally, the platoon should also allow merging vehicles that have no communication capabilities to merge inside the platoon at the junction.

Clearly the CACC system should be extended in order to support merging at a junction. In the next section we therefore propose a merging application to add this functionality to the CACC system.

5.1.2 The CACC merging application

In this section we present an application that is able to support automated CACC merging at a junction.

Previous research on automated merging focused on adapting the merging vehicle's speed to match existing gaps in the flow of highway traffic [84]. Such an approach does not work here however, as we assume highway vehicles to drive in platoon formation with little to no gaps to merge in. Other approaches assume that all vehicles involved are operated by CACC [85] [86] which obviously also does not apply here, as the CACC system has been designed to work with a mix of CACC and non-CACC traffic. We therefore propose a new merging system in which automated CACC merging can be performed assuming a mix of CACC and non-CACC traffic, and with highway vehicles adapting their speed to ensure that there is a gap in the flow of traffic for the merging vehicle to merge in.

The aim of our merging application is that when the merging vehicle reaches the merging area it will find a gap in the flow of traffic that it wants to join (in case of Fig. 5.1 the right-most road lane), large enough for it merge in. The merging vehicle should then align with the merging gap and merge inside the gap, after which normal CACC operation resumes. Gap creation must be done in such a way as to keep highway traffic string stable. We first define which CACC highway vehicle should create the merging gap.

The merging gap should have a certain size, should be ready at the moment the merging vehicle reaches the merging area, and should be present near the start of merging area at the moment the merging vehicle reaches the merging area. The double-headed arrow in Fig. 5.1 illustrates the required merging gap. Only a single gap in the flow of traffic should be created, i.e., at most one CACC vehicle should create a gap, and if a gap in the flow of traffic is already present no action should be taken.

To meet all needs with respect to the merging gap we formulate the following requirement: any CACC highway vehicle that is expected to occupy the gap area at any point in time should create the merging by increasing its headway. If a non-CACC vehicle is expected to occupy the gap area then it is left to the human driver to act. A non-CACC operated vehicle will typically drive with a larger headway, making it easier for the merging vehicle to merge inside the flow of traffic. If no vehicle is expected to occupy the gap area then the gap is already present. The distance in advance of the merging area that a CACC highway vehicle should start creating the merging gap, in order to do in as string-stable manner as possible, is still a subject of research. Especially in scenarios with multiple merging vehicles it is a challenge to determine the effect that merging has on CACC string stability.

To ensure that there will be a gap in the flow of traffic that allows the merging vehicle to merge we must first determine where it should be at what time and with what size. For this we need to determine the arrival time of the merging vehicle at the merging area, its location during the time it is inside the merging area, and the size of the gap. If the merging vehicle is a CACC vehicle it can calculate this on its own, given that is knows it own location, speed, and acceleration, the trajectory of the merging lane, and the location of the merging area. If the merging vehicle is a non-CACC vehicle some kind of RSU is needed however to track an approaching non-CACC merging vehicle and calculate its required merging gap. We therefore define that a RSU is located at the merging lane to calculate the required merging gap for approaching non-CACC merging vehicles. Approaching CACC merging vehicles may either calculate their own required merging gap and notify the RSU or have the RSU calculate it for them. Examples of such tracking systems are inductive-loop traffic detectors and on-road sensors [87]; the exact method employed to track an approaching merging vehicle is abstracted from here but we require that it should be able to calculate:

1. the moment the merging vehicle will reach the start of the merge area (denoted as t_{start});
2. the moment the merging vehicle will reach the end of the merge area (denoted as t_{end});
3. the required size of the merging gap to let the merging vehicle merge safely.

The amount of room that a vehicle needs in a platoon is by definition equal to the length of the vehicle plus the required headway in front of the vehicle and the required headway behind the vehicle. We use the same approach to calculate the required size of the merging gap. The headway required by the merging vehicle is defined as $h_{merging}$ (in s). To allow for some margin of safety the headway should be larger during the merging procedure than for normal CACC operation.

Once the merging gap has been calculated it must be communicated to any CACC highway vehicles approaching the merging area. The RSU must therefore be employed with communication capabilities and must be positioned in such a way that it can communicate directly with CACC vehicles driving on the highway. The RSU sends out so-called event messages containing the following fields:

id – Uniquely identifies a merging vehicle.
t_{create} – The moment that the message was created.
$t_{lifetime}$ – The lifetime of the message (in s). The information contained in the message is obsoleted $t_{lifetime}$ s after t_{create}.
a_1 – Gives the location of the start of the merging area in GPS coordinates.
a_2 – Gives the location of the end of the merging area in GPS coordinates.
t_{start} – The moment the merging vehicle is estimated to arrive at a_1.
t_{end} – The moment the merging vehicle is estimated to arrive at a_2.
μ – The headway required by the merging vehicle in front and behind.

Instead of separately defining the location of the merging vehicle at each moment during its time in the merging area, which would be rather inefficient to communicate, we assume that the merging moves with constant speed from the start of the merging area (a_1) to the end of the merging area (a_2), and that its location between t_{start} and t_{end} can therefore be calculated using the formula for linear motion. Field μ includes the length of the merging vehicle and is given by:

$$\mu = l/2 + h_{merging} \cdot v_{highway}, \tag{5.1}$$

where l is the length of the merging vehicle (in m), $v_{highway}$ is the speed of a highway vehicle (in m/s), and $h_{merging} \cdot v_{highway}$ is the required headway by the merging vehicle (in m). The value of $v_{highway}$ can be based on measurements (e.g., inductive-loop traffic detectors) or beacons received from highway vehicles.

Using the fields of the event message the CACC highway vehicle that should create a gap can now be formally specified. We require that any CACC highway vehicle that is expected to reach the merging area during the time period $[t_{start}, t_{end}]$ and is expected to be within μ meters of the merging vehicle at any moment of time during that period, should create a merging gap.

After having created the event message, the RSU forwards the message to the CACC highway vehicles. The RSU will calculate the required merging gap and send out the resulting event messages several times as a merging vehicle approaches the merging area. The time between two event messages relating to the same merging vehicle is a system parameter. As the merging vehicle comes closer to the merging area the estimations regarding its arrival time will become more precise; new event messages therefore obsolete older messages.

After an event message has been transmitted by the RSU it must be routed to any CACC highway vehicle that is expected to be within μ meters of the merging vehicle during the period $[t_{start}, t_{end}]$. In the next section we present a constrained geocast protocol capable of doing this.

A CACC highway vehicle that has received an event message, informing it that it is expected to be within μ meters of a merging vehicle during the period $[t_{start}, t_{end}]$, will create a gap by increasing its headway. The gap must should be finished when the merging vehicle reaches the merging area, i.e., at t_{start}. Gap creation does not necessarily need to start at the moment the vehicle receives the event message, but should be started such a distance in advance as to keep traffic disturbances due to the gap creation to a minimum. A CACC highway vehicle should therefore have received the event message regarding the merging vehicle before this time. We refer to the minimum distance ahead of the merging area at which a CACC highway vehicle should be notified of an approaching merging vehicle the *minimum notification distance*. The exact value of this distance is as of yet a subject of further research, but initial calculations strongly suggest that vehicles will still be outside the RSU's communication range. Multi-hop communication is therefore needed to route the event messages.

We ignore gap creation itself as it is a complex subject that falls outside the scope of this thesis. Instead we assume that, when the process is started in time, a CACC highway vehicle is capable of creating a gap in a string stable manner.

Having given a functional description of the our CACC merging application we show in the next section that the communication requirements of our application are an example of the spatiotemporal constraints typical of constrained geocast.

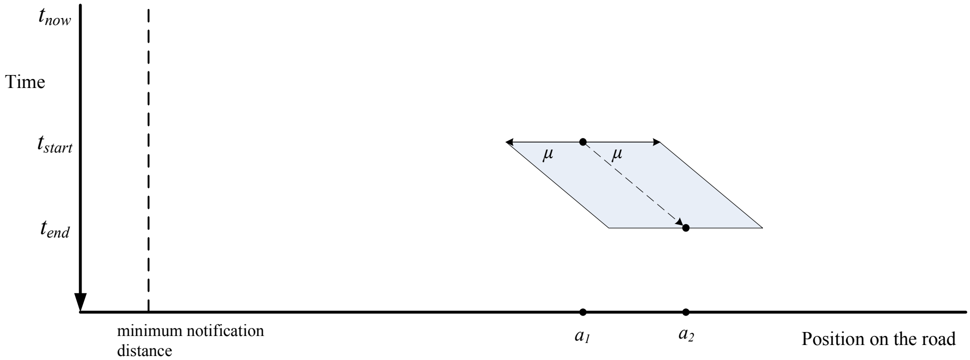

Figure 5.2: Spatiotemporal diagram of the merging gap. The dotted arrow represents the location of the merging vehicle on the road as given by $s_{merger}(t)$ in the interval $[t_{start}, t_{end}]$.

5.2 A constrained geocast scenario

In this section we first show that the communication requirements of our CACC merging application are a typical example of a constrained geocast scenario. We then specify a constrained geocast protocol for this particular scenario.

5.2.1 Spatiotemporal communication requirements

The CACC merging application requires that any CACC highway vehicle that is expected to be inside the required merging gap during the merging procedure, and that is driving on the lane in which the merging vehicle must merge, creates a merging gap, and starts doing so before it reaches the event area. Every node that is expected to be inside the required merging gap during the merging procedure must therefore receive an event message, informing the vehicle that it should create a gap. Nodes should furthermore be informed a minimum distance in advance of the merging area. These are very similar requirement to the requirements of constrained geocast, in which all nodes that are expected to be inside the event area during the event time should receive an event message. Below we formulate the communication requirements of the CACC application in constrained geocast terms.

Let the required merging gap be the event area and the period that the merging vehicle is in the merging area be the event time. The event area moves in time. For a moment in time t, $t \in [t_{start}, t_{end}]$, the event area runs from $s_{merger}(t) - \mu$ to $s_{merger}(t) + \mu$, $s_{merger}(t)$ being the position of the merging vehicle at time t, given by the formula of linear movement with zero acceleration:

$$s_{merger}(t) = a_1 + (t - t_{start})\frac{a_2 - a_1}{t_{end} - t_{start}}, \tag{5.2}$$

for $t \in [t_{start}, t_{end}]$. Fig. 5.2 shows the resulting event area in time and the minimum notification distance in a spatiotemporal diagram. The event area is defined in the time interval $[t_{start}, t_{end}]$; its size is as defined above. It can be seen how the centre area of the event area (i.e., the location of the merging vehicle during the event time) moves from a_1 to a_2, and how the event area runs from $s_{merger}(t) - \mu$ to $s_{merger}(t) + \mu$.

Although the merging gap is only required in the flow of traffic that the merging vehicle wishes to join, we define the event area to include all downstream lanes. Only destination nodes of the event area that are travelling in the right-most lane should create a merging gap; destination nodes travelling in other lanes should not create a gap but should be aware of the approaching merging vehicle, to prevent them from moving to the right-most lane.

Clearly the communication requirements of the CACC merging application fit our concept of constrained geocast as explained in the previous chapter. We implement a constrained geocast protocol for this particular scenario in the next section.

5.2.2 Constrained geocast protocol

In this section we implement a constrained geocast protocol to route event messages for our CACC merging application. We follow the general forwarding rules formulated at the end of the previous chapter regarding the forwarding of event messages, and show how we implement the routing issues discussed in the same chapter.

Any CACC highway vehicle that estimates that it will be inside the event area during the event time is considered a destination node. We assume that there are no on-ramps or off-ramps located directly upstream of the merging area, so that each vehicle that is located upstream of the merging area can be assumed to reach the event area eventually. Event messages are therefore only routed along the primary flow of traffic leading to the event area. Because we typically expect at most one destination vehicle, and the vehicle will be relatively close by, event messages are routed with no maximum to the distance they travel upstream.

To determine when a CACC highway vehicle will reach the merging area we again use the formula of linear motion with zero acceleration. We use this method because it is simple to implement, because it allows CACC highway vehicles to calculate their own future position, and because it allows them to calculate the future location of close-by CACC highway vehicles based only on the information contained in their network-level beacons. Because of its simplicity it may be somewhat inaccurate in cases where the assumption of zero acceleration does not hold. This inaccuracy is expected to be within reasonable bounds for most practical situations however. Moreover, in the future more advanced approximation methods may be used as well, as long as these methods also are relatively simple and allow nodes to calculate the future position of their neighbouring nodes based on received network-level beacons. Simplicity is required to keep routing scalable.

In previous work vehicles would estimate a range of future locations by taking into account a predefined maximum acceleration/deceleration value: in [4] a vehicle is considered a destination vehicle if for some acceleration/deceleration value that is less than the maximum the vehicle is estimated to be inside the event area during the event time, again using the formula for linear motion. With this method initially multiple vehicles will estimate to be inside the event area during the event time, consider themselves destination nodes, and therefore start creating a merging gap. As the platoon and the merging vehicles approach

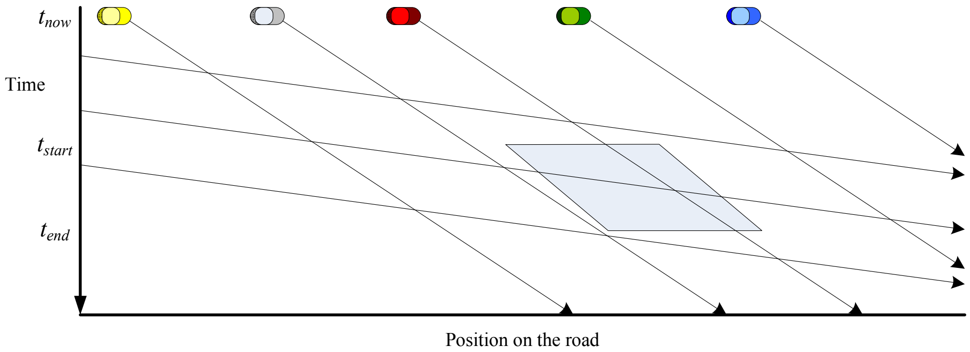

Figure 5.3: Spatiotemporal diagram of the merging gap and the CACC highway vehicle trajectories. The arrows represent the location of a vehicle in time.

the event area, the number of destination nodes becomes less as the effect of the acceleration value becomes less. In the end only one destination node should remain. Although this method ensures that in the end the CACC highway vehicle that is closest to the merging vehicle will have created a gap, its disadvantage is that determining the correct value for such an acceleration/deceleration maximum is non-trivial. If the maximum is too high the group of destination vehicles quickly becomes too large, resulting in unnecessary traffic disturbances. We therefore neglect the use of a predefined maximum acceleration/deceleration in this work. Note again however that in the future more advanced approximation methods may be used.

Fig. 5.3 again shows the event area in time but now together with the estimated trajectories of the downstream travelling highway vehicles in Fig. 5.1. The arrows denote the vehicle trajectories as calculated at time t_{now}. The lines of the platoon vehicles are straight since no acceleration is taken into account. Only the two red vehicles are estimated to be inside the event area during the event time; the rest of the vehicles either reaches the event area to soon or too late.

As the merging vehicle approaches the merging area successive estimates made by the RSU regarding the merging vehicle's arrival time at the merging area will be increasingly accurate. For each estimation a new event message is transmitted and routed upstream, obsoleting previous event messages. The time between two event messages should be less than the lifetime of an event message ($t_{lifetime}$).

All forwarding of event messages is done by means of piggybacking, i.e., event messages are attached to and transmitted along with the network-level beacons that each node regularly broadcasts. The timing of these beacons is not altered, meaning that a message will not be forwarded directly, but at the moment when the next beacon is scheduled for transmission. We use piggybacking as the forwarding method because the Connect & Drive CACC application is fully based on the regular transmission of network-level beacons, and we wish to keep the required changes to the communication system as small as possible.

Event messages are routed upstream of the merging area based on a set of rules that determine whether a node should forward an event message or not. Either the full event message is attached, or only its identifier, or it is not attached at all. Rules are based on whether nodes are estimated to be inside the event area during the event time, or whether they will reach it too soon or too late. Although event messages are routed strictly in an upstream direction, and are destined for nodes that are travelling in the downstream direction only, nodes that are travelling upstream may also forward the event messages. The rules are as follows:

1. If a node is a destination node it will attach the event message identifier (field *id*) for as long as the data is valid, to indicate its receipt.
2. Both nodes travelling downstream and upstream attach the entire event message in its beacon if they have a one-hop neighbour node that is a destination node, but that node did not include the event message identifier in the beacon most recently received by the reference node.
3. A node travelling downstream will also attach the entire event message if *(i)* it is estimated to be in front of the event area during the entire event time, and *(ii)* it has following one-hop neighbours (i.e., nodes that are within transmission range of the reference node, travelling downstream but located further upstream), none of which are estimated to be behind the event area during the entire event time. If the node has no following one-hop neighbours behind it then the node will attach the event message every third beacon.

Using the above rules event messages are actively forwarded in the upstream direction by downstream travelling nodes, up to the point where the destination node is located or, in case there is no destination node, up to the point where the destination node would be located if there was one. The latter scenario is covered by rule (3.ii). Upstream travelling nodes carry the event message further upstream but only forward the messages when they encounter a destination node that does not indicate that it has received the event message in its beacon. This technique is generally referred to as store-carry-forward. It is a relatively slow dissemination technique because the speed with which messages are disseminated in an upstream direction is equal to the speed of the vehicles carrying the message. To allow the upstream travelling vehicles to disseminate the messages for a considerable distance the event message lifetime should accordingly be set high enough.

It may be the case that due to speed differences there are multiple destination nodes. Using the above rules the event message may initially only be routed to the slower moving destination node, as this node will be closer to the merging area and will be the node that is moving on the slower-most lane that the merging vehicle wants to merge in. Any faster moving destination node will be located further upstream. The faster moving destination node is not required to create a merging gap, because it will either be driving in the slow lane, in which case it will have to decelerate anyway because of the slower moving destination vehicle driving in front of it, or because it is driving in the fast lane, in which case it does not need to create a merging gap. In the latter case it should receive the event message however to be warned about the merging vehicle. The faster moving destination node will either receive the message by a node travelling upstream, or when it gains on the slower moving destination node. The slower moving destination node thus acts as a gate node, forwarding the event message to any new destination nodes.

Rule 1 and 2 together act as a reliability mechanism to ensure that a destination node will receive the event message. This is done to increase the probability that a merging gap will be created.

To see if the constrained geocast protocol specified here is able to meet application requirements *and* to route event messages only to that part of the network where they are needed we evaluate its performance in the next section.

5.3 Performance evaluation

In this section we evaluate the performance of the constrained geocast protocol in the context of the CACC merging application and see how well it performs. We have evaluated the protocol using a simulation study in which a CACC merging scenario is simulated and constrained geocast is used to route event messages. To compare its performance with standard geocast we have also evaluated the performance of two standard geocast protocols. We evaluate whether the constrained geocast protocol is able to route messages both effective and selective, as defined in the previous chapter, and compare its performance to that of the standard geocast protocols. Below we first describe the two standard geocast protocols, present our simulation scenario, list our performance metrics, and in the end discuss the results.

5.3.1 Standard geocast protocols

We have implemented two standard geocast protocols to support the CACC merging application and to compare the performance of the constrained geocast protocol with. We refer to the first protocol as the simple geocast protocol and to the second as the restricted geocast protocol. The protocols differ in their forwarding rules but use the same destination areas. The destination areas have been defined as strict as possible such that the network load is minimised as much as possible without affecting the effectiveness of the protocols, in this way allowing a fair comparison with the constrained geocast protocol.

Standard geocast

This is the basic geocast forwarding algorithm as specified in [3], although adapted here for piggybacking. With this protocol all event messages are given a geographic destination area. Any vehicle that has received an event message and that is inside the destination area schedules to piggyback the event message once on its next beacon. The RSU acts as the source but is not necessarily included in the destination area. The destination area covers the entire road (downstream and upstream lanes), starts at the end of the merging area, and runs upstream for a distance that is equal to the maximum distance that a highway vehicle is allowed to travel during the time it takes the merging vehicle to reach the merge area. I.e., if at t_0 the merging vehicle is estimated to arrive at the start of the merging area (a_1) at t_{start}, and the highway speed limit is v_{max}, the maximum distance is given by $v_{max} \cdot (t_{start} - t_0)$. Fig. 5.4 shows the destination areas for two approaching merging vehicles.

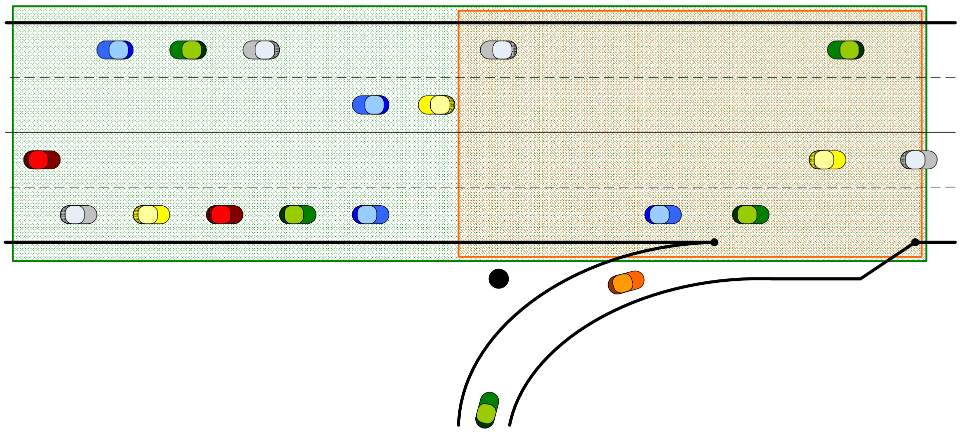

Figure 5.4: Destination areas for the two basic geocast protocols.

There may be multiple merging vehicles approaching the merging area at any one time. The RSU generates separate event messages for each approaching merging vehicle and each event message is routed separately. In [7] messages were routed using the simple geocast protocol as a single, aggregated event message, but it was shown that separate routing of event messages is more efficient because in this way event messages only reach those parts of the network where they are needed.

Restricted geocast

This protocol is based on the contention-based forwarding protocol specified in [3], although adapted here for piggybacking. With this protocol only nodes that are located progressively further upstream forward the event message.

Again all event messages are given a geographic destination area. Any vehicle that successfully receives an event message and that is inside the destination area schedules to forward the event message once by attaching it to its next scheduled beacon. However, if at the time of the next beacon the node has received the event message at least once from another node that is located further upstream (including the original sender), then it will cancel the forwarding of the event message. In this way the event message is forwarded in upstream direction only. The RSU acts as the source but is not necessarily included in the destination area.

The destination area is determined in the same way as for the simple geocast protocol. In [7] messages were routed using the restricted geocast protocol, both separately and aggregated. It was shown that separate routing of event messages gives a higher reliability. Event messages are therefore also routed separately here.

5.3.2 Simulation set-up

We have set up two simulation scenarios similar to the scenario shown in Fig. 5.1. We vary the number of road lanes and the node density per road lane to gauge the effect that the node density has on protocol performance, e.g., how scalable the protocols are and how their reliability is affected by changing densities. In the two-lane scenario there is one downstream lane and one upstream lane; in the four-lane scenario there are two downstream lanes and two upstream lanes. The RSU is located at the start of the merging area to ensure that it will be able to communicate directly with those CACC highway vehicles that are at the event area. The merging area has a length of 100 m. The maximum speed limit of all lanes is set to 120 km/h. Regarding the merging vehicle and the merging lane we assume the following. Merging vehicles approach every 7 seconds. After a merging vehicle has first been detected by the RSU it arrives at the start of the merging area 20 s later. Using Eq. (5.1) the size of the required merging gap (and thus of the event area), for the parameters chosen here, is always 45 m. The RSU generates and forwards new event messages every 6 seconds; accordingly $t_{lifetime}$ is also set to 6 s. We use this relatively high value for $t_{lifetime}$ to allow upstream travelling nodes to carry the information upstream, based on [7]. All nodes, including the RSU, beacon with a frequency of 1 Hz.

We have implemented our simulation scenario and the communication protocols in the OMNET++ 4.1 / MiXiM 1.2 network simulator [77] [79]. To model the behaviour of the IEEE 802.11p model as close as possible we have altered MiXiM's IEEE 802.11 MAC module in such a way that all parameters follow the IEEE 802.11p specification, although details in the 802.11p physical layer were abstracted from. Signal propagation is modelled using MiXiM's simple path loss model, with α set to 3.5, the center frequency set to 5.87 MHz, and the signal-to-noise ratio (SNR) threshold set to 0.1259. Propagation delay is ignored, and thermal noise is set to -110 dBm. All switching times were set to 0. In the MAC layer we set the access category to 0 and transmission speed to 3 Mbs, the most robust variant. The length of the transmission buffer is set to 14 packets, which is the default MiXiM value.

Packet sizes are as follows. A beacon is 3200 bits big. For each included event message 500 bits are added. For the constrained geocast protocol 10 bits are added for each included identifier.

Mobility is modelled using the intelligent driver model (IDM, see [88]). Mobility spacing is set to 6.7 m, acceleration to 0.73 m/s^2, deceleration to 1.67 m/s^2, and the acceleration exponent to 4. Vehicle lengths are set to 4 m and nodes are updated every 0.1 s. The desired velocity of vehicles has been adapted to meet the speed limits of a road lane.

The existence of line-of-sight (LOS) between a transmitter and receiver heavily influences the strength of the received signal. Recent experiments have shown that traffic on the road has a major impact on the existence of LOS and the resulting received signal strength. In for instance [14], [15] it can be seen how the probability of a successful transmission rapidly drops within the first few hundreds of meters due to obstruction of LOS by vehicles. Recent work has provided a propagation model that focuses on the effect of vehicles on the availability of LOS [89]. At the time when the simulation were performed however no such model was available. To still be able to emulate the effect traffic density has on the received signal strength, we use MiXiM's simple path loss model and vary the transmission power according to the traffic density. At the lowest density (5 veh./km/lane) the power is set to 1500mW, which gave a maximum communication range of 500 m. At higher densities power was varied between 77mW (200m) and 600mW (400m), to cover both a pessimistic and optimistic scenario. Additionally, ranges to where nodes were able to sense the medium as busy but unable to receive the packet were 100m (at 77mW), 200m (600mW), and 250m (1500mW).

5.3.3 Performance metrics

The main goals of our performance study are to determine *(i)* if the constrained geocast protocol is able to deliver event messages to destination nodes well in advance of those nodes reaching the event area, without delivering messages to parts of the network where they are not needed, and *(ii)* how the protocol performs with respect to standard geocast. Below we motivate our performance metrics.

The main requirement of the CACC merging application is that any CACC highway vehicle that is expected to be inside a merging vehicle's merging gap during the merging procedure receives an event message concerning the merging. Any such vehicle is therefore considered a destination node, and it should receive the event message well ahead of the merging area, so it has enough time to create a merging gap. The distance ahead of the merging area that a destination node receives it first event message is called the *notification distance*. Although we have not defined a minimum notification distance for the CACC merging application we do measure the notification distance of every destination node. To get an indication of the speed with which information is disseminated we also set the measured notification distance against the distance that the destination node was ahead of the merging area at the moment the RSU transmitted the event message. The difference between the two is the distance the destination node moved during the time it took to deliver the event message.

Note that although the CACC merging application requires a minimum notification distance, performance of the application does not necessarily improve if vehicles receive the notification further in advance, because the information contained in the event message has no practical use before this point.

The main aim of the constrained geocast concept is to route messages only to those parts of the network where they are needed, in this way reducing the load on the wireless medium. We therefore manually verify whether event messages are indeed only routed as far upstream as is needed to deliver them to the destination nodes when constrained geocast is used.

Because of the way that the scenario has been set up event messages are never routed further than 667 m upstream of the merging area with all three protocols. We therefore measure the *network load* on the wireless medium inside this region to compare how well the three protocols perform, i.e., we measure the percentage of time that a node inside the region on average experiences the medium to be busy.

Finally, to assess the reliability of the protocols we measure the percentage of all transmitted event messages that do not reach their destination node, called the *loss rate*.

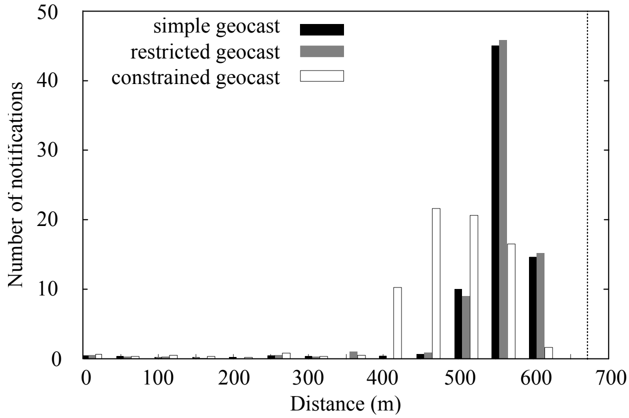

Figure 5.5: Notification distance for a two-lane scenario with a density of 10 v/km/lane. The dotted vertical line is the average distance between the RSU and the destination node at the time the RSU transmits the event message.

5.3.4 Results

In this section we evaluate *(i)* if the constrained geocast protocol is able to deliver event messages to destination nodes well in advance of those nodes reaching the event area, without delivering messages to parts of the network where they are not needed, and *(ii)* how the protocol performs with respect to the two standard geocast protocols. We start by making a number of general remarks that apply for each protocol and then discuss the performance of the constrained geocast protocol in detail and compare it with the two standard geocast protocols.

Note that for all shown mean results confidence intervals of the means have been left out but the 95% confidence intervals lie within 5 % of the shown means.

General remarks

Regardless of the protocol used the notification distance is determined by *(i)* the destination node's distance in advance of the merging area (and thus in advance of the RSU since it is located at the start of the merging area) at the moment the RSU transmits the first event message relating to a certain merging vehicle, and *(ii)* the end-to-end delay of forwarding this message from the RSU to the destination node.

The destination node's distance in advance of the merging area at the moment the RSU transmits the event message is defined by the speed of the highway nodes. The speed of highway vehicles, and consequently the distance from RSU to destination node, depends on the number of vehicles of the road. Fig. 5.5 shows a scenario in which traffic is free flowing at an average speed of around 120 km/h. Since an event message is first transmitted when the merging vehicle is 20 s away of the merging area the distance between RSU and destination node is around 670 m. As the vehicle density increases however highway traffic comes in a congested state causing vehicle speeds, as well as the resulting notification

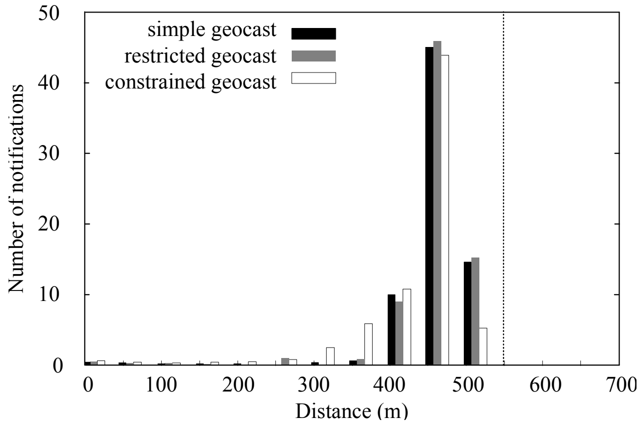

Figure 5.6: Notification distance for a two-lane scenario with a density of 50 v/km/lane. The dotted vertical line is the average distance between the RSU and the destination node at the time the RSU transmits the event message.

distance, to go down. Fig. 5.6 shows a scenario in which traffic is slightly congested and travels at speed of around 100 km/h. In this case the distance between RSU and destination node becomes less, around 560 m.

For a given distance between the RSU and a destination node the end-to-end delay to piggyback a message a certain distance is mainly determined by the beaconing frequency of the network nodes, the number of intermediate forwarding nodes, and the transmission range. During our experiments we have mainly varied the node density on the road (and to a lesser extent the transmission ranger, as a result of changing node densities). As the node densities increase more nodes act as intermediate forwarders and the forwarding delay between hops decreases, since the time it takes before a message is forwarded by a node becomes less as the number of forwarding nodes grows. This in turn leads to decreasing end-to-end delays and notification distances that lie closer to the RSU-to-destination-node distance at the moment the RSU transmits the event message. Although significantly less strong than the lessening RSU-to-destination-node distance due to decreasing node speeds, this effect can also be seen when comparing Fig. 5.5 and Fig. 5.6, albeit only limited.

Detailed discussion

Analysis of the results of the constrained geocast protocol show that the protocol is effective, especially in those crowded scenarios where the CACC merging application is most needed. However, although the protocol routes messages only to those parts of the network where they are needed, for this particular scenario constrained geocast does not significantly outperform the standard geocast protocols in terms of efficiency.

Verification of the simulation showed that with constrained geocast messages are routed as far upstream as is needed to deliver them to the destination nodes, and not any further. The constrained geocast protocol presented in this chapter is therefore able to meet the

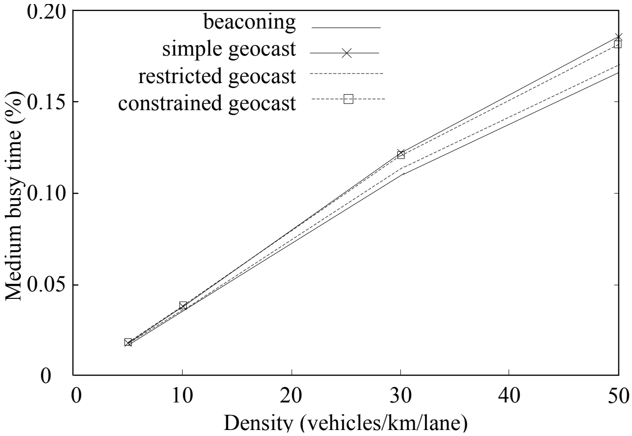

Figure 5.7: Network load for a two-lane scenario.

aim expressed in the previous chapter of only routing event messages to those parts of the network where they are needed. The advantage of this with respect to a standard geocast protocol is limited however because for this specific application, and with only a single flow of traffic, the destination area that is employed by the two standard geocast protocols is already quite selective (see Section 5.3.1). The standard geocast protocols therefore operate already quite efficient, sending messages only to that part of the network where they are needed. Moreover, inside this part of the network the network load of the constrained geocast protocol is relatively high due to the protocol's reliability mechanism: once an event message has been forwarded within transmission range of the destination node, every node that is within transmission range of the destination node will attach the event message to its beacon until it has received a beacon from the destination node indicating that it has received the event message (by attaching the event message's identifier to its beacon). Since no priority is given to the destination node's beacon, the event message may be forwarded by quite a large number of neighbouring nodes before the destination node has indicated that it has received the event message.

Comparing the network load of the three protocols we see the following trends. The added network load of each protocol with respect to the load of the beaconing protocol is relatively small. This is because of the small size of event messages compared to beacons and the fact that they are transmitted less often than beacons. The restricted geocast protocol adds the least amount of network load because of its restrictive forwarding rules: an event message is forwarded only a limited number of times with this protocol. The added network load of the constrained geocast protocol is comparable to that of the simple geocast protocol, and significantly higher than that of the restricted geocast protocol. These trends apply for all scenarios and have been visualised for a two-lane scenario in Fig. 5.7 and for a four-lane scenario with similar parameters in Fig. 5.8. Network loads increase roughly linearly with node density, as can also be seen when comparing the two figures.

The constrained geocast protocol is most effective in those scenarios where the CACC merging application is needed most, i.e., when node densities are high and inter-vehicle

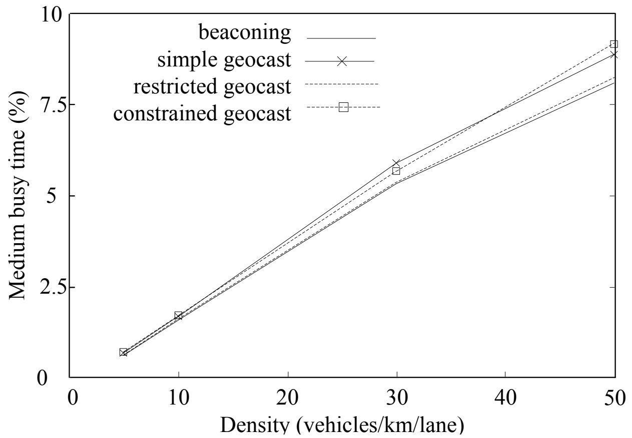

Figure 5.8: Network load for a four-lane scenario.

distances consequently short. In those scenarios the notification distance of the constrained geocast protocol is highest. When node densities grow sparse the protocol becomes less effective, leading to shorter notifications distances. In such situations inter-vehicle distances are already so large however that creating a merging gap for the merging vehicle is not a problem.

In scenarios where the node density is high the notification distance of the constrained geocast protocol is quite high as well, see for instance Fig. 5.6. CACC highway vehicles are therefore notified well in advance of the merging area that they should create a gap. The high notification distance is due to the increase in speed with which event messages are piggybacked when node densities go up, as was explained previously. When node densities decrease notification distances of the constrained geocast protocol become shorter, due to the decreasing speed with which event messages are piggybacked. As node densities become very low distances between vehicles become so large that communication gaps appear, i.e., nodes are no longer able to forward a message upstream. In these cases event messages must be carried upstream by upstream travelling nodes. This is a relatively slow method of disseminating information that leads to short notification distances, see for instance Fig. 5.5 In this two-lane scenario with a node density of 10 veh./km/lane CACC highway vehicles receive a notification distance a relative short distance in advance of the merging area. The figure also shows how notification distances become more variable; this is due to the increased variability of the end-to-end delay to disseminate an event message from RSU to destination node using upstream travelling nodes.

Comparing the notification distance of the three protocols we see the following trends. The notification distances of the two standard geo-broacast protocols are comparable and are always larger than the notification distance of the constrained geocast protocol. This is because with simple geocast and restricted geocast both downstream travelling nodes and upstream travelling nodes will actively forward an event message in the upstream direction, whereas with constrained geocast the upstream travelling nodes will only carry them for-

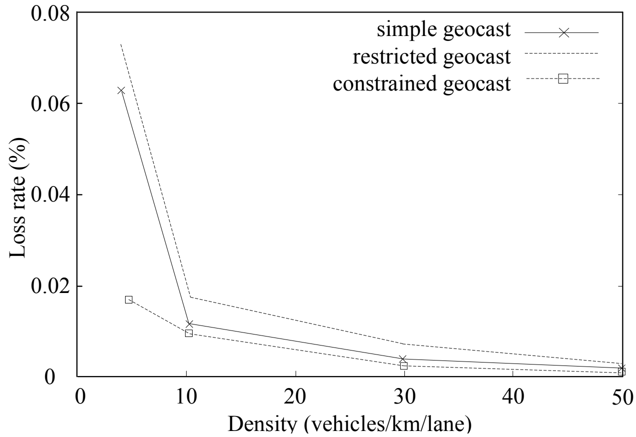

Figure 5.9: Loss rate of event messages for a two-lane scenario.

ward. In this way the number of nodes that piggyback the event messages with constrained geocast is effectively halved, thus increasing the end-to-end delay and decreasing the notification distance. This effect is strongest for low node densities, especially for those densities where the constrained geocast must employ upstream travelling nodes to bridge communication gaps between downstream travelling nodes, as can be seen in Fig. 5.5. For high node densities the absolute difference in end-to-end delay between the constrained geocast protocol and the two standard geocast protocols is so small that the resulting notification distances are comparable, see Fig. 5.6.

Due to its reliability mechanism the constrained geocast protocol has low loss rates (below 2 %) of event messages for all scenarios. Losses only occur in situations where there are no network nodes present to either actively forward or carry the event message to the destination node. For high node densities losses are therefore almost non-existent, see Fig. 5.9, which shows loss rates for the two-lane scenario, and Fig. 5.10, showing loss rates for a four-lane scenario. Loss rates of the two standard geocast protocols are comparably low for most scenarios, also below 2 %, except for very low node densities as can be seen in the two-lane scenario for a node density of 5 veh./km/lane. As neither of these protocols employs a reliability mechanism they both suffer from communication gaps caused by the high inter-vehicle distances in such scenarios. In such situations inter-vehicle distances are already so large however that creating a merging gap for the merging vehicle should not be a problem. Loss rates of the two standard geocast protocols decrease as node densities increase but never become as low as the constrained geocast protocol, since messages may still get lost due to transmission errors caused. The simple geocast protocol has lower loss rates than the restricted geocast protocol in all scenarios since messages are forwarded more often.

Finally, in our simulations we assume that highway vehicles do not exceed the maximum speed limit of 120 km/h. Should this happen however, then these destination vehicles are initially located well outside the standard geocast's destination area, see for example the second destination vehicle in Fig. 5.4. When messages are routed using standard

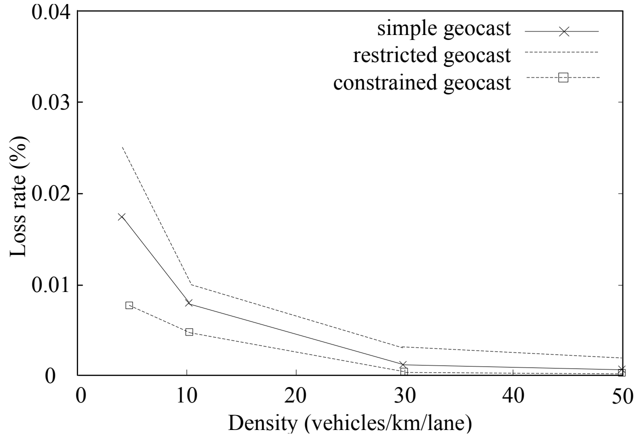

Figure 5.10: Loss rate of event messages for a four-lane scenario.

geocast these vehicle will initially therefore not receive any messages, not until they have approached the geocast destination area, or unless the destination area is increased. In contrast, with constrained geocast an event message will either be actively routed upstream by nodes that are aware of the far-away destination node, or it will be delivered by upstream travelling nodes that have carried the message upstream.

5.4 Conclusions

In this chapter we have presented a system to support automated CACC merging at a junction. The system senses approaching merging vehicles and informs the highway CACC vehicles of the arrival time of the merging vehicle at the merging area. When needed the CACC highway vehicles will then automatically create a gap in the flow of traffic to allow the merging vehicle to merge.

We have shown that the communication requirements of such an application of automated CACC merging at a junction are an example of constrained geocast, with the event area being defined by the merging gap required by the merging vehicle in the flow of highway traffic, and the time needed to perform the merging procedure. Any CACC highway vehicle that is expected to be inside the event area during the event time must be notified of this fact and must create a merging gap.

We have shown how to implement a constrained geocast protocol capable of routing messages to any node expected to be inside the event area during the event time. In this scenario messages are routed along a single flow of traffic, in the upstream direction, for as far as is needed to deliver them to the destination nodes. Event messages therefore only reach that part of the network where they are needed, which is the main goal of the constrained geocast concept. The methods used by this protocol, e.g., to estimate a vehicle's location at a future moment in time, can be applied in a similar manner to more complex constrained geocast scenarios in which multiple traffic flows are considered.

With automated CACC merging CACC highway vehicles must be explicitly notified to create a gap when inter-vehicle distances between highway vehicles are too small to allow a merging vehicle to merge inside the flow of traffic. The CACC merging application is therefore most needed in situations where node densities are average to high. Evaluation of the constrained geocast protocol by means of simulation shows that in those situations the protocol performs quite well, notifying vehicles well ahead of the merging area and delivering event messages with high probability. When node densities become less the protocol becomes less effective, warning destination nodes less far in advance of the merging area that they should create a gap. This is not a problem however as in these situations inter-vehicle distances are by definition quite large and it is not a problem for the merging vehicle to find a gap in the flow traffic to merge in.

Finally we have shown that in a scenario in which there is only a single flow of traffic and the event takes place only a limited time in the future, the advantage of using constrained geocast over a standard geocast protocol is limited. The main reason for this is because destination nodes are located quite close to the event area, along a single traffic flow, and as a result the destination area employed by the standard geocast protocol can be fitted quite accurately to deliver event messages only to that part of the network where they are needed. We believe however that in a more complex scenario where destination nodes may be located a greater distance away from the event area, be spread out over multiple traffic flows, and travelling at highly varying speeds, the increased uncertainty regarding the a priori location of destination nodes makes constrained geocast a more efficient method to route event messages.

Part III

Analytically modelling multi-hop forwarding protocols


TOSHIBA
Season's Greetings
DUNKIN' DONUTS
EGYPTAIR
Full flat bed seats
Daily non-stop to Cairo on EGYPTAIR
SONY
New York Police Dept

CHAPTER 6

Forwarding with random forwarding delays and fixed inter-node distances

In this chapter we present an analytical model that accurately describes the behaviour of a multi-hop location-based broadcast protocol (or [multi-hop] forwarding protocol for short) in a vehicular network when forwarding delays are either uniformly or exponentially distributed. The model covers the scenario in which a message is forwarded over a straight road with fixed inter-node distances and a fixed transmission range. For a given node density and source-to-sink distance, the model is able to capture the full distribution of *(i)* the delay of each hop, *(ii)* the length of each hop, *(iii)* the position of each forwarder, *(iv)* the required number of hops to cover the source-to-sink distance, and *(v)* the end-to-end delay to cover the source-to-sink distance.

As we will show in Section 6.1, when forwarding delays are distributed uniformly the forwarding protocol that we consider is functionally equivalent to a piggybacking protocol. With piggybacking messages are attached to, and transmitted along with, network-level beacons. It is a forwarding technique that is often used in vehicular networks to disseminate messages over multiple hops. Piggybacking was used in the previous chapter to disseminate event messages in an automated merging application. The insights gleaned in that work regarding the influence of network parameters on the performance of piggybacking served as motivation for the work presented in this chapter.

The outline of this chapter is as follows. We start by giving a short introduction of our analytical model in Section 6.1 and discuss related work on the analysis of multi-hop location-based broadcast protocols in vehicular networks in Section 6.2. The system model is presented in Section 6.3. The model analysis when forwarding delays are exponentially distributed is given in Section 6.4; the model analysis when forwarding delays are uniformly distributed is given in Section 6.5. We have verified our model analysis using extensive simulations; the simulation set-up is described in Section 6.6. We finally discuss the performance of our model in Section 6.6 and conclude the chapter in Section 6.7.

Image on previous page: cars queuing on Times Square, Manhattan, New York.

6.1 Introduction

In this chapter we analytically model the behaviour of a multi-hop location-based broadcast protocol in a vehicular network. Specifically we consider a scenario in which nodes are spread out over a straight line with the source at one end and a single sink at the other end[1]. The source node initiates the forwarding by broadcasting an application message. The message has a geographically defined destination address which is the position of the sink. All nodes apply the following forwarding rule: when a node receives a message for the first time, and the node is positioned closer to the sink than the previous sender, the node draws a time delay t from the forwarding delay distribution $T_{forwarding}$, and schedules to rebroadcast the message after t seconds. If before that time the node receives the message from another node that is positioned closer to the sink than the node itself, then the node will cancel the scheduled rebroadcast.

Multi-hop broadcast protocols such as these, in which nodes all have an identically distributed forwarding delays, are often employed by delay tolerant flooding protocols. These are protocols that aim to deliver information to all nodes within a certain region but that do not have strict delay requirements. In vehicular networks such flooding protocols are used to disseminate non-safety local traffic information, such as the average speed on the road or dangerous road conditions [33] [37].

Although multiple studies exist on analytically modelling multi-hop forwarding in wireless networks, so far we have not found any models that use assumptions that apply to our scenario, especially regarding the distribution of the forwarding delay. Moreover, existing models mainly target network connectivity, dissemination reliability, or give bounds on the end-to-end delay. We discuss some of these models in the next section.

The contribution of this chapter is an analytical model that expresses the performance of a multi-hop location-based broadcast protocol as presented above in terms of insightful and fast-to-evaluate formulas. Our model covers the scenario in which a message is forwarded a certain distance over a straight road, assuming fixed inter-node distances and a fixed transmission range. Forwarding delays are distributed either uniformly or exponentially. For each performance metric the full distribution is given, allowing us to express, a.o., the probability of having received a message within a certain time interval. In particular, for a given source-to-sink distance, transmission range, and forwarding delay distribution, the model gives expressions of the following performance metrics:

1. the distribution of the delay of each hop;
2. the distribution of the length of each hop;
3. the distribution of the position of the n^{th} forwarder;
4. the distribution of the required number of hops to reach the sink;
5. the distribution of the end-to-end delay.

When forwarding delays are exponentially distributed these performance metrics are expressed in closed form. Verification of the model by means of extensive simulation shows that results are accurate to within a few percent for distances up to ten times the transmission range.

[1] There may be multiple sinks but we consider each sink separately.

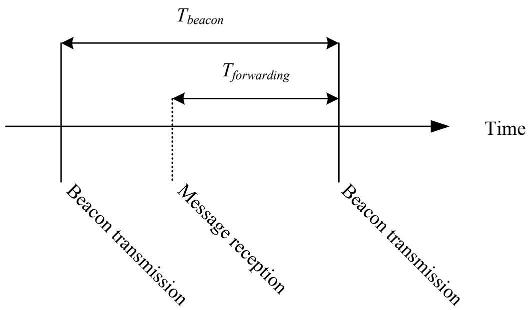

Figure 6.1: The relation between the timing parameters of a piggyback protocol (T_{beacon}) and a multi-hop forwarding protocol ($T_{forwarding}$).

When forwarding delays are distributed uniformly the forwarding protocol presented above is functionally equivalent to a piggybacking protocol. Here we briefly explain how the two protocols are equivalent and how the model presented in this chapter can be applied to model piggybacking. With piggybacking messages are attached to, and transmitted along with, network-level beacons. Beacons are typically sent at a fixed interval, e.g., every T_{beacon} seconds. When nodes receive a message they will attach it to their next scheduled beacon. The delay between the moment the node first receives the message and the moment it will forward it is therefore uniformly distributed between 0 and T_{beacon}, see Fig. 6.1 The analytical model that we present in this chapter can therefore be applied to model a piggybacking protocol by assuming $T_{forwarding}$ to be uniformly distributed between 0 and T_{beacon}.

In the next section we discuss briefly some of the work that has been performed on analytically modelling a multi-hop forwarding protocol. After that we present our forwarding model.

6.2 Related work

Although there is a plethora of performance studies on multi-hop forwarding protocols in vehicular networks, practically all of these studies are simulation based. What analytical studies there are contain overly simplified assumptions and often only focus on a limited number of performance metrics such as the network connectivity [90] [91] [92], without giving a full description of the end-to-end behaviour of a protocol. Below we give a brief overview of a number of analytical studies that we found to be the most relevant regarding multi-hop forwarding, and discuss their applicability to our forwarding scenario. It is the same body of work that is discussed in Chapters 7 and 8 but their applicability to the current forwarding protocol differs.

In [93] a scenario is considered in which a message is forwarded by means of broadcast transmissions over a straight line with fixed inter-node distances. Regarding single-hop transmissions all nodes within a certain range from the sender have the same probability

p ($0 \leq p \leq 1$) of correctly receiving the message in absence of interference. Interference of transmissions may be taken into account and if so will result in a loss. The model gives bounds on the end-to-end delay for an idealised dissemination strategy which ignores interference, and for two provably near-optimal dissemination strategies when interference is taken into account, none of which apply to our forwarding protocol.

In [94] the end-to-end delay of an emergency message dissemination protocol is analytically calculated. A unit-disc single-hop transmission model and exponentially distributed inter-node distances are assumed. Nodes are assumed to have formed communication clusters with each cluster of nodes having a cluster head node. All forwarding is done by the head nodes, which makes it relatively easy to calculate the end-to-end delay. This method of forwarding does not apply to our forwarding protocol however.

In [95] again a straight road with exponentially distributed inter-node distances and a unit-disc single-hop communication model are considered. Nodes that receive a message will forward the message with a certain probability p ($0 \leq p \leq 1$), making the approach of this work somewhat similar to [93]. The model gives bounds on the maximum end-to-end delay and shows that the value of p that gives the lowest end-to-end delay depends on the network density. A similar result was shown in [93]. The forwarding protocol assumed in this work does not apply to our forwarding protocol.

In [96] the required number of hops to disseminate a message from source to sink is analytically modelled in the context of a wireless sensor network. Nodes are again spread out over a straight line with exponentially distributed inter-node distances and the unit-disc model is again assumed for single-hop transmission. Multi-hop forwarding is assumed to go in synchronised communication rounds in which the node that has received the message and is positioned farthest in the direction of the sink forwards the message, similar to the forwarding protocol assumed in Chapter 8. It does not apply to the forwarding protocol assumed in this chapter however. The model gives approximations of the distance that a message has been forwarded for a given number communication rounds as well as the network connectivity as a function of the source-to-sink distance. The work does not address the delay to deliver a message to the sink. The model is quite accurate for high node densities and large distances but less so when densities are low and distances are short.

As can be seen none of the analytical models discussed can be applied to model our forwarding protocol, as their forwarding rules do not apply to ours. In the next sections we therefore present our system model and model analysis.

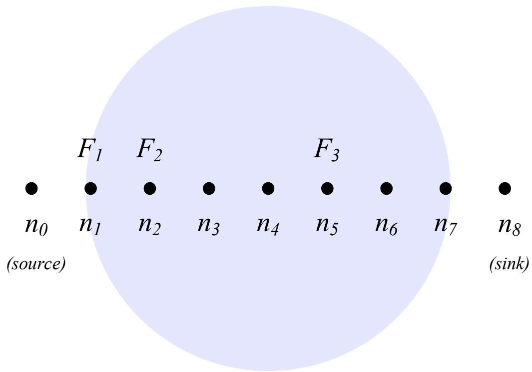

Figure 6.2: The system model with the eighth node being the sink and $R = 3$. The transmission range is shown for node 4.

6.3 The system model

In this section we present our forwarding model and introduce some definitions and notation that we use in our analysis.

Forwarding is done as described in Section 6.1. We model two different forwarding delay distributions $T_{forwarding}$ (in seconds): the first is exponentially distributed with mean T_d, the second is uniformly distributed between 0 and T_d.

Nodes are equidistantly spaced over a straight line with the source at one end and the sink at the other end. Nodes are numbered in ascending order from source to sink, node 0 being the source. Nodes are static: they remain at their position. Nodes all have the same transmission range R, R being the number of nodes in a given direction that receive a transmission with success probability 1; outside this range the success probability is 0. We thus ignore any transmission effects such as fading or interference. All delays related to transmitting and processing a signal (i.e., transmission delay, switching times, etc.) are furthermore set to zero.

The n^{th} forwarder is the node that retransmits the message for the n^{th} time after the source's original transmission; it is denoted F_n. Although not a forwarder since it originates the message, the source node is referred to as the 0^{th} forwarder, i.e., $F_0 = 0$. The n^{th} hop refers to the transmission made by the $(n-1)^{th}$ forwarder, i.e., the source's transmission is the first hop. The hop length of the n^{th} hop L_n is defined as the difference in position between the n^{th} forwarder and the $(n-1)^{th}$ forwarder, i.e., $L_n = F_n - F_{n-1}$. The hop delay D_n of the n^{th} hop refers to the time between the moment the $n - 1^{th}$ forwarder transmits the message and the moment the n^{th} forwarder transmits the message. The number of hops required to have the message forwarded by a node at or beyond position i is denoted N_i. The end-to-end delay to have the message forwarded by a node at or beyond position i is denoted E_i and is the sum of the required number of hops, given by $E_i = \sum_{n=1}^{N_i} D_n$.

Note that for a sink node at position i to receive the message, the message should be forwarded by a node at or beyond position $i - R$. We will therefore typically calculate the distribution of N_{i-R} and E_{i-R}. In the example shown in Fig. 6.2, $F_0 = 0$, $F_1 = 1$, $F_2 = 2$, and $F_3 = 5$; hence, $L_1 = 1$, $L_2 = 1$, and $L_3 = 3$. Furthermore, $N_5 = 3$, and $E_5 = D_1 + D_2 + D_3$.

Each time the message has been forwarded there will be a set of nodes that have all received the message and are all positioned closer to the sink node than the most recent forwarder. Since one of these nodes will become the next forwarder we call these nodes *candidate forwarders*, and the candidate forwarders to become the n^{th} forwarder the candidate n^{th} forwarders. The set of candidate forwarders is by definition of size R, except if the distance between the last forwarder and the sink is less than R. We ignore this last effect however, since in that case the sink has already received the message. In Fig. 6.2 the set of candidate first forwarders consists of the nodes 1, 2, and 3, the set of candidate second forwarders consists of nodes 2, 3, and 4, the set of candidate third forwarders consists of nodes 3, 4, and 5, and the set of candidate fourth forwarders consists of nodes 6, 7, and 8.

In the next two sections we first analyse our model when forwarding delays are exponentially distributed and then when they are distributed uniformly. As we will see both cases require their own approach.

6.4 Analysis with exponentially distributed forwarding delays

In this section we analyse our forwarding model, as presented in the previous section, when the forwarding delay distribution $T_{forwarding}$ is exponentially distributed with mean T_d. We calculate the distribution of the hop delays D_n in Section 6.4.1 and the distribution of the hop lengths L_n in Section 6.4.2. Using the latter result we calculate the distribution of the position of the n^{th} forwarder in Section 6.4.3 and the distribution of the required number of hops N_i to reach the sink node at position i in Section 6.4.4. Finally we combine these distributions to determine the distribution of the end-to-end delay E_i in Section 6.4.5.

6.4.1 Delay per hop

Let D_n be the delay of the n^{th} hop. In this section we determine D_n for $n \in \mathbb{N}^+$.

Let $t_{start} = 0$ be the moment that the source forwards the message; this is defined as the first hop. D_1 is thus the time between t_{start} and the first time the message is retransmitted by the first forwarder. After the source has transmitted the message at t_{start} there are R candidate forwarders (in Figure 6.2 nodes n_1,n_2, and n_3 are the candidate first forwarders). Each of these candidate forwarders draws a forwarding delay that is exponentially distributed with mean T_d. The candidate forwarder with the shortest forwarding delay forwards the message. The delay of the first hop, D_1, is therefore distributed as the minimum value of R exponentially distributed delays with mean T_d. This is itself exponentially distributed with mean $\frac{T_d}{R}$.

To calculate D_2 we are again interested in the moment when one of R nodes beacons for the first time. It is important to note here that some of the candidate forwarders may have received the message twice (from the source node and from the first forwarder), while the other nodes have only received it once (from the first forwarder). A part of the former group's forwarding delay has thus already passed. However, due to the memorylessness of the exponential distribution, this does not affect the distribution of the remaining forwarding delay of these nodes. The distribution of D_2 is therefore equal to the distribution of D_1. Since this argument applies for each hop we can state that the delays of successive hops are independent and identically exponentially distributed with mean $\frac{T_d}{R}$:

$$D_n \sim \text{Exp}(\frac{T_d}{R}),\ n \in \mathbb{N}+ . \tag{6.1}$$

6.4.2 Length of a hop

In this section we determine the length of the n^{th} hop L_n for $n \in \mathbb{N}^+$.

For every hop n there are R candidate n^{th} forwarders. The node that acts as the n^{th} forwarder is the candidate n^{th} forwarder that has the smallest forwarding delay. Since the distribution of the forwarding delay is i.i.d. for each hop and for each node, each candidate n^{th} forwarder has equal probability of becoming the n^{th} forwarder. L_n is therefore i.i.d. and given by

$$L_n \sim U(1, 2, \ldots, R),\ \ n \in \mathbb{N}^+, \tag{6.2}$$

where $U(1, 2, \ldots, R)$ denotes a discrete uniform distribution over the range $1, 2, \ldots, R$.

6.4.3 Position of the forwarder

In this section we determine the position of the node that is the n^{th} forwarder F_n for $n \in \mathbb{N}^+$.

Because the distribution of the hop length is i.i.d., the distribution of F_n is equal to the n-fold convolution of L_n, i.e.,

$$F_n = \sum_{j=1}^{n} L_j,\ \ n \in \mathbb{N}^+. \tag{6.3}$$

using the explicit expression for the n-fold convolution of a discrete uniform distribution derived in [97] we find:

$$P(F_n = f_n) = \frac{1}{R^n} \sum_{j=0}^{\lfloor f_n/R \rfloor} (-1)^j \binom{n}{j} \binom{i + f_n - R \cdot j - 1}{i - 1}. \tag{6.4}$$

6.4.4 Required number of hops

In this section we determine the required number of hops to have the message forwarded by a node at or beyond position i, denoted N_i for $i \in \mathbb{N}^+$. We give two methods to determine N_i. The first method uses the distribution of F_n and can be used regardless of the expected required number of hops. In the second method N_i is modelled as a renewal process; this method should be used if the expected required number of hops is high.

The position of the n^{th} forwarder is the sum of n hop lengths, see Eq. (6.3). For arbitrary values of $i > 0$ we can thus state

$$P(N_i \geq n) = P(F_n \leq i) = P(L_1 + \cdots + L_n \leq i). \tag{6.5}$$

Writing

$$P(F_n \leq i) = \sum_{f_n=0}^{f_n=i} P(F_n = f_n), \tag{6.6}$$

we can again use Eq. (6.4) to calculate the right-hand side of Eq. (6.5). According to [98] (page 5), when i becomes large, N_i has asymptotically the following normal distribution:

$$N_i \sim N(\frac{i}{\mu_{L_n}}, \sigma^2_{L_n} \frac{i}{(\mu_{L_n})^3}), \tag{6.7}$$

where μ_{L_n} and $\sigma^2_{L_n}$ are the mean and variance of the length of an individual hop, which can easily be calculated from Eq. (6.2).

When we calculate N_i in our discussion in Section 6.6 we use Eq. (6.6) when $i \leq 2R$, else we use Eq. (6.7).

Note that N_i denotes the required number of hops to have the message forwarded by a node at or beyond position i, but to have a sink node at position j receive the message one of nodes $n_{j-R}, \ldots, n_{j-1}$ must transmit the message. To calculate the required number of hops to have the message delivered at the sink node at position j we therefore determine the distribution of N_{j-R}.

6.4.5 End-to-end delay

Let E_i denote the end-to-end delay to have the message forwarded by a node at or beyond position i. In this section we determine E_i for $i \in \mathbb{N}^+$.

E_i is a function of the number of hops required to have the message forwarded by a node at or beyond position i (N_i) and the delay per hop (D_n):

$$E_i = \sum_{n=1}^{N_i} D_n. \tag{6.8}$$

Since the delay per hop is independent and identically exponentially distributed with mean $\frac{T_d}{R}$ the total delay for k hops is given by the Erlang distribution. The minimum number of hops required to have the message forwarded by a node at or beyond position i is $\lfloor \frac{i}{R} \rfloor$, the maximum is i. Since the length of a hop is i.i.d. the probability density function (PDF) of E_i is given by summing over all possible hop counts n:

$$f_{E_i}(t) = \sum_{n=\lfloor \frac{i}{R} \rfloor}^{i} P(N_i = n) \cdot \lambda^n \frac{t^{n-1}}{(n-1)!} e^{(-\lambda t)}, \quad t \geq 0, \quad i \in \mathbb{N}^+, \tag{6.9}$$

with the latter part of the equation being the Erlang distribution for n hops and rate $\lambda = \frac{T_d}{R}$.

6.5 Analysis with uniformly distributed forwarding delays

In this section we analyse our forwarding model when the forwarding delay distribution $T_{forwarding}$ is uniformly distributed between 0 and T_d. This relates to the use of a piggy-backing protocol with deterministic inter-beacon periods of length T_d. We first describe our approach in more general terms and then calculate the specific performance metrics.

We saw in the previous section that when forwarding delays are distributed exponentially the successive hop lengths are identically, discrete uniformly distributed. Therefore the required number of hops to reach the sink can be expressed as a simple convolution. Similarly, the hop delays are identically, independently, and exponentially distributed, which allows us to use the Erlang distribution to calculate the end-to-end delay for a given number of hops.

When forwarding delays are distributed uniformly however neither the hop lengths nor the hop delays are i.i.d, so we cannot take the same approach. Because both the hop length and the hop delay depend on the length and delay of *all* preceding hops, they must be explicitly calculated for each hop. This becomes rather complex and resource-intensive after the first few hops. For the delay of the third hop (and following hops) we therefore assume that it is independently distributed, identical to the distribution of the second hop. This allows us to express the end-to-end delay beyond the second hop as a convolution of i.i.d. hop delays. For the length of the fourth hop (and following hops) we furthermore assume that it is independently distributed, identical to the distribution of the third hop. This allows us to express the required number of hops to reach the sink beyond the third hop as a convolution of i.i.d. hop lengths. The validity of this assumption is evaluated in Section 6.6.

Our approach in this section is as follows. In Section 6.5.1 we calculate the distribution of the hop delay for the first two hops; we assume that the delay per hop of following hops is distributed identical to the hop delay of the second hop. In Section 6.5.2 we calculate the distribution of the position of the forwarder for the first three hops. Using this, we calculate the distribution of the hop length for the first three hops in Section 6.5.3; we assume that the hop length of following hops is distributed identical to the hop length of the third hop. Using this latter assumption we then approximate the distribution of the position of the fourth and following forwarders in Section 6.5.4. In Section 6.5.5 we calculate the required number of hops to reach the sink node: for the first three hops we use the distribution of the forwarder that was calculated in Section 6.5.2, the following hops are approximated as a convolution of i.i.d. hop lengths. Finally in Section 6.5.6 we calculate the distribution of the end-to-end delay: for the first hop we use the distributions of D_1 and D_2, the delay of following hops is expressed as a convolution of i.i.d. delays that are each distributed identically to D_2.

6.5.1 Delay per hop

We first consider the first-hop delay D_1, which is defined as the time between the moment that the source transmits the message and the moment the first forwarder transmits the message. After the source has transmitted the message at t_{start} there are R candidate first forwarders. Each of these candidate first forwarders draws a forwarding delay that is uniformly distributed between 0 and T_d. The cumulative probability function (CDF) of a random variable U that is uniformly distributed between a and b is given by

$$F_{U(a,b)}(t) = \frac{t-a}{b-a},\ a \leq t \leq b, \tag{6.10}$$

with $F_{U(a,b)}(t) = 0$ for $t < a$ and $F_{U(a,b)}(t) = 1$ for $t > b$. We state its general form here because we will need it later on. The CDF of the forwarding delay of a candidate first forwarder is thus given by $F_{U(0,T_d)}(t)$.

D_1 is distributed as the minimum value of R uniformly distributed forwarding delays, a distribution that is well known [99]. Because we will need this distribution as well later on we again state its general form here. Let U_{min} be the minimum value of k forwarding delays, each distributed uniformly between a and b. Its CDF is given by

$$F_{U_{min}}(t,a,b,k) = 1 - \Big(1 - \frac{t-a}{b-a}\Big)^k, \quad a \leq t \leq b. \tag{6.11}$$

with $F_{U_{min}}(t,a,b,k) = 0$ for $t < a$ and $F_{U_{min}}(t,a,b,k) = 1$ for $t > b$. The CDF of D_1 is then given by

$$F_{D_1}(d_1) = F_{U_{min}}(d_1, 0, T_d, R). \tag{6.12}$$

$F_{U_{min}}(t,a,b,k)$ gives the probability that *at least one* of k nodes will have forwarded the message in the period $\langle a, t]$. Because we will have need of it later on we define U_{max} as the probability that *none* of k nodes will have forwarded the message in this period, which is given by

$$F_{U_{max}}(t,a,b,k) = 1 - F_{U_{min}}(t,a,b,k). \tag{6.13}$$

When we want to determine the distribution of the second-hop delay D_2, which is defined as the time between the moment the first forwarder transmits the message and the moment the second forwarder transmits the message, we can no longer assume that forwarding delays of all the candidate second forwarders are i.i.d. The distribution of a candidate second forwarder's forwarding delay depends on whether the candidate forwarder received the message for the first time in the first hop from the source (such as is the case for the candidate second forwarder nodes 2 and 3 in the example in Fig. 6.2) or in the second hop from the first forwarder (such as is the case for the candidate second forwarder node 4 in Fig. 6.2). If it received the message for the first time from the first forwarder then its distribution is again uniformly distributed between 0 and T_d. If it already received the message from the source then the delay of the first hop must be taken into account: let d_1 be the delay of the first hop, then the *residual* forwarding delay of the candidate forwarder is uniformly distributed between 0 and $T_d - d_1$. We denote the set of candidate second forwarders that received the message from the source as $c_{2,0}$ and the set of candidate second forwarders that received the message for the first time from the first forwarder as $c_{2,1}$. The size of both of these sets is determined by the position of the first forwarder. For a given position of the first forwarder f_1 and a given delay of the first hop d_1 the CDF of D_2 for $0 \leq d_2 \leq T_d$ is then given by

$$F_{D_2}(d_2, f_1, d_1) = 1 - F_{U_{max}}(d_2, T_d - d_1, |c_{2,0}|) F_{U_{max}}(d_2, T_d, |c_{2,1}|), \tag{6.14}$$

with $F_{D_2}(d_2, f_1, d_1) = 0$ for $d_2 < 0$ and $F_{D_2}(d_2, f_1, d_1) = 1$ for $d_2 > T_d$.
$F_{U_{max}}(d_2, T_d - d_1, |c_{2,0}|)$ is the probability that none of the candidate second forwarders that first received the message from the source forwards the message in the interval $[d_1, d_2]$, $F_{U_{max}}(d_2, T_d, |c_{2,1}|)$ is the probability that none of the candidate second forwarders that first received the message from the first forwarder forwards the message in the interval $[d_1, d_1 + d_2]$, and the term $\left(1 - F_{U_{max}}(d_2, T_d - d_1, |c_{2,0}|)\; F_{U_{max}}(d_2, T_d, |c_{2,1}|)\right)$ expresses therefore the probability that at least one of the candidate second forwarders will have forwarded the message in the interval $[d_1, d_1 + d_2]$.

Taking into account all possible positions of the first forwarder and all possible delays of the first hop the CDF of D_2 for $0 \leq d_2 \leq T_d$ is given by

$$F_{D_2}(d_2) = \sum_{f_1=1}^{R} P(F_1 = f_1) \int_{d_1=0}^{T_d} f_{D_1}(d_1)\; F_{D_2}(d_2, f_1, d_1)\; \mathrm{d}d_1, \tag{6.15}$$

with $F_{D_2}(d_2) = 0$ for $d_2 < 0$, $F_{D_2}(d_2) = 1$ for $d_2 > T_d$, and $P(F_1 = f_1)$ being the probability that the node f_1 becomes the first forwarder. How to calculate this is tackled in the next section.

To calculate the distribution of D_3, D_4, etc., it is again necessary to take the distributions of the delays of the previous hops into account, as well as the positions of the previous forwarders. Calculating these distributions becomes resource-intensive for the third and following hops. As we will show in Section 6.6 however the distribution of D_n converges and, for the purpose of our model, does not change significantly beyond the second hop. For the remainder of our analysis we therefore state that the distribution of the delay of the third and following hops is identical to the distribution of the delay of the second hop, i.e.,

$$F_{D_n}(\cdot) \sim F_{D_2}(\cdot),\; n = 3, 4, \ldots. \tag{6.16}$$

6.5.2 Position of the forwarder for $n \leq 3$

We determine the position of the n^{th} forwarder F_n for $n \leq 3$. Calculating the distribution of the position of the forwarder becomes more complex with each following hop; for this reason we give an approximate method to calculate F_n for $n > 3$ in Section 6.5.4.

The distribution of F_n depends on two factors. The first factor is the set of positions of the previous forwarders. This determines the set of candidate n^{th} forwarders. The second factor is the set of delays of the previous $n - 1$ hops. These previous delays determine the distributions of the (residual) forwarding delays of the candidate n^{th} forwarders. Below we calculate in an iterative manner the distribution of the first three forwarders by taking into account for each hop all the possible positions of the previous forwarders and all the possible delays of the previous hops.

Calculating $\mathbb{P}(F_1 = f_1)$

To calculate the distribution of the position of the first forwarder no previous hops need to be taken into account. After the source has initially broadcasted the message all candidate first forwarders have an identical forwarding delay distribution. The probability that a candidate first forwarder will have the shortest forwarding delay is therefore equal for all candidate forwarders, so we can state

$$\mathbb{P}(F_1 = f_1) = \frac{1}{R}, \quad 1 \leq f_n \leq R. \tag{6.17}$$

Calculating $\mathbb{P}(F_2 = f_2)$

To calculate the distribution of the position of the second forwarder we need to take into account the position of the first forwarder and the delay of the first hop. This dependency is given by

$$\mathbb{P}(F_2 = f_2) = \sum_{f_1=1}^{R} \mathbb{P}(F_1 = f_1) \int_{d_1=0}^{T_d} f_{D_1}(d_1) \ \mathbb{P}(F_2 = f_2 \mid F_1 = f_1 \wedge D_1 = d_1) \, \mathrm{d}d_1. \tag{6.18}$$

The term $\mathbb{P}(F_2 = f_2 \mid F_1 = f_1 \wedge D_1 = d_1)$ is equal to the probability that the candidate second forwarder at position f_2 has a smaller (residual) forwarding delay than all the other candidate second forwarders, given that the first forwarder is at position f_1 and given that the first-hop delay is d_1. We calculate this in the following way. The set of candidate second forwarders, excluding the candidate forwarder at position f_2, is referred to as the set of *remaining* candidate second forwarders and is denoted $\bar{c}_2$. Let T_{f_2} be the distribution of the (residual) forwarding delay of the node at position f_2, and let $T_{\bar{c}_2}$ be the distribution of the minimum value of the (residual) forwarding delays of all the nodes in the set $\bar{c}_2$. The term $\mathbb{P}(F_2 = f_2 \mid F_1 = f_1 \wedge D_1 = d_1)$ can thus be expressed as

$$\mathbb{P}(F_2 = f_2 \mid F_1 = f_1 \wedge D_1 = d_1) = \mathbb{P}(T_{f_2} < T_{\bar{c}_2} \mid F_1 = f_1 \wedge D_1 = d_1). \tag{6.19}$$

To calculate $\mathbb{P}(T_{f_2} < T_{\bar{c}_2} \mid F_1 = f_1 \wedge D_1 = d_1)$ we integrate over all possible values of T_{f_2} multiplied by the probability that $T_{\bar{c}_2}$ has a larger value:

$$\mathbb{P}(T_{f_2} < T_{\bar{c}_2} \mid F_1 = f_1 \wedge D_1 = d_1) = \int_{t_2=0}^{T_d} f_{T_{f_2}}(t_2, f_1, d_1) \Big(1 - F_{T_{\bar{c}_2}}(t_2, f_1, d_1)\Big) \, \mathrm{d}t_2. \tag{6.20}$$

We thus need to determine the distribution of T_{f_2} and $T_{\bar{c}_2}$. The distribution of the (residual) forwarding delay of a candidate second forwarder depends on whether the node first received the message in the first hop or in the second hop and, if it first received the message in the second hop, on the delay of the first hop. We first show how to calculate the distribution of T_{f_2}, then how to calculate the distribution of $T_{\bar{c}_2}$.

If the candidate second forwarder at position f_2 received the message for the first time in the second hop then its forwarding delay T_{f_2} is uniformly distributed between 0 and T_d. If the candidate second forwarder first received the message in the first hop then it must take the delay of the first hop into account. For a given first-hop delay d_1, T_{f_2} is then uniformly distributed between 0 and $T_d - d_1$. Hence, for a given first-hop delay d_1 the CDF of T_{f_2} for $0 \leq t_2 \leq T_d$ is then given by

$$F_{T_{f_2}}(t_2, d_1) = \begin{cases} F_{U_{0,T_d}}(t_2) & f_2 > R \\ F_{U(0,T_d-d_1)}(t_2) & 0 < f_2 \leq R, \end{cases} \tag{6.21}$$

with $F_{T_{f_2}}(t_2, d_1) = 0$ for $t < 0$, $F_{T_{f_2}}(t_2, d_1) = 1$ for $t > T_d$.

$T_{\bar{c}_2}$ is distributed as the minimum value of the (residual) forwarding delays of all the remaining candidate second forwarders. For ease of notation we subdivide the set of remaining candidate second forwarders $\bar{c}_2$ into different subsets of nodes that all received the message from the same forwarder. We denote the set of remaining candidate second forwarders that first received the message in the first hop from the source as $\bar{c}_{2,0}$, the set of remaining candidate forwarders that received the message in the second hop from the first forwarder as $\bar{c}_{2,1}$. The size of these sets depends on the position of the first forwarder. All nodes in a set have identically distributed (residual) forwarding delays. For a given position of the first forwarder f_1 and a given first-hop delay d_1 the CDF of $T_{\bar{c}_2}$ for $0 \leq t_2 \leq T_d$ is then given by

$$F_{T_{\bar{c}_2}}(t_2, f_1, d_1) = 1 - F_{U_{max}}(t_2, T_d, |\bar{c}_{2,1}|)\, F_{U_{max}}(t_2, T_d - d_1, |\bar{c}_{2,0}|), \tag{6.22}$$

with $F_{T_{\bar{c}_2}}(t_2, f_1, d_1) = 0$ for $t_2 < 0$, $F_{T_{\bar{c}_2}}(t, f_1, d_1) = 1$ for $t_2 > T_d$, $|\bar{c}_{2,j}|$ being the number of candidate forwarders in the set $\bar{c}_{2,j}$. The term $F_{U_{max}}(t_2, T_d, |\bar{c}_{2,1}|) \cdot F_{U_{max}}(t_2, T_d - d_1, |\bar{c}_{2,0}|)$ expresses the probability that none of the remaining candidate second forwarders will have forwarded the message in the interval $[d_1, t_2]$.

Substituting Eq. (6.21) and Eq. (6.22) in Eq. (6.20) we thus have an expression for $\mathbb{P}(F_2 = f_2)$.

Calculating $\mathbb{P}(F_3 = f_3)$

To calculate the distribution of the position of the third forwarder we need to take in to account the position of the first two forwarders and the delays of the first two hops. This dependency is given by

$$\begin{aligned} \mathbb{P}(F_3 = f_3) = \sum_{f_1=1}^{R} \mathbb{P}(F_1 = f_1) \int_{d_1=0}^{T_d} f_{D_1}(d_1) \cdot \\ \sum_{f_2=f_1+1}^{f_1+R} \mathbb{P}(F_2 = f_2 \mid F_1 = f_1 \wedge D_1 = d_1) \int_{d_2=0}^{T_d} f_{D_2}(d_2, f_1, d_1) \cdot \\ \mathbb{P}(F_3 = f_3 \mid F_1 = f_1 \wedge D_1 = d_1 \wedge F_2 = f_2 \wedge D_2 = d_2), \end{aligned} \tag{6.23}$$

with $f_{D_2}(d_2, f_1, d_1)$ being the PDF of D_2, for a given position of the first forwarder and a given delay of the first hop, which can easily be derived from Eq. (6.14). The last term of Eq. (6.23) is equal to the probability that the candidate third forwarder at position f_3

has a smaller (residual) forwarding delay than all the other candidate third forwarders. Let T_{f_3} be the distribution of the (residual) forwarding delay of the candidate third forwarder at position f_3, and $T_{\bar{c}_3}$ the distribution of the minimum value of the (residual) forwarding delays of the remaining candidate third forwarders.
$\mathbb{P}(F_3 = f_3 \mid F_1 = f_1 \wedge D_1 = d_1 \wedge F_2 = f_2 \wedge D_2 = d_2)$ can thus be expressed as

$$\begin{aligned}&\mathbb{P}(F_3 = f_3 \mid F_1 = f_1 \wedge D_1 = d_1 \wedge F_2 = f_2 \wedge D_2 = d_2) = \\ &\mathbb{P}(T_{f_3} < T_{\bar{c}_3} \mid F_1 = f_1 \wedge D_1 = d_1 \wedge F_2 = f_2 \wedge D_2 = d_2).\end{aligned} \tag{6.24}$$

To calculate $\mathbb{P}(T_{f_3} < T_{\bar{c}_3} \mid F_1 = f_1 \wedge D_1 = d_1 \wedge F_2 = f_2 \wedge D_2 = d_2)$ we integrate over all possible values of T_{f_3} multiplied by the probability that $T_{\bar{c}_3}$ has a larger value:

$$\begin{aligned}&\mathbb{P}(T_{f_3} < T_{\bar{c}_3} \mid F_1 = f_1 \wedge D_1 = d_1 \wedge F_2 = f_2 \wedge D_2 = d_2) = \\ &\int_{t_3=0}^{T_d} f_{T_{f_3}}(t_3, f_1, d_1, f_2, d_2) \Big(1 - F_{T_{\bar{c}_3}}(t_3, f_1, d_1, f_2, d_2)\Big)\, \mathrm{d}t_3.\end{aligned} \tag{6.25}$$

We thus need to determine the conditional distributions of T_{f_3} and $T_{\bar{c}_3}$, given $F_1 = f_1 \wedge D_1 = d_1 \wedge F_2 = f_2 \wedge D_2 = d_2$. The distribution of the (residual) forwarding delay of a candidate third forwarder depends on the hop in which the node first received the message and, if it first received the message in one of the first two hops, on the delay of the first two hops. We first show how to calculate the distribution of T_{f_3}, then how to calculate the distribution of $T_{\bar{c}_3}$.

If the candidate third forwarder at position f_3 first received the message in the third hop (i.e., from the second forwarder) then its forwarding delay T_{f_2} is uniformly distributed between 0 and T_d, similar to how the delay of the first hop is distributed (see Eq. (6.12)). If the candidate third forwarder first received the message in the second hop (from the first forwarder) then it must take the delay of the second hop into account. For a given second-hop delay d_2, T_{f_2} is then uniformly distributed between 0 and $T_d - d_2$. If the candidate third forwarder first received the message in the first hop (from the source) then it must take the delay of the first two hops into account. For a given first-hop delay d_1 and second-hop delay d_2, T_{f_3} is then uniformly distributed between 0 and $T_d - d_1 - d_2$. For a given position of the first forwarder f_1, a given first-hop delay d_1, a given position of the second forwarder f_2, and a given second-hop delay d_2, the CDF of T_{f_3} for $0 \leq t_3 \leq T_d$ is then given by

$$F_{T_{f_3}}(t_3, f_1, d_1, d_2) = \begin{cases} F_{U(0,T_d)}(t_3) & f_3 > f_1 + R \\ F_{U(0,T_d-d_2)} & R < f_3 \leq f_1 + R \\ F_{U(0,T_d-d_1-d_2)} & f_3 \leq R, \end{cases} \tag{6.26}$$

with $F_{T_{f_3}}(t_3, f_1, d_1, d_2) = 0$ for $t < 0$ and $F_{T_{f_3}}(t_3, f_1, d_1, d_2) = 1$ for $t > T_d$.

$T_{\bar{c}_3}$ is distributed as the minimum value of the residual forwarding delays of all the remaining candidate third forwarders. We denote the set of remaining candidate third forwarders that received the message for the first time from the j^{th} forwarder as $\bar{c}_{3,j}$. The size of these sets depends on the position of the first two forwarders. All nodes in a set have identically distributed (residual) forwarding delays. For a given position of the first forwarder f_1, a given first-hop delay d_1, a given position of the second forwarder f_2, and a given second-hop delay d_2, the CDF of $T_{\bar{c}_3}$ for $0 \leq t_3 \leq T_d$ is given by

$$F_{T_{\bar{f}_3}}(t_3, f_1, f_2, h_1, h_2) = 1 - F_{U_{max}}(t_3, T_d, |\bar{c}_{3,2}|) \cdot F_{U_{max}}(t_3, T_d - d_2, |\bar{c}_{3,1}|) \cdot F_{U_{max}}(t_3, T_d - d_1 - d_2, |\bar{c}_{3,0}|) \tag{6.27}$$

with $F_{T_{\bar{c}_3}}(t_3, f_1, f_2, h_1, h_2) = 0$ for $t < 0$ and $F_{T_{\bar{c}_3}}(t_3, f_1, f_2, h_1, h_2) = 1$ for $t > T_d$. The term $\big(1 - F_{U_{max}}(t_3, T_d, |\bar{c}_{3,2}|) \cdot F_{U_{max}}(t_3, T_d - d_2, |\bar{c}_{3,1}|) \cdot F_{U_{max}}(t_3, T_d - d_1 - d_2, |\bar{c}_{3,0}|)\big)$ expresses the probability that at least one of the remaining candidate second forwarders will have forwarded the message in the interval $[d_1 + d_2, d_1 + d_2 + t_3]$.

Substituting Eq. (6.26) and Eq. (6.27) in Eq. (6.25) we thus have an expression for $\mathbb{P}(F_3 = f_3)$.

In a similar manner to how we have determined the probability distribution of F_1, F_2, and F_3 we can express the probability distribution of F_4, F_5, etc. This becomes relatively complex and resource-intensive however since we need to take into account the positions of the forwarders and the delay of each hop for an increasing number of previous hops. We therefore give an approximate method to calculate F_4, F_5, etc. in Section 6.5.4.

6.5.3 Length of a hop

In this section we determine the length of the n^{th} hop L_n for $n \leq 3$ in an exact manner and approximate L_n for $n > 3$.

The distribution of L_n can be expressed in terms of the distribution of F_n and F_{n-1}:

$$P(L_n = l_n) = \sum_{f_{n-1}=(n-1)}^{(n-1)R} P(F_{n-1} = f_{n-1}) \cdot P(F_n = f_{n-1} + l_n \mid F_{n-1} = f_{n-1}). \tag{6.28}$$

The distributions of the positions of the first three forwarders have been given in the previous section. Using these we have an exact expression for the distribution of L_n for $n \leq 3$.

As we will show in Section 6.6 the distribution of L_n converges and, for the purpose of our model, does not change significantly beyond the third hop, i.e.,

$$F_{L_n}(\cdot) \sim F_{L_3}(\cdot) \quad n > 3. \tag{6.29}$$

We thus assume that the lengths of the successive hops $n > 3$ are identically distributed and independent of the positions of the previous forwarders and the previous delays.

6.5.4 Approximated position of the forwarder for $n > 3$

We determine the position of the n^{th} forwarder F_n for $n > 3$.

In Section 6.5.2 we determined F_n for $n \leq 3$ in an exact manner, and using the assumption of Eq. (6.29) that the length of each following hop is i.i.d., the distribution of the position of every next forwarder approximated by

$$P(F_n = f_n) \approx \sum_{f_{n-1}=(n-1)}^{(n-1)R} P(F_{n-1} = f_{n-1}) \cdot P(L_n = f_i - f_{n-1}), \quad n > 3 \quad (6.30)$$

We thus have a recursive approximation of the position of the forwarder for the fourth hop and beyond.

6.5.5 Required number of hops

In this section we determine the required number of hops to have the message forwarded by a node at or beyond position i, denoted N_i. We first do so in an explicit manner as a convolution of hop lengths. For large values of i this method becomes quite resource-intensive however; in those cases we instead approximate N_i as a renewal process.

The first method makes use of the fact that the probability that *at most* n hops are required to have the message forwarded by a node at or beyond position i is equal to the probability that the n^{th} forwarder is at or beyond position i, i.e.,

$$P(N_i \leq n) = 1 - P(F_n < i), \quad (6.31)$$

where $P(F_n < i)$ is equal to the summed up probabilities that the forwarder is at position $0 \leq j < i$ given by Eq. (6.30), i.e.,

$$P(F_n < i) = \sum_{j=0}^{i-1} P(F_n = j). \quad (6.32)$$

In the second method we use the fact that F_n for $n > 3$ is a convolution of i.i.d. hop lengths, see Eq. (6.30). Let N_{i-f_3} be the number of hops required after the third forwarder has forwarded the message. According to [98] (page 5), when i becomes large, N_{i-f_3} has asymptotically the following normal distribution:

$$N_{i-f_3} \sim \mathcal{N}\left(\frac{i-f_3}{\mu_{L_3}}, \sigma^2_{L_3}\frac{i-f_3}{(\mu_{L_3})^3}\right), \quad i > f_3, \quad (6.33)$$

with $N_{i-f_3} = 0$ for $i \leq f_3$ and μ_{L_3} and $\sigma^2_{L_3}$ being the mean and variance of the distribution of the hop length L_3, which can easily be calculated using Eq. (6.29). Including the distribution of F_3, N_i is then distributed as

$$P(N_i = n) = \sum_{f_3=3}^{3R} P(F_3 = f_3) \cdot P(N_{i-f_3} = n - 3). \quad (6.34)$$

Note that N_i denotes the required number of hops to have the message forwarded by a node at or beyond position i, but to have a sink node at position j receive the message one of nodes $n_{j-R}, \ldots, n_{j-1}$ must transmit the message. To calculate the required number of hops to have the message delivered at the sink node at position j we therefore determine the distribution of N_{j-R}.

6.5.6 End-to-end delay

In this section we determine the end-to-end delay to have the message forwarded by a node at or beyond position i, denoted E_i for $i \in \mathbb{N}^+$, by combining the distributions of N_i and D_n. We assume that hop delays D_n are independent of the required number of hops N_i; the validity of this assumption is discussed in Section 6.6.

E_i is a function of the number of hops required to have the message forwarded by a node at or beyond position i (N_i), and the delay per hop (D_n). The distribution of the delay of the first hop is given by Eq. (6.12), the hop time of subsequent hops is given by Eq. (6.16). The minimum number of hops required to have the message forwarded by a node at or beyond position i is $\lfloor \frac{i}{R} \rfloor$, the maximum is i. Summing over all possible hop counts n and hop delays D_n the distribution of E_i is given by

$$F_{E_i}(t) = \sum_{n=\lfloor \frac{i}{R} \rfloor}^{i} P(N_i = n) \cdot F_{\sum\limits_{j=1}^{n} D_j}(t), \quad i \in \mathbb{N}^+. \tag{6.35}$$

Evaluating such an expression becomes rather resource-intensive for large values of i. Because we assume that the hop delays beyond the first hop are i.i.d. according to D_2 (see Eq. (6.16)) we can instead use the central limit theorem, which states that for n i.i.d. variables D_2 with mean μ_{D_2} and variance σ_{D_2}, $S_n := \sum_{i=1}^{n} D_2$ can be approximated by $S_n \sim \mathcal{N}(n \cdot \mu_{D_2}, n \cdot \sigma_{D_2})$. For a given required number of hops n, and taking the distribution of the delay of the first hop into account, the distribution of the end-to-end delay can then be expressed as (c.f. Eq. (6.35))

$$P(E_i = t \mid N_i = n) = \int\limits_{d_1=0}^{T_d} f_{D_1}(d_1) \cdot P(S_{n-1} = t - d_1) \, \mathrm{d}d_1. \tag{6.36}$$

Iterating over all the possible required number of hops we get

$$\mathbb{P}(E_i = t) = \sum_{n=\lfloor \frac{i}{R} \rfloor}^{i} \mathbb{P}(N_i = n) \ \cdot \ P(E_i = t \mid N_i = n), \quad i > 0, \quad t > 0. \tag{6.37}$$

6.6 Performance evaluation

We have performed an evaluation study to assess *(i)* how the performance of the forwarding protocol is affected by varying network parameters (for both forwarding delay distributions), and *(ii)* how well our analysis is able to capture the behaviour of the forwarding protocol. We have done so by evaluating a forwarding scenario for different network parameters, both by means of simulation and by means of our analysis. Below we briefly describe the scenario and the set-up of our simulation study, after which we discuss the results.

6.6.1 Set-up

The scenario is similar to the forwarding model shown in Section 6.3: a message is forwarded from source to sink over a straight road. The transmission range R is fixed for all experiments at 100 m. Inter-node distances are fixed per experiment, and are varied between experiments over values 50, 25, and 10 m. In our evaluation we will refer to the resulting number of nodes inside the transmission range as the node density $\rho = 2$, 4, and 10, respectively. The source-to-sink distance is varied between R, $2R$, $3R$, $4R$, $5R$, and $10R$. The forwarding rules are as described in Section 6.1. Forwarding delays are either exponentially distributed with a mean of 1 s or uniformly distributed between 0 and 1 s. To gain statistically significant results each experiment has been repeated at least 10,000 times with different random seeds.

Simulation experiments have been performed using the OMNET++ network simulator v4.1 [77] and using a self-modified version of the MiXiM framework v2.1 [79] to model the communication architecture. To model the behaviour of the 802.11p protocol as accurately as possible we have altered timing parameters in the IEEE 802.11 medium access module in such a way that all parameters follow the 802.11p specification [100]. The available 802.11 MiXiM physical layer has been adapted to include bit error ratios (BERs) and packet error ratios (PERs). The centre frequency was set to 5.9 MHz and AC 0 was used.

To emulate a deterministic, fixed transmission range, the physical layer was adapted in such a way that any node within R meters of a transmitting node will receive the transmitted signal at a fixed (and relatively high) power level. Outside this range a receiving node receives the signal at zero power. This effectively gives a unit-disc propagation model with reception probabilities one and zero (in case of an isolated transmission). Nodes use the 802.11p MAC as described above.

To focus on the multi-hop behaviour, the influence of packet collisions is kept as low as possible by using small packet sizes of 160 bits.

6.6.2 Results

The discussion of the results is split into two parts, one for each forwarding delay distribution, and for each distribution the impact of the network parameters are evaluated separately. We discuss the distribution of the delay of each hop, the distribution of the length of each hop, the distribution of the position of each forwarder, the distribution of the required number of hops, and the distribution of the end-to-end delay.

We use the Kolmogorov-Smirnov (K-S) statistic to express the difference between two distributions. The K-S statistic K for two distributions $F_1(x), F_2(x)$ is equal to the largest distance between the two CDFs, given by

$$K = \max\{|F_1(x) - F_2(x)|\} \quad \forall\, x. \tag{6.38}$$

Fig. 6.3 shows an example K-S statistic.

Performance metrics have been evaluated up to the tenth hop and for distances up to $10R$, and are all included in tables showing the K-S statistics of the resulting distributions. The figures show distribution for the first five hops and for distances up to $5R$. Results of following hops have been left out for the purpose of clarity of illustration. The solid lines

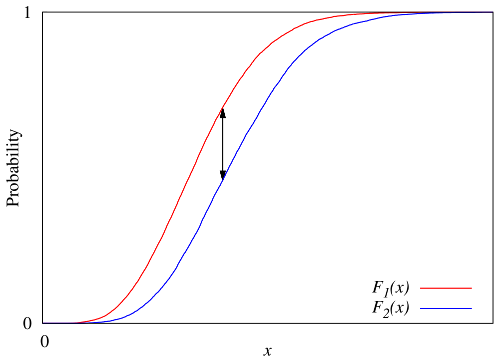

Figure 6.3: The arrow between the two CDFs is the K-S statistic.

represent analytical results, the dashed lines represent simulation results. In case of average values confidence intervals are less than 1 $\%$.

Exponentially distributed forwarding delays

We evaluate the performance of the forwarding protocol when forwarding delays are distributed exponentially.

Fig. 6.4 shows the distribution of the hop length of the first three hops for three values of ρ. Of the model analysis only the distribution of the hop length of the first hop is shown, as all hops have an identical hop length distribution. It can be seen that the probability of becoming the next forwarder is uniformly distributed over all the nodes for all values of ρ and for all shown hops. It can be seen in Fig. 6.4 as well as in Table 6.1 that, regarding the distribution of the hop length, results of the model simulation and the model analysis stay within 0.04 for $\rho = 2$ and within 0.01 for $\rho = 4, 10$.

Fig. 6.5 shows the distribution of the position of the first five forwarders for three values of ρ. As ρ increases the probability that a forwarder is positioned further away from the source increases, e.g., compare the distribution of the position of the fifth forwarder in all three figures. It can be seen in the figures as well as in Table 6.1 that regarding the distribution of the position of a forwarder, results of the model simulation and the model analysis stay within 0.05 for $\rho = 2$ and within 0.01 for $\rho = 4, 10$.

Fig. 6.6 shows the distribution of the required number of hops to have the sink receive the message N_i, for source-to-sink distances up to $5R$ and for three values of ρ. It can be seen that the required number of hops to have the sink receive the message grows linearly with the source-to-sink distance. This has been illustrated in Fig. 6.9a by plotting the required number of hops to have a 99 $\%$ probability that the source has received the message, for increasing source-to-sink distances: barring some variation caused by averaging (because the required number of hops must be expressed in integer values) the lines show a clear linear trend. The effect of increasing ρ is that the required number of hops to have the sink receive the message increase less than linear, as can be seen in Fig. 6.9b, which shows again the required number of hops to have a 99 $\%$ probability that the source has received the message but now for three values of ρ.

It can be seen in Fig. 6.6 and in Table 6.1 that regarding the distribution of the required number of hops to have the sink receive the message, results of the model simulation and the model analysis stay within 0.05 for $\rho = 2$ and within 0.01 for $\rho = 4, 10$, for distances up to $10R$.

Fig. 6.7 shows the distributions of the hop delay of the first four hops for three values of ρ. Of the model analysis only the distribution of the hop delay of the first hop is shown, as all hops have an identical hop delay distribution given by Eq. (6.1). It can be seen that the hop delay decreases as ρ increases.

It can be seen in Fig. 6.7 as well as in Table 6.1 that regarding the distribution of the hop delay, results of the model simulation and the model analysis stay within 0.03 for $\rho = 2$ and within 0.01 for $\rho = 4, 10$.

Fig. 6.8 shows the distribution of the end-to-end delay to have the sink receive the message for source-to-sink distances up to $5R$ and for three values of ρ. It can be seen that the end-to-end delay to have the sink receive the message grows linearly with the source-to-sink distance. This has been illustrated in Fig. 6.10a by plotting the delay after which the sink will have received the message with 99 % probability for increasing source-to-sink distances. The effect of increasing ρ is that the end-to-end delay to have the sink receive the message decreases, since the hop delay decreases as ρ increases. This decrease is less than linear however, as can be seen in Fig. 6.10b that shows again the delay after which the sink will have received the message with 99 % probability but now for differing values of ρ.

It can be seen in Fig. 6.8 and in Table 6.1 that regarding the distribution of the end-to-end delay, results of the model simulation and the model analysis stay within 0.04 for distances up to $10R$.

Overall we conclude that when forwarding delays are distributed exponentially our model analysis describes the behaviour of the forwarding protocol with a very high accuracy.

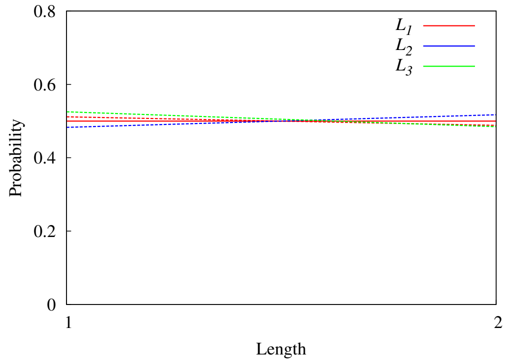

(a) For $\rho = 2$.

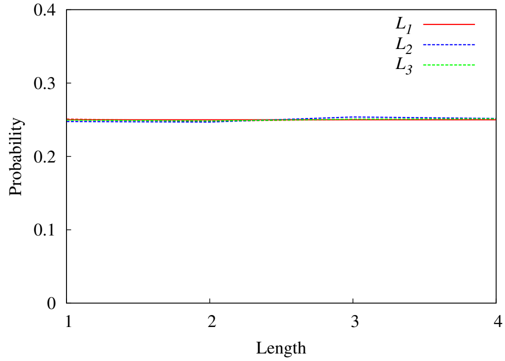

(b) For $\rho = 4$.

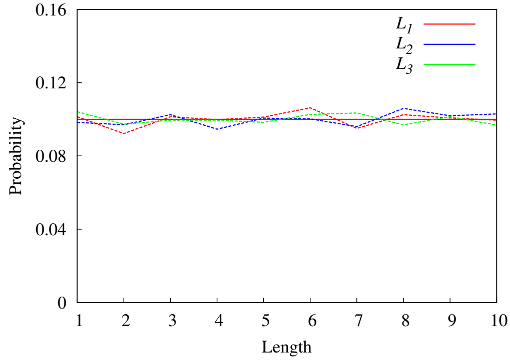

(c) For $\rho = 10$.

Figure 6.4: The distribution of the length of the first three hops for varying values of ρ when forwarding delays are exponentially distributed. Of the analytical results only the first hop is shown.

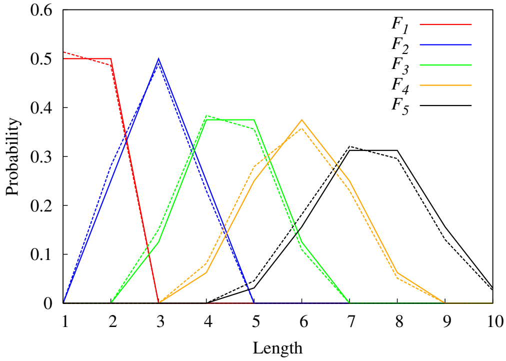

(a) For $\rho = 2$.

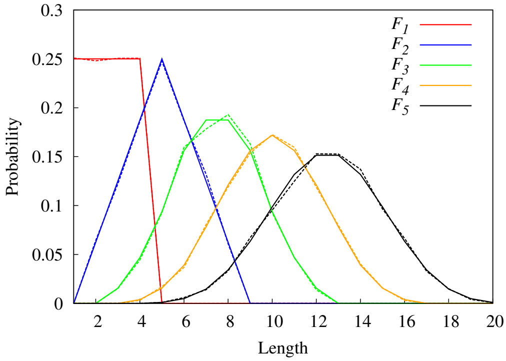

(b) For $\rho = 4$.

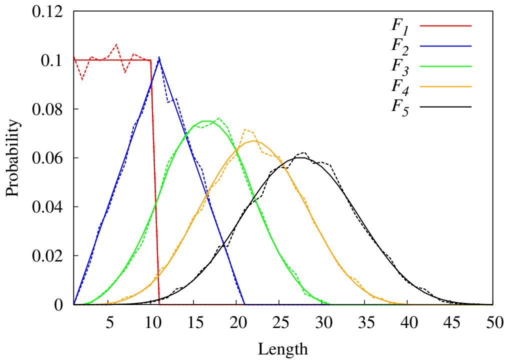

(c) For $\rho = 10$.

Figure 6.5: The position of the first five forwarders for varying values of ρ.

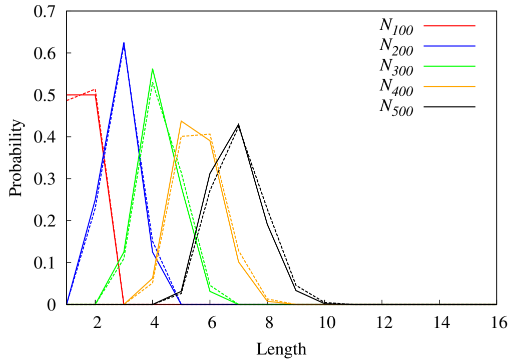

(a) For $\rho = 2$.

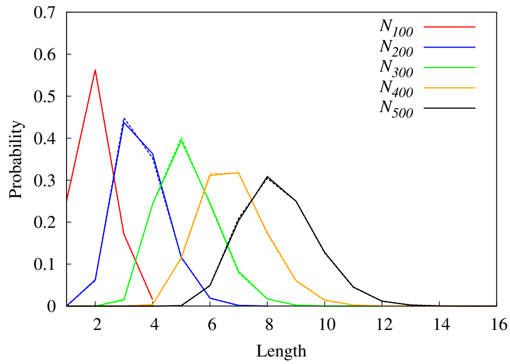

(b) For $\rho = 4$.

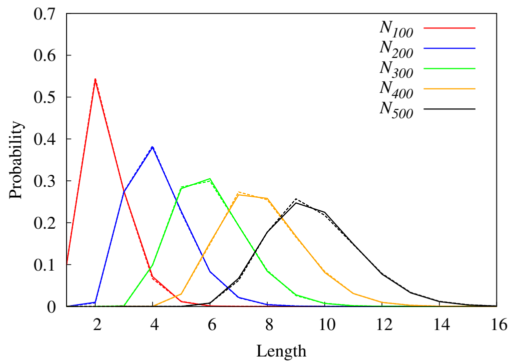

(c) For $\rho = 10$.

Figure 6.6: The distribution of the required number of hops to have the sink receive the message for varying source-to-sink distances and for various values of ρ, and when forwarding delays are exponentially distributed.

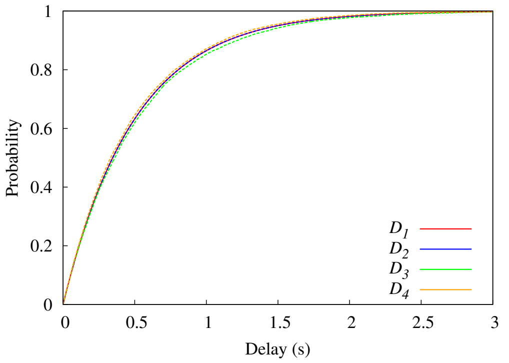

(a) For $\rho = 2$.

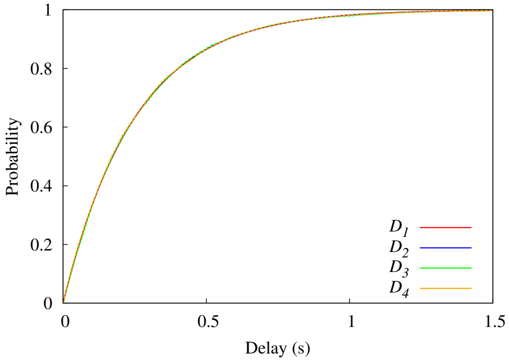

(b) For $\rho = 4$.

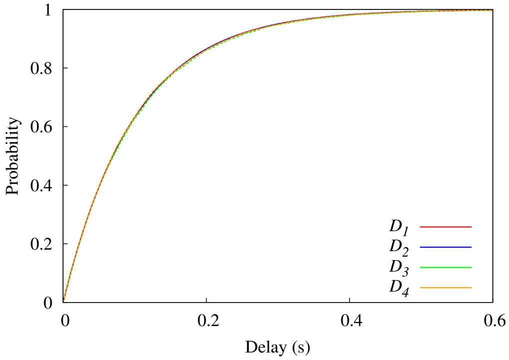

(c) For $\rho = 10$.

Figure 6.7: The hop delay of the first four hops for varying values of ρ when forwarding delays are exponentially distributed. Of the analytical results only the first hop is shown.

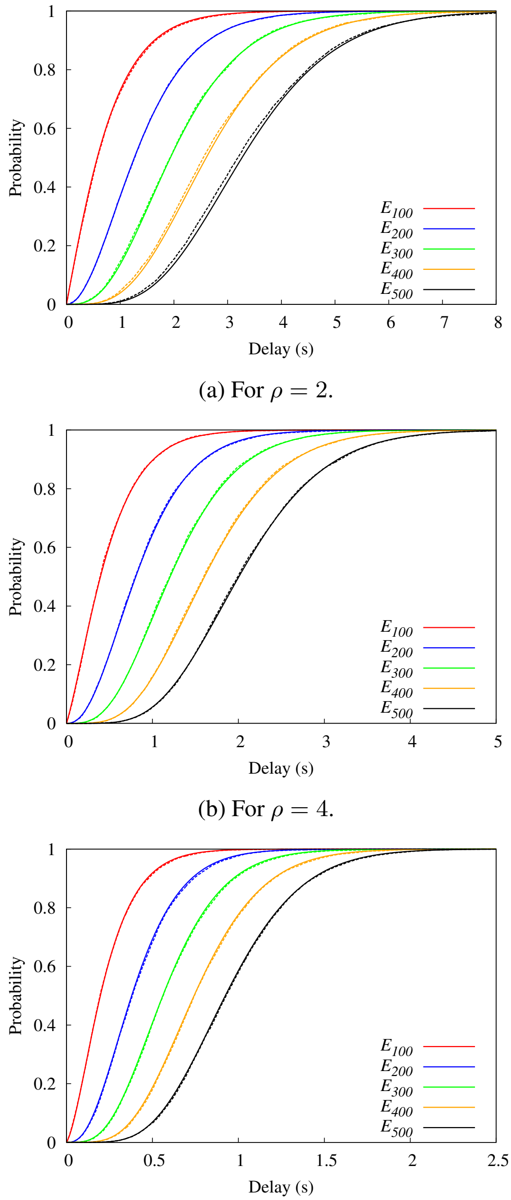

(a) For $\rho = 2$.

(b) For $\rho = 4$.

(c) For $\rho = 10$.

Figure 6.8: The distribution of the end-to-end delay to have the sink receive the message for varying source-to-sink distances and varying values of ρ, and when forwarding delays are exponentially distributed.

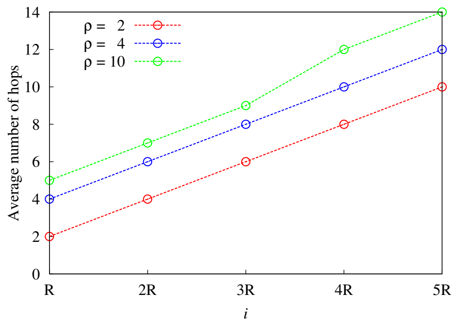

(a) For varying values of source-to-sink distance i.

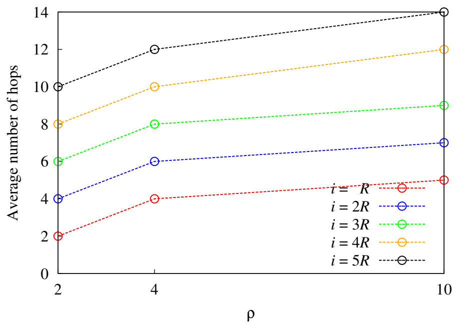

(b) For varying values of density ρ.

Figure 6.9: The required number of hops to have a 99 % probability that the source has received the message when forwarding delays are exponentially distributed. Only simulation results are shown.

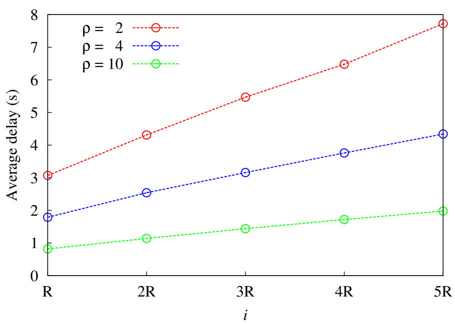

(a) For varying values of source-to-sink distance i.

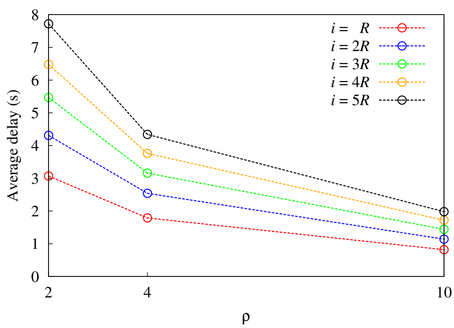

(b) For varying values of density ρ.

Figure 6.10: The delay after which the sink will have received the message with 99 % probability when forwarding delays are exponentially distributed. Only simulation results are shown.

Hop	1	2	3	4	5	10
R	Delay per hop					
2	0.015	0.015	0.022	0.027	0.019	0.023
4	0.009	0.009	0.008	0.014	0.011	0.012
10	0.008	0.006	0.010	0.007	0.008	0.005
R	Length of a hop					
2	0.014	0.037	0.025	0.033	0.029	0.028
4	0.001	0.006	0.002	0.008	0.008	0.003
10	0.006	0.011	0.005	0.010	0.007	0.004
R	Position of a forwarder					
2	0.014	0.031	0.035	0.048	0.048	0.051
4	0.001	0.006	0.010	0.004	0.007	0.005
10	0.006	0.012	0.006	0.005	0.007	0.006

Distance	R	$2R$	$3R$	$4R$	$5R$	$10R$
R	Required number of hops					
2	0.014	0.026	0.048	0.048	0.051	0.049
4	0.001	0.010	0.007	0.005	0.005	0.005
10	0.005	0.012	0.006	0.005	0.007	0.006
R	End-to-end delay					
2	0.009	0.004	0.013	0.020	0.027	0.043
4	0.012	0.008	0.010	0.010	0.010	0.006
10	0.007	0.013	0.009	0.010	0.008	0.007

Table 6.1: K-S statistics when comparing the results of the model analysis with the results of the model simulation, for exponential forwarding delays, calculated using Eq. (6.38).

Uniformly distributed forwarding delays

We evaluate the performance of the forwarding protocol when forwarding delays are distributed uniformly.

Fig. 6.11 shows the distribution of the hop length of the first four hops for three values of ρ. Of the model analysis only the distributions of the hop length of the first three hops are shown since in our analysis we assume that the hop length of the fourth and following hops is distributed identically to the hop length of the third hop. It can be seen that the hop length of the first hop is uniformly distributed over R, i.e., each node within R meters of the source (and located closer to the sink) has an equal probability of becoming the first forwarder. For following hops the distribution of the hop length is shifted: nodes that lie closer to the source have a higher probability of becoming the next forwarder, and hops subsequently become shorter. This effect is due to the fact that nodes that lie closer to the source often will receive the message in an earlier hop than nodes that lie further away, and will therefore have a shorter residual forwarding delay. This effect is strongest for $\rho = 2$, as can also be seen when comparing the figures. As ρ increases the effect grows less and the distribution of hop lengths becomes increasingly uniformly distributed: for $\rho = 10$ the difference between the distributions of the hop length of the first hop and of following hops is less than 0.01.

It can be seen in Fig. 6.11 and in Table 6.2 that regarding the distribution of the hop length, results of the model simulation and the model analysis stay within 0.01. This confirms our assumption that, for the purpose of our analysis, the distribution of the hop length of the fourth and following hops is identical to that of the third hop.

Fig. 6.12 shows the distribution of the position of the first five forwarders for three values of ρ. It can be seen that the resulting curves of the distributions are shifted toward the source compared to the case when forwarding delays are exponentially distributed, i.e., when forwarding delays are uniformly distributed the n^{th} forwarder is likely to be located closer to the source compared to when forwarding delays are distributed exponentially. This is a direct effect of the shortened hop lengths compared to the hop lengths when forwarding delays are distributed exponentially. As ρ increases however hop lengths become more uniformly distributed, similar to how hop lengths are distributed when forwarding delays are distributed exponentially, and the distribution of the position of a forwarder increasingly resembles the distribution of the position of a forwarder when forwarding delays are exponentially distributed. This can be seen in Fig. 6.18 which compares the distribution of the position of the fifth forwarder for both forwarding delay distributions and for all values of ρ.

In our model analysis we have assumed that, for the purpose of our model, hop lengths of consecutive hops beyond the third hop are i.i.d., and the position of the fourth and following forwarders is therefore calculated as a convolution of i.i.d. hop lengths. It can be seen in Fig. 6.12 as well as in Table 6.2 that, regarding the distribution of the position of a forwarder, results of the model simulation and the model analysis stay within 0.03. Results increase in accuracy as ρ increases. We therefore conclude that although our assumption is not wholly correct, causing some errors, results are still very accurate.

Fig. 6.13 shows the distribution of the required number of hops to have the sink receive the message for source-to-sink distances up to $5R$ and for three values of ρ. It can be seen that the required number of hops to have the sink receive the message grows linearly with the source-to-sink distance i. This has been illustrated in Fig. 6.16a by plotting the required number of hops to have a 99 % probability that the source has received the message for increasing source-to-sink distances: barring some variation caused by averaging (because the required number of hops must be expressed in integer values) the lines show a clear linear trend. The effect of increasing ρ is that the required number of hops to have the sink receive the message increases less than linear, as can be seen in Fig. 6.16b, which shows the required number of hops to have a 99 % probability that the source has received the message for differing values of ρ.

It can be seen in Fig. 6.13 and in Table 6.2 that, regarding the distribution of the required number of hops to have the sink receive the message results of the model simulation and the model analysis stay within 0.04, for distances up to $10R$.

Fig. 6.14 shows the distribution of the hop delay of the first three hops for three values of ρ. Of the model analysis only the distribution of the hop delay of the first two hops are shown since in our analysis we assume that the hop delay of the third and following hops is distributed identically to the hop delay of the second hop. It can be seen that as R increases the hop delay decreases. It can also be seen that whereas the difference between the distribution of the first hop and the distribution of the second hop is quite distinct, this difference is not significant for following hops. Furthermore, the difference between the distribution of the first hop and the distribution of the second hop decreases as ρ increases.

It can be seen in Fig. 6.14 as well as in Table 6.2 that regarding the distribution of the hop delay, results of the model simulation and the model analysis stay within 0.02. This confirms our assumption that, for the purpose of our analysis, the distribution of the hop delay of the third and following hops is identical to that of the second hop.

Fig. 6.15 shows the distribution of the end-to-end delay to have the sink receive the message for source-to-sink distances up to $5R$ and for three values of ρ. It can be seen that the end-to-end delay to have the sink receive the message grows linearly with the source-to-sink distance. This has been illustrated in Fig. 6.17b by plotting the delay after which the sink will have received the message with 99 % probability for differing values of ρ. The effect of increasing ρ is that the end-to-end delay to have the sink receive the message decreases, since the hop delay decreases as ρ increases. This decrease is less than linear however, as can be seen in Fig. 6.17a that shows the delay after which the sink has received the message with 99 % probability for increasing source-to-sink distances.

In our model analysis we have assumed that, for the purpose of our model, hop delays of consecutive hops beyond the second hop are i.i.d., and beyond the first hop the end-to-end delay for a given source-to-sink distance is therefore calculated as a convolution of i.i.d. hop delays. It can be seen in Fig. 6.15 and in Table 6.2 that regarding the distribution of the end-to-end delay, results of the model simulation and the model analysis stay within 0.07 for distances up to $10R$. We therefore conclude that although our assumption is not wholly correct, results are still quite accurate.

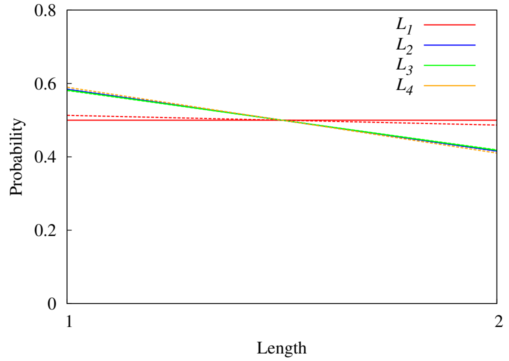

(a) For $\rho = 2$.

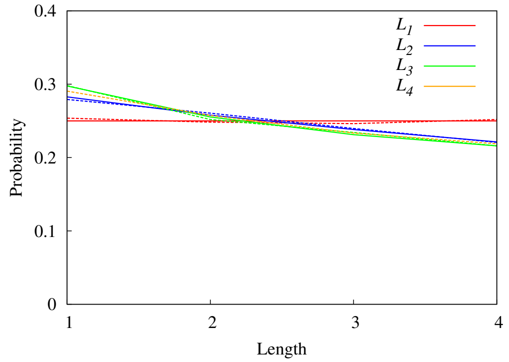

(b) For $\rho = 4$.

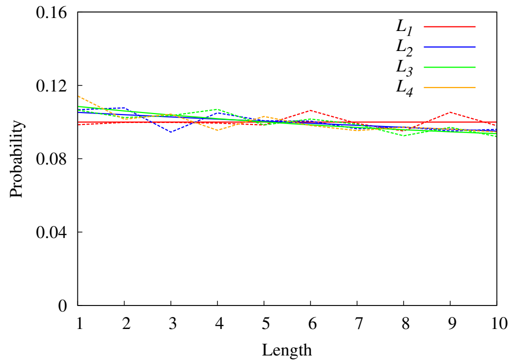

(c) For $\rho = 10$.

Figure 6.11: The distribution of the length of the first four hops for varying values of ρ when forwarding delays are uniformly distributed.

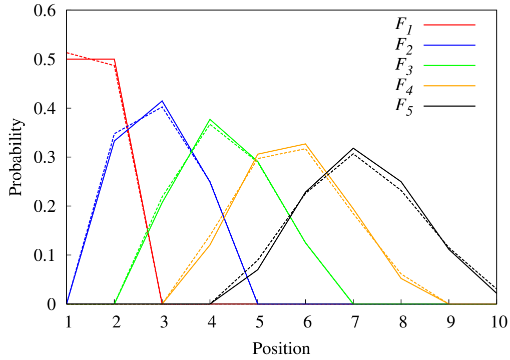

(a) For $\rho = 2$.

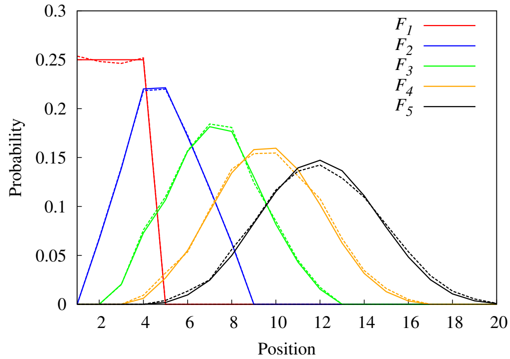

(b) For $\rho = 4$.

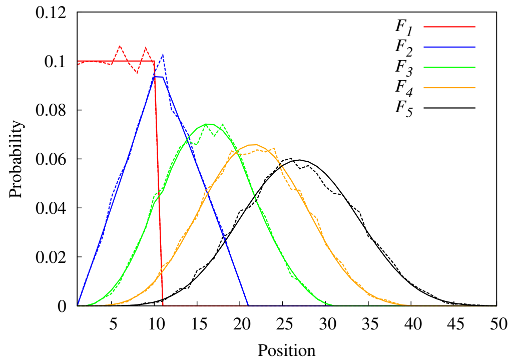

(c) For $\rho = 10$.

Figure 6.12: The position of the first five forwarders when forwarding delays are uniformly distributed, for varying values of ρ.

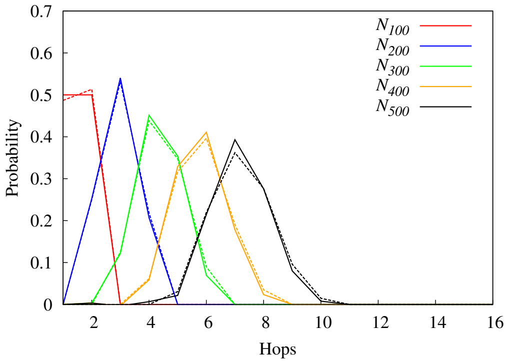

(a) For $\rho = 2$.

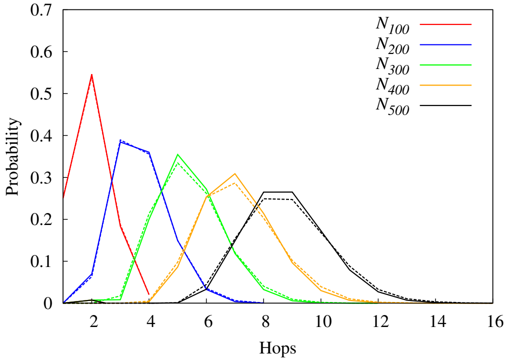

(b) For $\rho = 4$.

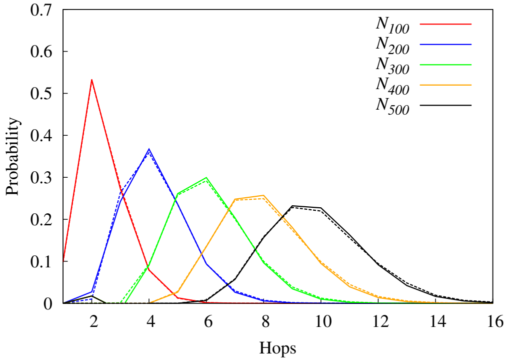

(c) For $\rho = 10$.

Figure 6.13: The distribution of the required number of hops to have the sink receive the message when forwarding delays are distributed uniformly, for varying source-to-sink distances and for various values of ρ.

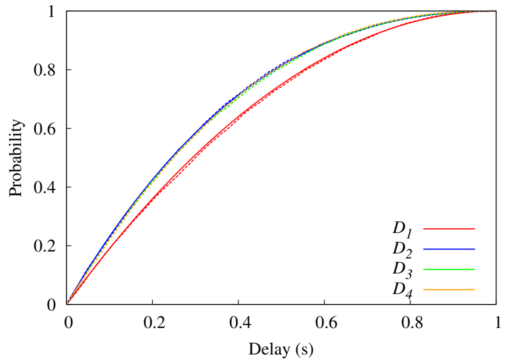

(a) For $\rho = 2$.

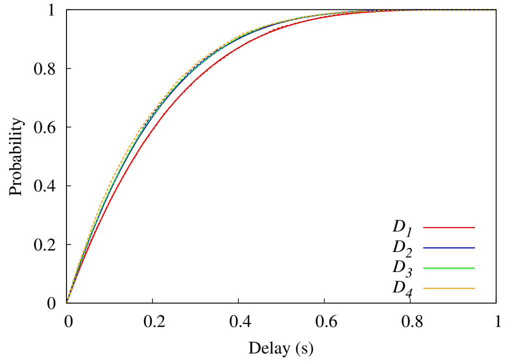

(b) For $\rho = 4$.

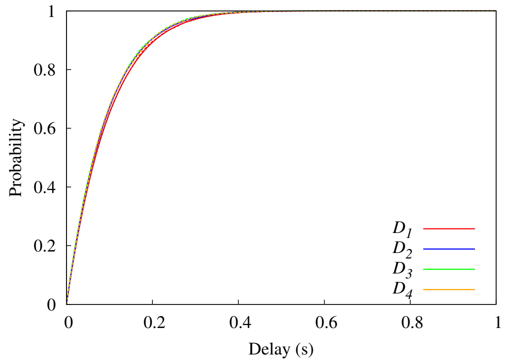

(c) For $\rho = 10$.

Figure 6.14: The CDF of the hop delay of the first four hops when forwarding delays are distributed uniformly, for varying values of ρ. Of the analytical results only the first two hops are shown.

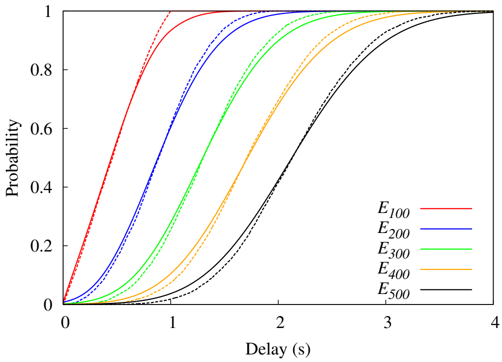

(a) For $\rho = 2$.

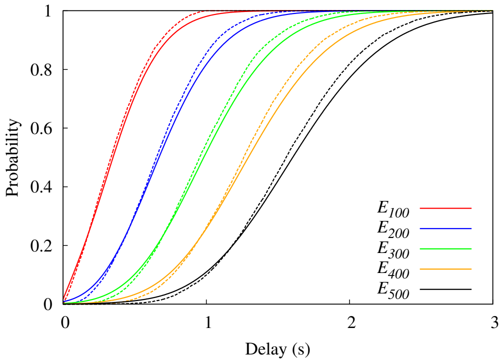

(b) For $\rho = 4$.

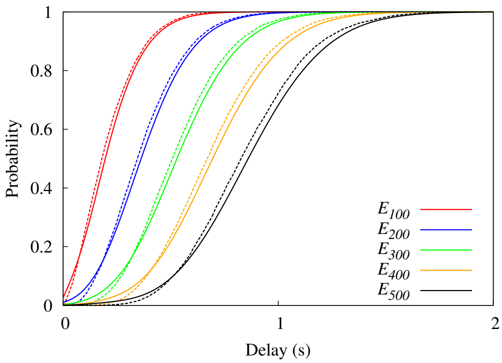

(c) For $\rho = 10$.

Figure 6.15: The distribution of the end-to-end delay to have the sink receive the message when forwarding delays are distributed uniformly for varying source-to-sink distances and varying values of ρ.

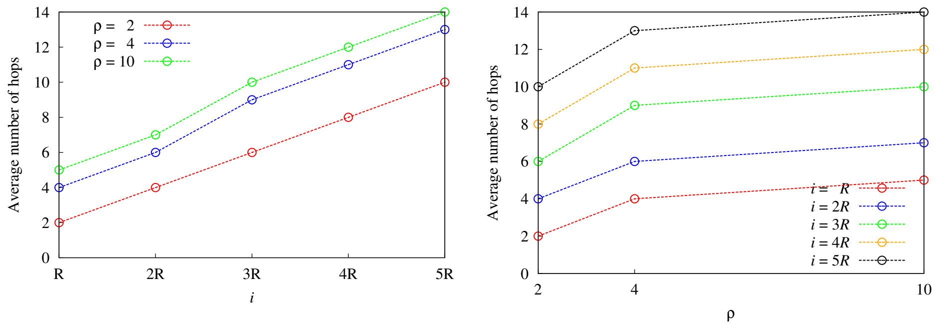

(a) For varying values of the source-to-sink distance i.

(b) For varying values of density ρ.

Figure 6.16: The required number of hops to have a 99 % probability that the source has received the message when forwarding delays are distributed uniformly. For clarity of illustration only simulation results are shown.

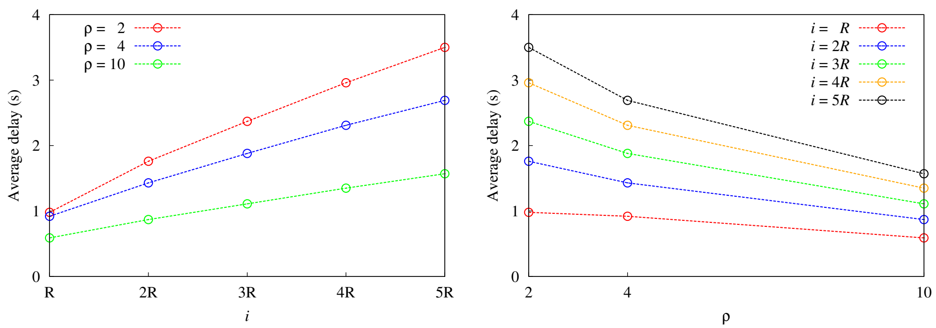

(a) For varying values of the source-to-sink distance i.

(b) For varying values of density ρ.

Figure 6.17: The delay after which the sink will have received the message with 99 % probability when forwarding delays are distributed uniformly. For clarity of illustration only simulation results are shown.

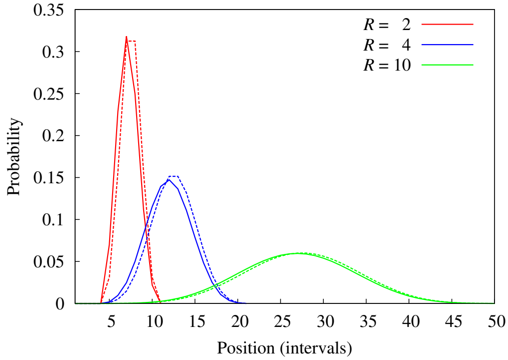

Figure 6.18: The position of the fifth forwarder when forwarding delays are distributed exponentially and uniformly, for varying values of ρ. The solid lines represent results when forwarding delays are uniformly distributed, the dashed lines represent results when forwarding delays are exponentially distributed. For clarity of illustration only analytical results are shown.

Hop	1	2	3	4	5	10
R	Delay per hop					
2	0.012	0.008	0.006	0.009	0.014	0.014
4	0.005	0.010	0.008	0.019	0.009	0.008
10	0.009	0.005	0.005	0.011	0.018	0.007
R	Length of a hop					
2	0.013	0.001	0.001	0.008	0.000	0.003
4	0.004	0.004	0.003	0.007	0.009	0.002
10	0.004	0.005	0.006	0.006	0.011	0.005
R	Position of a forwarder					
2	0.013	0.015	0.012	0.020	0.020	0.030
4	0.004	0.007	0.005	0.015	0.015	0.021
10	0.004	0.017	0.007	0.008	0.009	0.015

Distance	R	$2R$	$3R$	$4R$	$5R$	$10R$
R	Required number of hops					
2	0.013	0.011	0.020	0.024	0.024	0.035
4	0.003	0.006	0.015	0.021	0.021	0.027
10	0.005	0.017	0.017	0.017	0.017	0.005
R	End-to-end delay					
2	0.067	0.036	0.031	0.035	0.035	0.038
4	0.030	0.039	0.047	0.048	0.049	0.071
10	0.046	0.041	0.040	0.044	0.047	0.050

Table 6.2: K-S statistics when comparing the results of the model analysis with the results of the model simulation, for uniform forwarding delays, calculated using Eq. (6.38).

6.7 Conclusions

In this chapter we have shown how to analytically model a multi-hop location-based broadcast protocol when forwarding delays are either uniformly distributed or exponentially distributed. When forwarding delays are distributed uniformly such a forwarding protocol is functionally equivalent to a piggybacking protocol. Our model analysis is able to express the performance of the forwarding protocol in analytical and often even closed-form expressions. For a given node density and source-to-sink distance, the model is able to capture the full distribution of *(i)* the delay of each hop, *(ii)* the length of each hop, *(iii)* the position of each forwarder, *(iv)* the required number of hops to cover the source-to-sink distance, and *(v)* the end-to-end delay to cover the source-to-sink distance. Verification of the analysis by means of extensive simulation showed that results stay within 0.07, for distances up to ten times the transmission range. Model accuracy is best for high-density scenarios and over short distances.

As part of our work we have evaluated multi-hop forwarding using either uniformly or exponentially distributed forwarding delays. The node density and the source-to-sink distance were varied to assess their impact on performance: as the node density increases the required number of hops to cover the source-to-sink distance increases at a less-than-linear rate, whereas at the same time the end-to-end delay *de*creases at a less-than-linear rate. The latter is due to the fact that the effect of the decrease in the delay of each individual hop is stronger than the increase in the required total number of hops. As the source-to-sink distance is increased, both the required number of hops and the end-to-end delay increase linearly. It was furthermore shown that in case of high-density scenarios and when forwarding delays are distributed uniformly, the distribution of the length of a hop, the position of a forwarder, and the required number of hops to have the sink receive the message, is similar to when forwarding delays are distributed exponentially. For high-density scenarios we can therefore express these distributions using the same closed-form expressions as when forwarding delays are distributed exponentially.

Our evaluation of multi-hop forwarding showed that our model can considerably speed up such a study: whereas it took several days to generate the simulation results, results from our analytical model were generated in less than an hour.

In this chapter both the transmission range and the inter-node distances are assumed to be fixed. In the next chapter we will drop these assumptions and model multi-hop forwarding when traffic is free flowing and the probability of a successful single-hop transmission is modelled as a function of the distance between sender and receiver. For both assumptions we will see that our forwarding becomes more realistic but also more complex to analyse. Although we only model forwarding when forwarding delays are exponentially distributed in the next chapter, the method of analysis that has been presented in this chapter when forwarding delays are uniformly distributed can also be applied to the model presented in the next chapter.

CHAPTER 7

Forwarding with random forwarding delays and exponential inter-node distances

Similar to the previous chapter we present an analytical model that accurately describes the behaviour of a multi-hop location-based broadcast protocol (or [multi-hop] forwarding protocol for short) forwarding messages over a straight road using exponential forwarding delays. However, we no longer assume inter-node distances and the transmission range to be fixed. Instead we assume inter-node distances to be exponentially distributed, as previous research has shown that this distribution accurately describes inter-node distances when traffic is in a free-flowing state. We furthermore model the probability of a successful single-hop transmission as a function of the distance between sender and receiver, similar to the packet success ratio probability curve commonly used in literature [112].

The analytical model presented in this chapter focuses on forwarding a message over a specific distance. For a given node density our model analysis is then able to capture the full distribution of *(i)* the length of each hop, *(ii)* the delay of each hop, *(iii)* the success probability of each hop, *(iv)* the position of each intermediate forwarder, *(v)* the required number of hops to have the message forwarded over the entire distance, and *(vi)* the end-to-end delay to have the message forwarded over the entire distance. The last three metrics are calculated assuming that the message is successfully forwarded the entire forwarding distance.

The outline of this chapter is as follows. We start by giving a short introduction of our analytical model in Section 7.1 and discuss related work on the analysis of multi-hop forwarding in vehicular networks in Section 7.2. The system model is presented in Section 7.3 together with the notation used throughout the chapter. Our model analysis is split into two parts: the first part covers the behaviour of the first three hops in an exact manner in Section 7.4; the second part in Section 7.5 gives approximate expressions for the following hops. We have performed an evaluation study involving extensive simulations to study the performance of the forwarding protocol assumed in this chapter, as well as to verify the accuracy of our model analysis. Both the set-up of our evaluation study and its results are given in Section 7.6. We finally conclude the chapter in Section 7.7.

Image on previous page: pedestrians crossing a street in Tokyo.

7.1 Introduction

In this chapter we analytically model the behaviour of a multi-hop location-based broadcast protocol. Specifically we consider a scenario in which nodes are randomly spread out over a straight line with the source at one end and the sink at the other end. The source node initiates the forwarding by broadcasting an application message. The message has a geographically defined destination address which includes the position of the sink. All nodes apply the following forwarding rule: when a node receives a message for the first time, and the node is positioned closer to the sink than the previous sender, the node draws a forwarding delay from an exponential distribution with mean T_d. If before the end of the delay the node receives the message from another node that is positioned closer to the sink than the node itself, then the node will cancel the scheduled rebroadcast.

Multi-hop broadcast protocols such as these, in which nodes have identically distributed forwarding delays, are often employed by delay tolerant flooding protocols. These are protocols that aim to deliver information to all nodes within a certain region but that do not have strict delay requirements. In vehicular networks such flooding protocols are used to disseminate non-safety local traffic information, such as the average speed on the road or dangerous road conditions [33] [37].

Although several studies exist on analytically modelling multi-hop forwarding in wireless networks, so far we have not found any models that use assumptions that apply to our scenario. Especially regarding the level of realism of modelling single-hop transmissions existing work is lacking, as often a fixed transmission range is assumed. In contrast, in this chapter we model the probability of a successful single-hop transmission as a function of the distance between sender and receiver. Moreover, whereas the focus of existing models is often limited to network connectivity, dissemination reliability, or end-to-end delay bounds, our model gives a full distribution of a number of performance metrics.

The contribution of this chapter is an analytical model that expresses the performance of a multi-hop location-based broadcast protocol as presented above in terms of insightful and fast-to-evaluate formulas. Our model covers the scenario in which a message is forwarded a specific distance over a straight road, assuming exponentially distributed inter-node distances. In particular, for a given forwarding distance and transmission function, the model gives expressions of the following performance metrics:

1. the distribution of the length of each hop;
2. the distribution of the delay of each hop;
3. the success probability of each hop;
4. the distribution of the position of each forwarder;
5. the distribution of the required number of hops;
6. the distribution of the end-to-end delay.

The model analysis applies to messages that have successfully been forwarded over the entire forwarding distance; the effect of message loss on the end-to-end metrics is left for future work. The model has been verified using extensive simulations. For the most relevant scenarios results typically stay within 10%; as node densities decrease and the source-to-sink distance increases the model becomes less accurate.

We have split our model analysis into two parts: the first part shows how to express the behaviour of the first three hops of the forwarding protocol in an exact manner. Although this method can be applied for following hops as well, doing so becomes increasingly complex with each following hop. Based on the results of the first part we therefore show how to approximate the behaviour of the forwarding protocol for following hops in the second part.

Before presenting our analytical model we first discuss work that has been done previously on analytically modelling multi-hop forwarding in the next section.

7.2 Related work

Although there is a plethora of performance studies on multi-hop forwarding protocols in vehicular networks, practically all of these studies are simulation based. What analytical studies there are contain overly simplified assumptions and often only focus on a limited number of performance metrics such as the network connectivity [90] [91] [92], without giving a full description of the end-to-end behaviour of a protocol. Below we give a brief overview of a number of analytical studies that we found to be the most relevant regarding multi-hop location-based forwarding, and discuss their applicability to our forwarding scenario. It is the same body of work that is discussed in Chapters 6 and 8 but their applicability to the current forwarding protocol differs.

In [93] a scenario is considered in which a message is forwarded by means of broadcast transmissions over a straight line with fixed inter-node distances. Regarding single-hop transmissions all nodes within a certain range from the sender have the same probability p ($0 \leq p \leq 1$) of correctly receiving the message in absence of interference. Interference of transmissions may be taken into account and if so will result in a loss. The model gives bounds on the end-to-end delay for an idealised dissemination strategy which ignores interference, and for two provably near-optimal dissemination strategies when interference is taken into account, none of which apply to our forwarding protocol.

In [94] the end-to-end delay of an emergency message dissemination protocol is analytically calculated. A unit-disc single-hop transmission model and exponentially distributed inter-node distances are assumed. Nodes are assumed to have formed communication clusters with each cluster of nodes having a cluster head node. All forwarding is done by the head nodes, which makes it relatively easy to calculate the end-to-end delay. This method of forwarding does not apply to our forwarding protocol however.

In [95] again a straight road with exponentially distributed inter-node distances and a unit-disc single-hop communication model are considered. Nodes that receive a message will forward the message with a certain probability p ($0 \leq p \leq 1$), making the approach of this work somewhat similar to [93]. The model gives bounds on the maximum end-to-end delay and shows how the value of p that gives the lowest end-to-end delay depends on the network density. A similar result was shown in [93]. The forwarding protocol assumed in this work does not apply to our forwarding protocol.

In [96] the required number of hops to disseminate a message from source to sink is analytically modelled in the context of a wireless sensor network. Nodes are again spread out over a straight line with exponentially distributed inter-node distances and the unit-disc model is again assumed for single-hop transmission. Multi-hop forwarding is assumed to go in synchronised communication rounds in which the node that has received the message and is positioned farthest in the direction of the sink forwards the message, similar to the forwarding protocol assumed in Chapter 8. It does not apply to the forwarding protocol assumed in this chapter however. The model gives approximations for the distance that a message has been forwarded for a given number of communication rounds as well as for the network connectivity as a function of the source-to-sink distance and the node density. The work does not address the delay to deliver a message to the sink. The model is quite accurate for high node densities and large distances but less so when densities are low and distances are short.

As can be seen all of the studies discussed here assume an overly simplified transmission model and none of the protocols has forwarding rules that apply to our forwarding protocol. In the next sections we therefore present our system model and model analysis.

7.3 The system model

In this section we present our system model: an abstract representation of the forwarding scenario considered in this chapter that forms the basis of our analysis in subsequent sections. We also specify the forwarding rules of the protocol and introduce definitions and notations that are used throughout this chapter. A complete overview of these is given in Table 7.1.

We model a road as a straight line with vehicles (henceforth referred to as nodes) placed on this line, with the source node and sink node at either end of the line. Inter-node distances are exponentially distributed with mean d_{IN} (in meters). Previous studies suggest that this distribution gives a good approximation of the inter-vehicle distance in case of free flowing traffic [101] [102] [103]. Due to the differences in scale between the speed with which information is usually routed through a network (meter per millisecond) and the speed with which nodes move (meter per second), we assume the network to be static for the duration of time that a message is being forwarded from source to sink. Nodes are therefore immobile.

Fig. 7.1 illustrates the system model. Nodes are numbered and referred to with X_i, $i = 0, 1, \ldots, 10$. Node X_0 acts as the source, node X_{10} acts as the sink in this example. The first three hops are shown and with each hop the nodes that have received the message are coloured black. Initially only the source has the message.

To facilitate our analysis we divide the road into equal-sized intervals: starting from the source the road is divided into intervals of length d_{int}, with the i^{th} interval referring to the range $\langle (i-1) \cdot d_{int}, i \cdot d_{int}]$ from the source. In our analysis the size of d_{int} is such that the probability of having more than one node in an interval becomes negligible.

To model the propagation of a transmitted signal from a sender to a receiver we use a packet success ratio S_i that gives the success probability of a single-hop transmission as a function of the number of intervals i between sender and receiver. Each node thus has an independent probability S_i of receiving a transmission. The packet success ratio S_i is non-zero over the range $[1, R]$, where R is the maximum number of intervals away from the sender at which the receiver still has a non-zero probability of receiving the message. An abstraction such as S_i is commonly used to take into account fading effects that influ-

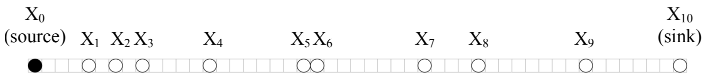

(a) Distances between the nodes are exponentially distributed.

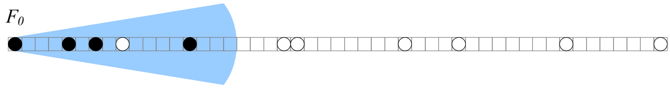

(b) First hop: the source broadcasts the message.

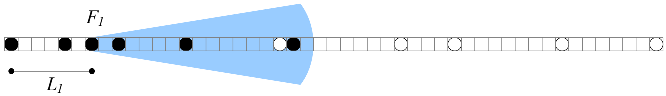

(c) Second hop: Node X_2 acts as the first forwarder and retransmits the message.

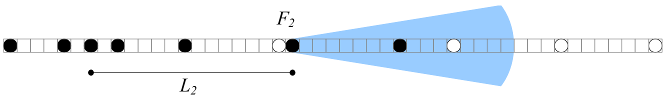

(d) Third hop: node X_6 acts as the second forwarder and retransmits the message.

Figure 7.1: The first, second, and third hop of an example scenario. The blue shape shows the maximum transmission distance R from the most recent forwarder. Black nodes have successfully received the message.

ence the reception of a signal. It ignores deterministic shadowing effects (e.g., due to an obstruction) however; the probability of successfully receiving a signal is independent for each node and for each interval. More background on radio wave propagation is given in Section 3.2.

All delays related to transmitting and processing a signal (i.e., transmission delay, propagation delay, switching times, etc.) are assumed to be negligible.

The source node initiates the forwarding by broadcasting an application message. The message has a geographically defined destination address which includes the position of the sink. All nodes apply the following forwarding rule: when a node receives a message for the first time, and the node is positioned closer to the sink than the sender, the node draws a forwarding delay from an exponential distribution with mean T_d. If before the end of the forwarding delay the node receives the message from another node that is positioned closer to the sink than the node itself, then the node will cancel the scheduled rebroadcast. In this way a message is progressively forwarded in the direction of the sink.

A_n	The number of additional candidate n^{th} forwarders, i.e., the number of candidate n^{th} forwarders i that first received the message from the $(n-1)^{\text{th}}$ forwarder. It holds that $A_n = C_n - C_{n-1}$.
$A_{n,i}$	The number of additional candidate n^{th} forwarders in interval i.
C_n	The number of candidate n^{th} forwarders.
$C_{n,i}$	The number of candidate n^{th} forwarders in interval i.
D_n	The hop delay (in seconds) of the n^{th} hop, i.e., the time between the moment the $(n-1)^{\text{th}}$ forwarder forwards the message and the moment the n^{th} forwarder forwards the message.
E_i	The end-to-end delay (in seconds) to have the message forwarded by a node that is positioned in interval i or beyond.
F_n	The position (in intervals) of the n^{th} forwarder, i.e., the forwarder that retransmits the message for the n^{th} time after the source's transmission. The source is by definition position in interval 0, i.e., $F_0 = 0$.
$G_{n,i}$	The number of n^{th} forwarders in interval i.
$H_{n,i}$	The number of candidate n^{th} forwarders in interval i, excluding the n^{th} forwarder.
$K_{n,i}$	The number of nodes in interval i that have not received the message from either the source or any of the first n forwarders. It holds that $K_{n,i} = V_{n,i} - C_{n,i}$.
L_n	The hop length (in intervals) of the n^{th} hop, defined as the distance between the $(n-1)^{\text{th}}$ forwarder and the n^{th} forwarder, i.e., $L_n = F_n - F_{n-1}$.
N_i	The number of hops required to have the message forwarded by a node that is positioned in interval i or beyond.
S_i	The single-hop packet reception probability as a function of the distance (in intervals) between the sender and receiver.
R	The maximum transmission range in intervals.
T_d	The mean per-hop forwarding delay in seconds.
V_i	The number of nodes in interval i.
Y_n	The probability of success of the n^{th} hop.

Table 7.1: Nomenclature used throughout this chapter.

We use the following notation throughout the chapter. The n^{th} forwarder is the node that retransmits the message for the n^{th} time after the source's original transmission; its position is denoted F_n. Although not a forwarder since it originates the message, the source node is referred to as the 0^{th} forwarder and is by definition positioned in interval 0, i.e., $F_0 = 0$. The n^{th} hop refers to the transmission made by the $(n-1)^{th}$ forwarder, i.e., the source's transmission is the first hop. Y_n denotes the probability of success of the n^{th} hop, i.e., the probability that there will be an n^{th} forwarder. The hop length of the n^{th} hop L_n refers to the distance in intervals between the $(n-1)^{th}$ forwarder and the n^{th} forwarder, i.e., $L_n = F_n - F_{n-1}$. The hop delay D_n of the n^{th} hop refers to the time between the moment the $(n-1)^{th}$ forwarder transmits the message and the moment the n^{th} forwarder transmits the message. Because there can be at most one node in an interval two forwarders can never be in the same interval, i.e., $F_n > F_k$ for $n > k$. In Fig. 7.1 F_0, F_1, and F_2 are given.

In our model we focus on the progress that a message makes as it is forwarded through the network. Let N_i denote the number of hops required to have the message forwarded i intervals, i.e., to have it forwarded by a node that is positioned in interval i or beyond. The end-to-end delay to have the message forwarded i intervals is denoted E_i and is the sum of the delays of the required hops, given by $E_i = \sum_{n=1}^{N_i} D_n$.

Each time the message has been forwarded there will be a set of nodes that have all successfully received the message and are all positioned closer to the sink node than the most recent forwarder. Since one of these nodes will become the next forwarder we call these nodes *candidate forwarders*. Let C_n be the number of candidates for the n^{th} forwarder, and let $C_{n,i}$ be the number of candidates for the n^{th} forwarder in interval i. In Fig. 7.1 nodes X_1, X_2, and X_4 are all candidate first forwarders. The number of nodes in interval i that have not received the message from either the source or one of the $n-1$ previous forwarder, and have therefore not become candidate n^{th} forwarder, is denoted $K_{n,i}$. In Fig. 7.1 node X_3 is the only such node that did not become a candidate first forwarder. By definition it holds that the total number of nodes in interval i, V_i, is given by

$$V_i = C_{n,i} + K_{n,i}, \quad n = 1, 2, \ldots, \quad i = F_{n-1} + 1, F_{n-1} + 2, \ldots \tag{7.1}$$

Sometimes we are interested in the set of candidate n^{th} forwarders that did not become the n^{th} forwarder. In Fig. 7.1 the set of candidate first forwarders that did not become the first forwarder consists of nodes X_1 and X_4. Let $H_{n,i}$ denote the number of candidate n^{th} forwarders in interval i, excluding the n^{th} forwarder itself, and let $G_{n,i}$ denote the number of n^{th} forwarders in interval i. By definition it holds that

$$C_{n,i} = H_{n,i} + G_{n,i}, \quad n = 1, 2, \ldots, \quad i = F_{n-1} + 1, F_{n-1} + 2, \ldots \tag{7.2}$$

For each hop beyond the first hop the set of candidate forwarders consists of nodes that received the message for the first time from the most recent forwarder and of nodes that received it before from some previous forwarder. The candidate n^{th} forwarders that received the message for the first time from the $(n-1)^{\text{th}}$ forwarder are referred to as additional candidate n^{th} forwarders. In Fig. 7.1c the set of additional candidate second forwarders consists of nodes X_3 and X_6. The number of additional candidate n^{th} forwarder is denoted A_n; the number of additional candidate n^{th} forwarder in interval i is denoted $A_{n,i}$. By definition it holds that

$$A_{n,i} = C_{n,i} - C_{n-1,i}, \quad n = 1, 2, \ldots, \quad i = F_{n-1} + 1, F_{n-1} + 2, \ldots \tag{7.3}$$

with $C_{0,i} = 0$ by definition.

7.4 Exact analysis of the first three hops

In this section we given an exact analysis of the system model for the first three hops. Although the method presented here can be applied for an arbitrary number of hops, it becomes increasingly complex with each hop however. We therefore determine the behaviour of the first three hops only. Based on the results of this section we then give a number of approximate methods in the next section that allow for fast calculation of hop metrics and end-to-end metrics for an arbitrary number of hops.

To determine the behaviour of a hop we require *(i)* the distribution of the number of candidate forwarders and *(ii)* the expected number of candidate forwarders in an interval. For the first two hops we specify both, allowing us to express the hop success probability, the position of the forwarder, the hop length, and the hop delay. For the third hop we specify the expected number of candidate forwarders in an interval only, and for this reason only express the position of the forwarder and the hop length. For all hop metrics a full distribution is given.

We specify the behaviour of each hop separately. For each hop holds that we first determine the distribution of the candidate forwarders and the expected number of candidate forwarders per interval, and then its hop metrics.

Throughout this section we clarify some of our modelling steps using (intermediate) numerical results from an evaluation study that we performed. The set-up of this study is described in Section 7.6.1. Results include both analytical results and simulation results; analytical results are illustrated using solid lines while simulation results are illustrated using dashed lines. For all figures holds that $d_{IN} = 50$ m and $d_{int} = 5$ m, other parameter settings can be found in Section 7.6.1.

7.4.1 First hop

Number of candidate forwarders

Since inter-node distances are distributed exponentially with mean d_{IN} m and intervals have a length of d_{IN} m, the distribution of V_i is given by the Poisson distribution with mean $\mathbb{E}(V_i)$ given by

$$\mathbb{E}(V_i) = \frac{d_{int}}{d_{IN}}, \quad i = 1, 2, \ldots \tag{7.4}$$

Note that the V_i's, $i = 1, 2, \ldots$, are independent.

Since a node in interval i has a probability S_i of becoming a candidate first forwarder, and the number of nodes in interval i is Poisson distributed with mean $\mathbb{E}(V_i)$, the number of candidate first forwarders in interval i is Poisson distributed with mean

$$\mathbb{E}(C_{1,i}) = \mathbb{E}(V_i) \cdot S_i, \quad i = 1, 2, \ldots, R, \tag{7.5}$$

with $\mathbb{E}(C_{1,i}) = 0$ for other values of i.

The total number of candidate first forwarders is equal to the sum of candidate first forwarders in the R intervals following the source. According to [99] the sum of a number of independent Poisson distributed random variables is also Poisson distributed, with its

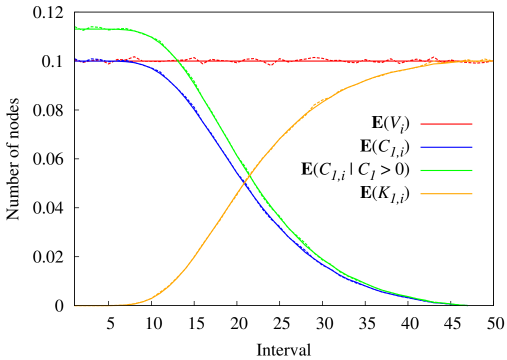

Figure 7.2: Expected values of V_i, $C_{1,i}$, $K_{1,i}$.

mean equal to the summed up means. Hence, C_1 has a Poisson distribution with mean

$$\mathbb{E}(C_1) = \sum_{i=1}^{R} \mathbb{E}(C_{1,i}) \tag{7.6}$$

$$= \sum_{i=1}^{R} S_i \mathbb{E}(V_i). \tag{7.7}$$

The probability of having at least one candidate first forwarder is given by

$$\mathbb{P}(C_1 > 0) = 1 - \mathbb{P}(C_1 = 0)$$
$$= 1 - e^{-\sum_{i=1}^{R} S_i \mathbb{E}(V_i)}. \tag{7.8}$$

Because we will need it later on, we determine here the distribution of the number of candidate first forwarders, given that there is at least one candidate first forwarder. It is calculated by normalising the distribution of C_1 with respect to $\mathbb{P}(C_1 > 0)$:

$$\mathbb{P}(C_1 = c_1 \mid C_1 > 0) = \frac{\mathbb{P}(C_1 = c_1 \wedge C_1 > 0)}{\mathbb{P}(C_1 > 0)} = \frac{\mathbb{P}(C_1 = c_1)}{\mathbb{P}(C_1 > 0)}$$
$$= \frac{\frac{\lambda^{c_1}}{c_1!} e^{-\lambda}}{1 - e^{-\lambda}}, \quad \lambda = \sum_{i=1}^{R} S_i \mathbb{E}(V_i), \quad c_1 \in \mathbb{N}^+, \tag{7.9}$$

with $\mathbb{P}(C_1 = c_1 \mid C_1 > 0) = 0$ for other values of c_1.

The expected number of candidate first forwarders in interval i, given that there is at least one candidate first forwarder is given by

$$\begin{aligned}
\mathbb{E}(C_{1,i} \mid C_1 > 0) &= \sum_{c_{1,i}=0}^{\infty} c_{1,i} \cdot \mathbb{P}(C_{1,i} = c_{1,i} \mid C_1 > 0) \\
&= \frac{1}{\mathbb{P}(C_1 > 0)} \cdot \sum_{c_{1,i}=1}^{\infty} c_{1,i} \cdot \mathbb{P}(C_1 > 0 \wedge C_{1,i} = c_{1,i}) \\
&= \frac{\mathbb{E}(C_{1,i})}{\mathbb{P}(C_1 > 0)} \\
&= \frac{S_i \mathbb{E}(V_i)}{1 - e^{-\sum_{j=1}^{R} S_j \mathbb{E}(V_j)}}, \quad i = 1, 2, \ldots, R, \qquad (7.10)
\end{aligned}$$

with $\mathbb{E}(C_{1,i} \mid C_1 > 0) = 0$ for other values of i. Fig. 7.2 shows $\mathbb{E}(C_{1,i} \mid C_1 > 0)$ as a function of interval number i.

Finally, since the number of candidate first forwarders in an interval is an independent Poisson process, the expected number of candidate first forwarders, given that there is at least one candidate first forwarder, is given by

$$\begin{aligned}
\mathbb{E}(C_1 \mid C_1 > 0) &= \sum_{i=1}^{R} \mathbb{E}(C_{1,i} \mid C_1 > 0) \\
&= \frac{\sum_{i=1}^{R} S_i \mathbb{E}(V_i)}{1 - e^{-\sum_{i=1}^{R} S_i \mathbb{E}(V_i)}}. \qquad (7.11)
\end{aligned}$$

Hop success probability

The probability of success of the first hop is equal to the probability of having a first forwarder, i.e., of having at least one candidate first forwarder:

$$\mathbb{P}(Y_1 = 1) = \mathbb{P}(C_1 > 0), \qquad (7.12)$$

with $\mathbb{P}(C_1 > 0)$ given by Eq. (7.8).

Position of the forwarder

For a given set of candidate forwarders, the candidate forwarder that has the shortest residual forwarding delay will become the next forwarder. Candidate forwarders draw their forwarding delay when they receive the message for the first time. Since the forwarding delay is distributed exponentially, and the exponential distribution is memoryless, the residual forwarding delay is i.i.d. with mean T_d for each candidate forwarder, regardless whether the candidate forwarder first received the message in the most recent hop or in some previous hop. Thus, for a given set of candidate forwarders the probability of becoming the next forwarder is equal for all candidate forwarders.

Since the probability of becoming the next forwarder is equal for all candidate forwarders, the probability that the first forwarder will be located in interval i, given that there

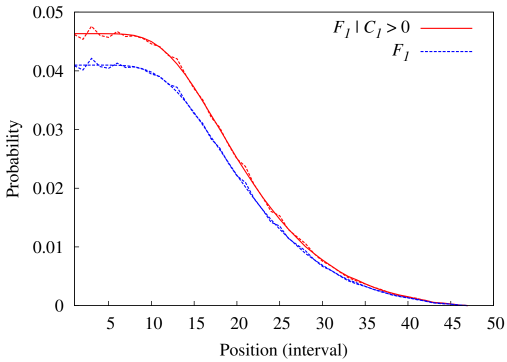

Figure 7.3: The distribution of the position of the first forwarder.

is a first forwarder, is equal to the expected value of the number of candidate forwarders in interval i normalised over the total number of candidate first forwarders, given that there is a first forwarder. As we prove in Appendix A.1 this results into

$$\begin{aligned} \mathbb{P}(F_1 = i \mid C_1 > 0) &= \mathbb{E}\Big(\frac{C_{1,i}}{C_1} \mid C_1 > 0\Big) \\ &= \frac{\mathbb{E}(C_{1,i})}{\mathbb{E}(C_1)}, \quad i = 1, 2, \ldots, R. \end{aligned} \tag{7.13}$$

with $\mathbb{P}(F_1 = i \mid C_1 > 0) = 0$ for other values of i.

It is easily seen that the probability that the first forwarder is positioned in interval i is equal to $\mathbb{P}(F_1 = i \mid C_1 > 0)$ multiplied with the probability that there is a first forwarder:

$$\mathbb{P}(F_1 = i) = \mathbb{P}(C_1 > 0) \cdot \mathbb{P}(F_1 = i \mid C_1 > 0), \quad i = 1, 2, \ldots, R, \tag{7.14}$$

with $\mathbb{P}(F_1 = i) = 0$ for other values of i and $\mathbb{P}(C_1 > 0)$ given by Eq. (7.8). Fig. 7.3 illustrates $\mathbb{P}(F_1 = i)$.

Given that there is a first forwarder, the expected number of first forwarders in interval i is equal to the probability that the first forwarder is positioned in interval i, i.e.,

$$\mathbb{E}(G_{1,i} \mid C_1 > 0) = \mathbb{P}(F_1 = i \mid C_1 > 0), \quad i = 1, 2, \ldots \tag{7.15}$$

Hop length

Since the source is by definition positioned in interval 0, the distribution of the hop length of the first hop is equal to the distribution of the position of the first forwarder, given that there is a first forwarder, i.e.,

$$\mathbb{P}(L_1 = l_1) = \mathbb{P}(F_1 = l_1 \mid C_1 > 0), \quad l_1 = 1, 2, \ldots, R, \tag{7.16}$$

with $\mathbb{P}(L_1 = l_1) = 0$ for other values of l_1.

Hop delay

For each hop holds that the candidate forwarder that has the shortest forwarding delay will become the next forwarder. The hop delay is therefore distributed as the minimum residual forwarding delay of all the candidate first forwarders. The candidate first forwarders draw their forwarding delay when they receive the message for the first time. Since the forwarding delay is distributed exponentially and the exponential distribution is memoryless, the forwarding delay of each candidate forwarder is identical, independent, and exponentially distributed with mean T_d. Given that there are c candidate forwarders, the hop delay is therefore distributed as the minimum value of c forwarding delays, that are each exponentially distributed with mean T_d. This minimum value is itself exponentially distributed with mean T_d/c. The CDF of the hop delay of the first hop (given that there is a first forwarder) is thus given by

$$F_{D_1}(t) = 1 - \sum_{c_1=1}^{\infty} \mathbb{P}(C_1 = c_1 \mid C_1 > 0) \ \cdot \ e^{-(c_1 \cdot \, t)/T_d}, \ \ t > 0, \tag{7.17}$$

with $\mathbb{P}(C_1 = c_1 \mid C_1 > 0)$ given by Eq. (7.9); $F_{D_1}(t) = 0$ for $t \leq 0$.

7.4.2 Second hop

Number of candidate forwarders

We first determine the expected number of candidate second forwarders in an interval, given the position of the first forwarder, denoted $\mathbb{E}(C_{2,i} \mid F_1 = j)$, and then the distribution of the total number of candidate second forwarders, given the position of the first forwarder, denoted $C_2 \mid F_1 = j$.

The set of candidate second forwarders in an interval consists of remaining candidate first forwarders (excluding the first forwarder itself) and additional candidate second forwarders, i.e., $C_{2,i} = H_{1,i} + A_{2,i}$. We are interested in their expected values for a given position j of the first forwarder:

$$\mathbb{E}(C_{2,i} \mid F_1 = j) = \mathbb{E}(H_{1,i} \mid F_1 = j) + \mathbb{E}(A_{2,i} \mid F_1 = j), \ \ i = j+1, j+2, \ldots \tag{7.18}$$

Below we first calculate $\mathbb{E}(H_{1,i} \mid F_1 = j)$ and then $\mathbb{E}(A_{2,i} \mid F_1 = j)$.

To calculate $\mathbb{E}(H_{1,i} \mid F_1 = j)$ we first determine $\mathbb{E}(H_{1,i} \mid C_1 > 0)$. We take the expected values of Eq. (7.2), condition on the existence of a first forwarder, and rearrange terms:

$$\mathbb{E}(H_{1,i} \mid C_1 > 0) = \mathbb{E}(C_{1,i} \mid C_1 > 0) - \mathbb{E}(G_{1,i} \mid C_1 > 0), \ \ i = 1, 2, \ldots, R, \tag{7.19}$$

with $\mathbb{E}(H_{1,i} \mid C_1 > 0) = 0$ for other values of i, $\mathbb{E}(C_{1,i} \mid C_1 > 0)$ given by Eq. (7.10) and $\mathbb{E}(G_{1,i} \mid C_1 > 0)$ given by Eq. (7.15). Fig. 7.4 illustrates $\mathbb{E}(H_{1,i} \mid C_1 > 0)$.

Because of the complexities involved, and in order to keep our discussion focussed, the method to explicitly calculate $\mathbb{E}(H_{1,i} \mid F_1 = j)$ is given in Appendix A.2. However, both extensive simulations and numerical calculations for a wide range of parameters have

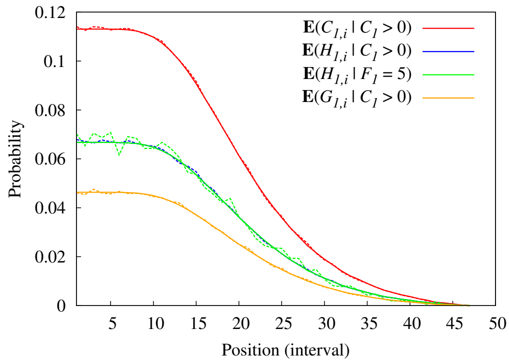

Figure 7.4: Expected values of $C_{1,i}$, $H_{1,i}$, and $G_{1,i}$. The analytical results of $\mathbb{E}(H_{1,i} \mid C_1 > 0)$ and $\mathbb{E}(H_{1,i} \mid F_1 = j)$ overlap.

shown that the expected number of candidate first forwarders in interval i, excluding the first forwarder, given that there is a first forwarder, is independent of the actual location of the first forwarder, i.e.,

$$\mathbb{E}(H_{1,i} \mid F_1 = j) = \mathbb{E}(H_{1,i} \mid C_1 > 0), \quad i = 1, 2, \ldots \quad j = 1, \ldots, R. \tag{7.20}$$

A formal proof of Eq. (7.20) in case of an ideal transmission model is given in Appendix A.3. Based on this proof, as well as on those results obtained by extensive simulations and numerical calculations, we conjecture that Eq. (7.20) also holds for the general case, i.e., for a non-ideal transmission model. As Eq. (7.20) is considerably faster than the method presented in Appendix A.2 we will use it to calculate $\mathbb{E}(H_{1,i} \mid F_1 = j)$ for the remainder of this chapter. The similarity of $\mathbb{E}(H_{1,i} \mid F_1 = j)$ and $\mathbb{E}(H_{1,i} \mid C_1 > 0)$ is illustrated in Fig. 7.4.

$\mathbb{E}(A_{2,i} \mid F_1 = j)$ is determined as follows. The number of additional candidate second forwarders in interval i is defined as the number of nodes in interval i that received the message for the first time from the first forwarder. The number of nodes that did not receive the message from the source in interval i, denoted $K_{1,i}$, has a Poisson distribution with mean

$$\mathbb{E}(K_{1,i}) = \mathbb{E}(V_i) \cdot (1 - S_i), \quad i = 1, 2, \ldots, R, \tag{7.21}$$

with $\mathbb{E}(K_{1,i}) = 0$ for other values of i. The distribution of $K_{1,i}$ is independent of the distribution of the number of candidate first forwarders. Fig. 7.2 shows $\mathbb{E}(K_{1,i})$.

Given that the first forwarder is positioned in interval j, the probability that a node in interval i successfully receives the message from the first forwarder is given by S_{i-j}, $i > j$. $A_{2,i} \mid F_1 = j$ is thus Poisson distributed with mean $\mathbb{E}(A_{2,i} \mid F_1 = j)$ given by

$$\mathbb{E}(A_{2,i} \mid F_1 = j) = \mathbb{E}(K_{1,i})\, S_{i-j}, \quad i = j + 1, \ldots, j + R, \tag{7.22}$$

with $\mathbb{E}(A_{2,i} \mid F_1 = j) = 0$ for other values of i. Fig. 7.5 illustrates $\mathbb{E}(A_{2,i} \mid F_1 = j)$.

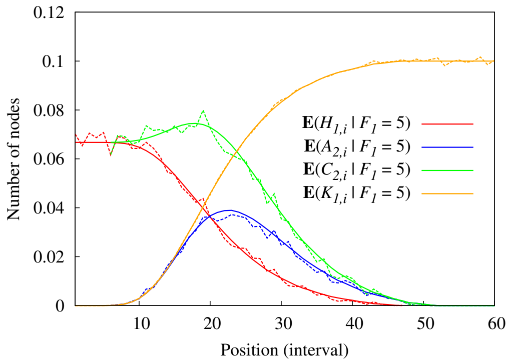

Figure 7.5: Expected values of $H_{1,i}$, $A_{2,i}$, and $C_{2,i}$.

Combining Eq. (7.20) and Eq. (7.22) into Eq. (7.18) we thus have an expression to calculate $\mathbb{E}(C_{2,i} \mid F_1 = j)$.

We now determine the distribution of $C_2 \mid F_1 = j$. Given that the first forwarder is positioned in interval j, the total number of candidate second forwarders C_2 is made up out the number of remaining candidate first forwarders in intervals $j+1$ through R, denoted $C_{1,j+1:R}$, plus the number of additional candidate second forwarders in intervals $j+1$ through $j+R$, i.e.,

$$\begin{aligned} \mathbb{P}(C_2 = c_2 \mid F_1 = j) = \quad & \mathbb{P}(C_{1,j+1:R} + A_2 = c_2 \mid F_1 = j) \\ = & \sum_{c_{1,j+1:R}=0}^{c_2} \mathbb{P}(C_{1,j+1:R} = c_{1,j+1:R} \mid F_1 = j) \cdot \\ & \qquad \mathbb{P}(A_2 = c_2 - c_{1,j+1:R} \mid F_1 = j), \\ c_2 \in \mathbb{N}, \quad j = 1, 2, \ldots, R, & \end{aligned} \tag{7.23}$$

with $\mathbb{P}(C_2 = c_2 \mid F_1 = j) = 0$ for other values of c_2, j. $\mathbb{P}(C_{1,j+1:R} = c_{1,j+1:R} \mid F_1 = j)$ is given by Eq. (A.25) in Appendix A.4. The distribution of $A_2 \mid F_1 = j$ is independent of the number of candidate first forwarders; it is Poisson distributed with mean

$$\mathbb{E}(A_2 \mid F_1 = j) = \sum_{i=j+1}^{j+R} \mathbb{E}(A_{2,i} \mid F_1 = j), \quad j = 1, 2, \ldots, R. \tag{7.24}$$

The distribution of the number of candidate second forwarders, given the position of the first forwarder and given that there is at least one candidate second forwarder, is given by

$$\mathbb{P}(C_2 = c_2 \mid F_1 = j \wedge C_2 > 0) = \frac{\mathbb{P}(C_2 = c_2 \mid F_1 = j)}{1 - \mathbb{P}(C_2 = 0 \mid F_1 = j)}, \quad j = 1, 2, \ldots, R. \tag{7.25}$$

Analogue to the first hop, see Eq. (7.10), the expected number of candidate second forwarders in interval i, given the position of the first forwarder and given that there is at least one candidate second forwarder, is given by

$$\mathbb{E}(C_{2,i} \mid F_1 = j \wedge C_2 > 0) = \frac{\mathbb{E}(C_{2,i} \mid F_1 = j)}{1 - \mathbb{P}(C_2 = 0 \mid F_1 = j)},$$
$$j = 1, 2, \ldots, R, \quad i = j+1, j+2, \ldots, j+R, \tag{7.26}$$

with $\mathbb{E}(C_{2,i} \mid F_1 = j \wedge C_2 > 0) = 0$ for other values of i, j.

Finally, because we will need it later on we express the expected number of nodes in an interval i following the first forwarder. Given that the first forwarder is positioned in interval j, the expected number of nodes in interval i is given by

$$\begin{aligned}\mathbb{E}(V_i \mid F_1 = j) &= \mathbb{E}(H_{1,i} + K_{1,i} \mid F_1 = j) \\ &= \mathbb{E}(H_{1,i} \mid F_1 = j) + \mathbb{E}(K_{1,i} \mid F_1 = j), \quad i = j+1, j+2, \ldots\end{aligned} \tag{7.27}$$

Hop success probability

The probability of success of the second hop is equal to the probability of having at least one candidate second forwarder. For a given position of the first forwarder it is therefore given by

$$\mathbb{P}(Y_2 = 1 \mid F_1 = i) = \mathbb{P}(C_2 > 0 \mid F_1 = i), \quad i = 1, 2, \ldots, R, \tag{7.28}$$

which can be calculated using Eq. (7.23). For an arbitrary position of the first forwarder (given that there is a first forwarder) the second-hop success probability is thus given by

$$\mathbb{P}(Y_2 = 1 \mid Y_1 = 1) = \sum_{i=1}^{R} \mathbb{P}(F_1 = i \mid C_1 > 0) \cdot \mathbb{P}(C_2 > 0 \mid F_1 = i), \tag{7.29}$$

with $\mathbb{P}(F_1 = i \mid C_1 > 0)$ given by Eq. (7.13). Finally, the unconditional probability of a successful second hop is given by

$$\mathbb{P}(Y_2 = 1) = \sum_{i=1}^{R} \mathbb{P}(F_1 = i) \cdot \mathbb{P}(C_2 > 0 \mid F_1 = i). \tag{7.30}$$

Position of the forwarder

We determine the distribution of the position of the second forwarder in a manner analogue to how the position of the first forwarder is calculated in Eq. (7.13):

$$\begin{aligned}\mathbb{P}(F_2 = i \mid F_1 = j \wedge C_2 > 0) &= \mathbb{E}\Big(\frac{C_{2,i}}{C_2} \mid F_1 = j \wedge C_2 > 0\Big) \\ &\approx \frac{\mathbb{E}(C_{2,i} \mid F_1 = j)}{\mathbb{E}(C_2 \mid F_1 = j)},\end{aligned}$$
$$j = 1, 2, \ldots, R, \quad i = j+1, \ldots, j+R, \tag{7.31}$$

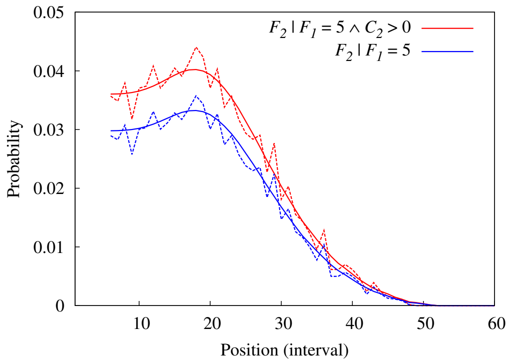

Figure 7.6: The distribution of the position of the second forwarder for a given position of the first forwarder.

with $\mathbb{P}(F_2 = i \mid F_1 = j \wedge C_2 > 0) = 0$ for other values of i. $\mathbb{E}(C_2 \mid F_1 = j)$ can easily be derived from Eq. (7.23). Note that Eq. (7.31) is an approximation because $\mathbb{E}\left(\frac{C_{2,i}}{C_2} \mid F_1 = j \wedge C_2 > 0\right) = \frac{\mathbb{E}(C_{2,i} \mid F_1=j)}{\mathbb{E}(C_2 \mid F_1=j)}$ only holds if both $C_{2,i} \mid F_1 = j \wedge C_2 > 0$ and $C_2 \mid F_1 = j \wedge C_2 > 0$ are Poisson distributed, which is not the case: both variables have a shifted Poisson distribution. For practical purposes the margin of error introduced by this approximation is negligible however, as will be shown in Section 7.6. Fig. 7.6 illustrates $\mathbb{P}(F_2 = i \mid F_1 = j \wedge C_2 > 0)$.

It is easily seen that $\mathbb{P}(F_2 = i \mid F_1 = j)$ can be calculated by multiplying $\mathbb{P}(F_2 = i \mid F_1 = j \wedge C_2 > 0)$ with the probability that there is a second forwarder:

$$\mathbb{P}(F_2 = i \mid F_1 = j) = \mathbb{P}(C_2 > 0 \mid F_1 = j) \cdot \mathbb{P}(F_2 = i \mid F_1 = j \wedge C_2 > 0),$$
$$j = 1, 2, \ldots, R, \quad i = j + 1, \ldots, j + R, \tag{7.32}$$

with $\mathbb{P}(F_2 = i \mid F_1 = j) = 0$ for other values of i and $\mathbb{P}(C_2 > 0 \mid F_1 = j)$ given by Eq. (7.23). Fig. 7.6 illustrates $\mathbb{P}(F_2 = i \mid F_1 = j)$ with respect to $\mathbb{P}(F_2 = i \mid F_1 = j \wedge C_2 > 0)$.

The probability that the second forwarder is in interval i, given that there is a first forwarder but irrespective of its position, is denoted $\mathbb{P}(F_2 = i \mid C_2 > 0)$. It is calculated by conditioning on the position of the first forwarder, given that there is a first forwarder:

$$\mathbb{P}(F_2 = i \mid C_2 > 0) = \sum_{j=1}^{R} \mathbb{P}(F_1 = j \mid C_1 > 0) \cdot \mathbb{P}(F_2 = i \mid F_1 = j \wedge C_2 > 0),$$
$$i = 2, 3, \ldots, 2R, \tag{7.33}$$

with $\mathbb{P}(F_2 = i \mid C_2 > 0) = 0$ for other values of i. Fig. 7.7 illustrates $\mathbb{P}(F_2 = i \mid C_2 > 0)$.

The probability that the second forwarder is in interval i is denoted $\mathbb{P}(F_2 = i)$ and is

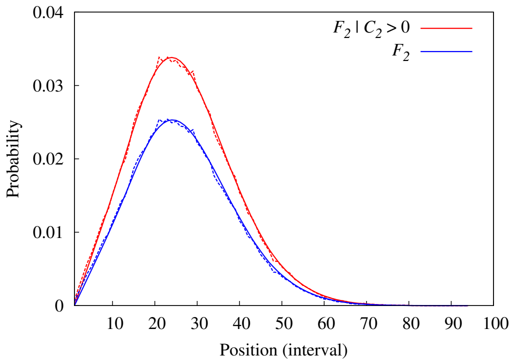

Figure 7.7: The distribution of the position of the forwarder.

calculated by conditioning on the possible positions of the first forwarder:

$$\mathbb{P}(F_2 = i) = \sum_{j=1}^{R} \mathbb{P}(F_1 = j) \cdot \mathbb{P}(F_2 = i \mid F_1 = j), \quad i = 2, 3, \ldots, 2R, \tag{7.34}$$

with $\mathbb{P}(F_2 = i) = 0$ for other values of i and $\mathbb{P}(F_1 = j)$ given by Eq. (7.14). Fig. 7.7 illustrates $\mathbb{P}(F_2 = i)$.

Finally, given that there is a second forwarder and given that the first forwarder is positioned in interval j, the expected number of second forwarders in interval i is given by

$$\mathbb{E}(G_{2,i} \mid F_1 = j \wedge C_2 > 0) = \mathbb{P}(F_2 = i \mid F_1 = j \wedge C_2 > 0)$$
$$j = 1, 2, \ldots, R, \quad i = j + 1, \ldots, j + R, \tag{7.35}$$

with $\mathbb{E}(G_{2,i} \mid F_1 = j \wedge C_2 > 0) = 0$ for other values of i, j.

Hop length

The distribution of the hop length of the second hop is calculated with respect to the position of the first forwarder. For a given position of the first forwarder the distribution of L_2 is given by

$$\mathbb{P}(L_2 = l_2 \mid F_1 = j) = \mathbb{P}(F_2 = j + l_2 \mid F_1 = j \wedge C_2 > 0), \quad l_2, j = 1, 2, \ldots, R, \tag{7.36}$$

with $\mathbb{P}(L_2 = l_2 \mid F_1 = j) = 0$ for other values of l_2, j. For an arbitrary position of the first forwarder the distribution of L_2 is given by conditioning on the position of the first forwarder:

$$\mathbb{P}(L_2 = l_2) = \sum_{j=1}^{R} \mathbb{P}(F_1 = j \mid C_1 > 0)\, \mathbb{P}(F_2 = j + l_2 \mid F_1 = j \wedge C_2 > 0),$$
$$l_2, j = 1, 2, \ldots, R, \tag{7.37}$$

with $\mathbb{P}(F_1 = j \mid C_1 > 0)$ given by Eq. (7.13) and $\mathbb{P}(F_2 = j + l_2 \mid F_1 = j \wedge C_2 > 0)$ given by Eq. (7.31); $\mathbb{P}(L_2 = l_2 \mid F_1 = j) = 0$ for other values of l_2.

Hop delay

Analogue to how the hop delay of the first hop is determined, the distribution of the hop delay of the second hop, denoted D_2, is given by conditioning on the number of candidate second forwarders (given that there is at least one candidate second forwarder). Given that the first forwarder is positioned in interval j, the CDF of the hop delay is given by

$$\mathbb{F}_{D_2 \mid F_1=j}(t) = 1 - \sum_{c_2=1}^{\infty} \mathbb{P}(C_2 = c_2 \mid F_1 = j \wedge C_2 > 0) \cdot e^{-(c_2 \cdot t)/T_d}, \quad t > 0, \tag{7.38}$$

with $\mathbb{P}(C_2 = c_2 \mid F_1 = j \wedge C_2 > 0)$ given by Eq. (7.25); $\mathbb{F}_{D_2 \mid F_1=j}(t) = 0$ for $t \leq 0$. For an arbitrary position of the first forwarder the distribution of D_2 is given by conditioning on the position of the first forwarder:

$$\mathbb{F}_{D_2}(t) = \sum_{j=1}^{R} \mathbb{P}(F_1 = j \mid C_1 > 0) \cdot \mathbb{F}_{D_2 \mid F_1=j}(t), \quad t > 0, \tag{7.39}$$

with $\mathbb{F}_{D_2}(t) = 0$ for $t \leq 0$.

7.4.3 Third hop

For this hop we determine the expected number of candidate third forwarders in an interval but not the distribution of the total number of candidate third forwarders. We can therefore only calculate the distribution of the position of the forwarder and the distribution of the hop length, but not the hop success probability or the hop delay, since these latter two metrics depend on the distribution of the total number of candidate third forwarders.

Number of candidate forwarders

We determine the expected number of candidate third forwarders in interval i, given that the first forwarder is positioned in interval j and the second forwarder is positioned in interval k, denoted $\mathbb{E}(C_{3,i} \mid F_1 = j \wedge F_2 = k)$.

The set of candidate third forwarders in an interval consists of remaining candidate second forwarders (excluding the second forwarder itself) and additional candidate third forwarders, i.e., $C_{3,i} = H_{2,i} + A_{3,i}$. Taking the expected values, for given positions of the first two forwarders, we get

$$\mathbb{E}(C_{3,i} \mid F_1 = j \wedge F_2 = k) = \mathbb{E}(H_{2,i} \mid F_1 = j \wedge F_2 = k) + \mathbb{E}(A_{3,i} \mid F_1 = j \wedge F_2 = k),$$
$$j = 1, 2, \ldots, R, \quad k = j+1, j+2, \ldots, j+R, \quad i = k+1, k+2, \ldots, k+R. \tag{7.40}$$

Below we first determine $\mathbb{E}(H_{2,i} \mid F_1 = j \wedge F_2 = k)$, then $\mathbb{E}(A_{3,i} \mid F_1 = j \wedge F_2 = k)$.

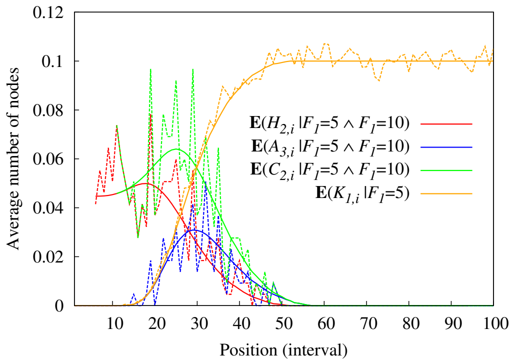

Figure 7.8: Expected values of $H_{2,i}$, $A_{3,i}$, $C_{3,i}$, and $K_{2,i}$.

Analogue to the second hop, see Eq. (7.20), we state

$$\mathbb{E}(H_{2,i} \mid F_1 = j \wedge F_2 = k) = \mathbb{E}(H_{2,i} \mid F_1 = j \wedge C_2 > 0),$$
$$j = 1, 2, \ldots, R, \quad i = j+1, j+2, \ldots, j+R, \tag{7.41}$$

with $\mathbb{E}(H_{2,i} \mid F_1 = j \wedge F_2 = k) = 0$ for other values of i, j. $\mathbb{E}(H_{2,i} \mid F_1 = j \wedge C_2 > 0)$ is, by definition, given by

$$\mathbb{E}(H_{2,i} \mid F_1 = j \wedge C_2 > 0) = \mathbb{E}(C_{2,i} \mid F_1 = j \wedge C_2 > 0) - \mathbb{E}(G_{2,i} \mid F_1 = j \wedge C_2 > 0),$$
$$j = 1, 2, \ldots, R, \quad i = j+1, j+2, \ldots, j+R, \tag{7.42}$$

with $\mathbb{E}(H_{2,i} \mid F_1 = j \wedge C_2 > 0) = 0$ for other values of i, j, $\mathbb{E}(C_{2,i} \mid F_1 = j \wedge C_2 > 0)$ given by Eq. (7.26), and $\mathbb{E}(G_{2,i} \mid F_1 = j \wedge C_2 > 0)$ given by Eq. (7.35).

$\mathbb{E}(A_{3,i} \mid F_1 = j \wedge F_2 = k)$ is determined as follows. The number of additional candidate third forwarders in interval i, $A_{3,i}$, is defined as the number of nodes in interval i that received the message for the first time from the second forwarder. It is a product of *(i)* the number of nodes in interval i that did not receive the message from either the source or the first forwarder, $K_{2,i}$, and *(ii)* the probability that a node in interval i successfully received the message from the second forwarder.

The number of nodes in interval i that did not receive the message from the source and did not receive the message from the first forwarder, given that the first forwarder is positioned in interval j, has a Poisson distribution with mean

$$\mathbb{E}(K_{2,i} \mid F_1 = j) = \begin{cases} \mathbb{E}(K_{1,i}) \cdot (1 - S_{i-j}), & i = j+1, \ldots, j+R, \\ \mathbb{E}(K_{1,i}), & i = j+R+1, j+R+2, \ldots, \end{cases} \tag{7.43}$$

with $\mathbb{E}(K_{2,i} \mid F_1 = j) = 0$ for other values of i. The distribution of $K_{2,i} \mid F_1 = j$ is independent of the distribution of the number of candidate second forwarders.

Given that the second forwarder is positioned in interval k, the probability that a node in interval i successfully receives the message from the second forwarder is given by S_{i-k},

$i > k$. $A_{3,i} \mid F_1 = j \wedge F_2 = k$ is thus Poisson distributed with mean

$$\mathbb{E}(A_{3,i} \mid F_1 = j \wedge F_2 = k) = \mathbb{E}(K_{2,i} \mid F_1 = j)\ S_{i-k},$$
$$j = 1, 2, \ldots, R, \quad k = j+1, j+2, \ldots, j+R, \quad i = k+1, k+2, \ldots, k+R, \tag{7.44}$$

with $\mathbb{E}(A_{3,i} \mid F_1 = j \wedge F_2 = k) = 0$ for other values of i, j, k, and with $\mathbb{E}(K_{1,i} \mid F_1 = j)$ given by Eq. (7.21).

Combining Eq. (7.41), Eq. (7.42), and Eq. (7.44), we thus have an expression to calculate Eq. (7.40). Fig. 7.8 shows the expected values of $H_{2,i}$, $A_{3,i}$, $C_{3,i}$, and $K_{2,i}$.

The expected total number of candidate third forwarders is then given by

$$\mathbb{E}(C_3 \mid F_1 = j \wedge F_2 = k) = \sum_{i=k+1}^{k+R} \mathbb{E}(C_{3,i} \mid F_1 = j \wedge F_2 = k),$$
$$j = 1, 2, \ldots, R, \quad k = j+1, j+2, \ldots, j+R, \tag{7.45}$$

with $\mathbb{E}(C_3 \mid F_1 = j \wedge F_2 = k) = 0$ for other values of j, k.

Lastly, because we will need it later on we express the expected number of nodes in an interval i following the second forwarder. Given that the first forwarder is positioned in interval j and the second forwarder is positioned in interval k, the expected number of nodes in interval i is given by

$$\mathbb{E}(V_i \mid F_1 = j \wedge F_2 = k) = \mathbb{E}(H_{2,i} \mid F_1 = j \wedge F_2 = k) + \mathbb{E}(K_{2,i} \mid F_1 = j \wedge F_2 = k),$$
$$i = j+1, j+2, \ldots, \tag{7.46}$$

Position of the forwarder

Analogue to the first and second hop the position of the third forwarder, given that there is a third forwarder and given the position of the first two forwarders, is approximated by

$$\mathbb{P}(F_3 = i \mid F_1 = j \wedge F_2 = k \wedge C_3 > 0) = \mathbb{E}(\frac{C_{3,i}}{C_3} \mid C_3 > 0)$$
$$\approx \frac{\mathbb{E}(C_{3,i})}{\mathbb{E}(C_3)},$$
$$j = 1, 2, \ldots, R, \quad k = j+1, j+2, \ldots, j+R, \quad i = k+1, k+2, \ldots, k+R. \tag{7.47}$$

When it is given that there is a third forwarder, the distribution of its position is calculated by conditioning on the position of the first two forwarder:

$$\mathbb{P}(F_3 = i \mid C_3 > 0) = \sum_{j=1}^{R} \sum_{k=j+1}^{j+R} \mathbb{P}(F_1 = j \mid C_1 > 0) \cdot \mathbb{P}(F_2 = i \mid F_1 = j \wedge C_2 > 0) \cdot$$
$$\mathbb{P}(F_3 = i \mid F_1 = j \wedge F_2 = k \wedge C_3 > 0),$$
$$i = 3, 4, \ldots, 3 \cdot R, \tag{7.48}$$

with $\mathbb{P}(F_3 = i \mid C_3 > 0) = 0$ for other values of i. Fig. 7.9 illustrates $\mathbb{P}(F_3 = i \mid C_3 > 0)$.

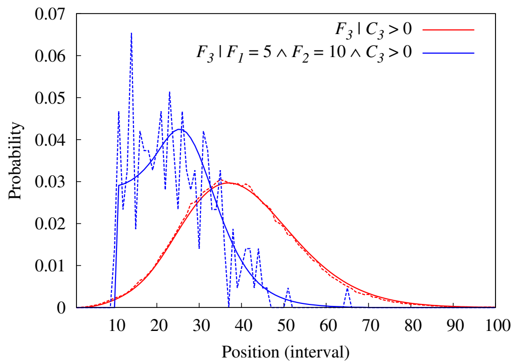

Figure 7.9: The distribution of the position of the third forwarder.

Hop length

The hop length of the third hop is calculated with respect to the position of the second forwarder. For a given position of the first two forwarders the distribution of L_3 is given by

$$\mathbb{P}(L_3 = l_3 \mid F_1 = j \wedge F_2 = k) = \mathbb{P}(F_3 = k + l_3 \mid F_1 = j \wedge F_2 = k \wedge C_3 > 0),$$
$$l_3 = 1, 2, \ldots, R, \tag{7.49}$$

with $\mathbb{P}(L_3 = l_3 \mid F_1 = j \wedge F_2 = k) = 0$ for other values of l_3, j, k. For arbitrary positions of the first two forwarders the distribution of L_3 is given by conditioning on the position of the first two forwarders:

$$\mathbb{P}(L_3 = l_3) = \sum_{j=1}^{R} \sum_{k=j+1}^{j+R} \mathbb{P}(F_1 = j \mid C_1 > 0)\, \mathbb{P}(F_2 = k \mid F_1 = j \wedge C_2 > 0) \cdot$$
$$\mathbb{P}(L_3 = l_3 \mid F_1 = j \wedge F_2 = k)$$
$$l_3 = 1, 2, \ldots, R, \tag{7.50}$$

with $\mathbb{P}(L_3 = l_3) = 0$ for other values of l_3.

7.5 Approximate analysis of following hops

In the previous section we determined the behaviour of the forwarding protocol in an exact manner. The complexity of the method we used grows exponentially with each hop, making it infeasible to determine the behaviour of the system for a large number of hops. In this section we therefore present a number of approximations to determine the behaviour of the forwarding model for an arbitrary number of hops. These methods are of limited complexity, allowing for fast evaluation.

7.5.1 Hop success probability

The probability of success of a hop (given that all the previous hops were successful) is approximated for the third and following hops by assuming that it is equal to the success probability of the second hop (given that first hop was successful), i.e.,

$$\mathbb{P}(Y_n = 1 \mid Y_{n-1} = 1) \approx \mathbb{P}(Y_2 = 1 \mid Y_1 = 1), \;\; n = 3, 4, \ldots, \tag{7.51}$$

with $\mathbb{P}(Y_2 = 1 \mid Y_1 = 1)$ given by Eq. (7.30). The unconditional probability of success of the n^{th} hop is then approximated by

$$\mathbb{P}(Y_n = 1) \approx \mathbb{P}(Y_1 = 1) \cdot \big(\mathbb{P}(Y_2 = 1)\big)^{n-1}, \;\; n = 3, 4, \ldots \tag{7.52}$$

7.5.2 Hop length

We approximate the distribution of the hop length of the fourth and following hops with the distribution of the hop length of the third hop. As we will find from the numerical results in Section 7.6.2, the distribution of the hop length of the n^{th} hop is significantly influenced by the hop lengths of previous hops. We therefore condition the distribution of the hop length of the n^{th} hop on the hop length of the $(n-1)^{\text{th}}$ hop, i.e.,

$$F_{L_n \mid L_{n-1}=l_{n-1}}(\cdot) \sim F_{L_3 \mid L_2=l_{n-1}}(\cdot), \;\; n = 4, 5, \ldots, \tag{7.53}$$

with the distribution of $L_3 \mid L_2 = l_{n-1}$ given by

$$\begin{aligned}
&\mathbb{P}(L_3 = l_3 \mid L_2 = l_2) = \\
&\sum_{i=1}^{R} \mathbb{P}(F_1 = i \mid C_1 > 0) \cdot \mathbb{P}(F_3 = i + l_2 + l_3 \mid F_1 = i \wedge F_2 = i + l_2 \wedge C_3 > 0), \\
&l_3 = 1, 2, \ldots, R, \;\; l_2 = 1, 2, \ldots, R,
\end{aligned} \tag{7.54}$$

with $\mathbb{P}(F_1 = i \mid C_1 > 0)$ given by Eq. (7.13) and
$\mathbb{P}(F_3 = i + l_2 + l_3 \mid F_1 = i \wedge F_2 = i + l_2 \wedge C_3 > 0)$ given by Eq. (7.47).

7.5.3 Position of the forwarder

We approximate the distribution of the position of the n^{th} forwarder ($n > 3$) in a recursive manner, assuming that there is such a forwarder, by taking into account the length of previous hops.

We have assumed in Eq. (7.53) that the hop length of each hop beyond the third hop (given the hop length of the previous hop) is distributed identically to the hop length of the third hop (given the hop length of the second hop). The position of the n^{th} forwarder, given that there is an n^{th} forwarder, can thus be approximated by conditioning on the position of the $(n-2)^{\text{th}}$ forwarder and the length of the $(n-1)^{\text{th}}$ hop, i.e.,

$$\begin{aligned}
\mathbb{P}(F_n = i \mid C_n > 0) \approx \sum_{j=n-2}^{(n-2)R} & \mathbb{P}(F_{n-2} = j \mid C_{n-2} > 0) \cdot \\
& \sum_{l_{n-1}=1}^{R} \mathbb{P}(F_{n-1} = j + l_{n-1} \mid F_{n-2} = j \wedge C_{n-1} > 0) \cdot \\
& \qquad \mathbb{P}(L_n = i - j - l_{n-1} \mid L_{n-1} = l_{n-1}), \\
n = 4, 5, \ldots, \quad i = n, n+1, \ldots, n \cdot R, & \qquad (7.55)
\end{aligned}$$

with $\mathbb{P}(F_n = i \mid C_n > 0) = 0$ for other values of i. The term $\mathbb{P}(F_{n-1} = j + l_{n-1} \mid F_{n-2} = j \wedge C_{n-1} > 0)$ denotes the probability that the $(n-1)^{\text{th}}$ forwarder is positioned in interval $j + l_{n-1}$, given that the $(n-2)^{\text{th}}$ forwarder is positioned in interval j and given that there is an $(n-1)^{\text{th}}$ forwarder. It is given by

$$\begin{aligned}
& \mathbb{P}(F_{n-1} = i \mid F_{n-2} = j \wedge C_{n-1} > 0) = \\
& \sum_{k=n-3}^{(n-3)R} \mathbb{P}(F_{n-3} = k \mid C_{n-3} > 0) \cdot \mathbb{P}(L_{n-1} = i - j \mid L_{n-2} = j - k), \\
& n = 3, 4, \ldots, \quad i = n, n+1, \ldots, n \cdot R, \qquad (7.56)
\end{aligned}$$

with $\mathbb{P}(L_{n-1} = i - j \mid L_{n-2} = j - k)$ given by Eq. (7.53); for other values of i $\mathbb{P}(F_n = i \mid F_{n-1} = j \wedge C_n > 0) = 0$.

7.5.4 Required number of hops

We determine the distribution of the required number of hops to have the message forwarded by a node at or beyond position i, denoted N_i. We make use of the fact that the probability that *at most* n hops are required to have the message forwarded by a node at or beyond position i is equal to the probability that the n^{th} forwarder is at or beyond position i, i.e.,

$$\begin{aligned}
\mathbb{P}(N_i \le n) &= \mathbb{P}(F_n \ge i \mid C_n > 0) \\
&= 1 - P(F_n < i \mid C_n > 0), \\
i = 1, 2, \ldots, & \quad n = 1, 2, \ldots \qquad (7.57)
\end{aligned}$$

where $\mathbb{P}(F_n < i \mid C_n > 0)$ is equal to the sum of the probabilities that the forwarder is at position $j = 1, \ldots, i-1$, given by

$$\begin{aligned}
& P(F_n < i \mid C_n > 0) = \sum_{j=1}^{i-1} \mathbb{P}(F_n = j \mid C_n > 0), \\
& n = 1, 2, \ldots, \quad i = 1, \ldots, n \cdot R, \qquad (7.58)
\end{aligned}$$

with $\mathbb{P}(F_n = j \mid C_n > 0)$ given by Eq. (7.55).

7.5.5 Hop delay

We approximate the hop delay of the n^{th} hop D_n for $n > 2$.

As we will find from the numerical results in Section 7.6.2 the distribution of the hop delay changes little after the first two hops. We therefore approximate the hop delay distribution of the n^{th} hop with the hop delay distribution of the second hop:

$$F_{D_n}(\cdot) \sim F_{D_2}(\cdot), \quad n = 3, 4, \ldots, \tag{7.59}$$

with $F_{D_2}(\cdot)$ given by Eq. (7.39). Moreover, for a given length of the $(n-1)^{\text{th}}$ hop l_{n-1} we approximate the hop delay distribution of the n^{th} hop by

$$F_{D_n \mid L_{n-1}=l_{n-1}}(\cdot) \sim F_{D_2 \mid F_1=l_{n-1}}(\cdot), \quad n = 3, 4, \ldots, \quad l_{n-1} = 1, 2, \ldots, R. \tag{7.60}$$

7.5.6 End-to-end delay

The end-to-end delay to have a message forwarded at least i intervals is a convolution of the required number of hops to have the message forwarded at least i intervals and the delay per hop. We therefore first determine the end-to-end delay to have the message forwarded at least i intervals in n hops, denoted $F_{E_i \mid N_i=n}$ and then condition on the required number of hops to have a message forwarded i intervals. For the first two hops the end-to-end delay is exact; for following hops the end-to-end delay is approximated.

The distribution of the end-to-end delay for the case that the sink is reached in a single hop is independent of the value of i and is equal to the distribution of the hop delay of the first hop, i.e.,

$$F_{E_i \mid N_i=1}(t) = F_{D_1}(t), \quad t > 0 \tag{7.61}$$

with $F_{D_1}(t)$ given by Eq. (7.17).

The distribution of the end-to-end delay to have a message forwarded i intervals when exactly two hops are needed is derived by conditioning on the position of the first forwarder and the delay of the first hop, given that the second forwarder is positioned at interval i or beyond. Normalising F_1 with respect to the fact that it must be within R intervals of interval i but not at or beyond interval i we get

$$F_{E_i \mid N_i=2}(t) = \sum_{j=\max(1,i-R)}^{\min(R,i-1)} \frac{\mathbb{P}(F_1 = j \mid C_1 > 0)}{\sum_{k=\max(1,i-R)}^{\min(R,i-1)} \mathbb{P}(F_1 = k \mid C_1 > 0)} \cdot \int_{t_1=0}^{t} f_{D_1}(t_1) \cdot \mathbb{F}_{D_2 \mid F_1=j}(t - t_1)\, \mathrm{d}t_1, \quad t > 0, \tag{7.62}$$

with $\mathbb{P}(F_1 = j \mid C_1 > 0)$ given by Eq. (7.13), $f_{D_1}(t_1)$ can easily be derived from Eq. (7.17), and $\mathbb{F}_{D_2 \mid F_1=j}(t - t_1)$ given by Eq. (7.38).

If $n > 2$ hops are needed to have the message forwarded i intervals then the average hop length l is given by i/n. To approximate the distribution of the end-to-end delay of n

hops we first approximate the end-to-end delay of the last $n-1$ hops as a convolution of $n-1$ independent hop delays distributed according to $F_{D_2 \mid F_1=l}(t)$. The delay of each of these $n-1$ hops is exponentially distributed with rate $\lambda = \mathbb{E}(C_2 \mid F_1 = l \wedge C_2 > 0)/T_d$, with $\mathbb{E}(C_2 \mid F_1 = l \wedge C_2 > 0)$ derived from Eq. (7.25). The distribution of the sum of $n-1$ of such independent exponential hop delays with identical rates is given by the Erlang distribution [99]. The end-to-end delay of n hops is then a convolution of the first hop, given by $f_{D_1}(t_1)$, and the $n-1$ remaining hops. $F_{E_i \mid N_i=n}(t)$ is therefore given by

$$F_{E_i \mid N_i=n}(t) \approx \int_{t_1=0}^{t} f_{D_1}(t_1) \cdot \Big(1 - \sum_{k=0}^{n-2} \frac{e^{-\lambda(t-t_1)}}{k!} (\lambda(t-t_1))^k\Big)\, \mathrm{d}t_1,$$
$$t > 0, \;\; n = 3, 4, \ldots, \;\; l = \lceil i/n \rceil. \tag{7.63}$$

Note that by assuming that each hop is of average length and consecutive hops are independent of each other we ignore any dependencies between consecutive hop lengths. The effect that this has on the accuracy of our model is discussed in detail in Section 7.6.2.

Finally, to calculate the end-to-end delay to have a message forwarded i intervals we condition on the required number of hops, such that the end-to-end delay is given by

$$F_{E_i}(t) = \sum_{n=1}^{\infty} \mathbb{P}(N_i = n) \cdot F_{E_i \mid N_i=n}(t), \;\; t > 0, \;\; i \in \mathbb{N}^+, \tag{7.64}$$

with $F_{E_i \mid N_i=n}(t)$ given by Eq. (7.61) for $n = 1$, by Eq. (7.62) for $n = 2$, and by Eq. (7.63) for $n > 2$.

7.6 Performance evaluation

Having analysed the forwarding protocol in an analytical manner in the previous sections, in this section we present the set-up and results of an evaluation study to assess *(i)* how the forwarding protocol described in Section 7.3 performs for varying network parameters, and *(ii)* how well our analysis presented in the previous section is able to capture its behaviour. We have done so by evaluating various scenarios with different network parameters, both by means of simulation and by means of our analysis. We discuss the performance of the forwarding protocol using the results of the simulation study and discuss the accuracy of our analysis by comparing the results of the simulation study and our analysis. Below we first describe the scenario and the set-up of our simulation study in Section 7.6.1 and then discuss the results in Section 7.6.2.

7.6.1 Experimental set-up

Nodes are positioned over a straight line of 3000 m with the source at one end and the message destination at the other end. The inter-node spacing is exponentially distributed with mean d_{IN} set to 10, 25, and 50 m. With each simulation experiment a message is initially broadcasted by the source and forwarded towards the message destination by the

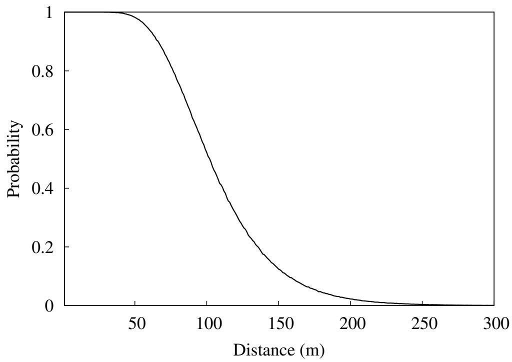

Figure 7.10: The packet reception curve S_i.

intermediate nodes, following the forwarding rules specified in Section 7.3 with the mean forwarding $T_d = 1$ s. To gain statistically significant results each experiment has been repeated at least 70,000 times with different random seeds.

Experiments have been performed using the OMNET++ network simulator v4.1 [77] and using a self-modified version of the MiXiM framework v2.1 [79] to model the communication architecture. To model the behaviour of the 802.11p protocol as accurately as possible we have altered the IEEE 802.11 medium access module in such a way that all parameters follow the 802.11p specification [100]. The available 802.11 MiXiM physical layer was adapted to include BERs and PERs for all transmission bit rates used in our experiments. The centre frequency was set to 5.9 MHz and IEEE 802.11 AC 0 was used. We use the log-normal shadowing model [22] for signal propagation with the path loss exponent set to 3.5 and the standard deviation to 6. Transmission power was set to 4 mW. To keep the influence of packet collisions due to hidden nodes as low as possible the packet sizes are kept small (only the headers are included) at 160 bits.

Our model analysis requires the packet reception ratio S_i as input. Using the above simulations settings we have measured the packet reception probabilities at intervals of one meter for $R = 300$ m, for a single node that broadcasted a packet ten thousand times without any interfering network traffic. The resulting packet reception curve S_i can be seen in Fig. 7.10; it has been used to calculate all of our analytical results presented in this chapter. The packet reception probability at the edge of the packet reception curve is less than 0.1.

Note that it is also possible to model S_i as a function of transmission power, propagation effects, BER, PER, and forward error correction; see for example [104].

7.6.2 Results

Our discussion of the results is split into two parts. We first show how the behaviour of a hop depends on the lengths of all previous hops, and how this affects performance. Then we discuss the results of our evaluation study.

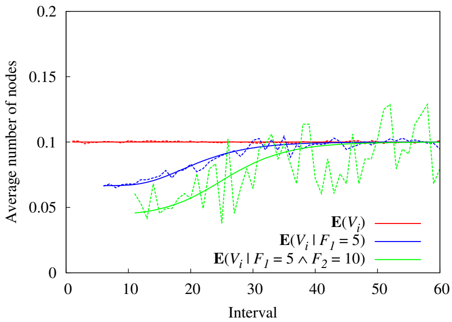

(a) Two short hops ($F_1 = 5, F_2 = 10$), $d_{IN} = 50$ m.

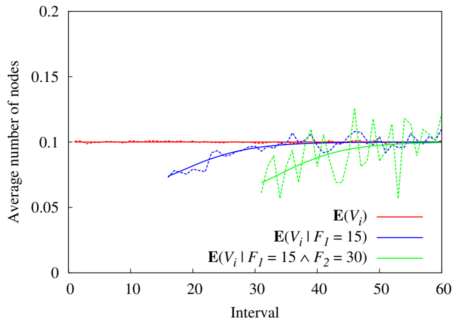

(b) Two long hops ($F_1 = 20, F_2 = 40$), $d_{IN} = 50$ m.

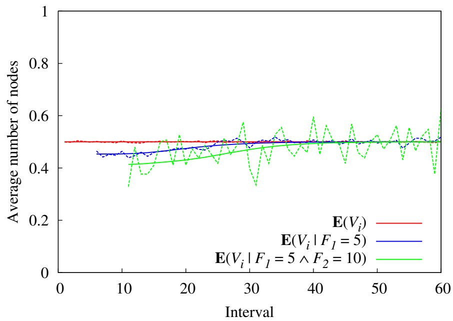

(c) Two short hops ($F_1 = 5, F_2 = 10$), $d_{IN} = 10$ m.

Figure 7.11: Average number of nodes in an interval following the source, following the first forwarder, and following the second forwarder, for different values of d_{IN} and different lengths of the first two hops.

Dependencies between consecutive hops

The behaviour of a hop depends on the behaviour of previous hops, especially regarding the lengths of those previous hop lengths. We explain why this is the case below and show how it affects performance. We conclude that to accurately analyse the behaviour of multiple hops, the length of each intermediate hop must be taken into account.

Each node that has received the message from a previous forwarder (or the source) has an equal probability of becoming the next forwarder. An interval that contains a higher than average number of nodes is therefore more likely to 'produce' a forwarder than an interval that contains a lower than average number of nodes and, consequently, an interval that does not produce a forwarder is more likely to have a lower than average number of nodes. This effect is illustrated in Fig. 7.11, which shows the average number of nodes in

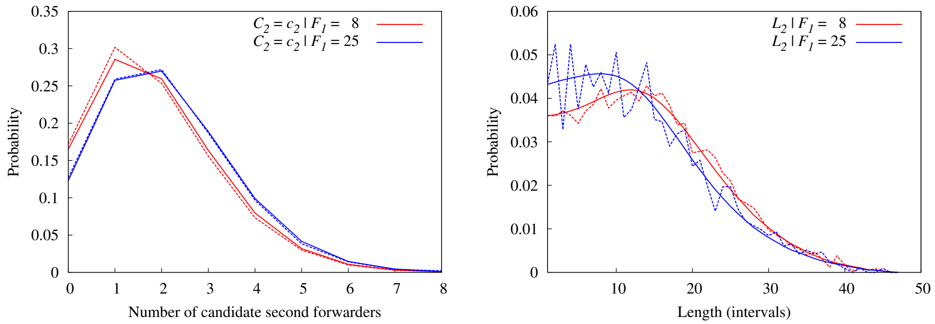

(a) Number of candidate forwarders.

(b) Hop length.

Figure 7.12: The distribution of *(a)* the number of candidate second forwarders C_2 and *(b)* the hop length of the second hop L_2, following a short first hop ($F_1 = 8$) and a long first hop ($F_1 = 25$), for $d_{IN} = 50$ m and $d_{int} = 5$ m.

an interval $\mathbb{E}(V_i)$, the average number of nodes in an interval following the first forwarder $\mathbb{E}(V_i \mid F_1 = j)$, and the average number of nodes in an interval following the second forwarder $\mathbb{E}(V_i \mid F_1 = j \wedge F_2 = k)$. It can be seen how this decrease in the average number of nodes in an interval becomes less as intervals are positioned further away from the forwarder, since the probability that these latter intervals will receive the message from the previous forwarder (and thus produce a forwarder) is lower. The relative decrease in the average number of nodes in an interval surrounding the forwarder is stronger for low node densities, since the impact of the position of a single node (the forwarder) is stronger when the total number of nodes is less. This can be seen when comparing Fig. 7.11a and Fig. 7.11c. The effect furthermore adds up for consecutive hops and is stronger when forwarders are positioned close together, i.e., when hop lengths are short. This can be seen when comparing Fig. 7.11a and Fig. 7.11b.

The effect that this decrease in the number of nodes in an interval surrounding the forwarder has on performance is significant, since the number of nodes per interval in the intervals following the previous forwarders determines the number of candidate forwarders per interval as well as the total number of candidate forwarders. Fig. 7.12a shows the distribution of the number of candidate second forwarders following a short first hop and a long first hop. It can be seen that on average there are more candidate second forwarders following a long hop, and that the probability of success of the second hop (i.e., of having at least one candidate second forwarder) is higher following a long hop. This dependency holds for each hop, i.e., the number of candidate forwarders following a long hop is on average always higher than the number of candidate forwarders following a short hop. A hop following one or more long hops therefore has a larger probability of being successful and will have a shorter hop delay.

The distribution of the hop length is also affected. Because the decrease in the average number of nodes intervals following the previous forwarder is stronger following a short hop, the number of candidate forwarders in an interval directly surrounding the previous forwarder is also less. As a result the probability that a candidate forwarder that is positioned further away from the forwarder becomes the next forwarder increases. Hop lengths are thus on average longer following one or more short hops. This has been illustrated in Fig. 7.12b for the second hop, showing the distribution of the hop length following a short first hop and a long first hop.

In conclusion, for all of the performance metrics discussed here it holds that to determine the performance of the n^{th} hop in an exact manner the length of all previous $n-1$ hops should be taken into account. Due to the complexities involved in doing so this is infeasible however, as we have argued in previous sections. In our analysis we therefore approximate the behaviour of the n^{th} hop by taking into account the length of the $(n-1)^{\text{th}}$ hop only or, in case of the end-to-end delay, by assuming that all $n-1$ preceding hops are of identical length. In the next section we show that such an approximation already gives very accurate results.

Protocol performance

We use the K-S statistic to express the difference between two distributions. The K-S statistic K for two distributions $F_1(x), F_2(x)$ is equal to the largest distance between the CDFs, given by

$$K = \max\{|F_1(x) - F_2(x)|\} \quad \forall\, x. \tag{7.65}$$

We discuss the following performance metrics in the same order in which we have presented them in Section 7.5: *(i)* the probability of success of each hop, *(ii)* the distribution of the hop length of each hop, *(iii)* the distribution of the position of each forwarder, *(iv)* the distribution of the number of hops to have a message forwarded i intervals, *(v)* the distribution of the hop delay of each hop, and *(vi)* the distribution of the end-to-end delay to have a message forwarded i intervals.

Per-hop performance metrics have been evaluated up to the tenth hop, while end-to-end metrics have been evaluated for distances up to 1000 m (on average 16 hops are needed to have the message forwarded over 1000 m). All results are included in Table 7.2, showing the K-S statistics of the resulting distributions. For clarity of illustration the figures showing the per-hop metrics only include distributions of the first five hops; the figures showing end-to-end metrics include results for up to 500 m. For all shown results $d_{int} = 1$ m unless specified otherwise. The solid lines represent analytical results, the dashed lines represent simulation results. In case of average values confidence intervals are less than 1 %.

In general we see that the accuracy of our model analysis is very high and that, except the end-to-end delay, all our analytical results stay within 0.1 of the simulation results. For the end-to-end delay results stay within 0.1 for high node densities and for forwarding scenarios in which the message is forwarded on average eight times or less.

Inaccuracies in our model analysis are mainly caused by *(i)* the fact that we ignore some effects caused by packet losses, such as the retransmission of messages, *(ii)* the fact that we ignore dependencies between consecutive hops following the third hop. The former holds for high-density scenarios in particular; the latter for low-density scenarios. Because of these conflicting effects we will sometimes see that results are most accurate for a medium-density scenario with $d_{IN} = 25$ m, as in such a scenario the sum of both effects is smallest.

Fig. 7.13 shows the *hop success probability* of the first ten hops. As there are less nodes on the road the probability that a message gets lost increases: whereas the probability of having a message forwarded ten times is 1 for $d_{IN} = 10$ m, it is almost 0 for $d_{IN} = 50$ m. It can be seen in the figure that, regarding the hop success probability, results of the model simulation and the model analysis stay within 0.03.

Fig. 7.14 shows the distribution of the *hop length* of the first four hops for three values of d_{IN}. Regarding the model analysis only the distributions of the hop length of the first three hops are shown, since in our analysis we assume that the distribution of the hop length of the fourth hop and following hops is identical to the distribution of the hop length of the third hop.

Because each candidate forwarder has an equal probability of becoming the next forwarder, the distribution of the hop length is mainly determined by the shape of the packet reception curve S_i and the distribution of the nodes following the most recent forwarder. Because of the dependency between hops that was discussed in the previous section, hops become increasingly longer with each hop. After the first few hops however the distribution of the hop length converges, such that the distribution of the hop length of the fourth hop is quite similar to the distribution of the hop length of the third hop.

As d_{IN} increases the dependency between successive hops increases as well, and the lengthening of successive hops becomes somewhat more pronounced, although the effect is limited. The average length of a hop changes but little as d_{IN} is varied because each candidate forwarder has an equal probability of becoming the next forwarder.

It can be seen in the figures as well as in Table 7.2 that, regarding the distribution of the hop length, results of the model simulation and the model analysis stay within 0.02. This confirms our assumption made in Eq. (7.53) that, for the purpose of our analysis and for the range of parameters tested here, the distribution of the hop length of the fourth hop (and of following hops) is identical to the distribution of the hop length of the third hop.

Fig. 7.15 shows the distribution of the *position of the forwarder* for the first five hops and for three values of d_{IN}. Since the impact of d_{IN} is limited on the distribution of the hop length, its impact on the position of a forwarder is similarly limited: the distribution of the position of the n^{th} forwarder does not change much as d_{IN} is varied.

In our model analysis the distribution of the position of the first three forwarders is calculated exactly (given the model assumptions); it can be seen in the figures as well as in Table 7.2 that, regarding the distribution of the position of the first three forwarders, results of the model simulation and the model analysis stay within 0.03. Our exact approach is thus very accurate, irrespective of the value of d_{IN}. Deviations are mainly caused by the effects of transmission errors that have not been taken into account.

The position of following forwarders is approximated in our model; it can be seen in the figures as well as in Table 7.2 that, regarding the distribution of the position of the fourth and following forwarders, results of the model simulation and the model analysis stay within 0.05 for the tenth forwarder. Results become less for each following hop because in our approximation we do not take into account the hop lengths of all preceding hops, but only the length of the most recent hop.

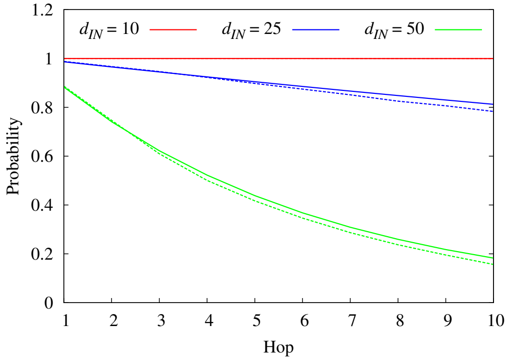

Figure 7.13: Hop success probability.

Fig. 7.16 shows the distribution of the *required number of hops* to have the message forwarded i intervals for three values of d_{IN}. Since it is a function of the hop length, the distribution of the number of hops changes but little as d_{IN} is varied. Fig. 7.19, which shows the average required number of hops as a function of d_{IN} and i, furthermore illustrate that the average required number of hops grows linearly as i increases.

It can be seen in the figures as well as in Table 7.2 that, regarding the distribution of the number of hops required to have the message forwarded i intervals, results of the model simulation and the model analysis stay within 0.1 for $d_{IN} = 50$ m, and generally become increasingly accurate as d_{IN} and i decrease. Inaccuracies are mainly caused by the fact that we do not take dependencies between successive hops into account in full.

Fig. 7.17 shows the distribution of the *hop delay* of the first four hops for three values of d_{IN}. Of the model analysis only the distribution of the hop delay of the first two hops are shown since in our analysis we assume that the distribution of the hop delay of the third hop (and of following hops) is identical to the hop delay of the second hop.

It can be seen that as d_{IN} decreases the average hop delay decreases, due to the increase in the number of candidate forwarders per hop. Although there is a small difference between the hop delay distribution of the first and the second hop, the differences between distribution of following hops is negligible.

It can be seen in the figures as well as in Table 7.2 that, regarding the distribution of the hop delay, results of the model simulation and the model analysis stay within 0.02. This confirms our assumption that, for the purpose of our analysis, the distribution of the hop delay of the third hop (and of following hops) is identical to the distribution of the hop delay of the second hop.

Fig. 7.18 shows the distribution of the *end-to-end delay* to have the message forwarded i intervals for three values of d_{IN}. Fig. 7.20 shows the average end-to-end delay for varying values of d_{IN} and i. It can be seen that the end-to-end delay increases linearly as i increases, and less than linearly as d_{IN} increases.

It can be seen in the figures as well as in Table 7.2 that, regarding the distribution of the end-to-end delay to have the message forwarded i intervals, results of the model simulation and the model analysis stay within 0.10 for $d_{IN} = 10$ m and within 0.19 for lower densities. For distances up to 500 m, which require on average eight hops to have the message forwarded this far, all results stay within 0.10. Regarding the average end-to-end delay results stay within 0.01 for $d_{IN} = 10, 25$ m, but become less accurate as d_{IN} decreases.

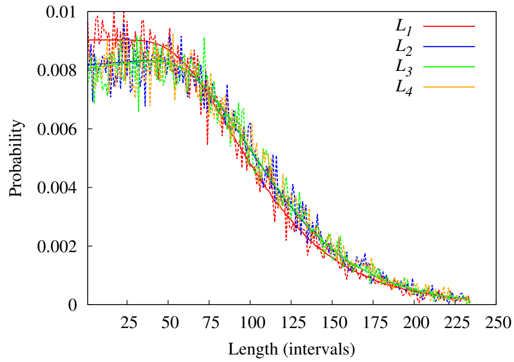

(a) For $d_{IN} = 10$ m.

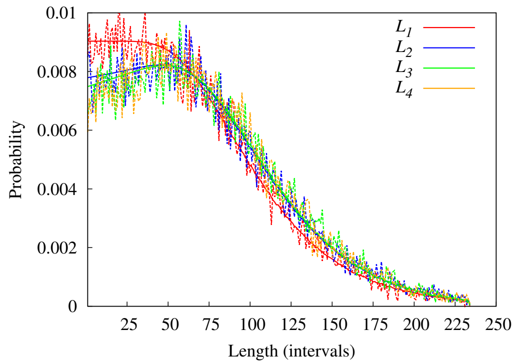

(b) For $d_{IN} = 25$ m.

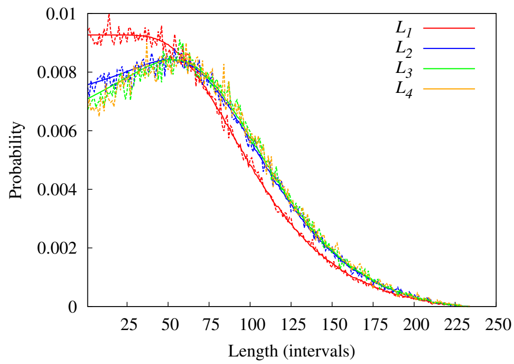

(c) For $d_{IN} = 50$ m.

Figure 7.14: The distribution of the length of the first hop for varying value of d_{IN}. Of the analytical results only the first three hops are shown.

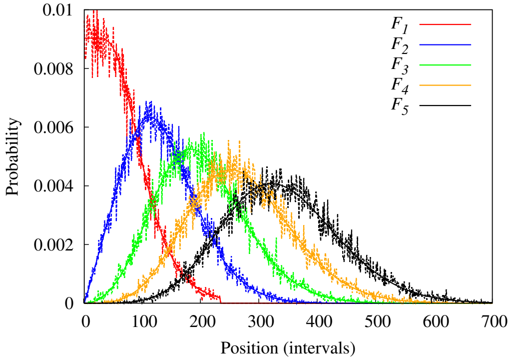

(a) For $d_{IN} = 10$ m.

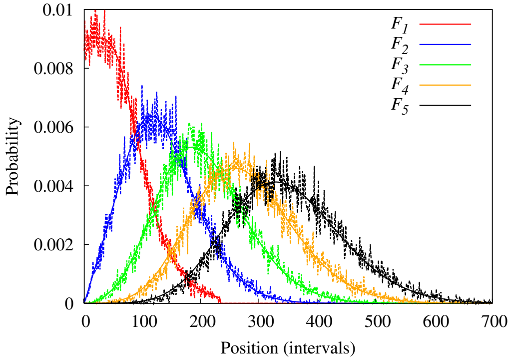

(b) For $d_{IN} = 25$ m.

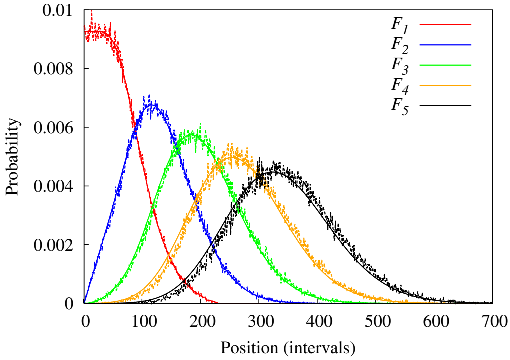

(c) For $d_{IN} = 50$ m.

Figure 7.15: The position of the first five forwarder for $d_{IN} = 50$.

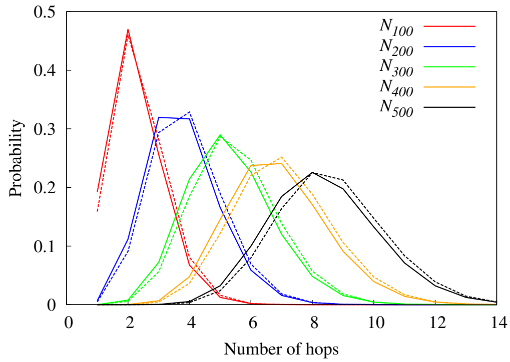

(a) For $d_{IN} = 10$ m.

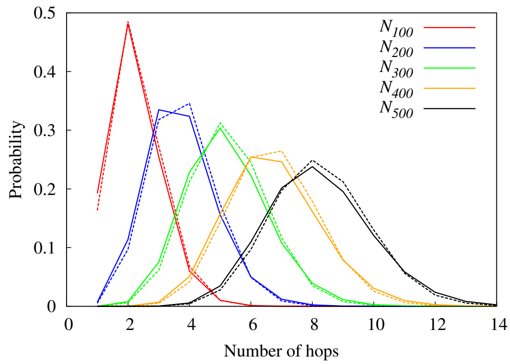

(b) For $d_{IN} = 25$ m.

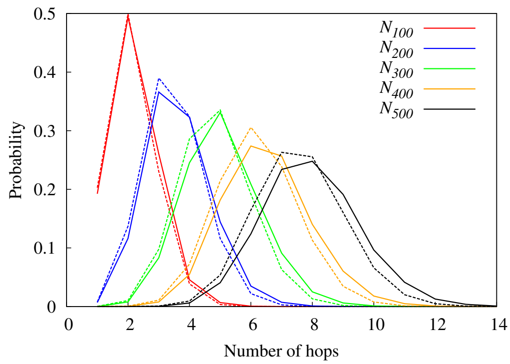

(c) For $d_{IN} = 50$ m.

Figure 7.16: The required number of hops to have the sink receive the message for source-to-sink distances of 100, 200, 300, 400, and 500 m, for $d_{IN} = 10$.

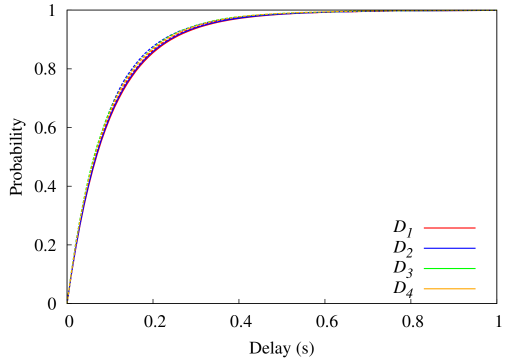

(a) For $d_{IN} = 10$ m.

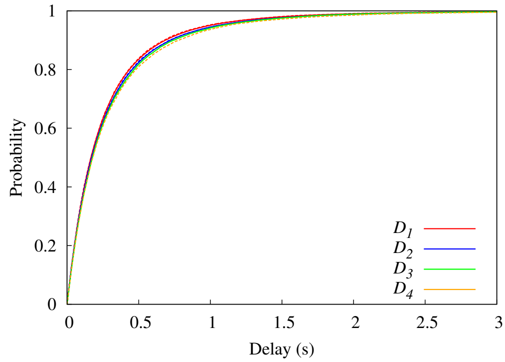

(b) For $d_{IN} = 25$ m.

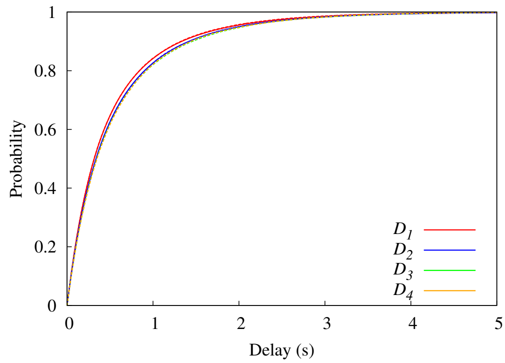

(c) For $d_{IN} = 50$ m.

Figure 7.17: The distribution of the hop delay of the first four hops for $d_{IN} = 50$.Of the analytical results only the first two hops are shown.

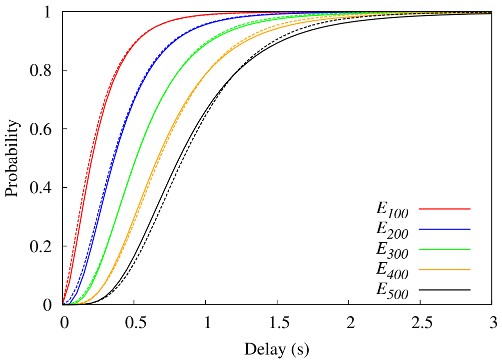

(a) For $d_{IN} = 10$ m.

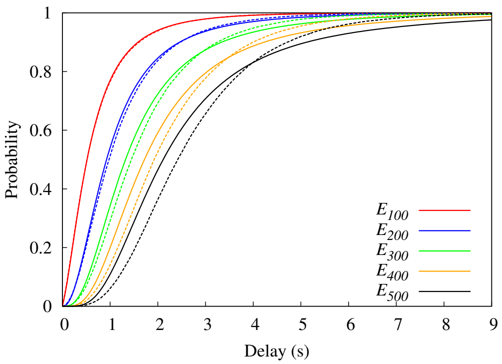

(b) For $d_{IN} = 25$ m.

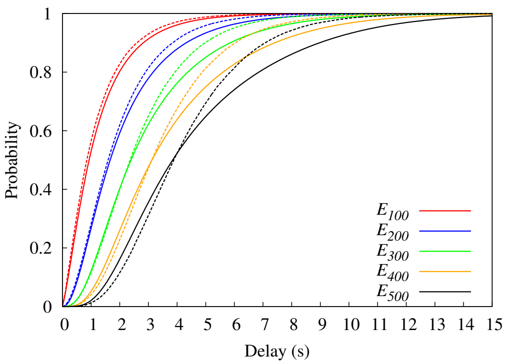

(c) For $d_{IN} = 50$ m.

Figure 7.18: The distribution of the end-to-end delay to have the message forwarded by a node at or beyond 100, 200, 300, 400, and 500 m.

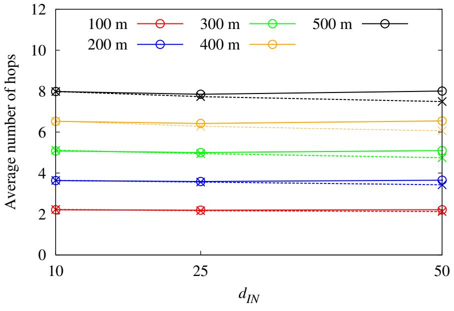

(a) For varying values of d_{IN}.

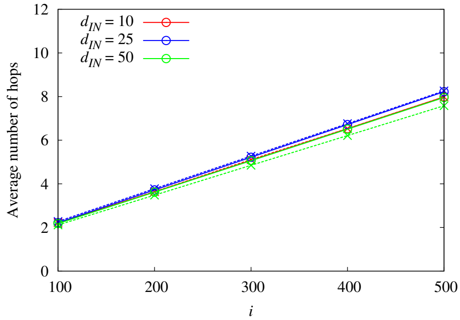

(b) For varying values of the source-to-sink distance i.

Figure 7.19: The average required number of hops to get the message at interval i.

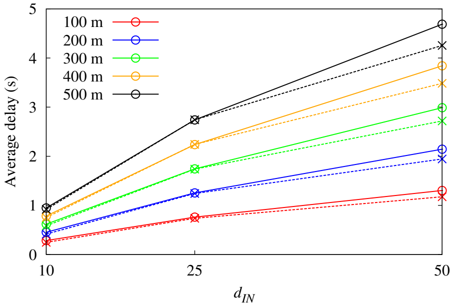

(a) For varying values of d_{IN}.

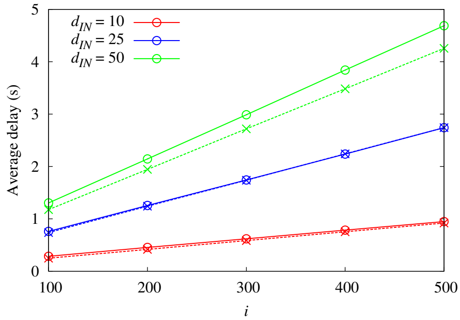

(b) For varying values of the source-to-sink distance i.

Figure 7.20: The average end-to-end delay to get the message at interval i.

Hop	1	2	3	4	5	6	7	8	9	10
d_{IN}	Position of forwarder									
10	0.008	0.018	0.026	0.032	0.038	0.040	0.041	0.044	0.046	0.047
25	0.011	0.020	0.026	0.028	0.29	0.030	0.029	0.030	0.029	0.029
50	0.008	0.012	0.011	0.013	0.016	0.021	0.025	0.028	0.031	0.033
d_{IN}	Hop length									
10	0.008	0.016	0.015	0.013	0.016	0.016	0.015	0.016	0.017	0.019
25	0.011	0.016	0.016	0.013	0.015	0.016	0.015	0.013	0.014	0.014
50	0.008	0.018	0.014	0.018	0.016	0.016	0.018	0.016	0.014	0.017
d_{IN}	Hop delay									
10	0.008	0.005	0.010	0.010	0.013	0.011	0.015	0.013	0.013	0.010
25	0.005	0.006	0.016	0.016	0.016	0.018	0.018	0.020	0.020	0.016
50	0.003	0.007	0.008	0.013	0.015	0.013	0.009	0.015	0.012	0.012

Distance	100	200	300	400	500	600	700	800	900	1000
d_{IN}	Required number of hops									
10	0.043	0.047	0.045	0.041	0.041	0.036	0.035	0.032	0.034	0.031
25	0.026	0.040	0.032	0.036	0.028	0.030	0.026	0.022	0.022	0.020
50	0.041	0.045	0.055	0.065	0.070	0.079	0.074	0.082	0.094	0.082
d_{IN}	End-to-end delay									
10	0.045	0.026	0.010	0.018	0.034	0.050	0.065	0.078	0.089	0.099
25	0.006	0.029	0.054	0.082	0.104	0.124	0.144	0.159	0.176	0.189
50	0.036	0.036	0.052	0.071	0.087	0.103	0.117	0.131	0.144	0.154

Table 7.2: K-S statistics when comparing the results of the model analysis with the results of the model simulation, calculated using Eq. (7.65). Distances in meters.

7.7 Conclusions

In this chapter we have shown how to analytically model a multi-hop location-based broadcast protocol that uses exponentially distributed forwarding delays, assuming exponentially distributed inter-node distances and a realistic transmission model. Our analysis is able to express the performance of the forwarding protocol in closed form formulas that allow for easy and fast evaluation of the protocol's performance, and that provide for an increased insight in the protocol's behaviour. Our analysis gives an exact description of the behaviour of the first three hops; following hops are approximated by assuming that they behave similar to the third hop.

For a given node density and a given transmission model the model is able to capture the full distribution of *(i)* the end-to-end delay to forward a message a specific distance, *(ii)* the required number of hops to forward a message a specific distance, *(iii)* the position of each intermediate forwarder, *(iv)* the length of each hop, *(v)* the delay of each hop, and *(vi)* the success probability of each hop. Verification of our model analysis by means of extensive simulations showed that our analysis is very accurate: all results of our model analysis stay within 0.10 of the simulated results for forwarding distances that require on average up to 8 hops, and within 0.19 for distances that require on average up to 16 hops. Especially regarding the required number of hops to disseminate the message accuracy is high, with results staying within 0.08 for distances that require on average up to 16 hops. Results are most accurate for high-density scenarios.

A main insight provided by our model is the interdependency that exists between consecutive hops, especially regarding the lengths of preceding hops. This interdependency has a significant effect on performance as it influences the success probability, length, and delay of each hop, especially in low-density scenarios. In our approximations of the performance of the n^{th} hop we therefore take into account the hop length of the $(n-1)^{\text{th}}$ hop. This interdependency applies for all multi-hop forwarding scenarios in which traffic is free flowing and should therefore always be taken into account to accurately describe the behaviour of a forwarding protocol.

CHAPTER 8

Forwarding with distance-based forwarding delays and exponential inter-node distances

In this chapter we present an analytical model that accurately describes the behaviour of a vehicular multi-hop location-based broadcast protocol (or [multi-hop] forwarding protocol for short) that uses distance-based forwarding delays, i.e., the node farthest in the direction of the sink forwards the message. We consider a similar scenario as in the previous chapter, with a message forwarded from source to sink over a straight road, with traffic assumed to be free flowing, and the probability of successfully receiving a single-hop transmission modelled as a function of the distance to the sender, similar to the packet success ratio probability curve commonly used in literature [112].

The analytical model presented in this chapter focuses on having a message forwarded from source to sink. For a given forwarding distance and a given node density our model analysis is able to capture the full distribution of *(i)* the length of each hop, *(ii)* the delay of each hop, *(iii)* the success probability of each hop, *(iv)* the position of each forwarder, *(v)* the required number of hops to have the message delivered to the sink, and *(vi)* the end-to-end delay to have the message delivered to the sink.

The outline of this chapter is as follows. We start by giving a short introduction in Section 8.1 and discuss related work on the analysis of multi-hop forwarding in vehicular networks in Section 8.2. The system model is presented in Section 8.3 together with the notation used throughout the chapter. Our analysis is given in Section 8.4. We have performed an evaluation study involving extensive simulations to study the performance of the forwarding protocol assumed in this chapter, as well as to verify the accuracy of our analytical model. Both the set-up of our evaluation study and its results are given in Section 8.5. We finally conclude the chapter in Section 8.6.

Image on previous page: motorbike riders taking shelter in the shade of the Skytrain in Bangkok.

8.1 Introduction

In this chapter we analytically model the behaviour of a multi-hop location-based broadcast protocol that uses distance-based forwarding delays. Specifically we consider a scenario in which nodes are spread out over a straight road with the source and sink at either end. The source node initiates the forwarding by broadcasting an application message with a geographically defined destination address that includes the position of the sink. All nodes apply the following forwarding rule: when a node receives a message for the first time, and the node is positioned closer to the destination than the previous sender, the node chooses a forwarding delay that is a function of its own distance to the destination and the previous sender's distance to the destination, and schedules to rebroadcast the message immediately after this forwarding delay. Nodes that are positioned closer to the destination will have shorter forwarding delays, so that the node that has received the message from the previous sender and is positioned closest to the destination will always be the next forwarder of the message. The other nodes will cancel their scheduled rebroadcast upon receiving the message from the node that is positioned closer to the destination. In this way a message is forwarded in as few hops as possible towards the destination.

The above protocol was first proposed in [105] in the context of mobile ad-hoc networks as the contention-based forwarding (CBF) protocol. It was applied to vehicular networks in [106] and has subsequently been standardised by ETSI as one of its primary means of disseminating vehicular (safety) messages to nodes that are positioned either directly in front of or behind the source vehicle [3]. Similar protocols have also been proposed for use in wireless sensor networks [107] to effectively and efficiently disseminate information throughout the entire network.

There exist a number of analytical studies that model the performance of forwarding protocols in which the node closest to the destination is the next forwarder [96] [108] [109]. So far however we have not found any study that uses assumptions that apply to our scenario however; especially regarding single-hop transmissions such studies typically use over-simplified assumptions. In contrast, in this chapter we model the probability of a successful single-hop transmission as a function of the distance between sender and receiver, an abstraction that is typically used to capture the behaviour of single-hop transmissions in a realistic manner, but that so far has not been applied to model multi-hop forwarding protocols. Moreover, whereas the focus of existing models is often limited to network connectivity, dissemination reliability, or end-to-end delay bounds, our model gives a full distribution of a number of performance metrics.

The contribution of this chapter is an analytical model that expresses the performance of the CBF protocol as presented above in terms of insightful and fast-to-evaluate formulas. Our model covers the scenario where the nodes on the road have exponentially distributed inter-node distances.

For a given source-to-sink distance, transmission model, and forwarding delay distribution, the model gives expressions of the following performance metrics:

1. the length of each hop;
2. the delay of each hop;
3. the success probability of each hop;
4. the position of each forwarder;
5. the required number of hops to have the message delivered to the sink; and
6. the end-to-end delay to have the message delivered to the sink.

Extensive verification has shown that the results of our model are very accurate.

In the next section we first discuss in some more detail the work that has previously been done on analytically modelling multi-hop broadcast. Our own analytical model is explained in full detail in Sections 8.3 and 8.4. The performance of the CBF protocol and the accuracy of our model is discussed in Section 8.5. This chapter is concluded in Section 8.6.

8.2 Related work

Although there is a plethora of performance studies on multi-hop forwarding protocols in vehicular networks, practically all of these studies are simulation based. What analytical studies there are contain overly simplified assumptions and often only focus on a limited number of performance metrics such as the network connectivity [90] [91] [92], without giving a full description of the end-to-end behaviour of a protocol. Below we give a brief overview of a number of analytical studies that we found to be the most relevant ones regarding multi-hop forwarding, and discuss their applicability to our forwarding scenario. It is the same body of work that is discussed in Chapters 6 and 7 but, as the forwarding scenario modelled in this chapter differs from the forwarding scenario in those chapters, so does (the discussion on) the applicability of these works with respect to our current forwarding scenario.

In [93] a scenario is considered in which a message is forwarded by means of broadcast transmissions over a straight line with fixed inter-node distances. Regarding single-hop transmissions all nodes within a certain range from the sender have the same probability p ($0 \leq p \leq 1$) of correctly receiving the message in absence of interference. Interference of transmissions may be taken into account and if so may result in a loss. The model gives bounds on the end-to-end delay for an idealised dissemination strategy which ignores interference, and for two provably near-optimal dissemination strategies when interference is taken into account, none of which apply to our forwarding protocol.

In [94] the end-to-end delay of an emergency message dissemination protocol is analytically calculated. A unit-disc single-hop transmission model and exponentially distributed inter-node distances are assumed. Nodes are assumed to have formed communication clusters with each cluster of nodes having a cluster head node. All forwarding is done by the head nodes, which makes it relatively easy to calculate the end-to-end delay. This method of forwarding does not apply to our forwarding protocol however.

In [95] again a straight road with exponentially distributed inter-node distances and a unit-disc single-hop communication model are considered. Nodes that receive a message will forward the message with a certain probability p ($0 \leq p \leq 1$), making the approach of this work somewhat similar to [93]. The model gives bounds on the maximum end-to-end delay and shows that the value of p that gives the lowest end-to-end delay depends on the network density. A similar result was shown in [93]. The forwarding protocol assumed in this work does not apply to our forwarding protocol.

In [96] the required number of hops to disseminate a message from source to sink is analytically modelled in the context of a wireless sensor network. Nodes are again spread out over a straight line with exponentially distributed inter-node distances and the unit-disc model is again assumed for single-hop transmission. Multi-hop forwarding is assumed to go in synchronised communication rounds in which the node that has received the message and is positioned farthest in the direction of the sink forwards the message, similar to our forwarding protocol. The model gives approximations of the distance that a message has been forwarded for a given number of communication rounds as well as the network connectivity as a function of the source-to-sink distance. The work does not address the delay to deliver a message to the sink. The model is quite accurate for high node densities and large distances but less so when densities are low and distances are short.

Among the studies considered here the forwarding protocol considered in [96] is most similar to the forwarding protocol considered in this chapter. The analytical model presented in [96] does not include the end-to-end delay to forwarding a message from source to sink however, and has an overly simplified single-hop transmission model. Regarding the other studies discussed here none of the forwarding protocols apply to the forwarding protocol considered in this chapter. In the next sections we therefore present our system model and model analysis.

8.3 The system model

In Section 8.1 we presented the forwarding scenario that we model in this chapter. In this section we present our system model: an abstract representation of the forwarding scenario that forms the basis of our analysis in subsequent sections. We also specify the forwarding rules of the CBF protocol and introduce some definitions and notations.

We model a road as a straight line with vehicles (henceforth referred to as nodes) placed on this line. Inter-node distances are exponentially distributed with mean d_{IN} (in meters). Previous studies suggest that this distribution gives a good approximation of the inter-vehicle distance in case of free flowing traffic [101] [102] [103]. Furthermore, due to the differences in scale between the speed with which information is usually routed through a network (meter per millisecond) and the speed with which nodes move (meter per second), we assume the network to be static for the duration of time that a message is being forwarded from source to sink.

To facilitate our analysis we divide the road into equal-sized intervals: starting from the source the road is divided into intervals of length d_{int}, with the i^{th} interval referring to the range $\langle (i-1) \cdot d_{int}, i \cdot d_{int}]$ from the source.

S_i denotes the probability that a node in the i^{th} interval from the sender successfully

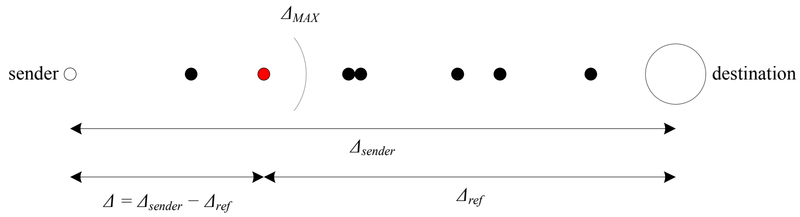

Figure 8.1: Forwarding progress Δ for the red reference node.

receives a transmitted message. The packet success ratio S_i is non-zero over the range $[0, R]$, where R is the maximum number of intervals away from the sender at which the receiver still has a non-zero probability of receiving the message, i.e., $S_i = 0$ for $i > R$. We assume $S_0 = 1$. An abstraction such as S_i is commonly used to take into account fading effects that influence the reception of a signal. It ignores deterministic shadowing effects (e.g., due to an obstruction) however; the occurrences of successfully receiving a signal are independent for all nodes and for all intervals. More background on radio wave propagation is given in Section 3.2.

All delays related to transmitting and processing a signal (i.e., transmission delay, propagation delay, switching times, etc.) are assumed to be negligible.

All nodes apply the following forwarding rules upon receiving a message for the first time. A message contains position information of the destination and of the previous sender, and nodes know their own position at all times. When a reference node receives the message it first calculates its own distance to the destination Δ_{ref} (in m) and the previous sender's distance to the destination Δ_{sender} (in m). The node then calculates the forwarding progress Δ (in m) if it were to become the next forwarder, defined as $\Delta = \Delta_{sender} - \Delta_{ref}$. In case the progress is positive then the reference node is positioned closer to the destination than the previous sender and it schedules to rebroadcast the message after $\tau_{CBF}(\Delta)$ ms. If the reference node receives the message from another node that is positioned closer to the destination than itself, before it has itself transmitted the message, then it will cancel its scheduled rebroadcast; otherwise it will rebroadcast the message as planned. $\tau_{CBF}(\Delta)$ is decreasing in Δ and is given by

$$\tau_{CBF}(\Delta) = \begin{cases} \tau_{min} + \left(1 - \dfrac{\Delta}{\Delta_{MAX}}\right) \cdot (\tau_{max} - \tau_{min}), & 0 \leq \Delta \leq \Delta_{MAX} \\ \tau_{min}, & \Delta > \Delta_{MAX}, \end{cases} \tag{8.1}$$

with $\Delta_{MAX} > 0$ being the maximum communication range (in m) assumed by the CBF protocol, τ_{min} being the minimum forwarding delay (in ms) and τ_{max} being the maximum forwarding delay (in ms). Fig. 8.1 illustrates Δ; Fig. 8.2 shows (an example of) $\tau_{CBF}(\Delta)$.

Δ_{MAX}, τ_{min}, and τ_{max} are all protocol parameters that serve as input to our analytical model. We define $\delta_{max} = \Delta_{MAX}/d_{int}$ as the maximum assumed protocol communication range measured in intervals and assume in our model that the maximum CBF communica-

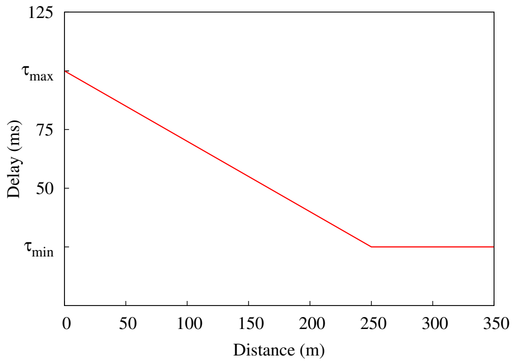

Figure 8.2: Distribution of the forwarding delay when $\Delta_{MAX} = 250$ m, $\tau_{min} = 25$ ms, and $\tau_{max} = 100$ ms.

tion range is equal to or greater than the actual maximum possible communication range, i.e., $R \leq \delta_{max}$.

Finally we use the following notation and definitions throughout the chapter. Note that the notation resembles the notation used in Chapter 7, but differs somewhat regarding the end-to-end metrics. The n^{th} forwarder is the node that retransmits the message for the n^{th} time after the source's original transmission; its position is denoted F_n. Although not a forwarder since it originates the message, the source node is referred to as the 0^{th} forwarder and is by definition positioned in interval 0, i.e., $F_0 = 0$. For reasons of brevity we denote the set of positions of the source and the first n forwarders as $\hat{F}_n = \langle F_0, \ldots, F_n \rangle$. The n^{th} hop refers to the transmission made by the $(n-1)^{th}$ forwarder, i.e., the source's transmission is the first hop. The hop length of the n^{th} hop L_n refers to the distance in intervals between the $(n-1)^{th}$ forwarder and the n^{th} forwarder, i.e., $L_n = F_n - F_{n-1}$. The hop delay D_n of the n^{th} hop refers to the time between the moment the $(n-1)^{th}$ forwarder transmits the message and the moment the n^{th} forwarder transmits the message. The number of hops after which a sink that is positioned in interval i first receives the message is denoted N_i. E_i is the end-to-end delay after which a sink that is positioned in interval i first receives the message.

The number of nodes in interval i is denoted V_i. Each time the message has been forwarded there will be a set of nodes that have all received the message and are all positioned closer to the sink node than the most recent forwarder. Since one of these nodes will become the next forwarder we call these nodes *candidate forwarders*. Let C_n be the number of candidates for becoming the n^{th} forwarder, and let $C_{n,i}$ be the number of candidates for the n^{th} forwarder in interval i. When it is given that the $(n-1)^{\text{th}}$ forwarder is positioned in interval j, it follows from Eq. (8.1) that $C_{n,i} = 0$ for any interval $i < j$. The number of nodes in interval i that have not received the message from either the source or one of the $n-1$ previous forwarder, and have therefore not become candidate n^{th} forwarder, is denoted $K_{n,i}$. By definition it holds that

$$V_i = C_{n,i} + K_{n,i}, \quad n = 1, 2, \ldots, \quad i = f_{n-1} + 1, f_{n-1} + 2, \ldots \tag{8.2}$$

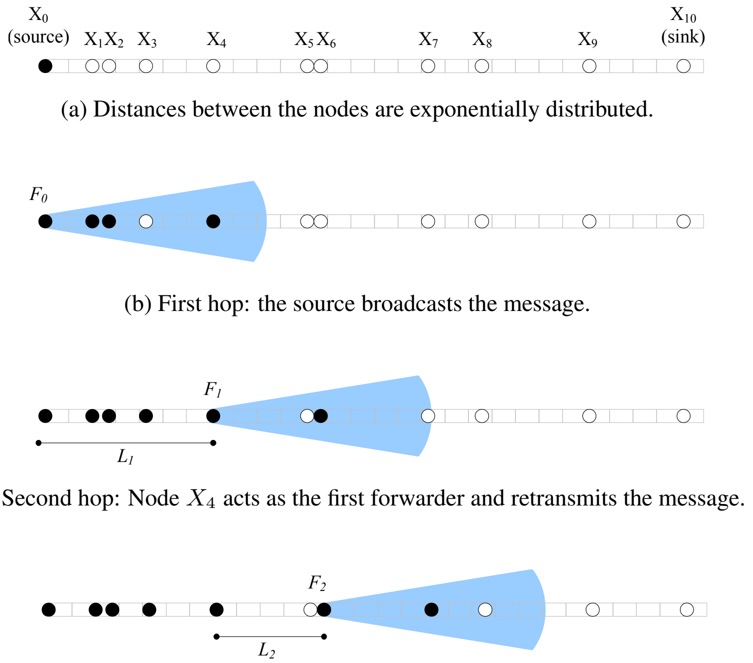

(a) Distances between the nodes are exponentially distributed.

(b) First hop: the source broadcasts the message.

(c) Second hop: Node X_4 acts as the first forwarder and retransmits the message.

(d) Third hop: Node X_6 acts as the second forwarder and retransmits the message.

Figure 8.3: The first, second, and third hop of an example scenario. The blue shape shows the maximum transmission distance R from the most recent forwarder. Black nodes have received the message.

We illustrate the above notation by means of an example. In Fig. 8.3b the source (F_0) broadcasts and nodes X_1, X_2, and X_4 all receive the message and become candidate first forwarders. In Fig. 8.3c node X_4, being closest to the destination and therefore having the shortest forwarding delay, acts as the first forwarder (F_1). The length of the first hop L_1 is defined as the distance between the position of the source and the position of the first forwarder, and has been illustrated in the figure. Node X_6 is the only candidate second forwarder and therefore acts as the second forwarder in Fig. 8.3d; the hop length of the second hop L_2 has been illustrated. The set of candidate third forwarders consists only of node X_7.

8.4 Model analysis

In this section we mathematically analyse the system model presented in the previous section. We start by giving an exact method to calculate the distribution of the position of a forwarder in Section 8.4.1. In Section 8.4.2 we determine the hop success probability and in Section 8.4.2 the distribution of the hop length. The method used in Section 8.4.1 to

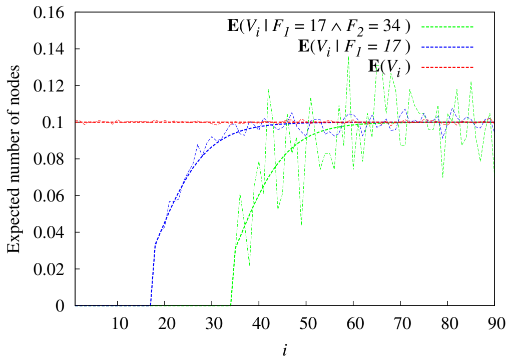

Figure 8.4: The expected number of nodes in intervals following a forwarder, for the source, the first forwarder, and the second forwarder, with $d_{int} = 5$ and $d_{IN} = 50$.

determine the position of a forwarder is infeasible for a large number of hops because of its complexity. In Section 8.4.4 we therefore give an approximate method to calculate the distribution of the position of the n^{th} forwarder for $n > 3$. The required number of hops to have the message delivered at the sink is determined in Section 8.4.5, the hop delay in Section 8.4.6, and finally the end-to-end delay in Section 8.4.7.

Throughout this section we clarify some of our modelling steps using (intermediate) results from a numerical evaluation study that we performed. The set-up of this study is described in Section 8.5.1. Results include both analytical results and simulation results; analytical results are illustrated using solid lines while simulation results are illustrated using dashed lines.

8.4.1 Exact position of a forwarder

In this section we determine the distribution of the position of the n^{th} forwarder in an exact manner. It is determined by the distribution of the candidate n^{th} forwarders, which in itself is determined by the distribution of the number of nodes in the R intervals following the most recent (i.e., $(n-1)^{\text{th}}$) forwarder. To calculate the distribution of the number of nodes in an interval we must in turn take into account the positions of the preceding $n-1$ forwarders.

Below we determine, for a given set of positions of the previous $n - 1$ forwarders, the distribution of the number of nodes in an interval i, denoted V_i, the distribution of the number of candidate n^{th} forwarders in an interval i, denoted $C_{n,i}$, and finally the distribution of the position of the forwarder, denoted F_n.

Determining the distribution of the position of the n^{th} forwarder in an exact manner quickly becomes complex, making it infeasible to calculate the distribution of F_n for large values of n. In Section 8.4.4 we therefore give a method to approximate the distribution of the position of the forwarder in a more efficient manner.

The distribution of V_i

Since inter-node distances are distributed exponentially with mean d_{IN} m and intervals have a length of d_{int} m, V_i is Poisson distributed with its mean given by

$$\mathbb{E}(V_i) = \frac{d_{int}}{d_{IN}}, \quad i \in \mathbb{N}^+. \tag{8.3}$$

The distribution of V_i is independent of the position of the source node, which is by definition interval 0. When the positions of successive forwarders are known however the distribution of V_i changes for the R intervals following the most recent forwarder. The number of nodes in interval i, given the position of the source and the first n forwarders, is Poisson distributed with its mean given by

$$\mathbb{E}(V_i \mid \hat{F}_n = \langle f_0, \ldots, f_n \rangle) = \mathbb{E}(V_i) \cdot \prod_{k=0}^{k=n-1} (1 - S_{i-f_k}),$$
$$n \in \mathbb{N}^+, \quad i = f_n + 1, f_n + 2, \ldots \tag{8.4}$$

Proof of Eq. (8.4) is given in Appendix B.1. Fig. 8.4 shows the resulting average number of nodes in an interval directly following the source, the first forwarder, and the second forwarder, given that first two forwarders are positioned in interval 17 and interval 34.

By definition no node positioned in an interval following the most recent forwarder can have received the message in one of the preceding hops, since in that case the node would have become the forwarder itself. On average the number of nodes in an interval directly following the most recent forwarder is therefore significantly lower than the average number of nodes in an interval. This effect can clearly be seen in Fig. 8.4.

The distribution of $C_{n,i}$

Let $C_{n,i} \mid \hat{F}_{n-1} = \langle f_0, \ldots, f_{n-1} \rangle$ denote the number of candidate n^{th} forwarders in interval i, given the positions of the source and the previous $n-1$ forwarders. Since candidate forwarders are by definition positioned closer to the destination than the most recent forwarder we determine $C_{n,i} \mid \hat{F}_{n-1} = \langle f_0, \ldots, f_{n-1} \rangle$ for $i \geq f_{n-1}$. By definition $C_{n,i} = 0$ for $i < f_{n-1}$.

All candidate n^{th} forwarders are nodes that receive the message for the first time from the $(n-1)^{\text{th}}$ forwarder. The expected number of candidate n^{th} forwarders in interval i is therefore a product of *(i)* the number of nodes in interval i that have not yet received the message and that are positioned closer to the destination than the $(n-1)^{\text{th}}$ forwarder, and *(ii)* the probability of receiving the $(n-1)^{\text{th}}$ forwarder's transmission. For interval $i = f_{n-1}$, given the positions of the previous $n-1$ forwarders, the number of nodes in interval i that have not yet received the message and that are positioned closer to the destination than the $(n-1)^{\text{th}}$ forwarder, is Poisson distributed with its mean given by $\mathbb{E}(V_i \mid \hat{F}_{n-1} = \langle f_0, \ldots, f_{n-1} \rangle)/2$ for $i > f_{n-2}$; proof of this is given in Appendix B.2. For intervals $i > f_{n-1}$ the number of nodes in interval i, given the positions of the previous $n-1$ forwarders, was shown in the previous section to be Poisson distributed with mean

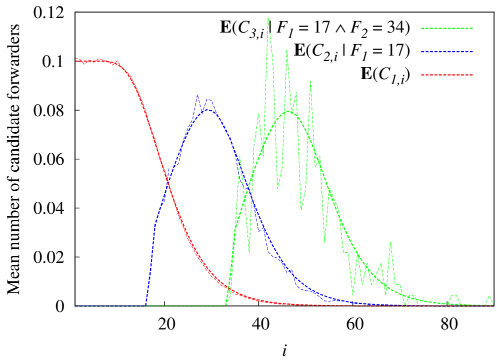

Figure 8.5: The expected number of candidate forwarders in an interval for the first three hops, with $d_{int} = 5$ m and $d_{IN} = 50$ m.

$\mathbb{E}(V_i \mid \hat{F}_{n-1} = \langle f_0, \ldots, f_{n-1} \rangle)$. Since a node in interval i has a probability of $S_{|i-f_{n-1}|}$ of receiving the $(n-1)^{\text{th}}$ forwarder's transmission, the distribution of the number of candidate n^{th} forwarders in interval i is thus Poisson distributed with its mean given by

$$\mathbb{E}(C_{n,i} \mid \hat{F}_{n-1} = \langle f_0, \ldots, f_{n-1} \rangle) = \begin{cases} 0 & i < f_{n-1}, \\ S_i \cdot \mathbb{E}(V_i) & n = 1, \\ \mathbb{E}(V_i \mid \hat{F}_{n-1} = \langle f_0, \ldots, f_{n-1} \rangle)/2 & n > 1, i = f_{n-1}, \\ S_{i-f_{n-1}} \cdot \mathbb{E}(V_i \mid \hat{F}_{n-1} = \langle f_0, \ldots, f_{n-1} \rangle) & n > 1, i > f_{n-1}, \end{cases} \tag{8.5}$$

for $n, i \in \mathbb{N}^+$ and $S_0 = 1$. Fig. 8.5 illustrates $\mathbb{E}(C_{n,i} \mid \hat{F}_{n-1} = \langle f_0, \ldots, f_{n-1} \rangle)$.

The total number of candidate n^{th} forwarders is equal to the sum of all the candidate n^{th} forwarders in the R intervals following the $(n-1)^{\text{th}}$ forwarder. According to [99] the sum of a number of independent Poisson distributed random variables is also Poisson distributed, with its mean equal to the summed up means. Hence, for a given set of positions of the source and the first $n-1$ forwarders, C_n has a Poisson distribution with mean

$$\mathbb{E}(C_n \mid \hat{F}_{n-1} = \langle f_0, \ldots, f_{n-1} \rangle) = \sum_{i=f_{n-1}}^{f_{n-1}+R} \mathbb{E}(C_{n,i} \mid \hat{F}_{n-1} = \langle f_0, \ldots, f_{n-1} \rangle), \quad n \in \mathbb{N}+. \tag{8.6}$$

The distribution of F_n

For a given set of candidate n^{th} forwarders the candidate forwarder that lies farthest in the direction of the destination becomes the n^{th} forwarder. The probability that the n^{th} forwarder is positioned in interval i is therefore equal to the probability that there is at least one candidate n^{th} forwarder in interval i *and* that there are no candidate n^{th} forwarders in any of the following intervals. The distribution of F_1 is therefore given by

$$\mathbb{P}(F_1 = i \mid F_0 = f_0) = \mathbb{P}(C_{1,i} > 0 \mid F_0 = f_0) \prod_{j=i+1}^{R} \mathbb{P}(C_{1,j} = 0 \mid F_0 = f_0),$$
$$i = 1, 2, \ldots, R, \tag{8.7}$$

with $f_0 = 0$. Note that since the source is by definition positioned in interval 0 the condition $F_0 = f_0$ may be left out, i.e., $\mathbb{P}(F_1 = i) = \mathbb{P}(F_1 = i \mid F_0 = f_0)$.

Generalising the above approach, the distribution of the position of the n^{th} forwarder ($n > 1$), given a set of positions of the source and the previous $n-1$ forwarders, is given by

$$\mathbb{P}(F_n = i \mid \hat{F}_{n-1} = \langle f_0, \ldots, f_{n-1} \rangle) =$$
$$\mathbb{P}(C_{n,i} > 0 \mid \hat{F}_{n-1} = \langle f_0, \ldots, f_{n-1} \rangle) \cdot \prod_{j=i+1}^{f_{n-1}+R} \mathbb{P}(C_{n,j} = 0 \mid \hat{F}_{n-1} = \langle f_0, \ldots, f_{n-1} \rangle),$$
$$n \in \mathbb{N}^+, \;\; i = f_{n-1}, f_{n-1}+1, \ldots, \tag{8.8}$$

with $\mathbb{P}(F_n = i \mid \hat{F}_{n-1} = \langle f_0, \ldots, f_{n-1} \rangle) = 0$ for $i < f_{n-1}$.

The probability of having n successive forwarders positioned in intervals $f_0, \ldots, f_n$ can now be expressed as

$$\mathbb{P}(\hat{F}_n = \langle f_0, \ldots, f_n \rangle) = \mathbb{P}(F_1 = f_1 \mid \hat{F}_0 = \langle f_0 \rangle) \cdot \mathbb{P}(F_2 = f_2 \mid \hat{F}_1 = \langle f_0, f_1 \rangle) \cdots$$
$$\mathbb{P}(F_n = f_n \mid \hat{F}_{n-1} = \langle f_0, \ldots, f_{n-1} \rangle) \tag{8.9}$$

Finally, to determine the distribution of F_n for $n > 1$ we sum over all possible positions of the previous $n-1$ forwarders:

$$\mathbb{P}(F_n = i) = \sum_{\langle f_0, \ldots, f_{n-1} \rangle} \mathbb{P}(\hat{F}_{n-1} = \langle f_0, \ldots, f_{n-1} \rangle) \cdot \mathbb{P}(F_n = i \mid \hat{F}_{n-1} = \langle f_0, \ldots, f_{n-1} \rangle),$$
$$n \in \mathbb{N}^+, \;\; i = 1, 2, \ldots, n \cdot R, \tag{8.10}$$

with $\mathbb{P}(F_n = i) = 0$ for other values of i. Fig. 8.6 illustrates $\mathbb{P}(F_1 = i)$, $\mathbb{P}(F_2 = i)$, and $\mathbb{P}(F_2 = i \mid F_1 = f_1)$.

Note that the expressions in Eq. (8.7), (8.8), and (8.10) to calculate the position of a forwarder all include the probability that there is no such forwarder, i.e., if we iterate over all the possible intervals in which the first forwarder can be positioned (using Eq. (8.7)), the total probability of having a first forwarder may be less than 1. Because we will need it later on we also define here the distribution of the position of the n^{th} forwarder when it is given that there is such a forwarder, denoted $F_n \mid C_n > 0$ since the probability of having an n^{th} forwarder is equal to the probability of having a candidate n^{th} forwarder. $\mathbb{P}(F_n = i \mid C_n > 0)$ is given by

$$\mathbb{P}(F_n = i \mid C_n > 0) = \frac{\mathbb{P}(F_n = i)}{\mathbb{P}(C_n > 0)}, \tag{8.11}$$

with $\mathbb{P}(C_n > 0)$ determined in the next section.

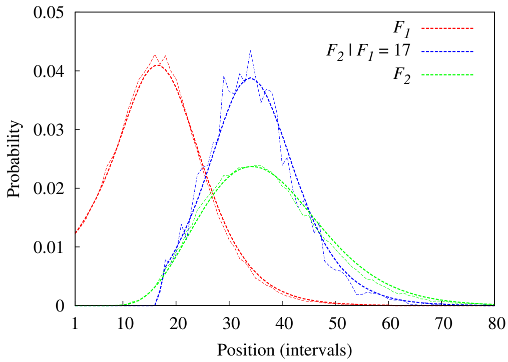

Figure 8.6: The probability distribution of the position of the first two forwarders, with $d_{int} = 5$ m and $d_{IN} = 50$ m.

8.4.2 Hop success probability

In this section we determine the probability of n successive hops and the individual probability of success of the n^{th} hop. The probability of n successive hops is equal to having at least one candidate n^{th} forwarder and is denoted $\mathbb{P}(C_n > 0)$. The n^{th} hop can be considered successful if there is at least one candidate n^{th} forwarder, while it is given that there is a candidate $(n-1)^{\text{th}}$ forwarder; its probability of success is therefore denoted $\mathbb{P}(C_n > 0 \mid C_{n-1} > 0)$ and (using the definition of conditional probabilities) is given by

$$\mathbb{P}(C_n > 0 \mid C_{n-1} > 0) = \frac{\mathbb{P}(C_n > 0)}{\mathbb{P}(C_{n-1} > 0)}, \quad n \in \mathbb{N}^+, \tag{8.12}$$

with $\mathbb{P}(C_0 > 0) = 1$ by definition.

Below we first determine $\mathbb{P}(C_n > 0)$ in an exact manner. Using Eq. (8.12) we thus also have an exact expression for $\mathbb{P}(C_n > 0 \mid C_{n-1} > 0)$. The complexity of calculating $\mathbb{P}(C_n > 0)$ increases exponentially with each hop however, making it infeasible to determine for large values of n. We therefore give an approximation of $\mathbb{P}(C_n > 0 \mid C_{n-1} > 0)$ for $n > 3$, and use this to approximate $\mathbb{P}(C_n > 0)$ for $n > 3$.

Note that in this section we determine the probability of success of a single hop or for multiple hops, and do not determine the probability that the sink will receive the message. The latter is determined in Section 8.4.5.

The n^{th}-hop success probability, given the position of the source and the positions of the preceding $n-1$ forwarders, is given by

$$\mathbb{P}(C_n > 0 \mid \hat{F}_{n-1} = \langle f_0, \ldots, f_{n-1} \rangle) = 1 - \mathbb{P}(C_n = 0 \mid \hat{F}_{n-1} \langle f_0, \ldots, f_{n-1} \rangle),$$
$$n \in \mathbb{N}^+, \tag{8.13}$$

with $C_n = 0 \mid \hat{F}_{n-1} \langle f_0, \ldots, f_{n-1} \rangle$ being Poisson distributed with its mean given by Eq. (8.6).

Summing over all possible positions of the preceding forwarders the probability of n successful hops is given by

$$\mathbb{P}(C_n > 0) = \sum_{\langle f_0,\ldots,f_{n-1}\rangle} \mathbb{P}(\hat{F}_{n-1} = \langle f_0, \ldots, f_{n-1}\rangle) \cdot \mathbb{P}(C_n > 0 \mid \hat{F}_{n-1} = \langle f_0, \ldots, f_{n-1}\rangle),$$
$$n \in \mathbb{N}^+, \tag{8.14}$$

with $\mathbb{P}(\hat{F}_{n-1} = \langle f_0, \ldots, f_{n-1}\rangle)$ given by Eq. (8.9).

Because of its complexity, the above method to determine the probability of n successful hops becomes infeasible for large values of n. Below we therefore given an approximate method to do so. First we state that (by using the rules of conditional probabilities) it by definition holds that

$$\mathbb{P}(C_n > 0) = \prod_{i=1}^{n} \mathbb{P}(C_i > 0 \mid C_{i-1} > 0), \;\; n \in \mathbb{N}^+. \tag{8.15}$$

Using Eq. (8.14) and (8.12) we can calculate $\mathbb{P}(C_i > 0 \mid C_{i-1} > 0)$ in an exact manner for small values of n. We then approximate the success probability of the n^{th} hop by assuming that its probability of success does not change beyond the third hop, i.e.,

$$\mathbb{P}(C_n > 0 \mid C_{n-1} > 0) \approx \mathbb{P}(C_3 > 0 \mid C_2 > 0), \;\; n = 4, 5, \ldots \tag{8.16}$$

Combining Eq. (8.16) with Eq. (8.15) we can thus approximate $\mathbb{P}(C_n > 0)$ for $n > 3$.

8.4.3 Hop length

In this section we determine the distribution of the hop length of the n^{th}-hop, denoted L_n. We give an exact expression to calculate L_n for arbitrary values of n and an approximate method to calculate L_n for $n > 3$.

The hop length of the n^{th} hop is defined as the distance between the $(n-1)^{\text{th}}$ forwarder and the n^{th} forwarder, i.e.,

$$L_n = F_n - F_{n-1}, \;\; n > 0, \tag{8.17}$$

with $F_0 = 0$. The length of the n^{th} hop is defined for successful hops only.

The distribution of the hop length of the first hop is identical to the distribution of the position of the first forwarder, given that there is a first forwarder, i.e.,

$$\mathbb{P}(L_1 = l_1) = \mathbb{P}(F_1 = l_1 \mid C_1 > 0), \;\; l_1 = 1, 2, \ldots, R, \tag{8.18}$$

with $\mathbb{P}(L_1 = l_1) = 0$ for other values of l_1. The distribution of the hop length of the n^{th} hop is given by conditioning on the positions of the first $n-1$ forwarders, given that there is such a forwarder:

$$\begin{aligned}\mathbb{P}(L_n = l_n) = \sum_{f_1=1}^{R} \quad & \mathbb{P}(F_1 = f_1 \mid \hat{F}_0 = \langle f_0 \rangle \wedge C_1 > 0) \ \cdots \\ \sum_{f_{n-1}=f_{n-2}}^{f_{n-2}+R} & \mathbb{P}(F_{n-1} = f_{n-1} \mid \hat{F}_{n-2} = \langle f_0, \ldots, f_{n-2} \rangle \wedge C_{n-1} > 0) \cdot \\ & \mathbb{P}(F_n = f_{n-1} + l_n \mid \hat{F}_{n-1} = \langle f_0, \ldots, f_{n-1} \rangle \wedge C_n > 0), \\ n = 2, 3, \ldots, \ \ l_n = 1, 2, \ldots, R. \qquad & \qquad (8.19)\end{aligned}$$

Calculating the distribution of the length of the n^{th} hop using the above method is infeasible for large values of n, due to its complexity. As we will show in Section 8.5.2 the distribution of L_n converges rapidly and, for the purpose of our analysis, does not change significantly beyond the third hop however. For the fourth and following hops we will therefore approximate the distribution of L_n by assuming it is identical to the distribution of L_3:

$$F_{L_n}(\cdot) \sim F_{L_3}(\cdot), \quad n = 4, 5, \ldots \qquad (8.20)$$

Moreover, we assume that L_n is not only identical but also independent of previous hop lengths for $n > 3$. We discuss the validity of this claim in Section 8.5.2.

8.4.4 Approximated position of a forwarder

In Section 8.4.1 the position of the n^{th} forwarder F_n is determined in an exact manner. Due to the complexity of this method, calculating the distribution of F_n in this manner is infeasible for large values of n. In this section we therefore approximate the distribution of F_n for $n > 3$. This approximation allows for a quick calculation of the distribution of F_n for large values of n.

Our approximation is as follows. In the previous section we have assumed that the hop length of each hop beyond the third hop is distributed independently and identical to L_3, see Eq. (8.20). The position of the n^{th} forwarder (for $n > 3$) is therefore a sum of $(n-3)$ i.i.d. hop lengths beyond the position of the third forwarder. Since the distribution of the hop length has been calculated assuming that the hop is successful, the success probability of each of these $(n-3)$ hops must also be taken into account. As was shown in the previous section we can approximate the success probability of each hop beyond the third hop using Eq. (8.16). The distribution of the position of the n^{th} forwarder is then given by the following recursive expression:

$$\begin{aligned}\mathbb{P}(F_n = f_n) \approx & \sum_{f_{n-1}=1}^{(n-1)R} \mathbb{P}(F_{n-1} = f_{n-1}) \cdot \mathbb{P}(L_3 = f_n - f_{n-1}) \cdot \mathbb{P}(C_3 > 0 \mid C_2 > 0), \\ n = 4, 5, \ldots, & \qquad (8.21)\end{aligned}$$

with $\mathbb{P}(F_n = f_n)$ given by Eq. (8.10) for $n \leq 3$.

8.4.5 Required number of hops

In this section we determine the hop in which the sink, positioned in interval i, first receives the message, denoted N_i.

The probability that the sink first receives the message in the first hop (i.e., directly from the source) is equal to S_i and is given by

$$\mathbb{P}(N_i = 1) = S_i, \;\; i \in \mathbb{N}^+. \tag{8.22}$$

$\mathbb{P}(N_i = 2 \mid F_1 = f_1)$ denotes the probability that the sink first receives the message in the second hop, i.e., from the first forwarder, given that the first forwarder is positioned in interval f_1. It is given by

$$\mathbb{P}(N_i = 2 \mid F_1 = f_1) = (1 - S_i) \cdot S_{|i-f_1|}, \;\; i \in \mathbb{N}^+, \tag{8.23}$$

where the term $(1 - S_i)$ denotes the probability that the sink did not receive the message in the first hop. To determine $\mathbb{P}(N_i = 2)$ we sum over all possible positions of the first forwarder, such that we get

$$\mathbb{P}(N_i = 2) = (1 - S_i) \cdot \sum_{f_1=1}^{R} \mathbb{P}(F_1 = f_1) \cdot S_{|i-f_1|}, \;\; i \in \mathbb{N}^+, \tag{8.24}$$

with $\mathbb{P}(F_1 = f_1)$ given by Eq. (8.7).

The probability that the sink first receives the message in the n^{th} hop from the $(n-1)^{\text{th}}$ forwarder, given the positions of the source and the first $n-1$ forwarders, is given by

$$\begin{aligned}&\mathbb{P}(N_i = n \mid \hat{F}_{n-1} = \langle f_0, \ldots, f_{n-1} \rangle) = \\ &(1 - S_i) \cdot (1 - S_{|i-f_1|}) \cdots (1 - S_{|i-f_{n-2}|}) \cdot S_{|i-f_{n-1}|}, \;\; i, n \in \mathbb{N}^+. \end{aligned}\tag{8.25}$$

Finally, the general case $\mathbb{P}(N_i = n)$ is obtained by summing over all possible positions of the first $n-1$ forwarders and then rewriting terms:

$$\begin{aligned}\mathbb{P}(N_i = n) = \sum_{\langle f_0, \ldots, f_{n-1} \rangle} &\mathbb{P}(\hat{F}_{n-1} = \langle f_0, \ldots, f_{n-1} \rangle) \cdot \\ &\mathbb{P}(N_i = n \mid \hat{F}_{n-1} = \langle f_0, \ldots, f_{n-1} \rangle), \;\; i, n \in \mathbb{N}^+, \end{aligned}\tag{8.26}$$

with $\mathbb{P}(\hat{F}_{n-1} = \langle f_0, \ldots, f_{n-1} \rangle)$ given by Eq. (8.9). Since the position of the source is fixed and each forwarder can be at R possible positions with respect to the position of the previous forwarder, calculating the distribution of N_i in this manner has a complexity of $R^{(n-1)}$.

8.4.6 Hop delay

In this section we determine the hop delay of the n^{th} hop, denoted D_n, and defined as the time between the moment the $(n-1)^{\text{th}}$ forwarder forwards the message and the moment

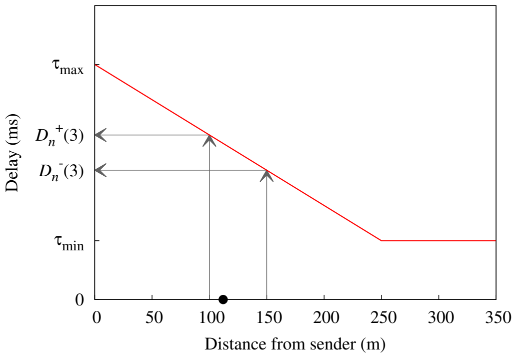

Figure 8.7: The minimum and maximum forwarding delay $D_n^-(3)$ and $D_n^+(3)$ for a hop three intervals long, with $d_{int} = 50$ m. The black dot represents a node in interval 3.

the n^{th} forwarder forwards the message. It is therefore equal to the delay of the candidate n^{th} forwarder that has the shortest forwarding delay (i.e., is positioned closest to the destination). A candidate forwarder's forwarding delay is determined by its distance to the previous sender, as defined in Eq. (8.1). D_n is therefore a function of L_n.

In Eq. (8.1) the forwarding delay is calculated based on the hop length in meters, whereas L_n gives the hop length in intervals that are d_{int} meter long. For a given length of the n^{th} hop l_n in intervals, the hop length in meters lies anywhere in the range $\langle (l_n - 1) \cdot d_{int}, l_n \cdot d_{int}]$. The forwarding delay of a candidate forwarder positioned inside an interval differs, depending on its position inside the interval. For a given length of the n^{th} hop l_n we therefore give a minimum resulting hop delay, denoted $D_n^-(l_n)$, and a maximum hop delay, denoted $D_n^+(l_n)$. $D_n^-(l_n)$ is given by

$$D_n^-(l_n) = \tau_{min} + (\delta_{max} - (l_n + 1)) \cdot \frac{\tau_{max} - \tau_{min}}{\delta_{max}},$$
$$n \in \mathbb{N}^+, \quad l_n = 0, 1, \ldots, \delta_{max}, \tag{8.27}$$

and $D_n^+(l_n)$ is given by

$$D_n^+(l_n) = \tau_{min} + (\delta_{max} - \max(l_n, 1) + 1) \cdot \frac{\tau_{max} - \tau_{min}}{\delta_{max}},$$
$$n \in \mathbb{N}^+, \quad l_n = 0, 1, \ldots, \delta_{max}. \tag{8.28}$$

Note that the equations allow for hop lengths of length 0 (i.e., two consecutive forwarders are positioned in the same interval), which for simplicity are treated as if they were of length 1. The relation between the hop length and the hop delay has been illustrated in Fig. 8.7.

To calculate the distribution of D_n we condition on the hop length and get

$$\mathbb{P}(D_n \in [D_n^-(l_n), D_n^+(l_n)]) = \mathbb{P}(L_n = l_n), \quad n \in \mathbb{N}^+, l_n = 0, 1, \ldots, R, \tag{8.29}$$

with $\mathbb{P}(L_n = l_n)$ given by Eq. (8.19). For a given hop length l_n we assume that the hop delay is uniformly distributed in the range $[D_n^-(l_n), D_n^+(l_n)]$.

8.4.7 End-to-end delay

In this section we determine in an exact manner the end-to-end delay to have the message delivered to a sink positioned in interval i, for a given maximum number of times that a message is transmitted, denoted $E_i \mid N_{\max}$. It is equal to the sum of the delays of the consecutive hops required to have the sink receive the message.

Given that the sink first receives the message in the n^{th} hop from the $(n-1)^{\text{th}}$ forwarder, the end-to-end delay is a sum of $n-1$ hop delays. The hop delay of the k^{th} hop, with hop length l_k, is assumed to be uniformly distributed in the range $[D_k^-(l_k), D_k^+(l_k)]$, as shown in the previous section. Given the positions of the $n-1$ forwarders, the end-to-end delay is thus a summation of $n-1$ uniformly distributed continuous hop delays D_k. Determining the distribution of such a sum in an explicit manner quickly becomes complex, so we approximate the end-to-end delay by assuming that it is uniformly distributed between the minimum end-to-end delay $E_i^-(l_1,\ldots,l_{n-1}) = \sum_{k=1}^{n-1} D_n^-(l_k)$ and the maximum end-to-end delay $E_i^+(l_1,\ldots,l_{n-1}) = \sum_{k=1}^{n-1} D_n^+(l_k)$. The distribution of the end-to-end delay, given that the sink first receives the message in the n^{th} hop and given that the position of the $n-1$ forwarders are known, denoted $E_i \mid N_i = n \wedge \hat{F}_{n-1} = \langle f_0,\ldots,f_{n-1}\rangle$, is thus uniformly distributed in the range $[E_i^-(l_1,\ldots,l_{n-1}), E_i^+(l_1,\ldots,l_{n-1})]$.

If the positions of the first $n-1$ forwarders are not known, using the rules of conditional probabilities, the probability that the sink first receives the message within time t, given that it first receives the message in the n^{th} hop, is given by

$$\mathbb{P}(E_i \le t \mid N_i = n) = \frac{\mathbb{P}(E_i \le t \wedge N_i = n)}{\mathbb{P}(N_i = n)}, \quad i,n \in \mathbb{N}^+, \tag{8.30}$$

with $\mathbb{P}(N_i = n)$ given by Eq. (8.26). To determine $\mathbb{P}(E_i \le t \wedge N_i = n)$ we sum over all possible positions of the source and the $n-1$ forwarders:

$$\begin{aligned}\mathbb{P}(E_i \le t \wedge N_i = n) = \sum_{\langle f_0,\ldots,f_{n-1}\rangle} & \mathbb{P}(N_i = n \wedge \hat{F}_{n-1} = \langle f_0,\ldots,f_{n-1}\rangle) \cdot \\ & \mathbb{P}(E_i \le t \mid N_i = n \wedge \hat{F}_{n-1} = \langle f_0,\ldots,f_{n-1}\rangle), \quad i,n \in \mathbb{N}^+,\end{aligned} \tag{8.31}$$

with $\mathbb{P}(N_i = n \wedge \hat{F}_{n-1} = \langle f_0,\ldots,f_{n-1}\rangle)$ (again using the rules of conditional probabilities) given by

$$\begin{aligned}&\mathbb{P}(N_i = n \wedge \hat{F}_{n-1} = \langle f_0,\ldots,f_{n-1}\rangle) = \\ &\mathbb{P}(\hat{F}_{n-1} = \langle f_0,\ldots,f_{n-1}\rangle) \cdot \mathbb{P}(N_i = n \mid \hat{F}_{n-1} = \langle f_0,\ldots,f_{n-1}\rangle), \quad n \in \mathbb{N}^+,\end{aligned} \tag{8.32}$$

with $\mathbb{P}(\hat{F}_{n-1} = \langle f_0,\ldots,f_{n-1}\rangle)$ given by Eq. (8.9) and $\mathbb{P}(N_i = n \mid \hat{F}_{n-1} = \langle f_0,\ldots,f_{n-1}\rangle)$ given by Eq. (8.25).

Finally, the probability that the sink first receives the message within time interval t, given that the message is transmitted a maximum of $n_{\max}$ times (including the source's transmission), is given by conditioning on the hop in which the sink first receives the mes-

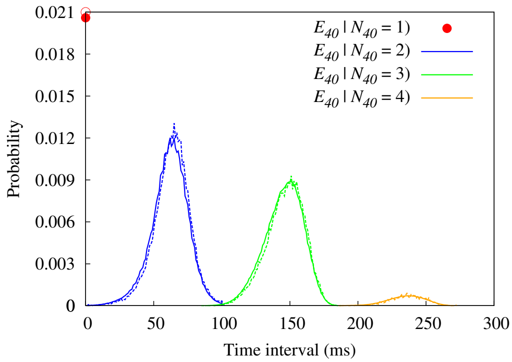

Figure 8.8: The end-to-end reception probability as a function of time, split up for each hop, with $d_{int} = 5$ m, $d_{IN} = 50$ m.

sage:

$$\mathbb{P}(E_i \leq t \mid N_{\max} = n_{\max}) = \sum_{n=1}^{n_{\max}} \mathbb{P}(N_i = n) \cdot \mathbb{P}(E_i \leq t \mid N_i = n),$$
$$n_{\max}, i \in \mathbb{N}^+, \tag{8.33}$$

with $\mathbb{P}(N_i = n)$ given by Eq. (8.26). It is possible to combine Eq. (8.31) and Eq. (8.26), since both sum over all possible positions of the $n - 1$ forwarders. Similar to Eq. (8.26) determining the distribution of $E_i \mid N_{\max} = n_{\max}$ is thus of complexity $R^{(n_{\max}-1)}$.

8.5 Performance evaluation

In this section we present the set-up and results of an evaluation study to assess *(i)* how the forwarding protocol described in Section 8.3 performs for varying network parameters, and *(ii)* how well our analysis presented in the previous section is able to capture the behaviour of the forwarding protocol. We have done so by evaluating a forwarding scenario for different network and protocol parameters, both by means of simulation and by means of our analysis. We first briefly describe the scenario and the set-up of our simulation study and then discuss the results.

8.5.1 Experimental set-up

Nodes are positioned over a straight line of 3000 m with the source at one end and the message destination at the other end. The inter-node spacing is exponentially distributed with mean d_{IN} set to 10, 25, or 50 m. Forwarding is done as specified in Section 8.3 with protocol parameters $\tau_{\min} = 1$ ms, $\tau_{\max} = 100$ ms, and $\Delta_{\max} = 300$ m. Additionally we determine a maximum number of hops a message is transmitted, including the source's original transmission, denoted $N_{\max}$. To gain statistically reliable results each experiment

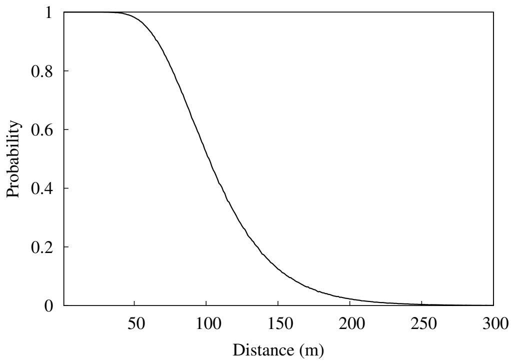

Figure 8.9: The packet reception curve S_i.

is repeated at least 30,000 times with different random seeds, and in some cases more than 100,000 times.

Experiments have been performed using the OMNET++ network simulator v4.1 [77] and using a self-modified version of the MiXiM framework v2.1 [79] to model the communication architecture. To model the behaviour of the 802.11p protocol as accurately as possible we have altered the IEEE 802.11 medium access module in such a way that all parameters follow the 802.11p specification [100]. The centre frequency was set to 5.9 MHz and AC 0 was used. We use the log-normal shadowing model [22] for signal propagation with the path loss exponent set to 3.5 and the standard deviation to 6. Transmission power was set to 4 mW, receiver sensitivity to -95 dBm, background noise to -99 dBm, and the required minimum SNR to 8 dBm. BER and PER calculations were ignored. To keep the influence of packet collisions due to hidden nodes as low as possible the packet sizes are kept small at 160 b.

Our model analysis requires the packet reception rate S_i as input. Using the above settings we measured the packet reception probabilities at intervals of one meter for a single node that broadcasted a packet ten thousand times without any interfering network traffic. The resulting packet reception curve S_i has been used to produce our analytical results. It can be seen in Fig. 8.9. At Δ_{max} m from the sender the probability of successfully receiving a packet is less than 0.1%.

Note that it is also possible to model S_i as a function of transmission power and propagation effects; see for example [104].

8.5.2 Results

Our discussion is split into two parts. We first look at protocol performance: for each performance metric we discuss how it is affected by changing network and protocol parameters, and compare how well the results of our analysis compare with the results of the simulation study, which serve as a baseline. As we will see the results of our analysis match those of the simulation most closely when the node density is low, and gradually become less accurate as the node density increases. This is due to the fact that multiple nodes often act as the n^{th} forwarder, causing a message to be forwarded in multiple waves. This effect, which is described in the second part of our discussion, is strongest for a high node density and has not been taken into account in our analysis.

Protocol performance

We look at the following performance metrics: *(i)* the hop success probability, *(ii)* the distribution of the hop length, *(iii)* the distribution of the position of the forwarder, *(iv)* the distribution of the hop delay, *(v)* the required number of hops to have the sink receive the message, and *(vi)* the end-to-end delay to have the sink receive the message.

Simulation results of the first four performance metrics have been generated with $N_{\max} = \infty$, i.e., the message is forwarded until it reaches the destination. Analytical results of these performance metrics have been calculated in an exact manner for the first three hops and have been approximated for following hops.

Simulation results of the two end-to-end performance metrics, the required number of hops and the end-to-end delay, have been generated with $N_{\max} = 6$, i.e., the message is transmitted a maximum of six hops. The position of the sink has been varied between 100, 200, 300, 400, 500, and 600 m. All analytical results of these performance metrics have been calculated in an exact manner.

We use the K-S statistic to express the difference between two distributions. The K-S statistic K for two distributions $F_1(x), F_2(x)$ is equal to the largest distance between the CDFs, given by

$$K = \max\{|F_1(x) - F_2(x)|\} \quad \forall\, x. \tag{8.34}$$

For clarity of illustration Fig. 8.11 - 8.14 show only distributions of the first five hops. For all shown results $d_{int} = 5$ m unless specified otherwise. The solid lines represent analytical results, the dashed lines represent simulation results. In case of average values confidence intervals are less than 1%. Fig. 8.12, 8.14, 8.15, 8.16, and 8.17 all include the probability that a message can be lost and illustrate it as a loss in probability mass, e.g., when comparing Fig. 8.12a and 8.12c it can be seen that the probability of having a fifth forwarder is significantly lower when $d_{IN} = 50$ m compared to when $d_{IN} = 10$ m.

In general we see that the accuracy of our model analysis is very high, with results of end-to-end metrics staying within 0.05 and per-hop metrics (such as the position of a forwarder) staying within 0.01-0.11, depending on the metric and the inter-node distance d_{IN}. Results become more accurate when d_{IN} increases, i.e., when there are less nodes on the road. This is because in our model analysis we do not take into account effects such as the simultaneous transmission of a message by two nodes, or how multiple nodes will act as the n^{th} forwarder and will all retransmit the message; effects which are more pronounced when there are more nodes on the road. Their impact on performance is described in the next section.

Fig. 8.10 shows the *hop success probability* of the first ten hops. As there are fewer nodes on the road the probability that a message gets lost increases: whereas the probability of having a message forwarded ten times is 1 for $d_{IN} = 10$ m, it is almost 0 for $d_{IN} = 50$

m. It can be seen in the figure as well as in Table 8.1 that, regarding the hop success probability, results stay within 0.02.

Fig. 8.11 shows the distribution of the *hop length* of the first five hops. Of the model analysis only the distributions of the hop length of the first three hops are shown since in our analysis we assume that the distribution of the hop length of the fourth hop (and of following hops) is identical to the distribution of the hop length of the third hop. It can be observed that *(i)* hop lengths of following hops are distributed almost identically and *(ii)* hops become longer as the density increases. The former is because the distribution of the number of nodes in intervals following the most recent forwarder quickly converges, as can also be seen in Fig. 8.4. This supports our assumption made in Eq. (8.20) that, for the purpose of our analysis and for the range of parameters tested here, the distribution of the hop length of the fourth hop (and of following hops) is identical to the distribution of the hop length of the third hop. The latter observation is due to the fact that as the probability of having a node in an interval increases, the probability of having a candidate forwarder in an interval positioned at a large distance from the previous sender increases.

Fig. 8.12 shows the distribution of the *position of a forwarder* of the first five hops. It can be seen that the n^{th} forwarder is more likely to be positioned further away from the source in a high-density scenario than in a low-density scenario, since hop lengths are on average longer in high-density scenarios. Furthermore, as node densities decrease, the probability of having an n^{th} forwarder decreases as well.

It can be seen in the figures as well as in Table 8.1 that, regarding the distribution of the position of the forwarder, depending on the hop and the node density, results of the model simulation and the model analysis stay between 0.01 and 0.11. Results become less accurate as the node density increases; this effect is explained in the next subsection. For low densities the accuracy remains the same for following hops, supporting our assumption that, for the purpose of our analysis, consecutive hop lengths are independent.

Fig. 8.13 shows the distribution of the *hop delay* of the first five hops. Of the model analysis only the distribution of the hop delay of the first three hops is shown, since in our analysis we assume that the distribution of the hop delay of the fourth hop (and of following hops) is identical to the hop delay of the third hop. Since a candidate forwarder's forwarding delay is a linear function of its distance to the previous sender, the distribution of the hop delay is a mirror image of the distribution of the hop length. It can be seen that if the node density increases the hop delay on average decreases, since hops become longer. Furthermore, apart from the hop delay of the first hop for $d_{IN} = 50$ m, the hop delays are distributed virtually identically. This is again because the distribution of the number of nodes in intervals following the most recent forwarder quickly converges

It can be seen in the figures as well as in Table 8.1 that, regarding the distribution of the hop delay, results of the model simulation and the model analysis stay within 0.04. This supports our assumption that, for the purpose of our analysis, the distribution of the hop delay of the third hop (and following) is identical to the distribution of the delay of the second hop.

Fig. 8.14 shows the distribution of the *required number of hops to have the sink first receive the message*. The figures show how fewer hops are needed to have the sink first receive the message as the node density increases, due the increased hop lengths. It can also be seen that the probability of the sink receiving the message at all decreases as the node density decreases. Fig. 8.18 shows trends of the average required number of hops to have a sink first receive the message (given that the sink does receive it); both as the source-to-sink distances increases, or the node density decreases, the average number of hops increases less than linearly.

It can be seen in the figures as well as in Table 8.2 that, regarding the distribution of the required number of hops to have the sink first receive the message, results of the model simulation and the model analysis stay within 0.01-0.05, depending on the source-to-sink distance and the value of d_{IN}.

Fig. 8.15, 8.16, and 8.17 show the distribution of the *end-to-end delay* to have the sink first receive the message. As the figures clearly illustrate end-to-end delay has a multi-modal distribution, with each mode corresponding to a specific hop in which the sink may first receive the message. I.e., when the sink is positioned at 200 m and $d_{IN} = 50$ m, the sink may either first receive the message in the first, second, third, or fourth hop, see Fig. 8.17c. This effect has also been illustrated in Fig. 8.8. Fig. 8.19 shows trends of the average end-to-end delay to have the sink first receive the message (given that the sink does receive it); both as the source-to-sink distances increases, or the node density decreases, the average number of hops increases less than linearly.

It can be seen in the figures as well as in Table 8.2 that, regarding the distribution of the end-to-end delay, results of the model simulation and the model analysis stay within 0.01-0.05, depending on the source-to-sink distance and the node density.

Waves of forwarding

When a message is being forwarded it may be that multiple nodes act as the n^{th} forwarder. Below we explain the cause of this effect and show how it affects performance. The effect has not been taken into account in our analytical model.

The first node to forward the message for the n^{th} time is the candidate forwarder positioned closest to the destination. However, candidate forwarders that are positioned less close to the destination may choose to forward the message as well in two cases. In the first case the candidate forwarder is positioned so close to the first n^{th}-hop forwarder that their forwarding delays are practically identical. This may result in the two candidate forwarders forwarding the message at (almost) the same time, causing the messages either to collide or to be transmitted back-to-back. It may also be however that the candidate forwarder is positioned such a distance behind (i.e., in the direction of the source) the first n^{th} forwarder that it fails to receive the first n^{th} forwarder's transmission. It will therefore assume that it is the candidate forwarder positioned most closely to the destination and also forward the message.

The effect that a message is being forwarded in multiple 'waves' has been illustrated in Fig. 8.20 for the first forwarder. The first wave in the figure refers to the candidate first forwarder that is the first to forward the message (the 'first first forwarder'), the second wave to candidate first forwarders that forward the message at (almost) the same moment and are positioned close (within one meter) behind the first first forwarder, and the third wave refers to candidate first forwarders that forward the message a little later that are positioned some distance behind the first first forwarder. The effect of multiple waves is strongest for a high

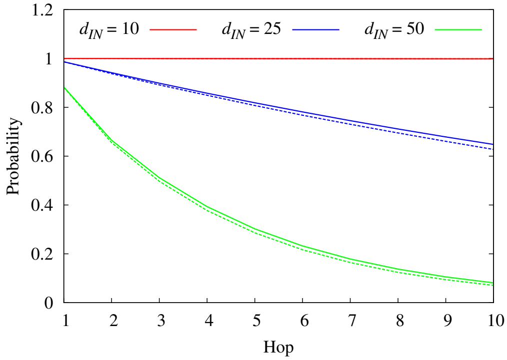

Figure 8.10: The hop success probability for various values of d_{IN}.

node density since in that situation there are more candidate forwarders. Fig. 8.21 shows the probability distribution of the position of the first three forwarders when all waves are taken into account, i.e., the simulation results include all nodes that act as the n^{th} forwarder. It can again be seen that for a high node density the number of additional forwarders is substantial.

The main effects that these waves of forwarding have on performance are *(i)* that the per-hop success probability and the end-to-end reception probability increase, because the third wave causes messages to be retransmitted, and *(ii)* that the length of a hop is influenced because of second-wave transmissions that either collide or are transmitted back-to-back. The impact of the first effect is limited since the effect of multiple waves is strongest for scenarios in which the hop success probability is already very high (i.e., for small values of d_{IN}). The impact of the second effect – although still limited – is strongest for small values of d_{IN}, see for instance Fig. 8.12a.

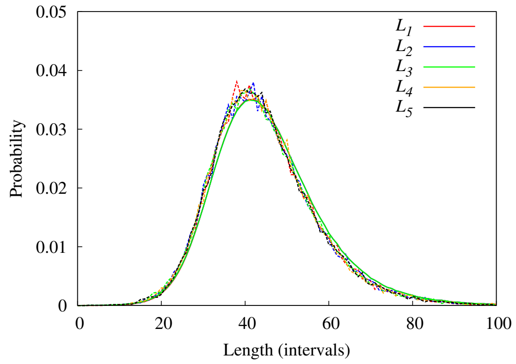

(a) For $d_{IN} = 10$ m.

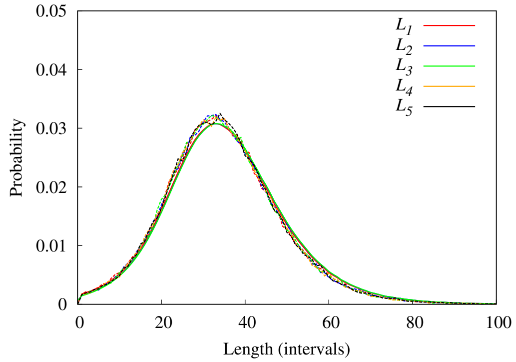

(b) For $d_{IN} = 25$ m.

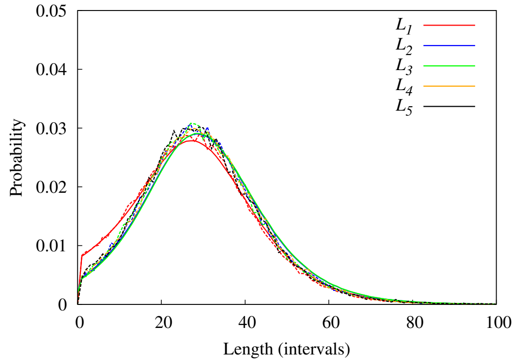

(c) For $d_{IN} = 50$ m.

Figure 8.11: The distribution of the hop length of the first five hops, for varying values of d_{IN}. For the analytical results only the first three hops are shown.

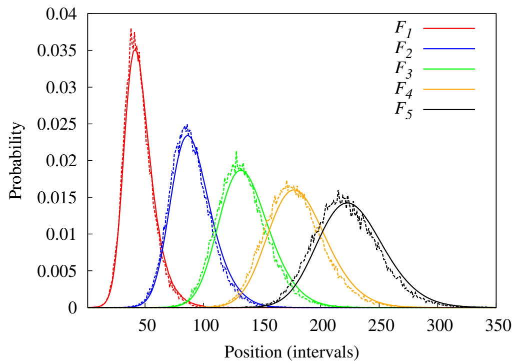

(a) For $d_{IN} = 10$ m.

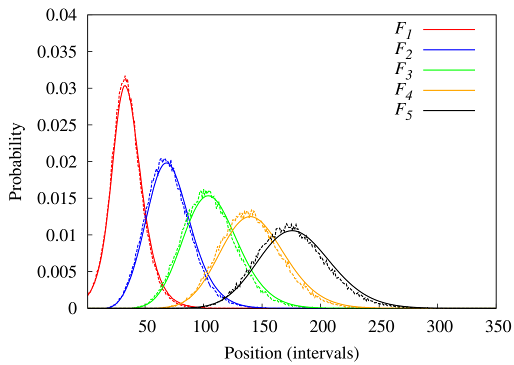

(b) For $d_{IN} = 25$ m.

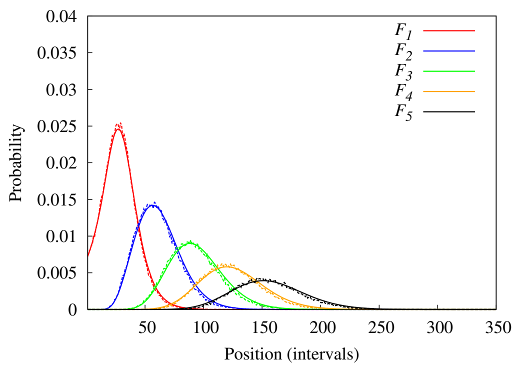

(c) For $d_{IN} = 50$ m.

Figure 8.12: The distribution of the position of the first five forwarders, for various values of d_{IN}.

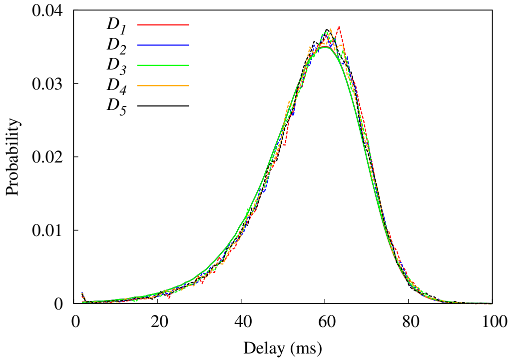

(a) For $d_{IN} = 10$ m.

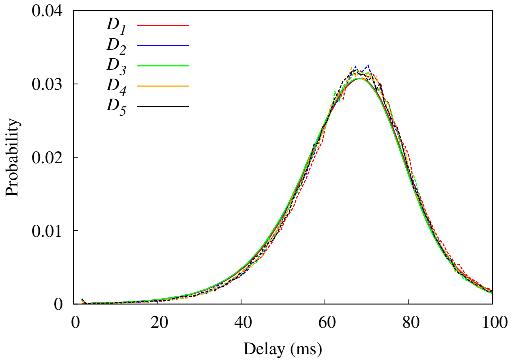

(b) For $d_{IN} = 25$ m.

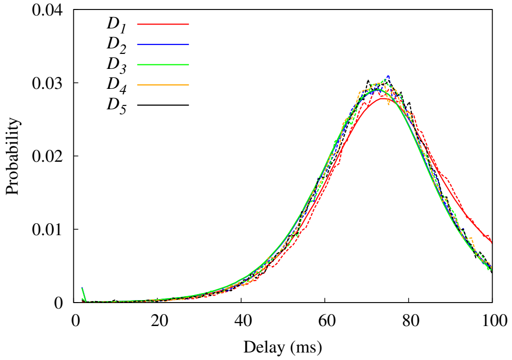

(c) For $d_{IN} = 50$ m.

Figure 8.13: The distribution of the hop delay of the first five hops, for varying values of d_{IN}. Of the analytical results only the first three hops are shown.

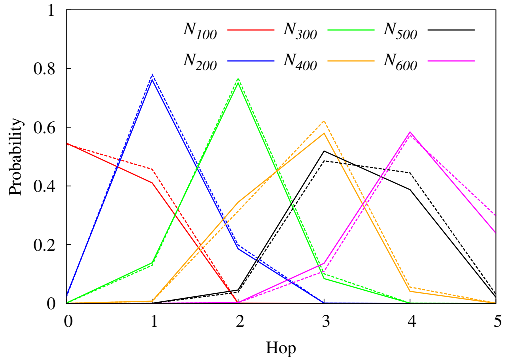

(a) For $d_{IN} = 10$ m.

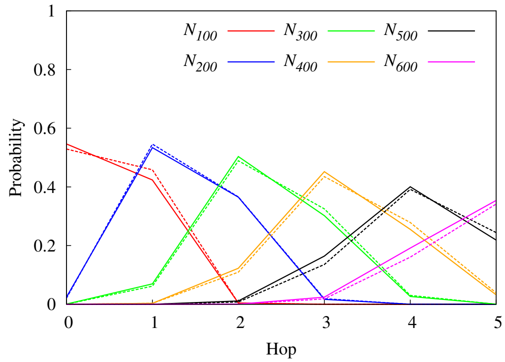

(b) For $d_{IN} = 25$ m.

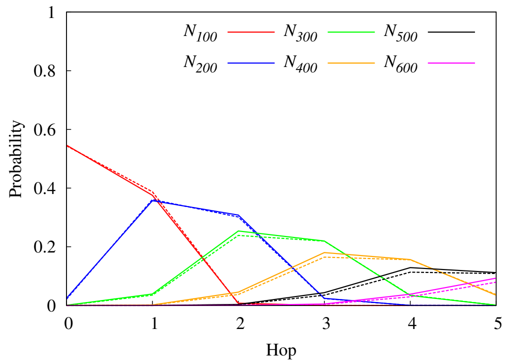

(c) For $d_{IN} = 50$ m.

Figure 8.14: The distribution of the required number of hops to have the sink receive the message, for varying values of d_{IN} and varying source-to-sink distances.

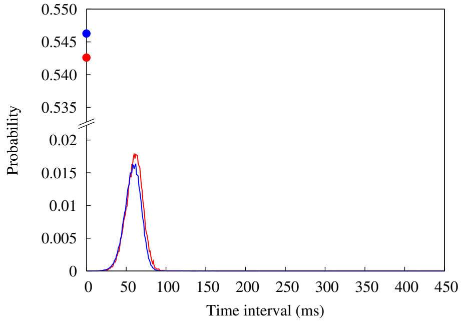

(a) Sink at 100 m.

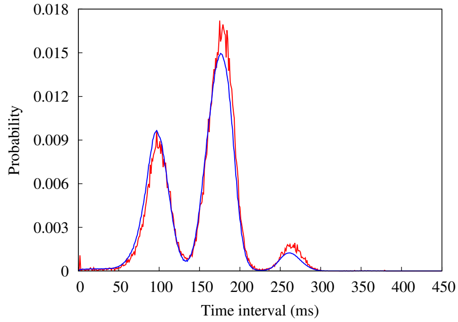

(b) Sink at 400 m.

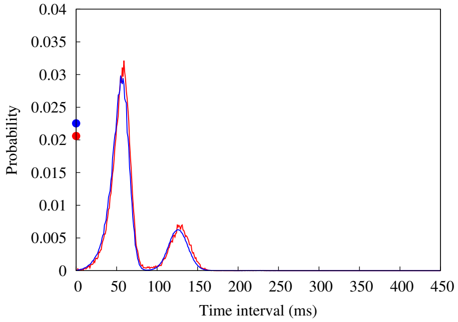

(c) Sink at 200 m.

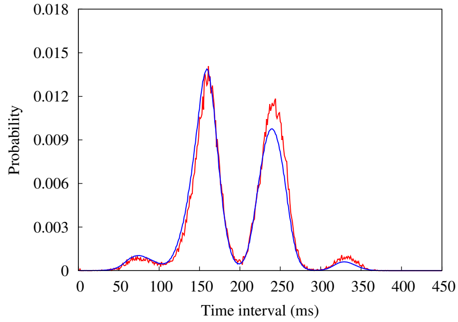

(d) Sink at 500 m.

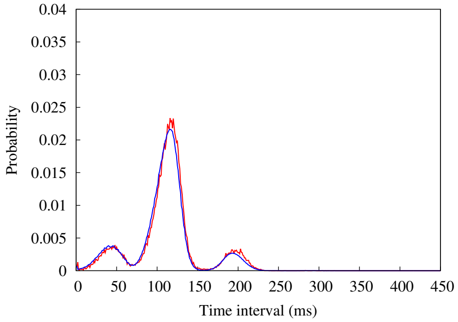

(e) Sink at 300 m.

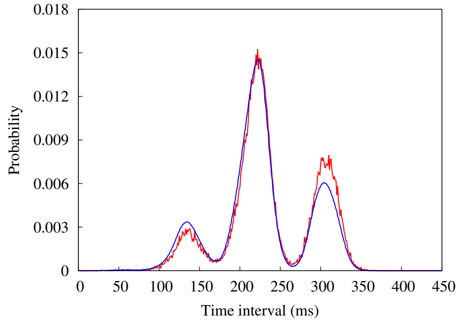

(f) Sink at 600 m.

Figure 8.15: The probability distribution of the end-to-end delay for $d_{IN} = 10$ and various source-to-sink distances. The blue lines represent analytical results, the red lines simulation results.

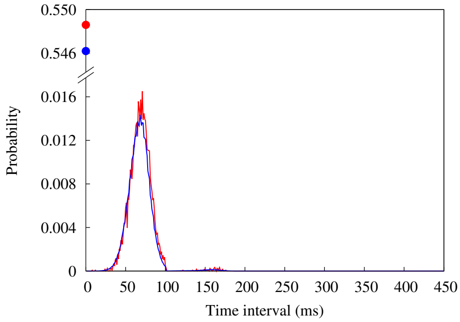

(a) Sink at 100 m.

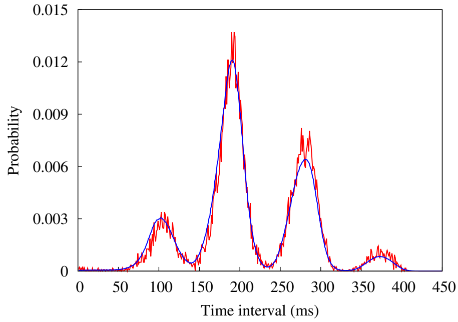

(b) Sink at 400 m.

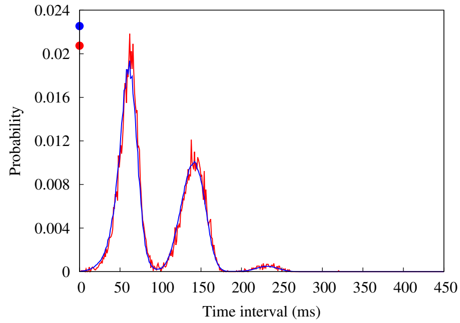

(c) Sink at 200 m.

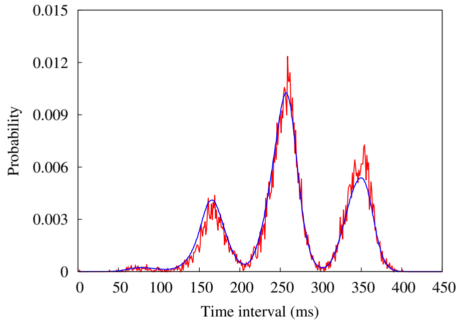

(d) Sink at 500 m.

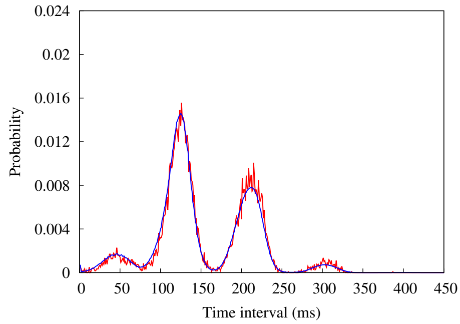

(e) Sink at 300 m.

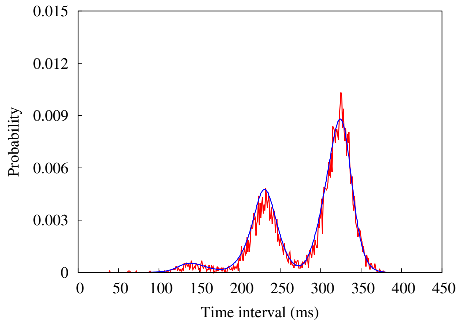

(f) Sink at 600 m.

Figure 8.16: The probability distribution of the end-to-end delay for $d_{IN} = 25$ and various source-to-sink distances. The blue lines represent analytical results, the red lines simulation results.

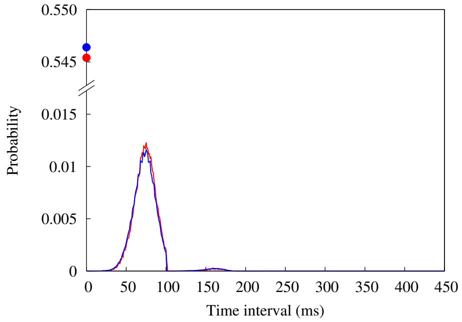

(a) Sink at 100 m.

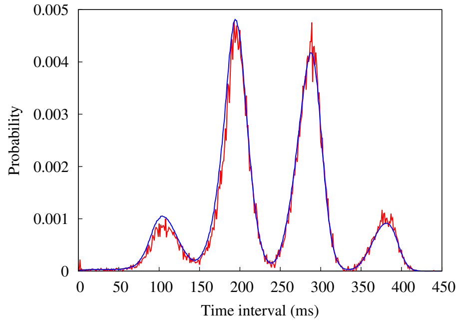

(b) Sink at 400 m.

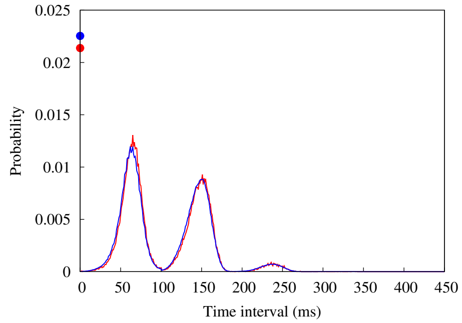

(c) Sink at 200 m.

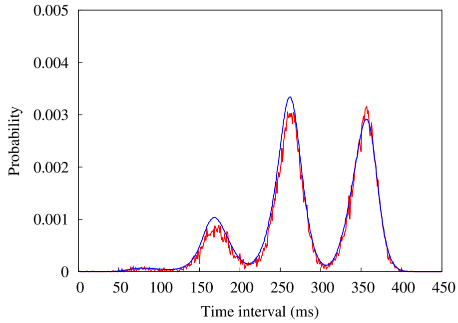

(d) Sink at 500 m.

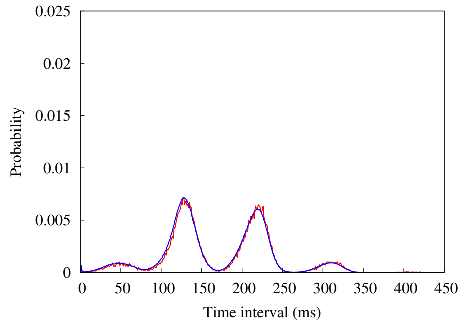

(e) Sink at 300 m.

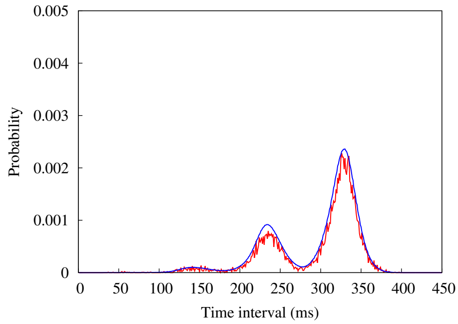

(f) Sink at 600 m.

Figure 8.17: The probability distribution of the end-to-end delay for $d_{IN} = 50$ and various source-to-sink distances. The blue lines represent analytical results, the red lines simulation results.

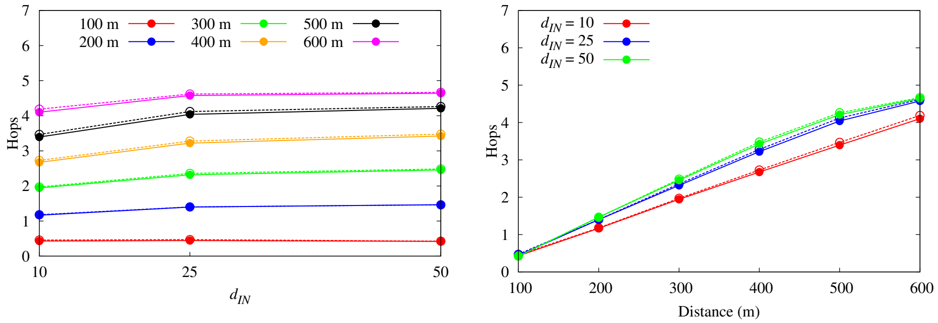

(a) For varying values of d_{IN}.

(b) For varying values of the source-to-sink distance i.

Figure 8.18: The average required number of hops to have the sink receive the message.

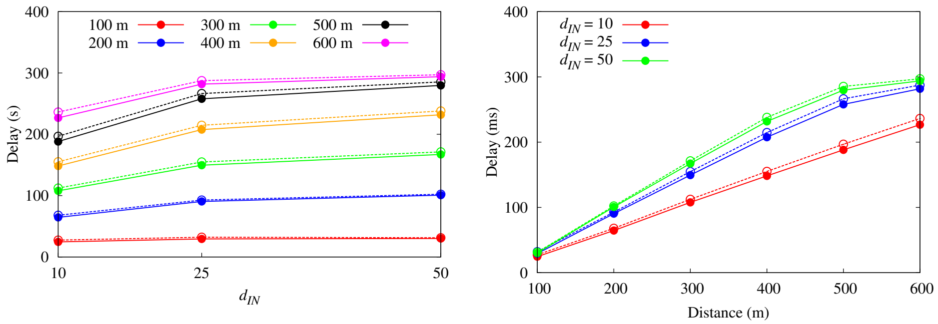

(a) For varying values of d_{IN}.

(b) For varying values of the source-to-sink distance i.

Figure 8.19: The average end-to-end delay to have the sink receive the message.

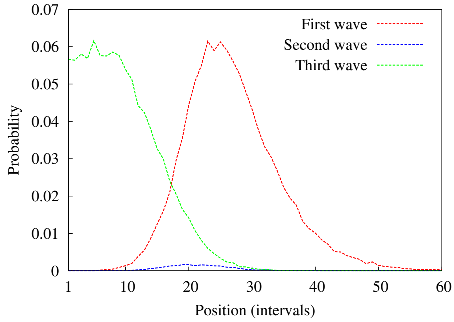

(a) For $d_{IN} = 10$ m.

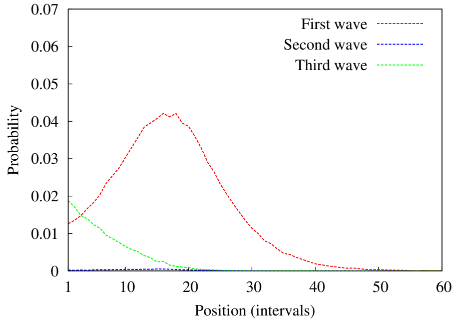

(b) For $d_{IN} = 50$ m.

Figure 8.20: The three forwarding waves of the first hop.

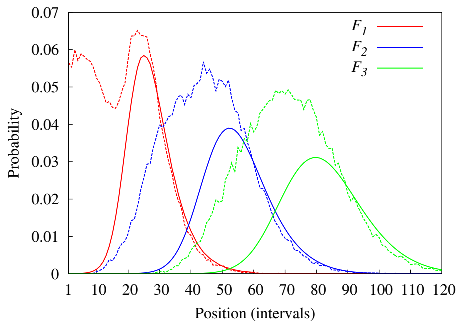

(a) For $d_{IN} = 10$ m.

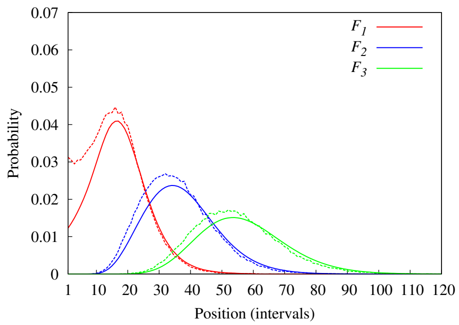

(b) For $d_{IN} = 50$ m.

Figure 8.21: The position of a forwarder. The simulation results include all forwarding waves.

Hop	1	2	3	4	5	6	7	8	9	10
d_{IN}	Hop length									
10	0.037	0.038	0.040	0.037	0.040	0.040	0.038	0.037	0.041	0.037
25	0.025	0.030	0.031	0.032	0.032	0.031	0.033	0.032	0.032	0.031
50	0.016	0.025	0.034	0.029	0.041	0.032	0.037	0.035	0.034	0.036
d_{IN}	Position of a forwarder									
10	0.036	0.049	0.061	0.068	0.079	0.083	0.091	0.096	0.103	0.109
25	0.024	0.032	0.038	0.039	0.037	0.034	0.032	0.031	0.030	0.027
50	0.013	0.012	0.013	0.014	0.015	0.015	0.014	0.013	0.011	0.010
d_{IN}	Hop delay									
10	0.044	0.029	0.032	0.029	0.032	0.032	0.030	0.028	0.031	0.029
25	0.030	0.023	0.025	0.026	0.025	0.024	0.027	0.026	0.025	0.025
50	0.021	0.021	0.029	0.025	0.036	0.028	0.033	0.030	0.029	0.032
d_{IN}	Hop success probability									
10	0.000	0.000	0.000	0.000	0.000	0.000	0.000	0.000	0.000	0.000
25	0.000	0.004	0.007	0.008	0.011	0.014	0.015	0.016	0.018	0.020
50	0.001	0.010	0.015	0.016	0.016	0.016	0.014	0.013	0.012	0.010

Table 8.1: K-S statistics when comparing the results of the model analysis with the results of the model simulation, calculated using Eq. (8.34). Analytical results beyond the third hop are approximations.

Distance	100	200	300	400	500	600
d_{IN}	Required number of hops					
10	0.043	0.027	0.024	0.031	0.041	0.039
25	0.017	0.011	0.022	0.030	0.041	0.049
50	0.010	0.007	0.020	0.024	0.028	0.024
d_{IN}	End-to-end delay					
10	0.043	0.050	0.044	0.044	0.053	0.054
25	0.025	0.030	0.035	0.039	0.049	0.053
50	0.010	0.020	0.026	0.027	0.029	0.024

Table 8.2: K-S statistics when comparing the results of the model analysis with the results of the model simulation, calculated using Eq. (8.34). Distances are in meters. Analytical results are exact.

8.6 Conclusions

In this chapter we have analytically modelled a multi-hop broadcast protocol that uses distance-based forwarding delays, such as is done in the CBF protocol. Our analysis is able to express the performance of the forwarding protocol in analytical expressions that allow for easy and fast evaluation of the protocol's performance, and that provide for an increased insight in the protocol's behaviour. For a given node density and a given source-to-sink distance the model is able to capture the full distribution of *(i)* the length of each hop, *(ii)* the delay of each hop, *(iii)* the success probability of each hop, *(iv)* the position of each forwarder, *(v)* the required number of hops to have the message delivered to the sink, and *(vi)* the end-to-end delay to have the message delivered to the sink.

Verification of the analysis by means of extensive simulations showed that the accuracy of our model analysis is very high, with results of end-to-end metrics staying within 0.05 and per-hop metrics (such as the position of a forwarder) staying within 0.01-0.11 for up to 10 hops, depending on the metric and the node density. Results become more accurate as the node density decreases. We have furthermore shown that the end-to-end delay has a multi-modal distribution, with each mode corresponding to a specific hop in which the sink may first receive the message.

The distributions of the hop length, the position of a forwarder, the hop delay, and the hop success probability, are given for any hop. The two end-to-end metrics – the required number of hops and the end-to-end delay to have the message delivered – are calculated for a given number of times n that a message is transmitted. Currently, the complexity of calculating the end-to-end metrics increases exponentially with each hop, and calculating these metrics is therefore infeasible for a large number of retransmissions. In future work we plan to approximate end-to-end metrics such that they can be obtained for an arbitrary number of hops.

The granularity of our analysis is determined by parameter R, which determines the number of intervals into which the maximum transmission range of a node is broken down. Calculating end-to-end metrics for n transmissions has a complexity of $R^{(n-1)}$. A finer granularity (i.e., a larger R) will give more accurate results, whereas a more coarse granularity will keep the computation time low. For our verification we used $R = 60$, which allowed us to calculate end-to-end metrics for up to six hops ($n = 6$) with a high accuracy (as stated above) and in a short amount of time. Calculations using our analytical model took less than 9 minutes, whereas simulating the same scenario took more than a day for the high-density scenario on a cluster of 10 compute nodes with dual Intel E5335 CPUs and 24GB RAM. Using our analytical model we can thus determine the behaviour of the CBF protocol with high accuracy in only a fraction of the time required when simulating the protocol.

Part IV

Conclusion


CONSTANTINOPLE

CHAPTER 9

Concluding remarks

We conclude this thesis by giving a short summary of our contributions, answering the research questions posed in the first chapter, and giving an outlook on future directions of research.

The first part of this thesis has given an introduction to the subject of vehicular networks and an overview of current technologies regarding location-based forwarding in such networks, such as georouting.

In the second part we focused on georouting of ITS application data in a vehicular network. We have shown that existing georouting solutions are often unable to properly distinguish nodes that should receive certain ITS data (i.e., destination nodes) from other nodes. The reason for this inefficiency is the fact that with standard georouting nodes are distinguished based on their current position only, a method which poorly meets the requirements of a typical ITS scenario where a node's trajectory from its current position onward is important. To overcome this problem we have proposed and implemented a novel georouting method called constrained geocast, in which nodes are distinguished based on their future position. The future position of a node is conjectured based on its current position, heading, and speed. In this way it is possible to distinguish destination nodes that are expected to be at a specific event location in the near future, and ignore other nodes. Such a method better suits the requirements of a typical ITS application. It also answers our first research question: *How can we distinguish destination nodes that require certain ITS application data from other nodes?*

Having distinguished which nodes are the destination nodes, we have then defined a set of generic forwarding rules for constrained geocast: messages regarding some event are forwarded from the event area outward, in an upstream direction against any flows of traffic that lead to the event area. We have verified these rules by means of a simulation study for a small-scale scenario, in which there was a single flow of traffic. Our results showed that it was possible to route messages in an effective manner based on the conjectured future position of a node. We also found that in such a small-scale scenario the gain in efficiency is little to none when comparing constrained geocast with existing georouting solutions. This is mainly due to the fact that in such a scenario destination nodes can relatively accurately be distinguished from other nodes based on their current position alone, making existing georouting solutions quite efficient already. Based on the insight gained from our study however we expect that in a larger-scale scenario, in which the position of a destination node

Image on previous page: red lights at an intersection in Enschede.

is much less certain, constrained geocast will be considerably more efficient than existing georouting solutions. In future research we therefore suggest to investigate the performance of constrained geocast for such large-scale scenarios. We have thus partially answered our second research question: *How can we route the ITS application data both effectively (to as many destination nodes as possible) and efficiently (to as few non-destination nodes as possible)?*

The main motivation of our work on constrained geocast has been to increase the scalability of vehicular networks. It is expected that deployment of the first commercial vehicular networks will start in the next few years. The potential scale of these networks is enormous, and a wide range of ITS applications has already been proposed in literature. Once these networks have been deployed, situations may occur that were unforeseen and untested, in particular regarding scalability. We argue therefore that extreme care should be taken in the deployment phase with regard to the introduction of (communication-based) ITS applications, initially only deploying a limited set of safety applications. Moreover, for individual ITS applications the number of message transmissions should be reduced as much as possible, as aimed for by the proposed constrained geocast concept.

The third part of this thesis focused on analytically modelling multi-hop forwarding in a vehicular network. Existing studies typically employ overly-simplified assumptions and give only a limited level of understanding of the system, with little details regarding system performance. We have therefore performed a detailed study on the behaviour of three multi-hop forwarding protocols, deriving analytical expressions that allow for easy and fast evaluation of a protocol's performance. We consider a scenario in which nodes are spread out over a straight road, with the source and sink positioned at either end, and a message is forwarded from source to sink by intermediate forwarders. The probability of a successful single-hop transmission is modelled as a function of the distance between sender and receiver, an abstraction that is typically used to capture the behaviour of single-hop transmissions in a realistic manner. The progress of a message as it is being forwarded from source to sink is then modelled as a stochastic process according to the rules of the forwarding protocol. Because the complexity of our analysis grows exponentially with each hop, we have also included approximations to describe the behaviour of the forwarding protocol for a large number of hops. The protocols differ in their forwarding delays: the first protocol uses uniformly distributed forwarding delays, similar to how messages are piggybacked on so-called beacons. The second uses exponentially distributed forwarding delays, and the forwarding delay of the third protocol depends on a forwarder's distance to the previous sender, similar to the recently standardised CBF protocol. In our investigations regarding the first protocol some simplifications have been assumed regarding the network parameters (i.e., inter-nodes distances and the transmission range are both fixed), but all protocol parameters have been modelled with a very high level of detail. For the second and third protocol this high level of detail has been applied both to the network parameters and the protocol parameters. This represents the outcome of our third research question: *How can we express the behaviour of a multi-hop location-based forwarding protocol in a vehicular network in an analytical manner, using realistic assumptions that fully capture the behaviour of the protocol and the network?*

In our analyses we take into account the full distribution of each hop metric, instead of assuming average values as is commonly done. For a given node density and a given source-to-sink distance our analytical models therefore capture the full probability distribution of *(i)* the length of each hop, *(ii)* the delay of each hop, *(iii)* the success probability of each hop, *(iv)* the position of each forwarder, *(v)* the required number of hops to have the message delivered, and *(vi)* the end-to-end delay to have the message delivered. The accuracy of the analytical results has been verified by means of simulation for all performance metrics and was shown to be very high. This answers our fourth and final research question: *How can we express performance of a multi-hop location-based forwarding protocol in more detail?*

Our analytical models are effective tools to study and compare the performance of the considered multi-hop forwarding protocols. For example, by comparing the performance of the second and third protocol, which have been evaluated in similar scenarios, we have quantified the benefit of using distance-based forwarding delays over exponentially distributed forwarding delays. Results clearly show that fewer hops are needed to cover the source-to-sink distance when forwarding delays are distance-based because of the increased length of each hop, leading to lower end-to-end delays. However, depending on the scenario, this increase in hop length may come at the cost of a lowered end-to-end reception probability: the additional hops needed when forwarding delays are exponentially distributed make sure that more intermediate nodes will receive it, ensuring a higher level of reliability.

Due to their high level of detail our analytical models also provide great insight into the behaviour of the protocols, and show how performance is affected by changing network and protocol parameters. We have shown for instance that how the distribution of the length of a hop is influenced by the length of the previous hop(s). When forwarding delays are distance-based the effect is almost non-existent and can be ignored, but for other forwarding protocols this effect has a significant impact on performance, especially in low-density traffic scenarios. It was furthermore shown that when traffic is free flowing the distribution of the hop length changes for the first few hops, with hops becoming increasingly longer, after which the distribution converges. Again this effect is strongest in low-density traffic scenarios.

Compared to existing simulation models our analytical models allow for very fast evaluation of a forwarding scenario, decreasing the computation time from hours (or even days) to minutes. By using our analytical models to emulate the (computationally highly demanding) communication layer of in simulation models, the simulation of higher-level ITS application scenarios will therefore be speeded up considerably.

Currently our analytical models consider a forwarding scenario in which a message is forwarded over a straight road with free-flowing traffic, and single-hop transmissions have been modelled taking signal attenuation into account, but ignoring shadowing or the effect of hidden nodes. In future research we suggest to investigate more elaborate traffic scenarios, and to expand our single-hop transmission model to include these latter transmission effects. Once these effects have been included, and using similar modelling techniques such as presented in this thesis, analysing the performance of a multi-hop forwarding protocol can be done along the lines presented in this thesis. We expect that in the future, as understanding of (multi-hop) forwarding in vehicular networks grows, more and more analytical models such as our own will be developed and may be used to replace existing simulation models, thus further speeding up the simulation of higher-level ITS application scenarios.

Although we have performed our analytical work in the context of a vehicular network, all three analytical models and their findings can be applied to similar CSMA-based networks, such as for instance wireless sensor networks [110].

In conclusion, the results of this thesis improve the efficiency and understanding of location-based forwarding in vehicular networks. The insights provided by our work can be used to increase the effectiveness of vehicular communication protocols and in this way advance the overall performance of ITS applications.

APPENDIX A

Derivations of some intermediate results used in chapter 7

This appendix is meant to support Chapter 7. We provide a number of proofs regarding first-hop calculations. First we re-introduce some of our notation however.

Let V_i be the number of nodes in interval i. C_1 denotes the total number of candidate first forwarders, $C_{1,i}$ denotes the number of candidate first forwarders in interval i, and $C_{1,j:k}$ denotes the total number of candidate first forwarders in intervals j through k. Furthermore, let $H_{1,i}$ be the number of candidate first forwarders in i, excluding the candidate forwarder that became the first forwarder, and let $G_{1,i}$ be the number of first forwarders in interval i, such that $C_{1,i} = H_{1,i}+G_{1,i}$. The position of the first forwarder is denoted F_1. Finally, S_i denotes the probability that a receiver successfully receives a message transmitted by a sender that is located i intervals away.

A.1 Calculating $\mathbb{E}(\frac{C_{1,i}}{C_1} \mid C_1 > 0)$

We prove that $\mathbb{E}(\frac{C_{1,i}}{C_1} \mid C_1 > 0) = \frac{\mathbb{E}(C_{1,i})}{\mathbb{E}(C_1)}$. Let X substitute $C_{1,i}$ and let Y be $C_1 - C_{1,i}$; X and Y are independent. X is Poisson distributed with mean $\lambda_i = S_i\mathbb{E}(V_i)$ and Y is Poisson distributed with mean $\mu = \sum_{\substack{j=1\\j\neq i}}^{R} S_j\mathbb{E}(V_j)$. Then

$$\begin{aligned}
\mathbb{E}(\frac{C_{1,i}}{C_1} \mid C_1 > 0) &= \sum_{k=0}^{\infty}\sum_{j=0}^{\infty}\frac{k}{k+j}\cdot\mathbb{P}(X = k \wedge Y = j \mid X+Y > 0)\\
&= \sum_{k=0}^{\infty}\sum_{j=0}^{\infty}\frac{k}{k+j}\cdot\frac{\mathbb{P}(X = k \wedge Y = j \wedge X+Y > 0)}{\mathbb{P}(X+Y>0)}\\
&= \frac{1}{\mathbb{P}(X+Y>0)}\cdot\sum_{k=0}^{\infty}\sum_{j=0}^{\infty}\frac{k}{k+j}\cdot\mathbb{P}(X = k \wedge Y = j \wedge X+Y > 0)\\
&= \frac{1}{\mathbb{P}(X+Y>0)}\cdot\sum_{k=1}^{\infty}\sum_{j=0}^{\infty}\frac{k}{k+j}\cdot\mathbb{P}(X = k \wedge Y = j)\\
&= \frac{1}{1-e^{-(\lambda_i+\mu)}}\cdot\sum_{k=1}^{\infty}\sum_{j=0}^{\infty}\frac{k}{k+j}\cdot\frac{\lambda_i^k}{k!}e^{-\lambda_i}\cdot\frac{\mu^j}{j!}e^{-\mu}
\end{aligned}$$

$$= \frac{\lambda_i e^{-\lambda_i} e^{-\mu}}{1 - e^{-(\lambda_i + \mu)}} \cdot \sum_{k=1}^{\infty} \sum_{j=0}^{\infty} \frac{1}{k+j} \cdot \frac{\lambda_i^{k-1}}{(k-1)!} \cdot \frac{\mu^j}{j!}$$

$$= \frac{\lambda_i e^{-\lambda_i} e^{-\mu}}{1 - e^{-(\lambda_i + \mu)}} \cdot \sum_{k=0}^{\infty} \sum_{j=0}^{\infty} \frac{1}{k+j+1} \cdot \frac{\lambda_i^{k}}{k!} \cdot \frac{\mu^j}{j!}$$

$$= \frac{\lambda_i \mathbb{E}(\frac{1}{X+Y+1})}{1 - e^{-(\lambda_i + \mu)}} \tag{A.1}$$

According to [111] (see Eq. (32) for $Q = X + Y, a = 1$), as $X + Y$ is Poisson distributed with mean $\lambda_i + \mu$, the term $\mathbb{E}(\frac{1}{X+Y+1})$ is equal to $\frac{1-e^{-(\lambda_i+\mu)}}{\lambda_i+\mu}$. So we get

$$\mathbb{E}(\frac{C_{1,i}}{C_1} \mid C_1 > 0) = \frac{\lambda_i}{\lambda_i + \mu}$$

$$= \frac{\mathbb{E}(C_{1,i})}{\mathbb{E}(C_1)}, \quad i = 1, 2, \ldots, R. \tag{A.2}$$

A.2 Calculating $\mathbb{E}(H_{1,i} \mid F_1 = j)$

We show how to calculate $\mathbb{E}(H_{1,i} \mid F_1 = j)$. We first condition on the number of candidate first forwarders, given that the first forwarder is in interval j:

$$\mathbb{E}(H_{1,i} \mid F_1 = j) = \sum_{c_1=1}^{R} \mathbb{P}(C_1 = c_1 \mid F_1 = j)\, \mathbb{E}(H_{1,i} \mid F_1 = j \wedge C_1 = c_1),$$
$$i = 1, 2, \ldots, R, \quad j = 1, 2, \ldots, R. \tag{A.3}$$

In the next two subsections we show how to calculate $\mathbb{P}(C_1 = c_1 \mid F_1 = j)$ and $\mathbb{E}(H_{1,i} \mid F_1 = j \wedge C_1 = c_1)$ respectively.

A.2.1 $\mathbb{P}(C_1 = c_1 \mid F_1 = j)$

Following the rules of conditional probability $\mathbb{P}(C_1 = c_1 \mid F_1 = j)$ is given by

$$\mathbb{P}(C_1 = c_1 \mid F_1 = j) = \mathbb{P}(C_1 = c_1)\, \frac{\mathbb{P}(F_1 = j \mid C_1 = c_1)}{\mathbb{P}(F_1 = j)}, \quad i = 1, \ldots, R, \tag{A.4}$$

with C_1 being Poisson distributed with its mean given by Eq. (7.6) and $\mathbb{P}(F_1 = i)$ given by Eq. (7.14). $\mathbb{P}(F_1 = i \mid C_1 = c_1)$ is calculated in a manner similar to Eq. (7.13), given that there are exactly c_1 first-hop candidate forwarders:

$$\mathbb{P}(F_1 = i \mid C_1 = c_1) = \mathbb{E}\Big(\frac{C_{1,i}}{C_1} \mid C_1 = c_1\Big), \quad i = 1, 2, \ldots, R. \tag{A.5}$$

$\mathbb{E}\Big(\frac{C_{1,i}}{C_1} \mid C_1 = c_1\Big)$ is calculated as follows. C_1 is Poisson distributed with mean $\sum_{j=1}^{R} S_j \cdot \mathbb{E}(V_j)$, $C_{1,i}$ is Poisson distributed with mean $S_i \cdot \mathbb{E}(V_i)$, and the number of candidate first forwarders in the remaining $R-1$ intervals is Poisson distributed with mean $\sum_{\substack{j=1\\j\neq i}}^{R} S_j \cdot \mathbb{E}(V_j)$. For readability we substitute λ for $\sum_{j=1}^{R} S_j \cdot \mathbb{E}(V_j)$ and λ_i for $S_i \cdot \mathbb{E}(V_i)$. We can then write

$$\begin{aligned}
\mathbb{E}\Big(\frac{C_{1,i}}{C_1} \mid C_1 = c_1\Big) &= \frac{1}{\mathbb{P}(C_1 = c_1)} \sum_{c_{1,i}=0}^{c_1} \frac{c_{1,i}}{c_1} \cdot \mathbb{P}(C_{1,i} = c_{1,i}) \cdot \mathbb{P}(C_1 - C_{1,i} = c_1 - c_{1,i}), \\
&= \frac{1}{\frac{\lambda^{c_1}}{c_1!}e^{-\lambda}} \sum_{c_{1,i}=0}^{c_1} \frac{c_{1,i}}{c_1} \cdot \frac{\lambda_i^{c_{1,i}}}{c_{1,i}!} e^{-\lambda_i} \cdot \frac{(\lambda-\lambda_i)^{c_1-c_{1,i}}}{(c_1-c_{1,i})!} e^{\lambda-\lambda_i}, \\
&= \frac{c_1!}{\lambda^{c_1}} \sum_{c_{1,i}=0}^{c_1} \frac{c_{1,i}}{c_1} \cdot \frac{\lambda_i^{c_{1,i}}}{c_{1,i}!} \cdot \frac{(\lambda-\lambda_i)^{c_1-c_{1,i}}}{(c_1-c_{1,i})!}, \\
&= \frac{1}{c_1 \cdot \lambda^{c_1}} \sum_{c_{1,i}=1}^{c_1} \frac{c_1!}{(c_{1,i}-1)!(c_1-c_{1,i})!} \lambda_i^{c_{1,i}} (\lambda-\lambda_i)^{c_1-c_{1,i}}, \\
&= \frac{\lambda_i}{c_1 \cdot \lambda^{c_1}} \sum_{c_{1,i}=0}^{c_1-1} \frac{c_1!}{c_{1,i}!(c_1-c_{1,i}-1)!} \lambda_i^{c_{1,i}} (\lambda-\lambda_i)^{c_1-c_{1,i}-1}, \\
&= \frac{\lambda_i}{\lambda^{c_1}} \sum_{c_{1,i}=0}^{c_1-1} \binom{c_1-1}{c_{1,i}} \lambda_i^{c_{1,i}} (\lambda-\lambda_i)^{c_1-c_{1,i}-1}. \qquad \text{(A.6)}
\end{aligned}$$

Using $(a+b)^n = \sum_{j=0}^{n} a^j b^{n-j} \binom{n}{j}$, we can state

$$\begin{aligned}
\mathbb{E}\Big(\frac{C_{1,i}}{C_1} \mid C_1 = c_1\Big) &= \frac{\lambda_i}{\lambda}, \\
&= \frac{\mathbb{E}(C_{1,i})}{\mathbb{E}(C_1)}. \qquad \text{(A.7)}
\end{aligned}$$

A.2.2 $\mathbb{E}(H_{1,i} \mid F_1 = j \wedge C_1 = c_1)$

To calculate $\mathbb{E}(H_{1,i} \mid F_1 = j \wedge C_1 = c_1)$ we condition on the number of first-hop candidate forwarders in interval i, given that the first forwarder is positioned in interval j and there are exactly c_1 first-hop candidate forwarders:

$$\begin{aligned}
&\mathbb{E}(H_{1,i} \mid F_1 = j \wedge C_1 = c_1) = \\
&\sum_{c_{1,i}=0}^{c_1} \mathbb{P}(C_{1,i} = c_{1,i} \mid F_1 = j \wedge C_1 = c_1) \cdot \mathbb{E}(H_{1,i} \mid F_1 = j \wedge C_{1,i} = c_{1,i} \wedge C_1 = c_1), \\
&\sum_{c_{1,i}=1}^{c_1} \mathbb{P}(C_{1,i} = c_{1,i} \mid F_1 = j \wedge C_1 = c_1) \cdot \mathbb{E}(H_{1,i} \mid F_1 = j \wedge C_{1,i} = c_{1,i}), \\
&i = 1, 2, \ldots, R, \quad j = 1, 2, \ldots, R. \qquad \text{(A.8)}
\end{aligned}$$

It should be clear that $\mathbb{E}(H_{1,i} \mid F_1 = j \wedge C_{1,i} = c_{1,i}) = c_{1,i}$ for $i \neq j$ and $\mathbb{E}(H_{1,i} \mid F_1 = j \wedge C_{1,i} = c_{1,i}) = c_{1,i} - 1$ for $i = j$. We therefore only have to determine $\mathbb{P}(C_{1,i} = c_{1,i} \mid F_1 = j \wedge C_1 = c_1)$ which we do below.

Using the rules of conditional probability $\mathbb{P}(C_{1,i} = c_{1,i} \mid F_1 = j \wedge C_1 = c_1)$ can be rewritten as

$$\begin{aligned}&\mathbb{P}(C_{1,i} = c_{1,i} \mid C_1 = c_1 \wedge F_1 = j) = \\ &\mathbb{P}(C_1 = c_1 \wedge F_1 = j \mid C_{1,i} = c_{1,i}) \cdot \frac{\mathbb{P}(C_{1,i} = c_{1,i})}{\mathbb{P}(F_1 = j \wedge C_1 = c_1)}, \\ &i = 1, 2, \ldots, R, \quad j = 1, 2, \ldots, R,\end{aligned} \tag{A.9}$$

with $C_{1,i}$ being Poisson distributed with mean $S_i \cdot \mathbb{E}(V_i)$. We determine $\mathbb{P}(F_1 = j \wedge C_1 = c_1)$ and $\mathbb{P}(C_1 = c_1 \wedge F_1 = j \mid C_{1,i} = c_{1,i})$ below.

$\mathbb{P}(F_1 = j \wedge C_1 = c_1)$ is given by

$$\mathbb{P}(F_1 = j \wedge C_1 = c_1) = \mathbb{P}(F_1 = j \mid C_1 = c_1) \cdot \mathbb{P}(C_1 = c_1), \quad i = 1, 2, \ldots, R, \tag{A.10}$$

with both right-hand terms known.

$\mathbb{P}(C_1 = c_1 \wedge F_1 = j \mid C_{1,i} = c_{1,i})$ can be written as

$$\begin{aligned}&\mathbb{P}(F_1 = j \wedge C_1 = c_1 \mid C_{1,i} = c_{1,i}) = \\ &\mathbb{P}(F_1 = j \mid C_1 = c_1 \wedge C_{1,i} = c_{1,i}) \cdot \mathbb{P}(C_1 = c_1 \mid C_{1,i} = c_{1,i}), \\ &i = 1, 2, \ldots, R, \quad j = 1, 2, \ldots, R.\end{aligned} \tag{A.11}$$

Below we first determine $\mathbb{P}(C_1 = c_1 \mid C_{1,j} = c_{1,j})$ and then $\mathbb{P}(F_1 = i \mid C_1 = c_1 \wedge C_{1,j} = c_{1,j})$.

$\mathbb{P}(C_1 = c_1 \mid C_{1,i} = c_{1,i})$ is equal to the probability of having exactly $c_1 - c_{1,i}$ first-hop candidate forwarders in the $R - 1$ intervals excluding interval i. Using the notation Substituting $\lambda = \sum_{j=1}^{R} S_j \cdot \mathbb{E}(V_j)$ and $\lambda_i = S_i \cdot \mathbb{E}(V_i)$, we have

$$\mathbb{P}(C_1 = c_1 \mid C_{1,i} = c_{1,i}) = \frac{(\lambda - \lambda_i)^{(c_1 - c_{1,i})}}{(c_1 - c_{1,i})!} e^{-(\lambda - \lambda_i)}, \quad i = 1, 2, \ldots, R. \tag{A.12}$$

$\mathbb{P}(F_1 = i \mid C_1 = c_1 \wedge C_{1,j} = c_{1,j})$ can be calculated by conditioning on the number of candidate first forwarders in interval i:

$$\begin{aligned}&\mathbb{P}(F_1 = i \mid C_1 = c_1 \wedge C_{1,j} = c_{1,j}) = \\ &\sum_{c_{1,i}=1}^{c_1 - c_{1,j}} \mathbb{P}(C_{1,i} = c_{1,i} \mid C_1 = c_1 \wedge C_{1,j} = c_{1,j}) \cdot \\ &\mathbb{P}(F_1 = i \mid C_1 = c_1 \wedge C_{1,i} = c_{1,i} \wedge C_{1,j} = c_{1,j}), \quad i = 1, 2, \ldots, R,\end{aligned} \tag{A.13}$$

We determine both right hand side terms below.

Since the probability of becoming the next forwarder is equal for all candidate forwarders $\mathbb{P}(F_1 = i \mid C_1 = c_1 \wedge C_{1,i} = c_{1,i} \wedge C_{1,j} = c_{1,j})$ is obtained by dividing the number of first-hop candidate forwarders in interval i by the total number of first-hop candidate forwarders:

$$\mathbb{P}(F_1 = i \mid C_1 = c_1 \wedge C_{1,i} = c_{1,i} \wedge C_{1,j} = c_{1,j}) = \frac{c_{1,i}}{c_1},$$
$$i = 1, 2, \ldots, R, \quad j = 1, 2, \ldots, R. \tag{A.14}$$

Using the notation $\lambda = \sum_{j=1}^{R} S_j \cdot \mathbb{E}(V_j)$, $\lambda_i = S_i \cdot \mathbb{E}(V_i)$, and $\lambda_j = S_j \cdot \mathbb{E}(V_j)$, the other term in the right hand side of Eq. (A.13) is given by

$$\begin{aligned}\mathbb{P}(C_{1,i} = c_{1,i} \mid C_1 = c_1 \wedge C_{1,j} = c_{1,j}) &= \frac{\mathbb{P}(C_{1,i} = c_{1,i})}{\mathbb{P}(C_1 - C_{1,j} = c_1 - c_{1,j})} \cdot \\ &\quad \mathbb{P}(C_1 - C_{1,i} - C_{1,j} = c_1 - c_{1,i} - c_{1,i}), \\ &= \frac{\frac{\lambda_i^{c_{1,i}}}{c_{1,i}!} e^{-\lambda_i} \frac{(\lambda-\lambda_i-\lambda_j)^{c_1-c_{1,i}-c_{1,j}}}{(c_1-c_{1,i}-c_{1,j})!} e^{-(\lambda-\lambda_i-\lambda_j)}}{\frac{(\lambda-\lambda_j)^{c_1-c_{1,j}}}{(c_1-c_{1,j})!} e^{-(\lambda-\lambda_j)}}, \\ i = 1, 2, \ldots, R, &\quad j = 1, 2, \ldots, R. \end{aligned} \tag{A.15}$$

A.3 Proof for $\mathbb{E}(H_{1,i} \mid F_1 = j) = \mathbb{E}(H_{1,i} \mid C_1 > 0)$

We prove Eq. (7.20) in case of an ideal transmission model, i.e., $S_i = 1$ for $i = 1, 2, \ldots, R$ and $S_i = 0$ otherwise.

Proof. We write out $\mathbb{E}(H_{1,i} \mid C_1 > 0)$ and $\mathbb{E}(H_{1,i} \mid F_1 = j)$ in full in the next two subsections and show that they are equal.

A.3.1 $\mathbb{E}(H_{1,i} \mid C_1 > 0)$

Assuming the ideal transmission model and substituting $\mathbb{E}(V_i)$ by λ, writing out $\mathbb{E}(H_{1,i} \mid C_1 > 0)$ in full gives

$$\begin{aligned}\mathbb{E}(H_{1,i} \mid C_1 > 0) &= \mathbb{E}(C_{1,i} \mid C_1 > 0) - \mathbb{E}(G_{1,i} \mid C_1 > 0) \\ &= \frac{\mathbb{E}(C_{1,i})}{1 - \mathbb{P}(C_1 = 0)} - \mathbb{P}(F_1 = i \mid C_1 > 0) \\ &= \frac{\lambda}{1 - e^{-R\lambda}} - \frac{\mathbb{E}(C_{1,i} \mid C_1 > 0)}{\mathbb{E}(C_1 \mid C_1 > 0)} \\ &= \frac{\lambda}{1 - e^{-R\lambda}} - \frac{\lambda}{R\lambda} \\ &= \frac{\lambda}{1 - e^{-R\lambda}} - \frac{1}{R}, \quad i = 1, 2, \ldots, R, \end{aligned} \tag{A.16}$$

with $\mathbb{E}(H_{1,i} \mid C_1 > 0) = 0$ for $i < 0$ and $\mathbb{E}(H_{1,i} \mid C_1 > 0) = 0$ for $i > R$.

A.3.2 $\mathbb{E}(H_{1,i} \mid F_1 = j)$

Writing out $\mathbb{E}(H_{1,i} \mid F_1 = j)$ in full gives

$$\mathbb{E}(H_{1,i} \mid F_1 = j) = \sum_{c_1=1}^{\infty} \Bigg(\mathbb{P}(C_1 = c_1 \mid F_1 = j)\ \mathbb{E}(H_{1,i} \mid F_1 = j \wedge C_1 = c_1) \Bigg)$$
$$= \sum_{c_1=1}^{\infty} \Bigg(\mathbb{P}(C_1 = c_1)\ \frac{\mathbb{P}(F_1 = j \mid C_1 = c_1)}{\mathbb{P}(F_1 = j)}\ \mathbb{E}(H_{1,i} \mid F_1 = j \wedge C_1 = c_1) \Bigg)$$
$$= \sum_{c_1=1}^{\infty} \Bigg(\mathbb{P}(C_1 = c_1)\ \frac{\mathbb{E}(\frac{C_{1,j}}{C_1} \mid C_1 > 0)}{\mathbb{P}(C_1 > 0) \cdot \mathbb{E}(\frac{C_{1,j}}{C_1})} \cdot$$
$$\sum_{c_{1,i}=0}^{c_1} \Bigg(\mathbb{P}(C_{1,i} = c_{1,i} \mid F_1 = j \wedge C_1 = c_1)\ \mathbb{E}(H_i \mid F_1 = j \wedge C_{1,i} = c_{1,i} \wedge C_1 = c_1) \Bigg) \Bigg). \tag{A.17}$$

Since $\mathbb{E}(\frac{C_{1,i}}{C_1} \mid C_1 > 0) = \mathbb{E}(\frac{C_{1,i}}{C_1})$ and
$\mathbb{E}(H_i \mid F_1 = j \wedge C_{1,i} = c_{1,i} \wedge C_1 = c_1) = \mathbb{E}(H_i \mid F_1 = j \wedge C_{1,i} = c_{1,i})$, and summing over $c_{1,i}$, we can write

$$\mathbb{E}(H_{1,i} \mid F_1 = j) = \sum_{c_1=1}^{\infty} \Bigg(\frac{\mathbb{P}(C_1 = c_1)}{\mathbb{P}(C_1 > 0)} \cdot$$
$$\sum_{c_{1,i}=1}^{c_1} \Bigg(\mathbb{P}(C_1 = c_1 \wedge F_1 = j \mid C_{1,i} = c_{1,i})\ \frac{\mathbb{P}(C_{1,i} = c_{1,i})}{\mathbb{P}(F_1 = j \wedge C_1 = c_1)} \cdot$$
$$\mathbb{E}(H_i \mid F_1 = j \wedge C_{1,i} = c_{1,i}) \Bigg) \Bigg)$$
$$= \sum_{c_1=1}^{\infty} \Bigg(\frac{\mathbb{P}(C_1 = c_1)}{\mathbb{P}(C_1 > 0)} \cdot$$
$$\sum_{c_{1,i}=1}^{c_1} \Bigg(\mathbb{P}(F_1 = j \mid C_1 = c_1 \wedge C_{1,i} = c_{1,i})\ \mathbb{P}(C_1 = c_1 \mid C_{1,i} = c_{1,i}) \cdot$$
$$\frac{\mathbb{P}(C_{1,i} = c_{1,i})}{\mathbb{P}(F_1 = j \mid C_1 = c_1)\ \mathbb{P}(C_1 = c_1)}\ \mathbb{E}(H_i \mid F_1 = j \wedge C_{1,i} = c_{1,i}) \Bigg) \Bigg)$$
$$= \sum_{c_1=1}^{\infty} \Bigg(\frac{\mathbb{P}(C_1 = c_1)}{\mathbb{P}(C_1 > 0)} \cdot$$
$$\sum_{c_{1,i}=1}^{c_1} \Bigg(\sum_{c_{1,j}=1}^{c_1 - c_{1,i}} \Bigg(\mathbb{P}(C_{1,j} = c_{1,j} \mid C_1 = c_1 \wedge C_{1,i} = c_{1,i}) \cdot$$

$$\mathbb{P}(F_1 = j \mid C_1 = c_1 \wedge C_{1,j} = c_{1,j} \wedge C_{1,i} = c_{1,i})\Big) \, \mathbb{P}(C_1 = c_1 \mid C_{1,i} = c_{1,i}) \cdot$$
$$\frac{\mathbb{P}(C_{1,i} = c_{1,i})}{\mathbb{P}(F_1 = j \mid C_1 = c_1)\,\mathbb{P}(C_1 = c_1)} \, \mathbb{E}(H_i \mid F_1 = j \wedge C_{1,i} = c_{1,i})\Big)\Big)$$
$$= \sum_{c_1=1}^{\infty} \Bigg(\frac{\mathbb{P}(C_1 = c_1)}{\mathbb{P}(C_1 > 0)\mathbb{P}(C_1 = c_1)} \cdot$$
$$\sum_{c_{1,i}=1}^{c_1} \Bigg(\sum_{c_{1,j}=1}^{c_1 - c_{1,i}} \Bigg(\mathbb{P}(C_{1,j} = c_{1,j} \mid C_1 = c_1 \wedge C_{1,i} = c_{1,i}) \cdot \frac{c_{1,j}}{c_1} \Bigg) \cdot$$
$$\mathbb{P}(C_1 = c_1 \mid C_{1,i} = c_{1,i}) \cdot \frac{\mathbb{P}(C_{1,i} = c_{1,i})}{\mathbb{P}(F_1 = j \mid C_1 = c_1)\,\mathbb{P}(C_1 = c_1)} \cdot$$
$$\mathbb{E}(H_{1,i} \mid F_1 = j \wedge C_{1,i} = c_{1,i})\Bigg)\Bigg),$$
$$i = 1, 2, \ldots, R, \quad j = 1, 2, \ldots, R. \tag{A.18}$$

Assuming the ideal transmission model, substituting $\mathbb{E}(V_{1,i})$ by λ, using the relation $\mathbb{E}(H_{1,i} \mid F_1 = j \wedge C_{1,i} = c_{1,i}) = c_{1,i}$ for $i \neq j$ and (for now) ignoring the case $i = j$, the equation above can be rewritten as follows

$$\mathbb{E}(H_{1,i} \mid F_1 = j) = \sum_{c_1=1}^{\infty} \Bigg(\frac{\mathbb{P}(C_1 = c_1)}{\mathbb{P}(C_1 > 0)} \cdot$$
$$\sum_{c_{1,i}=1}^{c_1} \Bigg(\sum_{c_{1,j}=1}^{c_1 - c_{1,i}} \Bigg(\mathbb{P}(C_{1,j} = c_{1,j} \mid C_1 = c_1 \wedge C_{1,i} = c_{1,i}) \cdot \frac{c_{1,j}}{c_1} \Bigg) \cdot$$
$$\mathbb{P}(C_1 = c_1 \mid C_{1,i} = c_{1,i}) \, \frac{\mathbb{P}(C_{1,i} = c_{1,i})}{\mathbb{P}(F_1 = j \mid C_1 = c_1)\,\mathbb{P}(C_1 = c_1)} \, c_{1,i}\Bigg)\Bigg)$$
$$= \sum_{c_1=1}^{\infty} \Bigg(\frac{\frac{(R\lambda)^{c_1}}{c_1!} e^{-R\lambda}}{1 - e^{-R\lambda}} \cdot$$
$$\sum_{c_{1,i}=1}^{c_1} \Bigg(\sum_{c_{1,j}=1}^{c_1 - c_{1,i}} \Bigg(\frac{\frac{\lambda^{c_{1,j}}}{c_{1,j}!} e^{-\lambda} \cdot \frac{(R-2)\lambda^{c_1 - c_{1,j} - c_{1,i}}}{(c_1 - c_{1,j} - c_{1,i})!} e^{-(R-2)\lambda}}{\frac{(R-1)\lambda^{c_1 - c_{1,i}}}{(c_1 - c_{1,i})!} e^{-(R-1)\lambda}} \cdot \frac{c_{1,j}}{c_1} \Bigg) \cdot$$
$$\frac{((R-1)\lambda)^{c_1 - c_{1,i}}}{(c_1 - c_{1,i})!} e^{-(R-1)\lambda} \, \frac{\frac{\lambda^{c_{1,i}}}{c_{1,i}!} e^{-\lambda}}{\frac{1}{R} \, \frac{(R\lambda)^{c_1}}{c_1!} e^{-R\lambda}} \, c_{1,i}\Bigg)\Bigg),$$
$$i = 1, 2, \ldots, R, \quad j = 1, 2, \ldots, R, \quad i \neq j. \tag{A.19}$$

Renaming c_1 to c, $c_{1,i}$ to k, and $c_{1,j}$ to n, and still assuming $i \neq j$, $\mathbb{E}(H_{1,i} \mid F_1 = j)$ can be written as

$$\mathbb{E}(H_{1,i} \mid F_1 = j) = \frac{1}{1-e^{-R\lambda}} \cdot$$
$$\sum_{c=1}^{\infty}\left(\frac{(R\lambda)^c}{c!}e^{-R\lambda}\sum_{k=1}^{c}\left(\sum_{n=1}^{c-k}\left(\frac{\frac{\lambda^n}{n!}e^{-\lambda}\frac{((R-2)\lambda)^{c-n-k}}{(c-n-k)!}e^{-(R-2)\lambda}}{\frac{((R-1)\lambda)^{c-k}}{(c-k)!}e^{-(R-1)\lambda}}\cdot\frac{n}{c}\cdot\right.\right.\right.$$
$$\left.\left.\left.\frac{((R-1)\lambda)^{c-k}}{(c-k)!}e^{-(R-1)\lambda}\cdot\frac{\frac{\lambda^k}{k!}e^{-\lambda}}{\frac{1}{R}\frac{(R\lambda)^c}{c!}e^{-R\lambda}}\cdot k\right)\right)\right)$$
$$= \frac{R}{1-e^{-R\lambda}}\sum_{c=1}^{\infty}\left(\sum_{k=1}^{c}\left(\sum_{n=1}^{c-k}\left(\frac{\lambda^n}{n!}e^{-\lambda}\cdot\frac{((R-2)\lambda)^{c-n-k}}{(c-n-k)!}e^{-(R-2)\lambda}\cdot\frac{n}{c}\cdot\frac{\lambda^k}{k!}e^{-\lambda}\cdot k\right)\right)\right),$$
$$i = 1,2,\ldots,R, \;\; j = 1,2,\ldots,R, \;\; i \neq j. \tag{A.20}$$

Rearranging summations followed by a number of substitutions gives us

$$\mathbb{E}(H_{1,i} \mid F_1 = j) =$$
$$\frac{R}{1-e^{-R\lambda}}\sum_{k=1}^{\infty}\left(\sum_{n=1}^{\infty}\left(\sum_{c=0}^{\infty}\left(\frac{\lambda^n}{n!}e^{-\lambda}\cdot\frac{((R-2)\lambda)^{c-n-k}}{(c-n-k)!}e^{-(R-2)\lambda}\cdot\frac{n}{c}\cdot\frac{\lambda^k}{k!}e^{-\lambda}\cdot k\right)\right)\right)$$
$$= \frac{R}{1-e^{-R\lambda}}\sum_{k=1}^{\infty}\left(\sum_{n=1}^{\infty}\left(\sum_{c=0}^{\infty}\left(\frac{\lambda^n}{n!}e^{-\lambda}\cdot\frac{((R-2)\lambda)^{c}}{c!}e^{-(R-2)\lambda}\cdot\frac{n}{c+k+n}\cdot\frac{\lambda^k}{k!}e^{-\lambda}\cdot k\right)\right)\right)$$
$$= \frac{\lambda^2 R}{1-e^{-R\lambda}}\sum_{k=1}^{\infty}\left(\sum_{n=1}^{\infty}\left(\sum_{c=0}^{\infty}\left(\frac{\lambda^n}{n!}e^{-\lambda}\cdot\frac{((R-2)\lambda)^{c}}{c!}e^{-(R-2)\lambda}\cdot\frac{\lambda^k}{k!}e^{-\lambda}\cdot\frac{1}{c+k+n+2}\right)\right)\right)$$
$$= \frac{\lambda^2 R}{1-e^{-R\lambda}}\mathbb{E}(\frac{1}{X+Y+Z+2}), \;\; i = 1,2,\ldots,R, \;\; j = 1,2,\ldots,R, \;\; i \neq j, \tag{A.21}$$

with X being Poisson distributed with mean λ, Y being Poisson distributed with mean λ, and Z being Poisson distributed with mean $(R-2)\lambda$. Let $Q = X + Y + Z$, then Q is Poisson distributed with mean $R\lambda$. It has been shown in [111] that

$$\mathbb{E}(\frac{1}{Q+a}) = \frac{(a-1)!(-1)^{a-1}}{\mu^a}\Big(1 - e^{-\mu}\sum_{r=1}^{a-1}\frac{(-\mu)^r}{r!}\Big), \;\; a \in \mathbb{N}^+ \tag{A.22}$$

with Q being Poisson distributed with mean μ. Thus we can state

$$\mathbb{E}(\frac{1}{X+Y+Z+2}) = \frac{R\lambda - (1-e^{-R\lambda})}{(R\lambda)^2}, \tag{A.23}$$

and

$$\begin{aligned}\mathbb{E}(H_{1,i} \mid F_1 = j) &= \frac{\lambda^2 R}{1-e^{-R\lambda}}\mathbb{E}(\frac{1}{X+Y+Z+2}) \\ &= \frac{\lambda^2 R}{1-e^{-R\lambda}} \cdot \frac{R\lambda - (1-e^{-R\lambda})}{(R\lambda)^2} \\ &= \frac{R\lambda - (1-e^{-R\lambda})}{R(1-e^{-R\lambda})} \\ &= \frac{\lambda}{1-e^{-R\lambda}} - \frac{1}{R} \\ & i = 1,2,\dots,R, \quad j = 1,2,\dots,R, \quad i \neq j. \end{aligned} \tag{A.24}$$

Hence, cf. Eq. (A.16), $\mathbb{E}(H_{1,i} \mid F_1 = j) = \mathbb{E}(H_{1,i} \mid C_1 > 0)$, which completes our proof.

A.4 Calculating the distribution of $C_{1,j+1:R} \mid F_1 = j$

Given that the first forwarder is positioned in interval j we calculate the total number of candidate first forwarders in intervals $j+1$ through R, $C_{1,j+1:R}$. Although the number of first-hop candidate forwarders in interval i is Poisson distributed, this does no longer hold when it is given that the first forwarder is positioned in interval j. We therefore give a step-by-step breakdown of how to calculate the distribution of $C_{1,j+1:R}$. We start by conditioning on the number of first-hop candidate forwarders, given that the first forwarder is positioned in interval j:

$$\begin{aligned}\mathbb{P}(C_{1,j+1:R} = c_{1,j+1:R} \mid F_1 = j) = \sum_{c_1=1}^{\infty} & \mathbb{P}(C_1 = c_1 \mid F_1 = j) \cdot \\ & \mathbb{P}(C_{1,j+1:R} = c_{1,j+1:R} \mid F_1 = j \wedge C_1 = c_1), \\ & c_{1,j+1:R} = 0,1,2,\dots, \quad j = 1,2,\dots,R, \end{aligned} \tag{A.25}$$

with $\mathbb{P}(C_1 = c_1 \mid F_1 = j)$ given by Eq. (A.4).

$\mathbb{P}(C_{1,j+1:R} = c_{1,j+1:R} \mid F_1 = j \wedge C_1 = c_1)$ can be rewritten as

$$\begin{aligned}&\mathbb{P}(C_{1,j+1:R} = c_{1,j+1:R} \mid F_1 = j \wedge C_1 = c_1) = \\ &\mathbb{P}(F_1 = j \wedge C_1 = c_1 \mid C_{1,j+1:R} = c_{1,j+1:R}) \cdot \frac{\mathbb{P}(C_{1,j+1:R} = c_{1,j+1:R})}{\mathbb{P}(F_1 = j \wedge C_1 = c_1)}, \\ &c_{1,j+1:R} = 0,1,2,\dots, \quad j = 1,2,\dots,R, \end{aligned} \tag{A.26}$$

with $\mathbb{P}(F_1 = j \wedge C_1 = c_1)$ given by Eq. (A.10). Below we show how to calculate first $\mathbb{P}(C_{1,j+1:R} = c_{1,j+1:R})$ and then $\mathbb{P}(F_1 = j \wedge C_1 = c_1 \mid C_{1,j+1:R} = c_{1,j+1:R})$.

As was already stated in the beginning of this section the number of first-hop candidate forwarders in interval i is Poisson distributed with mean $\mathbb{E}(C_{1,i})$, given by Eq. (7.5), so $\mathbb{P}(C_{1,j+1:R} = c_{1,j+1:R})$ in Eq. (A.26) is Poisson distributed with mean $\sum_{i=j+1}^{R} \mathbb{E}(C_{1,i})$.

The rest of this section focuses on calculating $\mathbb{P}(F_1 = j \wedge C_1 = c_1 \mid C_{1,j+1:R} = c_{1,j+1:R})$. We first rewrite it as

$$\mathbb{P}(F_1 = j \wedge C_1 = c_1 \mid C_{1,j+1:R} = c_{1,j+1:R}) =$$
$$\mathbb{P}(F_1 = j \mid C_1 = c_1 \wedge C_{1,j+1:R} = c_{1,j+1:R}) \cdot \mathbb{P}(C_1 = c_1 \mid C_{1,j+1:R} = c_{1,j+1:R}),$$
$$j = 1, 2, \ldots, R, \;\; c_1 = 0, 1, 2, \ldots, \;\; c_{1,j+1:R} = 0, 1, 2, \ldots \tag{A.27}$$

$\mathbb{P}(F_1 = j \mid C_1 = c_1 \wedge C_{1,j+1:R} = c_{1,j+1:R})$ can be calculated by conditioning on the number of first-hop candidate forwarders in interval i, given that there are c_1 first-hop candidate forwarders and $c_{1,j+1:R}$ remaining first-hop candidate forwarders:

$$\mathbb{P}(F_1 = j \mid C_1 = c_1 \wedge C_{1,j+1:R} = c_{1,j+1:R}) =$$
$$\sum_{c_{1,i}=1}^{c_1 - c_{1,j+1:R}} \mathbb{P}(C_{1,j} = c_{1,j} \mid C_1 = c_1 \wedge C_{1,j+1:R} = c_{1,j+1:R})\, \mathbb{P}(F_1 = i \mid C_{1,i} = c_{1,i} \wedge C_{=} c_1),$$
$$j = 1, 2, \ldots, R, \;\; c_1 = 0, 1, 2, \ldots, \;\; c_{1,j+1:R} = 0, 1, 2, \ldots \tag{A.28}$$

Since each candidate forwarder has an equal probability of becoming the next forwarder, $\mathbb{P}(F_1 = i \mid C_{1,i} = c_{1,i} \wedge C_1 = c_1)$ is given by $\frac{c_{1,j}}{c_1}$.

By definition $C_1 = C_{1,j-1} + C_{1,j} + C_{1,j+1:R}$ and $C_{1,1:j} = C_{1,j-1} + C_{1,j}$. $\mathbb{P}(C_{1,j} = c_{1,j} \mid C_1 = c_1 \wedge C_{1,j+1:R} = c_{1,j+1:R})$ is therefore given by

$$\mathbb{P}(C_{1,j} = c_{1,j} \mid C_1 = c_1 \wedge C_{1,j+1:R} = c_{1,j+1:R}) =$$
$$\frac{\mathbb{P}(C_{1,j} = c_{1,j}) \cdot \mathbb{P}(C_{1,1:j-1} = c_{1,1:j-1})}{\mathbb{P}(C_{1,1:j} = c_{1,1:j})},$$
$$j = 1, 2, \ldots, R, \;\; c_1 = 0, 1, 2, \ldots, \;\; c_{1,j+1:R} = 0, 1, 2, \ldots, \tag{A.29}$$

Again the number of first-hop candidate forwarders in interval i is Poisson distributed with mean $\mathbb{E}(C_{1,i})$, given by Eq. (7.5), so $C_{1,j}$ is Poisson distributed with mean $\mathbb{E}(C_{1,j})$, $C_{1,1:j-1}$ is Poisson distributed with mean $\sum_{i=1}^{j-1} \mathbb{E}(C_{1,i})$, and $C_{1,1:j}$ is Poisson distributed with mean $\sum_{i=1}^{j} \mathbb{E}(C_{1,i})$.

APPENDIX B

Derivations of some intermediate results used in chapter 8

This appendix is meant to support Chapter 8. In Section B.1 we prove that the number of nodes in an interval following the most recent forwarder is Poisson distributed. In Section B.2 we show that the number of nodes in an interval that did not become candidate forwarder is Poisson distributed as well. First we re-introduce some of our notation however.

Let V_i be the number of nodes in interval i. C_n denotes the number of candidate n^{th} forwarders and $C_{n,i}$ denotes the number of candidate n^{th} forwarders in interval i. Furthermore, let $K_{n,i}$ be the number of nodes in interval i that (after the $(n-1)^{\text{th}}$ forwarder has forwarded the message) did not receive the message yet and therefore did not become candidate n^{th} forwarder. Finally, S_i denotes the probability that a receiver successfully receives a message transmitted by a sender that is located i intervals away.

B.1 Number of nodes in intervals following the most recent forwarder

The number of nodes in an interval i, given the position of the first n forwarders, is denoted $V_i \mid \hat{F}_n = \langle f_0, \dots, f_n \rangle$. In this section we prove that $V_i \mid \hat{F}_n = \langle f_0, \dots, f_n \rangle$ is Poisson distributed with mean $\mathbb{E}(V_i) \cdot (1 - S_i) \cdots (1 - S_{i-f_{n-1}})$ for $i > f_n$. For reasons of clarity we first show our proof for $n = 1$ and $n = 2$, and finally give the proof for the general case $n \in \mathbb{N}^+$. For all three cases we use the same line of reasoning.

B.1.1 Calculating the distribution of $V_i \mid \hat{F}_1 = \langle f_0, f_1 \rangle$

To determine the distribution of $V_i \mid \hat{F}_1 = \langle f_0, f_1 \rangle$ we first require the distribution of $C_{1,i}$

The distribution of $C_{1,i}$ is determined as follows. The number of nodes in interval i is Poisson distributed with mean $\mathbb{E}(V_i)$ given by Eq. (8.3). Since a node in interval i has a probability S_i of receiving the source's transmission and becoming a first-hop candidate forwarder, $C_{1,i}$ is Poisson distributed with mean $S_i \cdot \mathbb{E}(V_i)$. Furthermore, for a given number of nodes v in an interval i, $C_{1,i}$ has a Binomial distribution with success probability S_i.

When the first forwarder is positioned in interval f_1 then by definition there are no first-hop candidate forwarders in any interval following interval f_1, i.e., $C_{1,i} = 0$ for $i > f_1$.

Using the notation $p_1 = (1 - S_i)$ and $\lambda = \mathbb{E}(V_i)$, the distribution of $V_i \mid \hat{F}_1 = \langle f_0, f_1 \rangle$ for $i > f_1$ is given by:

$$\begin{aligned}
\mathbb{P}(V_i = v \mid \hat{F}_1 = \langle f_0, f_1 \rangle) &= \mathbb{P}(V_i = v \mid C_{1,i} = 0), \\
&= \frac{\mathbb{P}(V_i = v) \cdot \mathbb{P}(C_{1,i} = 0 \mid V_i = v)}{\mathbb{P}(C_{1,i} = 0)}, \\
&= \frac{\mathbb{P}(V_i = v) \cdot \mathbb{P}(C_{1,i} = 0 \mid V_i = v)}{\sum\limits_{v=0}^{v=\infty} \mathbb{P}(V_i = v) \cdot \mathbb{P}(C_{1,i} = 0 \mid V_i = v)}, \\
&= \frac{\frac{\lambda^v}{v!} e^{-\lambda} \cdot p_1^v}{\sum\limits_{v=0}^{\infty} \frac{\lambda^v}{v!} e^{-\lambda} \cdot p_1^v}, \\
&= \frac{\frac{(p_1 \lambda)^v}{v!} e^{-\lambda}}{e^{p_1 \lambda} e^{-\lambda}}, \\
&= \frac{(p_1 \lambda)^v}{v!} e^{-p_1 \lambda}, \quad i = f_1 + 1, f_1 + 2, \ldots. \qquad \text{(B.1)}
\end{aligned}$$

Hence, $V_i \mid \hat{F}_1 = \langle f_0, f_1 \rangle$ is Poisson distributed with mean $p_1 \lambda = (1 - S_i) \cdot \mathbb{E}(V_i)$ for $i = f_1 + 1, f_1 + 2, \ldots$ Note that the distribution of the number of nodes in an interval, given that there is a first forwarder, is thus independent of the position of the first forwarder.

B.1.2 Calculating the distribution of $V_i \mid \hat{F}_2 = \langle f_0, f_1, f_2 \rangle$

We determine the distribution of $V_i \mid \hat{F}_2 = \langle f_0, f_1, f_2 \rangle$ in a similar manner as we did for $V_i \mid \hat{F}_1 = \langle f_0, f_1 \rangle$. First we require the distribution of $C_{2,i} \mid \hat{F}_1 = \langle f_0, f_1 \rangle$, which we give below. We then give the expression of the distribution of $V_i \mid \hat{F}_2 = \langle f_0, f_1, f_2 \rangle$.

As we showed in the previous section, when it is given that $\hat{F}_1 = \langle f_0, f_1 \rangle$, the number of nodes in interval i is Poisson distributed with mean $(1 - S_i) \cdot \mathbb{E}(V_i)$ for $i > f_1$. By definition no node that is positioned in an interval following the first forwarder has received the source's transmission, else it would have become the first forwarder itself. Since a node in interval i has a probability S_{i-f_1} of receiving the first forwarder's transmission and becoming a second-hop candidate forwarder, $C_{2,i} \mid \hat{F}_1 = \langle f_0, f_1 \rangle$ is Poisson distributed with mean $S_{i-f_1} \cdot (1 - S_i) \cdot \mathbb{E}(V_i)$. Furthermore, for a given number of nodes v in an interval i, $C_{2,i}$ has a Binomial distribution with success probability S_{i-f_1}.

When the second forwarder is positioned in interval f_2 then by definition there are no candidate first forwarders in any interval following interval f_2, i.e., $C_{2,i} = 0$ for $i > f_2$. Using the notation $p_1 = (1 - S_i)$, $p_2 = (1 - S_{i-f_1})$, and $\lambda = \mathbb{E}(V_i)$, the distribution of

$V_i \mid \hat{F}_2 = \langle f_0, f_1, f_2 \rangle$ is given by

$$
\begin{aligned}
\mathbb{P}(V_i = v \mid \hat{F}_2 = \langle f_0, f_1, f_2\rangle) &= \mathbb{P}(V_i = v \mid \hat{F}_1 = \langle f_0, f_1\rangle \wedge C_{2,i} = 0), \\
&= \frac{\mathbb{P}(F_1 = f_1 \wedge C_{2,i} = 0 \mid V_i = v) \cdot \mathbb{P}(V_i = v)}{\mathbb{P}(F_1 = f_1 \wedge C_{2,i} = 0)}, \\
&= \frac{\mathbb{P}(C_{2,i} = 0 \mid F_1 = f_1 \wedge V_i = v) \cdot \mathbb{P}(F_1 = f_1 \mid V_i = v) \cdot \mathbb{P}(V_i = v)}{\mathbb{P}(F_1 = f_1) \cdot \mathbb{P}(C_{2,i} = 0 \mid F_1 = f_1)}, \\
&= \frac{\mathbb{P}(C_{2,i} = 0 \mid F_1 = f_1 \wedge V_i = v) \cdot \frac{\mathbb{P}(V_i = v \mid F_1 = f)\mathbb{P}(F_1 = f)}{\mathbb{P}(V_i = v)} \cdot \mathbb{P}(V_i = v)}{\mathbb{P}(F_1 = f_1) \cdot \mathbb{P}(C_{2,i} = 0 \mid F_1 = f_1)}, \\
&= \frac{\mathbb{P}(C_{2,i} = 0 \mid F_1 = f_1 \wedge V_i = v) \cdot \mathbb{P}(V_i = v \mid F_1 = f)}{\mathbb{P}(C_{2,i} = 0 \mid F_1 = f_1)}, \\
&= \frac{p_2^v \cdot \mathbb{P}(V_i = v \mid F_1 = f)}{\sum\limits_{v=0}^{\infty} \mathbb{P}(V_i = v \mid F_1 = f_1) \cdot \mathbb{P}(C_{2,i} = 0 \mid F_1 = f_1 \wedge V_i = v)}, \\
&= \frac{p_2^v \cdot \frac{(p_1\lambda)^v}{v!} e^{-p_1\lambda}}{\sum\limits_{v=0}^{\infty} \frac{(p_1\lambda)^v}{v!} e^{-p_1\lambda} \cdot p_2^v}, \\
&= \frac{p_2^v \cdot \frac{(p_1\lambda)^v}{v!} e^{-p_1\lambda}}{e^{p_2 p_1 \lambda} e^{-p_1\lambda}}, \\
&= \frac{(p_1 p_2 \lambda)^v}{v!} e^{-p_1 p_2 \lambda}, \\
i = f_2 + 1, f_1 + 2, \ldots, \quad & f_1 = 1, \ldots, d_{max}, \quad f_2 = f_1, \ldots, f_1 + d_{max} \qquad \text{(B.2)}
\end{aligned}
$$

Hence, $V_i \mid \hat{F}_2 = \langle f_0, f_1, f_2\rangle$ is Poisson distributed with mean $p_1 p_2 \lambda = (1 - S_{i-f_1}) \cdot (1 - S_i) \cdot \mathbb{E}(V_i)$ for $i = f_2 + 1, f_1 + 2, \ldots$. Note that the distribution of the number of nodes in an interval, given that there are two forwarders, is thus independent of the position of the second forwarder.

B.1.3 Calculating the distribution of $V_i \mid \hat{F}_n = \langle f_0, \ldots, f_n\rangle$

We have shown above that $V_i \mid \hat{F}_1 = \langle f_0, f_1\rangle$ is Poisson distributed with mean $(1 - S_i) \cdot \mathbb{E}(V_i)$ and that $V_i \mid \hat{F}_2 = \langle f_0, f_1, f_2\rangle$ is Poisson distributed with mean $(1 - S_{i-f_1}) \cdot (1 - S_i) \cdot \mathbb{E}(V_i)$. Below we give the general form of the distribution of $V_i \mid \hat{F}_n = \langle f_0, \ldots, f_n\rangle$ and show that it is Poisson distributed with mean $(1 - S_{i-f_{n-1}}) \cdots (1 - S_i) \cdot \mathbb{E}(V_i)$ for $i = f_n + 1, f_n + 2, \ldots$.

First we determine the distribution of $C_{n,i} \mid \hat{F}_{n-1} = \langle f_0, \ldots, f_{n-1}\rangle$. Assuming that $\hat{F}_{n-1} = \langle f_0, \ldots, f_{n-1}\rangle$, the number of nodes in interval i is Poisson distributed with mean $(1 - S_{i-f_{n-2}}) \cdots (1 - S_i) \cdot \mathbb{E}(V_i)$ for $i > f_{n-1}$. By definition no node that is positioned in an interval following the n^{th} forwarder has received the $(n-1)^{\text{th}}$ forwarder's transmission, else it would have become the n^{th} forwarder itself. Since a node in interval i has a probability $S_{i-f_{n-1}}$ of receiving the $(n-1)^{\text{th}}$ forwarder's transmission and becoming a candidate n^{th} forwarder, $C_{n,i} \mid \hat{F}_{n-1} = \langle f_0, \ldots, f_{n-1} \rangle$ is Poisson distributed with mean $S_{i-f_{n-1}} \cdots (1 - S_i) \cdot \mathbb{E}(V_i)$. Furthermore, for a given number of nodes v in an interval i, $C_{n,i}$ has a Binomial distribution with success probability $S_{i-f_{n-1}}$.

When the n^{th} forwarder is positioned in interval f_n then by definition there are no candidate n^{th} forwarders in any interval following interval f_n, i.e., $C_{n,i} = 0$ for $i > f_n$. Using the notation $p_k = (1 - S_{i-f_{k-1}})$ and $\lambda = \mathbb{E}(V_i)$, the distribution of $V_i = v \mid \hat{F}_n = \langle f_0, \ldots, f_n \rangle$ is given by

$$\mathbb{P}(V_i = v \mid \hat{F}_n = \langle f_0, \ldots, f_n \rangle) = \frac{\mathbb{P}(V_i = v \wedge \hat{F}_{n-1} = \langle f_0, \ldots, f_{n-1} \rangle \wedge C_{n,i} = 0)}{\mathbb{P}(\hat{F}_{n-1} = \langle f_0, \ldots, f_{n-1} \rangle \wedge C_{n,i} = 0)},$$

$$= \frac{\mathbb{P}(C_{n,i} = 0 \mid V_i = v \wedge \hat{F}_{n-1} = \langle f_0, \ldots, f_{n-1} \rangle) \cdot \mathbb{P}(V_i = v \wedge \hat{F}_{n-1} = \langle f_0, \ldots, f_{n-1} \rangle)}{\mathbb{P}(C_{n,i} = 0 \mid \hat{F}_{n-1} = \langle f_0, \ldots, f_{n-1} \rangle) \cdot \mathbb{P}(\hat{F}_{n-1} = \langle f_0, \ldots, f_{n-1} \rangle)},$$

$$= \mathbb{P}(\hat{F}_{n-1} = \langle f_0, \ldots, f_{n-1} \rangle) \cdot$$

$$\frac{\mathbb{P}(C_{n,i} = 0 \mid V_i = v \wedge \hat{F}_{n-1} = \langle f_0, \ldots, f_{n-1} \rangle) \cdot \mathbb{P}(V_i = v \mid \hat{F}_{n-1} = \langle f_0, \ldots, f_{n-1} \rangle)}{\mathbb{P}(C_{n,i} = 0 \mid \hat{F}_{n-1} = \langle f_0, \ldots, f_{n-1} \rangle) \cdot \mathbb{P}(\hat{F}_{n-1} = \langle f_0, \ldots, f_{n-1} \rangle)},$$

$$= \frac{\mathbb{P}(C_{n,i} = 0 \mid V_i = v \wedge \hat{F}_{n-1} = \langle f_0, \ldots, f_{n-1} \rangle) \cdot \mathbb{P}(V_i = v \mid \hat{F}_{n-1} = \langle f_0, \ldots, f_{n-1} \rangle)}{\mathbb{P}(C_{n,i} = 0 \mid \hat{F}_{n-1} = \langle f_0, \ldots, f_{n-1} \rangle)},$$

$$= \frac{\mathbb{P}(C_{n,i} = 0 \mid V_i = v \wedge F_{n-1} = f_{n-1}) \cdot \mathbb{P}(V_i = v \mid \hat{F}_{n-1} = \langle f_0, \ldots, f_{n-1} \rangle)}{\sum_{v=0}^{\infty} \mathbb{P}(V_i = v \mid \hat{F}_{n-1} = \langle f_0, \ldots, f_{n-1} \rangle) \cdot \mathbb{P}(C_{n,i} = 0 \mid V_i = v \wedge \hat{F}_{n-1} = \langle f_0, \ldots, f_{n-1} \rangle)},$$

$$= \frac{p_n^v \cdot \frac{(p_1 \cdots p_{n-1} \lambda)^v}{v!} e^{-p_1 \cdots p_{n-1} \lambda}}{\sum_{v=0}^{\infty} \frac{(p_1 \cdots p_{n-1} \lambda)^v}{v!} e^{-p_1 \cdots p_{n-1} \lambda} \cdot p_n^v},$$

$$= \frac{\frac{(p_1 \cdots p_n \lambda)^v}{v!} e^{-p_1 \cdots p_n \lambda}}{e^{-p_1 \cdots p_n \lambda} e^{p_1 \cdots p_n \lambda}},$$

$$= \frac{(p_1 \cdots p_n \lambda)^v}{v!} e^{-p_1 \cdots p_n \lambda}, \quad n \in \mathbb{N}^+, \quad i = f_n + 1, f_n + 2, \ldots, \quad f_1 = 1, 2, \ldots, \delta_{max},$$

$$f_n = f_{n-1}, f_{n-1} + 1, \ldots, f_{n-1} + \delta_{max}.$$

Hence, $V_i \mid \hat{F}_n = \langle f_0, \ldots, f_n \rangle$ is Poisson distributed with mean $p_1 \cdots p_n \lambda = (1 - S_{i-f_{n-1}}) \cdots (1 - S_i) \cdot \mathbb{E}(V_i)$, for $i = f_n + 1, f_n + 2, \ldots$. Again note that the distribution of the number of nodes in an interval, given that there are n forwarders, is thus independent of the position of the n^{th} forwarder.

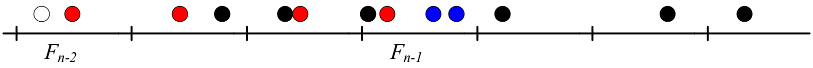

Figure B.1: Example instance of distance-based forwarding over a road divided into fixed-size intervals. The white node is the $(n-2)^{\text{th}}$ forwarder, the red nodes are candidate $(n-1)^{\text{th}}$ forwarders, and the right-most red node is the $(n-1)^{\text{th}}$ forwarder. The blue nodes are nodes positioned in the same interval as the $(n-1)^{\text{th}}$ forwarder that have not received the $(n-2)^{\text{th}}$ forwarder's transmission and that are positioned closer to the destination than the $(n-1)^{\text{th}}$ forwarder. The black nodes represent the other nodes that did not receive the $(n-2)^{\text{th}}$ forwarder's transmission.

B.2 The number of non-candidate forwarders in an interval

Given that the source and the first $n-1$ forwarders are positioned in intervals $f_0, f_1, \ldots, f_{n-1}$, we determine the distribution of the number of nodes in interval f_{n-1} that have not received the message from the $(n-2)^{\text{th}}$ forwarder, and that are positioned closer to the destination than the $(n-1)^{\text{th}}$ forwarder. Below we show how to do so but first exemplify the situation by means of Fig. B.1: in the figure the white node is the $(n-2)^{\text{th}}$ forwarder. The red nodes have all received the message from the $(n-2)^{\text{th}}$ forwarder and are therefore candidate $(n-1)^{\text{th}}$ forwarders, of which the right-most red node has become the $(n-1)^{\text{th}}$ forwarder. The black and blue nodes have not received the message from the $(n-2)^{\text{th}}$ forwarder. We are interested in the number of nodes in interval f_{n-1} that have not yet received the message after the $(n-2)^{\text{th}}$ forwarder has forwarded the message and that are positioned closer to the destination than the $(n-1)^{\text{th}}$ forwarder, i.e., the blue nodes in the figure.

Let $K_{k-1,j} \mid \hat{F}_{k-2} = \langle f_0, \ldots, f_{k-2} \rangle$ denote the number of nodes in interval j that did not become candidate $k-1^{\text{th}}$ forwarder, given the positions of the source and the first $k-2$ forwarders. To determine the number of nodes in interval f_{n-1} that have not yet received the message after the $(n-2)^{\text{th}}$ forwarder has forwarded the message and that are positioned closer to the destination than the $(n-1)^{\text{th}}$ forwarder, we require the distribution of $K_{n-1,f_{n-1}} \mid \hat{F}_{n-1} = \langle f_0, \ldots, f_{n-1} \rangle$. Below we first determine the distribution of $K_{n-1,f_{n-1}} \mid \hat{F}_{n-2} = \langle f_0, \ldots, f_{n-2} \rangle$; based on that we obtain the distribution of $K_{n-1,f_{n-1}} \mid \hat{F}_{n-1} = \langle f_0, \ldots, f_{n-1} \rangle$. Finally we determine how many of $K_{n-1,f_{n-1}} \mid \hat{F}_{n-1} = \langle f_0, \ldots, f_{n-1} \rangle$ nodes are positioned closer to the destination than $(n-1)^{\text{th}}$ forwarder.

In the previous section we proved that the number of nodes in interval f_{n-1}, given the position of the source and the first $n-2$ forwarders, is Poisson distributed with mean $(1 - S_{f_{n-1}-f_{n-3}}) \cdots (1 - S_{f_{n-1}-f_0}) \cdot \mathbb{E}(V_{f_{n-1}})$. The probability number of nodes in interval f_{n-1} that does not receive the $(n-2)^{\text{th}}$ forwarder's transmission (i.e., K_{n-1}, f_{n-1}), given $\hat{F}_{n-2} = \langle f_0, \ldots, f_{n-2} \rangle$, is thus Poisson distributed with mean $(1 - S_{f_{n-1}-f_{n-2}}) \cdot (1 - S_{f_{n-1}-f_{n-3}}) \cdots (1 - S_{f_{n-1}}) \cdot \mathbb{E}(V_{f_{n-1}})$.

To determine the distribution of $K_{n-1,f_{n-1}} \mid \hat{F}_{n-1} = \langle f_0, \ldots, f_{n-1} \rangle$ we note that (given the positions of the source and the first $n-2$ forwarders) the distribution of the number of nodes in an interval i that did not receive the message from the $(n-2)^{\text{th}}$ forwarder is independent of the number of nodes in interval i that did receive the message from the $(n-2)^{\text{th}}$ forwarder. The distribution of $K_{n-1,f_{n-1}} \mid \hat{F}_{n-2} = \langle f_0, \ldots, f_{n-2} \rangle$ does therefore not change when the position of the $(n-1)^{\text{th}}$ forwarder is given, i.e., $K_{n-1,f_{n-1}} \mid \hat{F}_{n-1} = \langle f_0, \ldots, f_{n-1} \rangle$ has the same distribution as $K_{n-1,f_{n-1}} \mid \hat{F}_{n-2} = \langle f_0, \ldots, f_{n-2} \rangle$.

Now that the distribution of $K_{n-1,f_{n-1}} \mid \hat{F}_{n-1} = \langle f_0, \ldots, f_{n-1} \rangle$ is known we need to determine how many of these nodes are positioned closer to the destination than the $(n-1)^{\text{th}}$ forwarder. Because the probability of successfully receiving a transmission is i.i.d. for each node in an interval, the position of the $(n-1)^{\text{th}}$ forwarder in interval f_{n-1} is random with respect to the position of the nodes in that interval that did not become a candidate $(n-1)^{\text{th}}$ forwarder. Each node that did not become a candidate forwarder therefore has a probability of $1/2$ of being positioned closer to the destination than the $(n-1)^{\text{th}}$ forwarder, and the number of nodes in interval f_{n-1} (for $f_{n-1} > f_{n-2}$) that did not receive the message from the $(n-2)^{\text{th}}$ forwarder and that are positioned closer to the destination than the $(n-1)^{\text{th}}$ forwarder is therefore Poisson distributed with mean $(1 - S_{f_{n-1}-f_{n-2}}) \cdot (1 - S_{f_{n-1}-f_{n-3}}) \cdots (1 - S_{f_{n-1}-f_0}) \cdot \mathbb{E}(V_{f_{n-1}})/2$, which is equal to $\mathbb{E}(V_{f_{n-1}} \mid \hat{F}_{n-1} = \langle f_0, \ldots, f_{n-1} \rangle)/2$.

Bibliography

[1] J. Ploeg, A. Serrarens, and G. Heijenk, "Connect & Drive: Design and Evaluation of Cooperative Adaptive Cruise Control for Congestion Reduction," *Journal of Modern Transportation*, vol. 19, no. 3, pp. 207–213, 2011.

[2] B. van Arem, C. van Driel, and R. Visser, "The Impact of Cooperative Adaptive Cruise Control on Traffic-Flow Characteristics," *Intelligent Transportation Systems, IEEE Transactions on*, vol. 7, no. 4, pp. 429–436, 2006.

[3] "Intelligent Transport Systems (ITS) – Vehicular Communications – Geonetworking – Part 4: Geographical Addressing and Forwarding for Point-to-Point and Point-to-Multipoint Communications – Sub-Part 1: Media-Independent Functionality," European Telecommunications Standards Institute, Technical Specification 102 636-4-1, 2011.

[4] W. Klein Wolterink, G. Karagiannis, and G. Heijenk, "A Dynamic Geocast Solution to Support Cooperative Adaptive Cruise Control (CACC) Merging," in *Fourth ERCIM Workshop on eMobility*, 2010, p. 113.

[5] W. Klein Wolterink, G. Heijenk, and G. Karagiannis, "Constrained Geocast to Support Cooperative Adaptive Cruise Control (CACC) Merging," in *2010 IEEE Vehicular Networking Conference (VNC)*. pp. 41–48.

[6] W. Klein Wolterink, G. Heijenk, and G. Karagiannis, "Automated Merging in a Cooperative Adaptive Cruise Control (CACC) System," in *Fifth ERCIM workshop on eMobility*, 2011, p. 23.

[7] W. Klein Wolterink, G. Heijenk, and G. Karagiannis, "Dissemination Protocols to Support Cooperative Adaptive Cruise Control (CACC) Merging," in *International Conference on ITS Telecommunications*, 2011.

[8] W. Klein Wolterink, G. Heijenk, and G. Karagiannis, "Information Dissemination in VANETs by Piggybacking on Beacons - An Analysis of the Impact of Network Parameters," in *2011 IEEE Vehicular Networking Conference (VNC)*.

[9] W. Klein Wolterink, G. Heijenk, and H. van den Berg, "Analytically Modelling the Performance of Piggybacking on Beacons in VANETs," in *Proceedings of the Ninth ACM International Workshop on VehiculAr inter-NETworking (VANET), systems, and applications*. 2012, pp. 43–52.

[10] J.L. van den Berg, W. Klein Wolterink, G. Heijenk, "An Analytical Model for the Performance of Geographical Multi-Hop Broadcast," in *Proceedings of the 2012 IEEE Vehicular Networking Conference (VNC)*.

[11] "Shuets Udono: http://www.flickr.com/photos/udono/408633225/ [cc-by-sa-2.0 (http://creativecommons.org/licenses/by-sa/2.0)], via wikimedia commons."

[12] "On the Intelligent Car Initiative – "Raising Awareness of ICT for Smarter, Safer and Cleaner Vehicles"," European Commission, Brussels, Belgium, Tech. Rep., 2006.

[13] Y. Sugiyama, M. Fukui, M. Kikuchi, K. Hasebe, A. Nakayama, K. Nishinari, S. Tadaki, and S. Yukawa, "Traffic Jams without Bottlenecks: Experimental Evidence for the Physical Mechanism of the Formation of a Jam," *New Journal of Physics*, vol. 10, p. 033001, 2008.

[14] J. University of Nagoya, "Shockwave Traffic Jams Recreated for First Time," Online: http://www.youtube.com/watch?v=Suugn-p5C1M.

[15] M. van Eenennaam, W. Klein Wolterink, G. Karagiannis, and G. Heijenk, "Exploring the Solution Space of Beaconing in VANETs," in *Vehicular Networking Conference (VNC), 2009 IEEE*. IEEE, pp. 1–8.

[16] C. Lei, E. M. van Eenennaam, W. Klein Wolterink, G. Karagiannis, G. J. Heijenk, and J. Ploeg, "Impact of Packet Loss on CACC String Stability Performance," in *Proceedings of the Eleventh International Workshop on ITS Telecommunications, Saint-Petersburg, Russia*. Russia: IEEE Communications Society, August 2011, pp. 381–386.

[17] J. Spilker, *The Global Positioning System: Theory and Applications*. Aiaa, 1996, vol. 2.

[18] "European GNSS Agency," http://www.gsa.europa.eu/.

[19] R. Schubert, M. Schlingelhof, H. Cramer, and G. Wanielik, "Accurate Positioning for Vehicular Safety Applications – The SAFESPOT Approach," in *Vehicular Technology Conference, 2007. VTC2007-Spring. IEEE 65th*. IEEE, 2007, pp. 2506–2510.

[20] P. Papadimitratos, A. La Fortelle, K. Evenssen, R. Brignolo, and S. Cosenza, "Vehicular Communication Systems: Enabling Technologies, Applications, and Future Outlook on Intelligent Transportation," *Communications Magazine, IEEE*, vol. 47, no. 11, pp. 84–95, 2009.

[21] "Intelligent Transport Systems - Communications Access for Land Mobiles (CALM) – Architecture," ISO Technical Committee 204 WG16, Tech. Rep. ISO/DIS 21217, work in progress, September 2009.

[22] T. Rappaport *et al.*, *Wireless Communications: Principles and Practice*. Prentice Hall PTR New Jersey, 1996, vol. 207.

[23] "IEEE Standard for Information Technology – Telecommunications and Information Exchange Between Systems Local and Metropolitan Area networks – Specific Requirements Part 11: Wireless LAN Medium Access Control (MAC) and Physical Layer (PHY) Specifications," Institute of Electrical and Electronics Engineers (IEEE), Tech. Rep., March 2012.

[24] "Intelligent transport systems (ITS) – European profile standard for the physical and medium access control layer of intelligent transport systems operating in the 5 ghz frequency band," European Telecommunications Standards Institute, European Standard 202 663, January 2010.

[25] M. Torrent-Moreno, D. Jiang, and H. Hartenstein, "Broadcast Reception Rates and Effects of Priority Access in 802.11-based Vehicular Ad-hoc Networks," in *Proceedings of the 1st ACM international workshop on Vehicular ad hoc networks*. ACM, 2004, pp. 10–18.

[26] J. Blum and A. Eskandarian, "Avoiding Timeslot Boundary Synchronization for Multihop Message Broadcast in Vehicular Networks," in *Vehicular Technology Conference, 2009. VTC Spring 2009. IEEE 69th*. IEEE, 2009, pp. 1–5.

[27] "Trial-use Standard for Wireless Access in Vehicular Environments (WAVE) – Multi-Channel Operation (IEEE 1609.4)," IEEE, Tech. Rep., 2006.

[28] U. F. C. Commission *et al.*, "R&O FCC 03–324," *Dedicated Short Range Communications Report and Order*, 2003.

[29] "Intelligent Transport Systems (ITS) – Vehicular Communications – Geographical Area Definition," European Telecommunications Standards Institute, European Standard (draft) 302 931, 2010.

[30] C. Maihöfer, T. Leinmüller, and E. Schoch, "Abiding geocast: time–stable geocast for ad hoc networks," in *Proceedings of the 2nd ACM international workshop on Vehicular ad hoc networks*. ACM, 2005, pp. 20–29.

[31] A. Castro, G. Serugendo, and D. Konstantas, "Hovering information–self-organizing information that finds its own storage," *Autonomic Communication*, pp. 111–145, 2009.

[32] A. Vinel, Y. Koucheryavy, S. Andreev, and D. Staehle, "Estimation of a successful beacon reception probability in vehicular ad-hoc networks," in *Proceedings of the 2009 International Conference on Wireless Communications and Mobile Computing: Connecting the World Wirelessly*. ACM, 2009, pp. 416–420.

[33] R. Schmidt, T. Leinmüller, E. Schoch, F. Kargl, and G. Schäfer, "Exploration of adaptive beaconing for efficient intervehicle safety communication," *Network, IEEE*, vol. 24, no. 1, pp. 14–19, 2010.

[34] T. Tielert, D. Jiang, Q. Chen, L. Delgrossi, and H. Hartenstein, "Design methodology and evaluation of rate adaptation based congestion control for vehicle safety communications," in *Vehicular Networking Conference (VNC), 2011 IEEE*. IEEE, 2011, pp. 116–123.

[35] T. Tielert, D. Jiang, H. Hartenstein, and L. Delgrossi, "Joint power/rate congestion control optimizing packet reception in vehicle safety communications," in *Proceedings of the Tenth ACM International Workshop on VehiculAr Inter-NETworking, Systems, and Applications (VANET)*, Taipei, Taiwan, 2013.

[36] M. van Eenennaam, L. Hendriks, G. Karagiannis, and G. Heijenk, "Oldest packet drop (OPD): A buffering mechanism for beaconing in ieee 802.11p VANETs (poster)," in *Vehicular Networking Conference (VNC), 2011 IEEE*. IEEE, 2011, pp. 252–259.

[37] C. Sommer, O. Tonguz, and F. Dressler, "Traffic information systems: efficient message dissemination via adaptive beaconing," *Communications Magazine, IEEE*, vol. 49, no. 5, pp. 173–179, 2011.

[38] ETSI, "TS 102 637-2 vehicular communications; basic set of applications; part 2: Specification of cooperative awareness basic service," 2010.

[39] B. Karp and H. Kung, "GPSR: Greedy perimeter stateless routing for wireless networks," in *Proceedings of the 6th annual international conference on Mobile computing and networking*. ACM, 2000, pp. 243–254.

[40] C. Lochert, M. Mauve, H. Füßler, and H. Hartenstein, "Geographic routing in city scenarios," *ACM SIGMOBILE Mobile Computing and Communications Review*, vol. 9, no. 1, pp. 69–72, 2005.

[41] C. Lochert, H. Hartenstein, J. Tian, H. Fussler, D. Hermann, and M. Mauve, "A routing strategy for vehicular ad hoc networks in city environments," in *Intelligent Vehicles Symposium, 2003. Proceedings. IEEE*. Ieee, 2003, pp. 156–161.

[42] V. Dumitrescu and J. Guo, "Context assisted routing protocols for inter-vehicle wireless communication," in *Intelligent Vehicles Symposium, 2005. Proceedings. IEEE*. IEEE, 2005, pp. 594–600.

[43] M. Jerbi, R. Meraihi, S. Senouci, and Y. Ghamri-Doudane, "GyTAR: improved greedy traffic aware routing protocol for vehicular ad hoc networks in city environments," in *Proceedings of the 3rd international workshop on Vehicular ad hoc networks*. ACM, 2006, pp. 88–89.

[44] J. LeBrun, C. Chuah, D. Ghosal, and M. Zhang, “Knowledge-based opportunistic forwarding in vehicular wireless ad hoc networks,” in *Vehicular Technology Conference, 2005. VTC 2005-Spring. 2005 IEEE 61st*, vol. 4. IEEE, 2005, pp. 2289–2293.

[45] F. Li and Y. Wang, “Routing in vehicular ad hoc networks: A survey,” *Vehicular Technology Magazine, IEEE*, vol. 2, no. 2, pp. 12–22, 2007.

[46] J. Bernsen and D. Manivannan, “Unicast routing protocols for vehicular ad hoc networks: A critical comparison and classification,” *Pervasive and Mobile Computing*, vol. 5, no. 1, pp. 1–18, 2009.

[47] O. Tonguz, N. Wisitpongphan, F. Bai, P. Mudalige, and V. Sadekar, “Broadcasting in VANET,” in *2007 Mobile Networking for Vehicular Environments*. IEEE, 2007, pp. 7–12.

[48] N. Wisitpongphan, O. Tonguz, J. Parikh, P. Mudalige, F. Bai, and V. Sadekar, “Broadcast storm mitigation techniques in vehicular ad hoc networks,” *Wireless Communications, IEEE*, vol. 14, no. 6, pp. 84–94, 2007.

[49] R. Schwartz, K. Das, H. Scholten, and P. Havinga, “Exploiting beacons for scalable broadcast data dissemination in VANETs,” in *Proceedings of the ninth ACM international workshop on Vehicular inter-networking, systems, and applications*. ACM, 2012, pp. 53–62.

[50] L. Wischhof, A. Ebner, and H. Rohling, “Information dissemination in self-organizing inter-vehicle networks,” *Intelligent Transportation Systems, IEEE Transactions on*, vol. 6, no. 1, pp. 90–101, 2005.

[51] T. Little and A. Agarwal, “An information propagation scheme for VANETs,” in *Intelligent Transportation Systems, 2005. Proceedings. 2005 IEEE*. IEEE, 2005, pp. 155–160.

[52] J. Blum, A. Eskandarian, and L. Hoffman, “Mobility management in IVC networks,” in *Intelligent Vehicles Symposium, 2003. Proceedings. IEEE*. IEEE, 2003, pp. 150–155.

[53] R. Santos, A. Edwards, R. Edwards, and N. Seed, “Performance evaluation of routing protocols in vehicular ad-hoc networks,” *International Journal of Ad Hoc and Ubiquitous Computing*, vol. 1, no. 1, pp. 80–91, 2005.

[54] P. Papadimitratos, L. Buttyan, T. Holczer, E. Schoch, J. Freudiger, M. Raya, Z. Ma, F. Kargl, A. Kung, and J. Hubaux, “Secure vehicular communication systems: design and architecture,” *Communications Magazine, IEEE*, vol. 46, no. 11, pp. 100–109, 2008.

[55] M. Feiri, J. Petit, and F. Kargl, “Evaluation of congestion-based certificate omission in VANETs,” in *Proceedings of the IEEE Vehicular Networking Conference 2012 (VNC 2012)*, IEEE. Seoul, Korea: IEEE, 11/2012 2012.

[56] F. Dressler, F. Kargl, J. Ott, O. Tonguz, and L. Wischhof, “Research challenges in intervehicular communication: lessons of the 2010 Dagstuhl seminar,” *Communications Magazine, IEEE*, vol. 49, no. 5, pp. 158–164, 2011.

[57] “Intelligent transport systems (ITS) – vehicular communications – basic set of applications – definitions,” European Telecommunications Standards Institute, Technical Report 102 638, 2009.

[58] A. Vinel, “3GPP LTE versus IEEE 802.11p/WAVE: Which technology is able to support cooperative vehicular safety applications?” *Wireless Communications Letters, IEEE*, vol. 1, no. 2, pp. 125–128, 2012.

[59] S. Eichler, “Performance evaluation of the IEEE 802.11p WAVE communication standard,” in *Vehicular Technology Conference, 2007. VTC-2007 Fall. 2007 IEEE 66th*. IEEE, 2007, pp. 2199–2203.

[60] T. Kosch, C. Adler, S. Eichler, C. Schroth, and M. Strassberger, "The scalability problem of vehicular ad hoc networks and how to solve it," *Wireless Communications, IEEE*, vol. 13, no. 5, pp. 22–28, 2006.

[61] "Safespot EU FP6 project website," http://www.safespot-eu.org.

[62] "CVIS EU FP6 project website," http://www.cvisproject.org.

[63] "Network on Wheels (NoW) German project website," http://www.network-on-wheels.de/about.html.

[64] "COMmunication for eSafety (COMeSafety) EU FP6 project," http://www.comesafety.org.

[65] "SeVeCom EU FP6 project website," http://www.network-on-wheels.de/about.html.

[66] "Official website of National ITS Architecture," http://www.iteris.com/itsarch/index.htm/.

[67] "Trial-use standard for wireless access in vehicular environments (WAVE) – resource manager (IEEE 1609.1)," IEEE, Tech. Rep., 2006.

[68] "Trial-use standard for wireless access in vehicular environments (WAVE) – security services for applications and management message (IEEE 1609.2)," IEEE, Tech. Rep., 2006.

[69] "IEEE trial-use standard for wireless access in vehicular environments (WAVE) – networking services (IEEE 1609.3)," IEEE, Tech. Rep., 2006.

[70] Intellidrive project, "Vehicle safety applications," in *ITS Joint program Office*. USDOT.

[71] "PATH project website," http://www.path.berkeley.edu/PATH/Research/projects.html.

[72] "Official website of the V2V safety roadmap," http://www.intellidriveusa.org/research/v2v-safety-roadmap.php.

[73] H. Matsumoto, H. Sonoda, M. Yoshioka, T. Tanino, "Study of how to protect ETC system security," in *15th World Congress on Intelligent Transportation Systems (ITS WC08)*, 2008.

[74] "Official website of the advanced cruise assist highway systems research association (AHSRA)," http://www.ahsra.or.jp/eng/index.htm.

[75] "Intelligent transport systems – communications access for land mobiles (CALM) – CALM M5," ISO, ISO Technical Committee 204, ISO/DIS 21215, April 2009.

[76] C. Sommer, R. German, and F. Dressler, "Bidirectionally coupled network and road traffic simulation for improved IVC analysis," *Mobile Computing, IEEE Transactions on*, vol. 10, no. 1, pp. 3–15, 2011.

[77] OmNet++ network simulation framework. [Online]. Available: http://www.omnetpp.org/

[78] SUMO website: http://sumo.sourceforge.net.

[79] MiXiM website: http://mixim.sourceforge.net/

[80] M. Piorkowski, M. Raya, A. Lugo, P. Papadimitratos, M. Grossglauser, and J. Hubaux, "TraNS: realistic joint traffic and network simulator for VANETs," *ACM SIGMOBILE Mobile Computing and Communications Review*, vol. 12, no. 1, pp. 31–33, 2008.

[81] NS website: http://www.isi.edu/nsnam/ns.

[82] "JiST / SWANS," http://jist.ece.cornell.edu/.

[83] B. van Arem, C. van Driel, and R. Visser, "The impact of cooperative adaptive cruise control on traffic-flow characteristics," *Intelligent Transportation Systems, IEEE Transactions on*, vol. 7, no. 4, pp. 429–436, 2006.

[84] A. Hsu, S. Sachs, F. Eskafi, and P. Varaiya, "The design of platoon maneuvers for IVHS," in *American Control Conference, 1991*. IEEE, 1991, pp. 2545–2550.

[85] S. Hallé, B. Chaib-draa, and J. Laumonier, "Car platoons simulated as a multiagent system," in *Agent Based Simulation*, vol. 4. Citeseer, 2003, pp. 57–63.

[86] L. Baskar, B. De Schutter, and H. Hellendoorn, "Hierarchical traffic control and management with intelligent vehicles," in *Intelligent Vehicles Symposium, 2007 IEEE*. IEEE, 2007, pp. 834–839.

[87] W. Birk, J. Eliasson, P. Lindgren, E. Osipov, and L. Riliskis, "Road surface networks technology enablers for enhanced ITS," in *Vehicular Networking Conference (VNC), 2010 IEEE*. IEEE, 2010, pp. 152–159.

[88] M. Treiber, A. Hennecke, and D. Helbing, "Congested traffic states in empirical observations and microscopic simulations," *Physical Review E*, vol. 62, no. 2, p. 1805, 2000.

[89] M. Boban, T. Vinhoza, M. Ferreira, J. Barros, and O. Tonguz, "Impact of vehicles as obstacles in vehicular ad hoc networks," *Selected Areas in Communications, IEEE Journal on*, vol. 29, no. 1, pp. 15–28, 2011.

[90] Y. Zhuang, J. Pan, and L. Cai, "A probabilistic model for message propagation in two-dimensional vehicular ad-hoc networks," in *Proceedings of the seventh ACM international workshop on VehiculAr InterNETworking*. ACM, 2010, pp. 31–40.

[91] K. Viswanath and K. Obraczka, "Modeling the performance of flooding in wireless multi-hop ad hoc networks," *Computer Communications*, vol. 29, no. 8, pp. 949–956, 2006.

[92] S. Yousefi, E. Altman, R. El-Azouzi, and M. Fathy, "Analytical model for connectivity in vehicular ad hoc networks," *Vehicular Technology, IEEE Transactions on*, vol. 57, no. 6, pp. 3341 –3356, nov. 2008.

[93] G. Resta, P. Santi, and J. Simon, "Analysis of multi-hop emergency message propagation in vehicular ad hoc networks," in *Proceedings of the 8th ACM international symposium on Mobile ad hoc networking and computing*. ACM, 2007, pp. 140–149.

[94] K. Abboud and W. Zhuang, "Modeling and analysis for emergency messaging delay in vehicular ad hoc networks," in *Global Telecommunications Conference, 2009. GLOBECOM 2009. IEEE*. IEEE, 2009, pp. 1–6.

[95] K. Rostamzadeh and S. Gopalakrishnan, "Analysis of emergency message dissemination in vehicular networks," in *Wireless Communications and Networking Conference (WCNC), 2011 IEEE*. IEEE, 2011, pp. 575–580.

[96] S. Vural and E. Ekici, "Probability distribution of multi-hop-distance in one-dimensional sensor networks," *Computer Networks*, vol. 51, no. 13, pp. 3727–3749, 2007.

[97] L. Mattner and B. Roos, "Maximal probabilities of convolution powers of discrete uniform distributions," *Statistics & Probability Letters*, vol. 78, no. 17, pp. 2992–2996, 2008.

[98] H. Tijms, "Stochastic modelling and analysis: a computational approach," 1986.

[99] S. Ross, *Introduction to probability models*. Academic Pr, 2009.

[100] "IEEE standard for information technology – telecommunications and information exchange between systems – local and metropolitan area networks – specific requirements part 11: Wireless LAN medium access control (MAC) and physical layer (PHY) specifications – amendment 6: Wireless access in vehicular environments," IEEE Computer Society, Tech. Rep., 2010.

[101] F. Bai and B. Krishnamachari, "Spatio-temporal variations of vehicle traffic in VANETs: facts and implications," in *Proceedings of the sixth ACM international workshop on VehiculAr InterNETworking*. ACM, 2009, pp. 43–52.

[102] M. Schönhof, A. Kesting, M. Treiber, and D. Helbing, "Coupled vehicle and information flows: Message transport on a dynamic vehicle network," *Physica A: Statistical Mechanics and its Applications*, vol. 363, no. 1, pp. 73–81, 2006.

[103] V. Arasan and R. Koshy, "Methodology for modeling highly heterogeneous traffic flow," *Journal of Transportation Engineering*, vol. 131, p. 544, 2005.

[104] D. Moltchanov, Y. Koucheryavy, and J. Harju, "Cross-layer modeling of wireless channels for data-link and ip layer performance evaluation," *Computer communications*, vol. 29, no. 7, pp. 827–841, 2006.

[105] H. Füßler, J. Widmer, M. Käsemann, M. Mauve, and H. Hartenstein, "Contention-based forwarding for mobile ad hoc networks," *Ad Hoc Networks*, vol. 1, no. 4, pp. 351–369, 2003.

[106] H. Füßler, H. Hartenstein, J. Widmer, M. Mauve, and W. Effelsberg, "Contention-based forwarding for street scenarios," in *1st International Workshop in Intelligent Transportation (WIT 2004)*, 2004, pp. 155–159.

[107] S. Son, B. Blum, T. He, and J. Stankovic, "IGF: A state-free robust communication protocol for wireless sensor networks," Citeseer, Tech. Rep., 2003.

[108] S. Vural and E. Ekici, "On multihop distances in wireless sensor networks with random node locations," *Mobile Computing, IEEE Transactions on*, vol. 9, no. 4, pp. 540–552, 2010.

[109] N. Wisitpongphan, F. Bai, P. Mudalige, V. Sadekar, and O. Tonguz, "Routing in sparse vehicular ad hoc wireless networks," *Selected Areas in Communications, IEEE Journal on*, vol. 25, no. 8, pp. 1538–1556, 2007.

[110] ZigBee website: http://www.zigbee.org.

[111] K. Audenaert, "Inverse moments of univariate discrete distributions via the poisson expansion," *arXiv preprint arXiv:0809.4155*, 2008.

[112] M. Killat and H. Hartenstein, "An empirical model for probability of packet reception in vehicular ad hoc networks," *EURASIP Journal on Wireless Communications and Networking*, vol. 2009, p. 4, 2009.